270

UCRL-53632

SAI
T&MSS
LIBRARY

Field Investigation of Keyblock Stability

Jesse Lewis Yow, Jr.

(Doctor of Philosophy)

April 1985

DISCLAIMER

This document was prepared as an account of work sponsored by an agency of the United States Government. Neither the United States Government nor the University of California nor any of their employees, makes any warranty, express or implied, or assumes any legal liability or responsibility for the accuracy, completeness, or usefulness of any information, apparatus, product, or process disclosed, or represents that its use would not infringe privately owned rights. Reference herein to any specific commercial products, process, or service by trade name, trademark, manufacturer, or otherwise, does not necessarily constitute or imply its endorsement, recommendation, or favoring by the United States Government or the University of California. The views and opinions of authors expressed herein do not necessarily state or reflect those of the United States Government or the University of California, and shall not be used for advertising or product endorsement purposes.

Work performed under the auspices of the U.S. Department of Energy by Lawrence Livermore National Laboratory under Contract W-7405-Eng-48.

UCRL-53632
Distribution Category UC-70

Field Investigation of Keyblock Stability

Jesse Lewis Yow, Jr.

(Doctor of Philosophy)

Manuscript date: April 1985

SAI
T&MSS
LIBRARY

LAWRENCE LIVERMORE LABORATORY
University of California • Livermore, California • 94550

Available from: National Technical Information Service • U.S. Department of Commerce
5285 Port Royal Road • Springfield, VA 22161 • $20.50 per copy • (Microfiche $4.50)

Field Investigation of Keyblock Stability

By

Jesse Lewis Yow, Jr.

B.S. (University of Missouri, Rolla) 1974
M.S. (University of Missouri, Rolla) 1976

DISSERTATION

Submitted in partial satisfaction of the requirements for the degree of

DOCTOR OF PHILOSOPHY

in

Engineering

in the

GRADUATE DIVISION

OF THE

UNIVERSITY OF CALIFORNIA, BERKELEY

Approved: ...Richard E. Goodman... Mar 27, 1985
Chairman Date
..... April 9, 1985
..... April 9, 1985

.....

PREFACE

This report develops three-dimensional techniques to assess the behavior of underground openings in cases where opening stability is controlled by rock mass structures such as joints. These techniques for evaluating stability complement rather than replace other excavation design approaches. The techniques are suitable for cylindrical openings like waste package emplacement holes and are good approximations for certain other excavation geometries as well. Emplacement hole stability is important for waste package integrity and retrieval and can also be a factor in emplacement hole construction.

A subsequent report will use currently available site geologic information from exploratory drilling with the methods developed herein to examine the stability of waste package emplacement holes that may be constructed at Yucca Mountain, NV. Example solutions in this subsequent report will illustrate the effects of emplacement hole orientation and data variability on opening stability. A final analysis of stability is planned for when fracture characterization data are available from the Exploratory Shaft facilities. This work is funded in the Nuclear Waste Management Group of Lawrence Livermore National Laboratory as part of the Nevada Nuclear Waste Storage Investigations Project of the U.S. Department of Energy.

Field Investigation of Keyblock Stability

Jesse L. Yow, Jr.

Doctor of Philosophy

Lawrence Livermore National Laboratory

Civil Engineering
Geological Engineering

Richard E. Goodman
Committee Chairman

Discontinuities in a rock mass can intersect an excavation surface to form discrete blocks (keyblocks) which can be unstable. This engineering problem is divided into two parts: block identification, and evaluation of block stability. Keyblocks can be identified from discontinuity and excavation geometry using a whole stereographic projection. Once a block is identified, the forces affecting it can be calculated to assess its stability. The normal and shear stresses on each block face before displacement are calculated using elastic theory and are modified in a nonlinear way by discontinuity deformations as the keyblock displaces. The stresses are summed into resultant forces to evaluate block stability. Since the resultant forces change with displacement, successive increments of block movement are examined to see whether the block ultimately becomes stable or fails.

One stable keyblock and thirteen fallen keyblocks were observed in field investigations at the Nevada Test Site. Nine blocks were measured in detail sufficient to allow back-analysis of their stability. Measurements included block geometry, and discontinuity roughness and compressive strength. Back-analysis correctly predicted stability or failure in all but two cases. These two exceptions

involved situations that violated the stress assumptions of the stability calculations. Keyblock faces correlated well with known joint set orientations. The effect of tunnel orientation on keyblock frequency was apparent. Back-analysis of physical models successfully predicted block pullout force for two-dimensional models of unit thickness.

Two-dimensional (2D) and three-dimensional (3D) analytic models for the stability of simple pyramidal keyblocks were examined. Calculated stability is greater for 3D analyses than for 2D analyses. Calculated keyblock stability increases with larger in situ stress magnitudes, larger lateral stress ratios, and larger shear strengths. Discontinuity stiffness controls block displacement more strongly than it does stability itself. Large keyblocks are less stable than small ones, and stability increases as blocks become more slender. Rock mass temperature decreases reduce the confining stress magnitudes and can lead to failure. The pattern of stresses affecting each block face explains conceptually the occurrence of pyramidal keyblocks that are truncated near their apex.

TABLE OF CONTENTS

LIST OF FIGURES iv

LIST OF TABLES. x

NOMENCLATURE. xi

ACKNOWLEDGMENTS xiii

CHAPTER 1 INTRODUCTION. 1

Definition of the Block Stability Problem 1

Scope of Work 11

CHAPTER 2 IDENTIFICATION OF KEYBLOCKS 13

Approaches for Identifying Critical Blocks. 13

Block Theory and Keyblock Identification. 20

CHAPTER 3 KEYBLOCK STABILITY ANALYSIS METHODS 28

Approaches for Evaluating Keyblock Stability. . . . 28

Stability Analysis Assumptions. 31

Keyblock Instability and Displacement 33

Discontinuity Shear Strength. 37

Discontinuity Stiffness 38

Load and Stress Conditions. 52

Formulation of Keyblock Stability Equations 57

CHAPTER 4 FIELD OBSERVATIONS OF KEYBLOCKS 69
Observations at the Nevada Test Site. 69
Techniques Used for Field Observations. 73
Field Observations of Keyblock Occurrences. 83
Analyses of Keyblock Stability. 101
Analyses of Physical Models 105

CHAPTER 5 PARAMETER EFFECTS ON KEYBLOCK STABILITY 110
Description of Keyblocks Used for Studies 110
Limitations of Stability Analysis Method. 114
Keyblock Displacement 117
Discontinuity Shear Strength. 125
Discontinuity Stiffness 130
Stresses and Loads. 133
Block Geometry. 139

CHAPTER 6 CONCLUSIONS AND APPLICATIONS. 146
Design Use of Keyblock Behavior Models. 147
Excavation Depth and Keyblock Stability 149
Thermal Effects 153
Keyblock Geometry and Discontinuity Strength. . . .156
Excavation Sequence and Techniques. 157
Possible Stabilization Measures 159
Keyblock Displacement without Failure 159

REFERENCES. 161

APPENDIX 1. Two-dimensional keyblock stability analysis
program BSTB2D 170

APPENDIX 2. Three-dimensional keyblock stability analysis
program BSTB3D 185

LIST OF FIGURES

1.1 Two-dimensional schematic diagram of a keyblock in the roof of an underground excavation. 2

1.2 Sketch of large block encountered in Morrow Point powerhouse cavern (after Cording et al, 1971) 3

1.3 Typical blocks encountered in Washington, D.C. subway tunnels (after Cording and Mahar, 1974). 5

1.4 Fallen block sequence in model of Kielder Tunnel (after Ward, 1978). 6

1.5a Tunnel in continuous rock mass. 9

1.5b Tunnel in rock mass containing a single ubiquitous discontinuity set. 9

1.5c Tunnel in rock mass with several discrete discontinuities 10

1.5d Tunnel in rock mass with discontinuities intersecting to form keyblocks. 10

2.1 Planar discontinuity dipping at 30° below horizontal. . . . 15

2.2 Typical lower hemisphere stereographic construction for Ubiquitous Joint Method (after Cartney, 1977).. 16

2.3 Repeated stereographic constructions needed for the Inclined Hemisphere Projection Method (after Priest, 1980). 18

2.4 Types of blocks in a discontinuous rock mass (after Goodman and Shi, 1985) 21

2.5 Typical plot of discontinuities on a whole stereographic projection. 25

2.6 Identification of blocks from whole stereographic projection. 26

3.1 Typical geometry of pyramidal keyblock. 32

3.2 Representation of rock mass by system of springs of varying stiffness 34

3.3 Keyblock failure by free fall (all faces separate) and by sliding (one or two faces remain in contact) 35

3.4 Shear strength calculated using linear and nonlinear approaches. 39

3.5 Typical form of normal deformations resulting from axial loading of a rock sample containing a discontinuity. 41

3.6 Linear and nonlinear representations of discontinuity normal stiffness. 42

3.7 Constant stiffness and peak displacement (variable stiffness) representations of shear stiffness 49

3.8 Effect of unrecoverable closure on discontinuity normal stiffness. 51

3.9 Geometry used in Kirsch two-dimensional solution for stresses around a circular hole 55

3.10 Coordinate systems used in three-dimensional block analyses 59

3.11 Typical grid of points used to calculate initial stresses for each keyblock face. 60

3.12 F/W ratio as function of displacement (block reaction curve) for falling keyblock. 66

3.13 Block reaction curves for stable, marginal, and unstable falling keyblocks 68

4.1 Location map for the Nevada Test Site (after Langkopf and Eshom, 1982) 70

4.2 Layout of drifts at 420 meter level of Climax stock, NTS 71

4.3 Typical keyblock at springline (shoulder) of Piledriver drift. 74

4.4 Typical keyblocks in crown of Piledriver drift 75

4.5 Location of observations in G-Tunnel (map after Langkopf and Eshom, 1982). 76

4.6 Keyblock in rib of G-Tunnel. 77

4.7 Correction curves for Schmidt hammer orientation 82

4.8 Lower hemisphere concentrations of poles of fractures mapped in Spent Fuel Test-Climax drifts. 84

4.9a Keyblock analysis for north shoulder of Piledriver drift. 85

4.9b Keyblock analysis for rib of Piledriver drift. 86

4.9c Keyblock analysis for north shoulder of Spent Fuel Test canister drift. 87

4.9d Keyblock analysis for rib of Spent Fuel Test canister drift. 88

4.10 Lower hemisphere concentrations of poles of fractures mapped in G-Tunnel rock mechanics drift 89

4.11 Keyblock in north shoulder of Piledriver drift 95

4.12 Keyblock in crown of Piledriver drift. 97

4.13 Keyblock in south rib of Piledriver drift. 99

4.14a Geometry of physical model tested by Crawford and Bray (1983). 106

4.14b Geometry used with 2D code to back-analyze model 107

4.15 Back-analysis of pullout force measured in physical model by Crawford and Bray (1983). 109

5.1a Typical symmetric keyblock used for two-dimensional studies. 111

5.1b Typical symmetric keyblock used for three-dimensional studies. 112

5.2 Block reaction curves for 2D and 3D analyses 118

5.3 Block reaction curves of 3D keyblock for linear and nonlinear discontinuity models 119

5.4a Variation of normal stress along face with increasing block displacement 122

5.4b Variation of shear stress along face with increasing block displacement 123

5.4c Variation in stress at a point on block face near apex during displacement. 124

5.5a Variation of minimum F/W ratio with Joint Roughness Coefficient (JRC) 126

5.5b Variation of minimum F/W ratio with Joint Compressive Strength (JCS). 128

5.5c Variation of minimum F/W ratio with residual friction angle (ϕ_r). 129

5.6 Initial normal stiffness versus no-load aperture 131

5.7 Miminum F/W ratio versus initial normal stiffness. 132

5.8 Variation of E_{mass} with in situ stress 134

5.9 Minimum F/W ratio versus in situ vertical stress magnitude with 0.5 lateral stress ratio. 135

5.10 Minimum F/W ratio versus lateral stress ratio at constant in situ vertical stress. 137

5.11 Variation of minimum F/W ratio caused by temperature change in tunnel. 138

5.12 Minimum F/W ratio versus acuteness of apex 140

5.13 Minimum F/W ratio versus keyblock size 141

5.14 Minimum F/W ratio versus scale of keyblock and tunnel. . . 143

5.15 Tensile stress on possible truncated surface near apex of keyblock. 144

6.1 Lateral stress ratio required in situ for F/W ratio of zero. 152

6.2 Typical linear stress changes around circular tunnel caused by temperature changes within tunnel 154

A1.1 Geometry used in two-dimensional keyblock stability model. 171

LIST OF TABLES

3.1 Analytic models for keyblock stability. 30

3.2 Coordinate systems used in three-dimensional keyblock behavior analysis. 61

4.1 Summary of field observations of keyblocks. 78

4.2 Keyblock measurements. 80

4.3 Summary descriptions of measured keyblocks. 91

4.4 Summary of data used in back-analysis of keyblocks. 102

4.5 Results of back-analysis of keyblocks 103

5.1 Parameters examined for effect on keyblock stability. . . .113

6.1 Relative influence of parameters affecting stability of keyblock in crown of tunnel. 150

NOMENCLATURE

a, b	coefficients used in hyperbolic stiffness equation
a_o	average no-load aperture of discontinuity
D	displacement
E	Young's modulus
E_m, E_{mass}	rock mass deformation modulus
F/W	ratio of support force to keyblock weight
G	shear modulus
i	dilatancy angle of discontinuity
JCS	compressive strength of joint surface
JRC	coefficient of roughness of joint surface
k_n	normal stiffness
k_{ni}	initial normal stiffness
k_s	shear stiffness
L	length of block face in direction of sliding
P	pressure in tunnel
r, R	radius
S	spacing between discontinuities of a given set
S_H	horizontal stress
S_V	vertical stress
ΔT	change in temperature
ΔU	shear displacement
ΔV	normal displacement
V_m	maximum closure of discontinuity
W	weight of keyblock
X, Y, Z	Cartesian coordinate system

NOMENCLATURE (continued)

α	coefficient of linear thermal expansion
β	angle between block face and displacement vector
γ	weight per unit volume
ν	Poisson's ratio
σ	normal stress
σ_1, σ_2, σ_3	principal stresses
σ_r, σ_θ	radial and tangential normal stresses
τ	shear stress
τ_a	available shear strength
ϕ	friction angle of discontinuity
θ	tangential coordinate

ACKNOWLEDGMENTS

The author is grateful to many people for their support and encouragement during preparation of this work. Professor Richard Goodman was instrumental in calling attention to the fundamental problems of the behavior of discontinous rock. Professors Tor Brekke and Malcolm McPherson helped focus the work with their comments and questions. Derek Elsworth, a former fellow graduate student now teaching at the University of Toronto, was the first investigator to analyze generalized two-dimensional keyblock stability in a hydrostatic initial stress field. Graduate students William Boyle, John Tinucci, Lap Yan Chan, and Glenn Boyce all made many helpful comments and suggestions. Gen-hua Shi, a visiting scholar at the University of California, Berkeley, developed the mathematical basis of the keyblock identification procedures that complement this work, and wrote the computer programs that draw whole stereographic projections.

This effort was funded in the Lawrence Livermore National Laboratory (LLNL) Nuclear Waste Management Group as part of the U.S. Department of Energy's Nevada Nuclear Waste Storage Investigations Project. A special note of thanks goes to Virginia Oversby, who recognized the potential of the work when it was proposed and arranged for it to be funded. Dale Wilder, Wes Patrick, Harold Ganow, Lyn Ballou, and Larry Ramspott, all at LLNL, supported and encouraged this undertaking and provided the assignment and schedule flexibility

necessary for its completion. The figures in this dissertation were expertly drawn by Priscilla Proctor, and Barbara Bryan speedily deciphered my scribbled text and compiled it into a clean, typed manuscript.

Finally, I would like to acknowledge the patience, support, and love of my wife, Dorcas, and children, David and Rachel.

Sola Deo Gloria

CHAPTER 1 INTRODUCTION

Definition of the Block Stability Problem

Rock masses in which excavations are constructed almost always contain discontinuities such as joints, shears, and faults. Often, these discontinuities will intersect to create blocks of rock in the perimeter of an excavation. These blocks can have shapes so as to be able to displace into the excavation, unobstructed by adjacent rock. A simple form of such a block is shown in two dimensions in Figure 1.1. Blocks of more complex shape may be encountered, but are usually formed by combinations of geometrically simpler blocks (Goodman and Shi, 1985). The behavior and stability of these relatively simple blocks is therefore a problem of fundamental interest in the design and use of underground excavations.

Many block stability problems have been described in the rock mechanics literature in the past several years, and the stabilizing influence of confining stresses in situ has been recognized qualitatively as well (Brekke, 1968). The blocks themselves have been called wedges, keystones, or keyblocks by various investigators. Keyblocks are encountered on a range of scales, varying in size from small pieces of rock found ubiquitously along a tunnel rib to large monoliths that dominate an entire excavation surface. Cording et al (1971) described examples of the latter: a 2000 cubic yard (1529 m^3) block in an excavation at the Nevada Test Site, and a block measuring over 50 feet (15 m) from base to apex at Morrow Point power

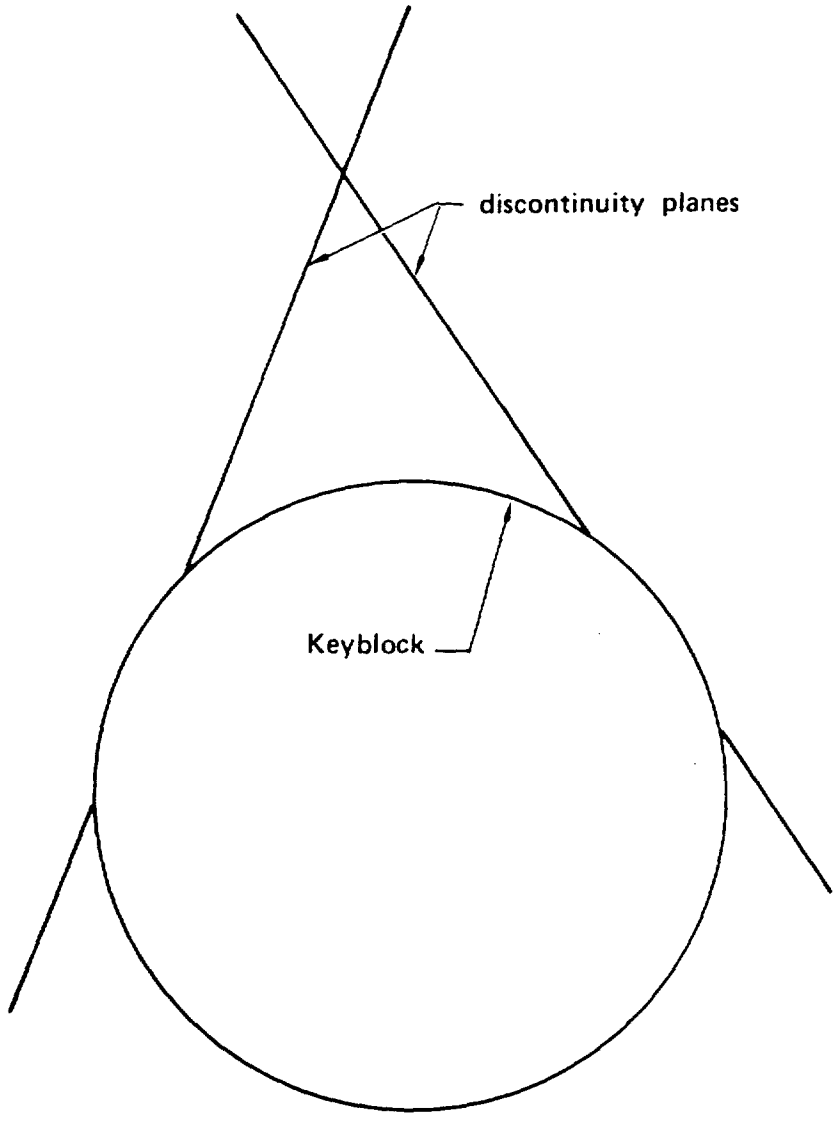

Figure 1.1 Two-dimensional schematic diagram of a keyblock in the roof of an underground excavation.

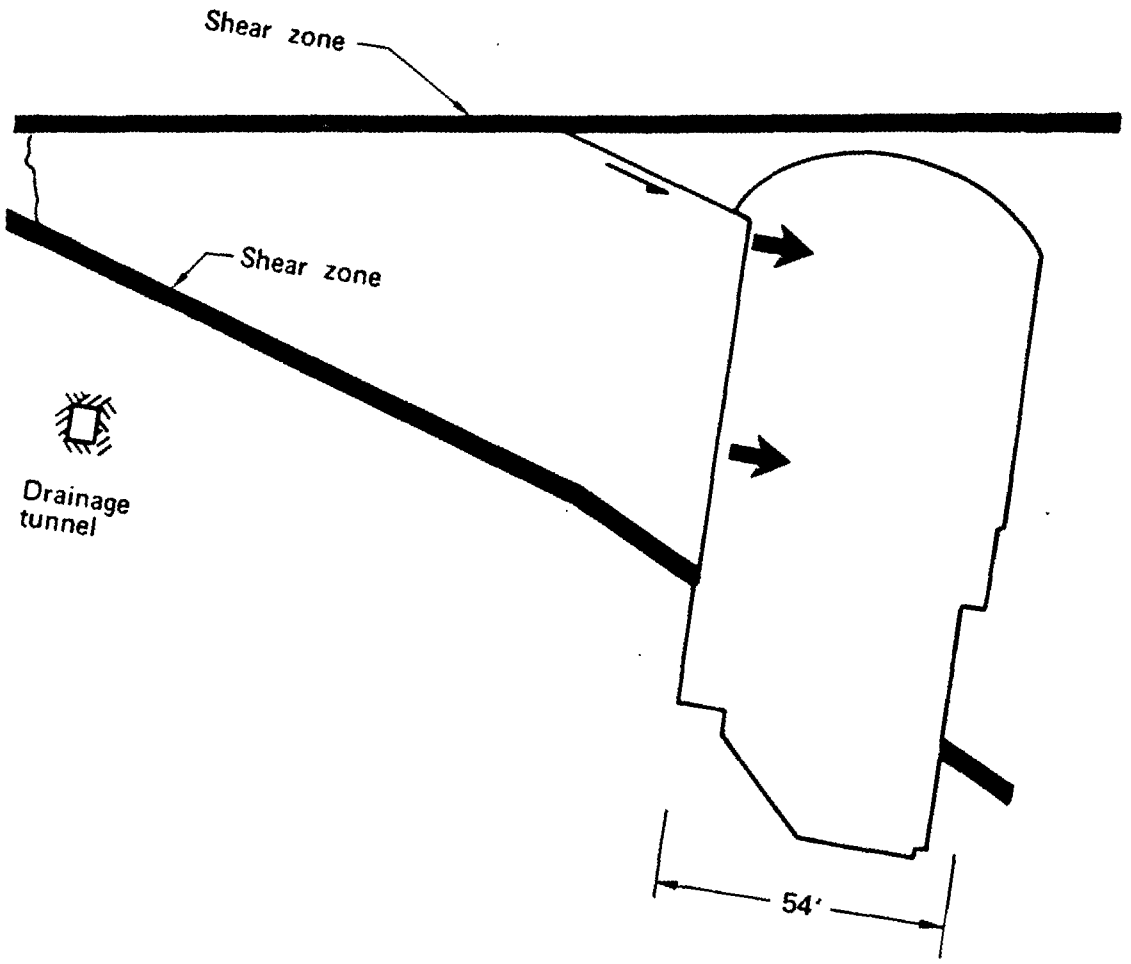

Figure 1.2 Sketch of large block encountered in Morrow Point powerhouse cavern (after Cording et al, 1971).

station (Figure 1.2). Cording and Mahar (1974) summarized the forms of blocks of lesser scale found in New York City and Washington, D.C. subway excavations (Figure 1.3).

The behavior of keyblocks can seriously affect the construction and use of an underground opening. While failure of a very large keyblock could entirely halt the use of an excavation, even small keyblock failures can be a safety hazard and can cause construction delays, rockfall cleanup expenses, and unexpected ground support costs. In extreme cases, keyblock displacement could lead to ravelling of the overlying ground; Ward (1978) described how a progressive failure can occur in regularly jointed rocks (Figure 1.4). Even if a fall did not occur, partial displacement of a keyblock adjacent to a tunnel would cause dilation and opening of the discontinuities bounding the keyblock. This would create a zone of increased permeability and decreased rock mass stiffness next to the excavation. In addition to other areas of mining and civil works, the problem is of interest in nuclear waste disposal, where excavation performance over several decades is critical for waste repository operation. In particular, waste package retrieval from emplacement holes (which may not be lined) must be possible for a specified length of time.

Analysis of the stability and behavior of a keyblock adjacent to an underground opening is a two-step problem. The first step is identification of the keyblock, while the second is a quantitative analysis of its response to the stresses and loads acting upon it.

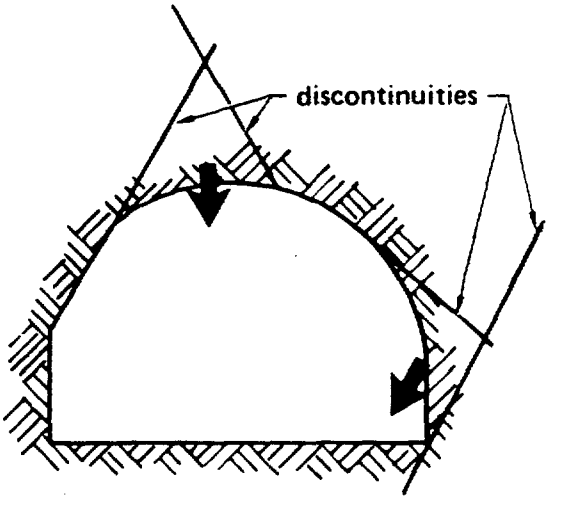

Figure 1.3 Typical blocks encountered in Washington,D.C. subway tunnels (after Cording and Mahar,1974).

Figure 1.4 Fallen block sequence in model of Kielder Tunnel (after Ward, 1978).

The first step is based upon an understanding of the discontinuities in the geologic setting and the orientation and size of the planned excavation. The second step requires measured or assumed values for discontinuity parameters and for the stress and load conditions around the excavation. Both steps need to be carried forward as far as possible prior to construction of the opening so as to allow the analysis to be of benefit in excavation design. Preliminary analysis of keyblocks can help evaluate how well discontinuity orientations and other parameters must be known for design purposes.

Conventional design approaches for excavation stability analysis usually include assumptions regarding the rock mass and its properties. Figure 1.5 illustrates common ways of treating the rock mass in calculations of excavation stability or deformation. Figure 1.5a shows a tunnel sited in a continuous rock mass, i.e., rock containing no discontinuities. This allows continuum methods of elasticity to be used in either closed form expressions or finite element approaches to estimate stresses and deformations around the excavation. Since rock is usually discontinuous, this approach is a simplification that often underestimates excavation deformations and does not allow all possible failure modes to be addressed.

Figure 1.5b shows a tunnel in rock containing a single ubiquitous set of discontinuities; this concept can be used with closed form solutions (Daemen, 1983) or with finite element schemes to locate and determine the size of zones around the excavation in which slip is expected to occur as construction or post-construction loading

proceeds. Scoping calculations can be readily made with this type of model; the results are useful to get an overall impression of the limits of opening behavior.

Figure 1.5c illustrates a tunnel in a rock mass containing several discrete discontinuities. Like the ubiquitous discontinuities, this can be examined with a finite element method of analysis to obtain excavation behavior estimates for specific situations (e.g., Heuze et al, 1983). However, a considerable amount of information on the discontinuity and excavation geometries is needed, and each situation to be analyzed requires setting up a new finite element mesh for the numerical code that is used for the solution.

Figure 1.5d shows a tunnel in rock containing discontinuities that intersect to form keyblocks. This work is an approach for solving this class of problems which is intended to complement rather than replace the three preceding methods of analysis. Each of the three preceding methods can be readily used for a two-dimensional analysis or, with some difficulty, a three-dimensional analysis. However, the keyblock approach allows keyblocks in three dimensions to be identified using procedures developed by Goodman and Shi (1981), and allows the stability and displacement behavior of keyblocks to be estimated using methods developed here. The calculations involved are simple enough to allow use of the method for general scoping calculations as well as for analysis of specific problems.

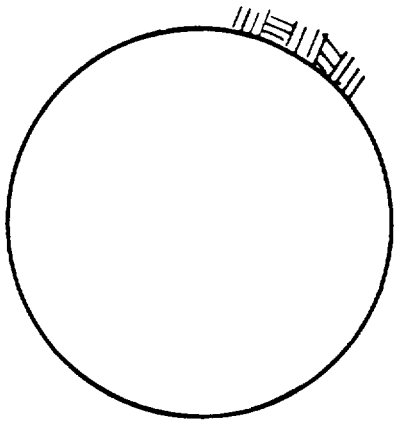

Figure 1.5a Tunnel in continuous rock mass.

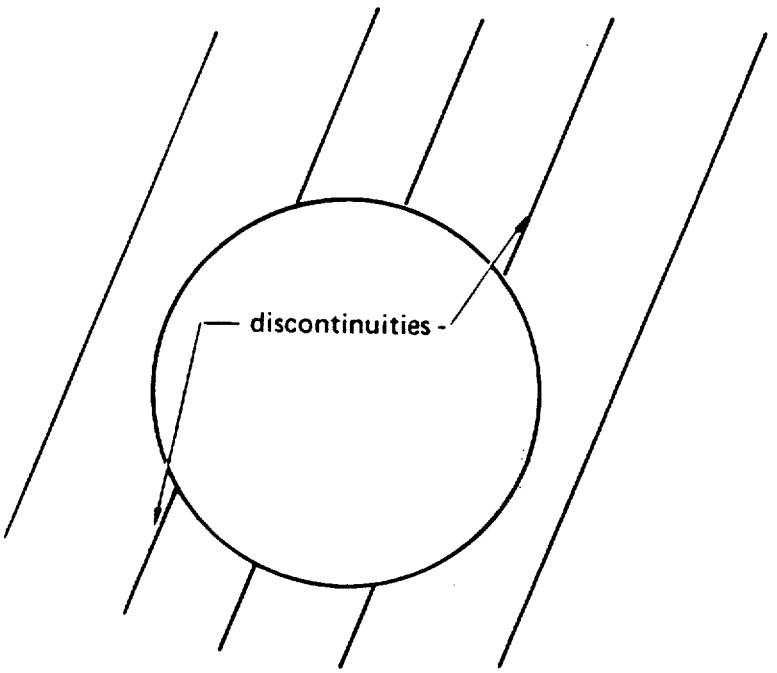

Figure 1.5b Tunnel in rock mass containing a single ubiquitous discontinuity set.

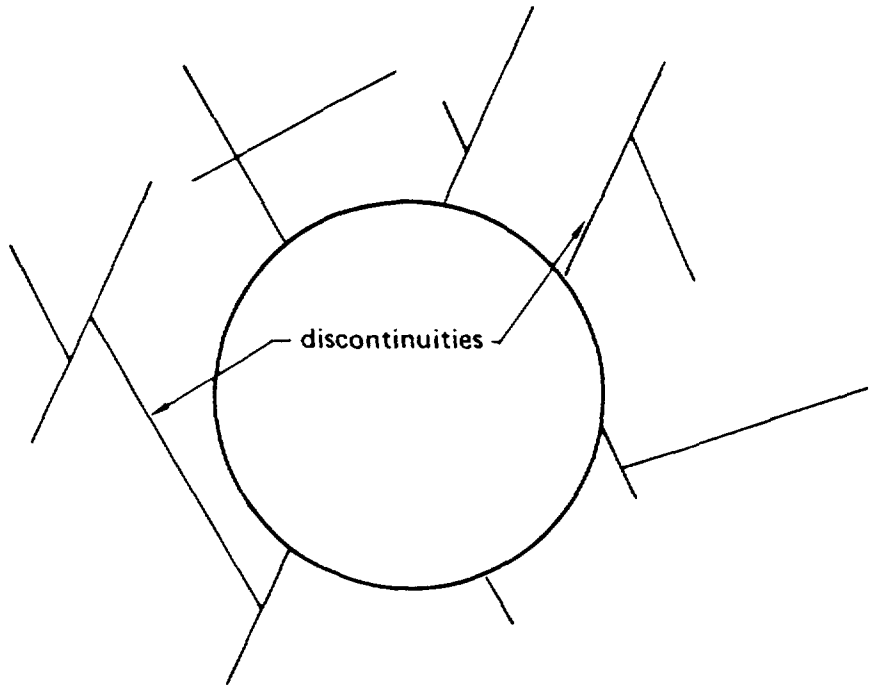

Figure 1.5c Tunnel in rock mass with several discrete discontinuities.

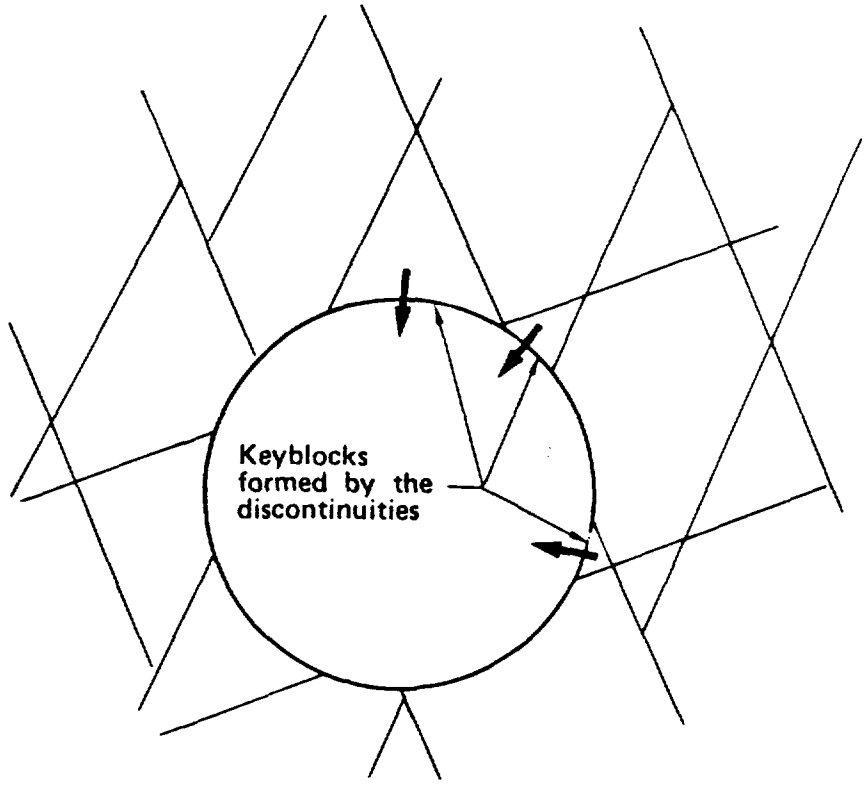

Figure 1.5d Tunnel in rock mass with discontinuities intersecting to form keyblocks.

Scope of Work

The scope of this research can be summarized in four parts: development of methods with which to analyze keyblock behavior, field observations of keyblocks, back-analysis of the stability of observed and modeled keyblocks, and interpretation and extrapolation of the analytic results.

Development of methods to analyze keyblock behavior requires that the keyblocks be identified from geologic data. Methods with which keyblocks can be identified for analysis are reviewed and compared briefly in Chapter 2. The most versatile of the available methods, the Keyblock Method by Goodman and Shi (1981) is then described in somewhat greater detail. Complete details about the Keyblock Method and its basis have been published by Goodman and Shi (1985). The second step, analysis of keyblock behavior, requires that techniques be devised to evaluate and relate keyblock behavior to factors that include block and excavation geometry, pre-existing and excavation-induced stresses, thermal stresses, and discontinuity strengths and stiffnesses. This is the thrust of the first part of the work. Fluid pressures within the discontinuities and dynamic loads, however, were beyond the scope of this stage of the work. These new techniques for analyzing keyblock behavior are developed in Chapter 3.

The second part of the work involved field observations of keyblocks. Fallen and stable keyblocks were observed in tunnels in

granite and in tuff at the Nevada Test Site. These observations allowed the keyblock analysis techniques to be checked in the third part of the work, where the stability of each keyblock measured in the field was back-analyzed using the methods of Chapter 3. Model studies published by Crawford and Bray (1983) were also back-analyzed. Comparison of the observations and calculations in Chapter 4 gives important insights about keyblock behavior and the sensitivities of the models used to describe it.

The fourth part of the work involves interpretation of the analyses and extrapolation for other field conditions. Limitations of the new methods of stability analysis and the effects of keyblock displacement, discontinuity strength, discontinuity stiffness, in situ stress magnitude, lateral stress ratio, thermal stresses, and keyblock geometry are each described in Chapter 5. Chapter 6 then elaborates on the engineering implications of the results. Two-dimensional and three-dimensional models for keyblock behavior were coded in BASIC; computer code listings are provided in the Appendices.

CHAPTER 2 IDENTIFICATION OF KEYBLOCKS

Approaches for Identifying Critical Blocks

Solution of the problem of potentially unstable rock blocks (keyblocks) in the perimeter of an underground opening can be divided into two steps: identification of the keyblocks, and analysis of their stability. Methods for identification and analysis of the failure modes, surface areas, and volumes of blocks defined by discontinuities have been presented by Goodman (1976). Subsequently, procedures have been published with which sets of rock mass discontinuities of known orientation can be examined to identify combinations forming keyblocks in underground openings. In order of publication these methods are the Ubiquitous Joint Method (Cartney, 1977), the Inclined Hemisphere Projection Method (Priest, 1980), the Keyblock Method (Goodman and Shi, 1981), and a method that uses the Keyblock Method in conjunction with principles from graph theory (Chan and Goodman, 1983). Other methods have been developed for defining kinematic modes of block failure (e.g., Lucas, 1980, and Warburton, 1981), but these other approaches do not address the necessary first step of block identification.

The three-dimensional procedures listed above all use either graphical techniques or vector analysis to examine the ways in which discontinuity planes may intersect to form keyblocks in excavation surfaces. The methods also include an assessment of possible translational keyblock failure modes (falling or sliding); rotational

failures such as toppling are not considered. Some of the procedures require more geologic data than others, and the procedures are not equally versatile in handling a range of excavation surface orientations. Since keyblock behavior should be considered as part of the excavation design for underground openings in jointed rock, it is advantageous to be able to commence the analysis with a minimum amount of geologic data. The analysis can then be refined as more information becomes available, and can even help guide the site exploration and data acquisition program.

The first approach published specifically for underground excavations with which all joint sets could be examined simultaneously for block-forming set combinations was the Ubiquitous Joint Method by Cartney (1977). The method, which was used in cavern design for the Dinorwic Power Station (Douglas et al, 1979), involves plotting great circle representations of each discontinuity set on a lower hemisphere stereographic projection. The excavation surface under examination and the discontinuity planes are thus passed through a common point at the center of the sphere, allowing identification of pyramidal wedges (keyblocks) that are kinematically capable of failure. An example plot of a single discontinuity is shown in Figure 2.1b, and a typical stereographic construction from Cartney's 1977 paper is shown in Figure 2.2. "Ubiquitious" refers conceptually to the possibility of encountering joints of a given orientation anywhere in the excavation. This "ubiquitous joint" concept was named by Goodman (1967).

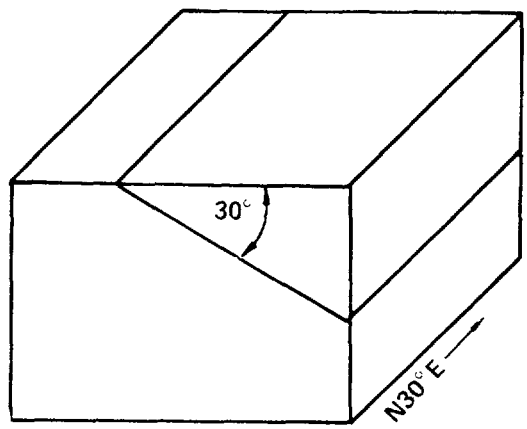

(a) Block diagram showing discontinuity in rock mass.

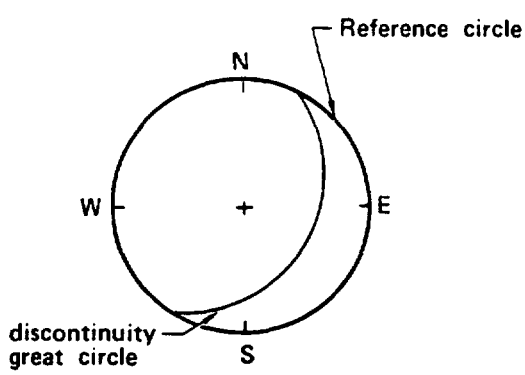

(b) Lower hemisphere stereographic plot of discontinuity in (a).

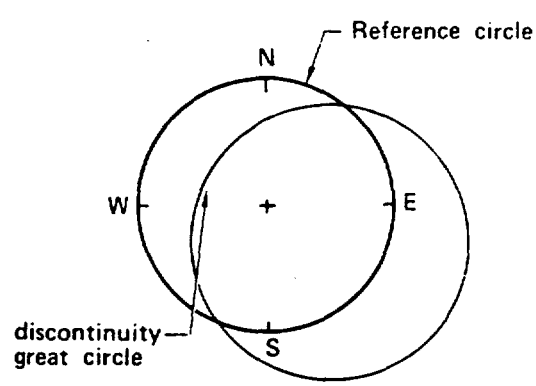

(c) Plot of discontinuity (a) on upper hemisphere whole stereographic projection.

Figure 2.1 Planar discontinuity dipping at 30° below horizontal.

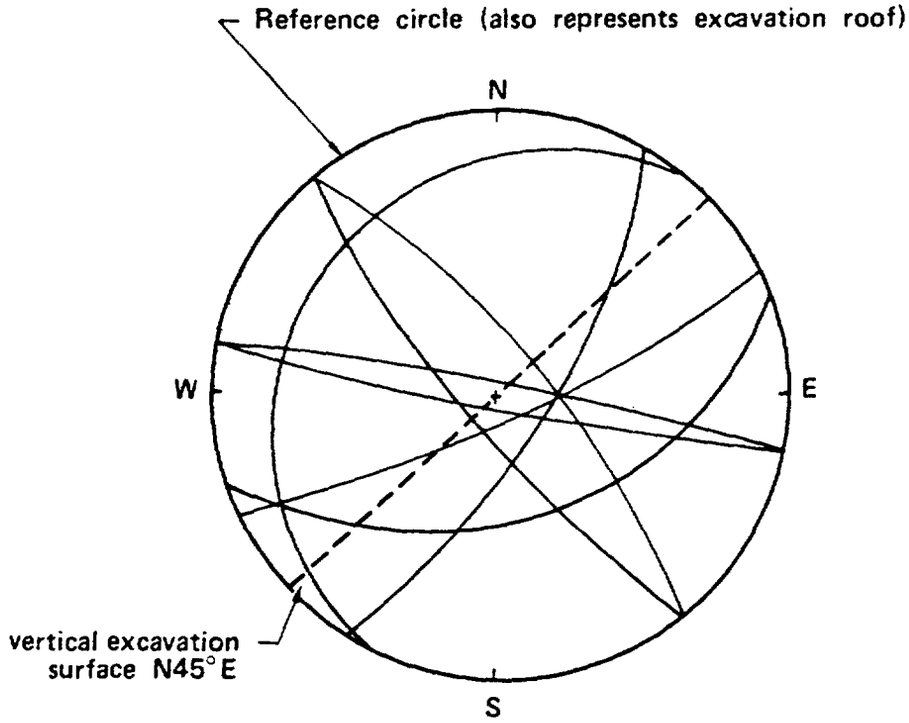

Figure 2.2 Typical lower hemisphere stereographic construction for Ubiquitous Joint Method (after Cartney,1977)

In the Ubiquitous Joint Method, excavation surfaces are all assumed to be either vertical or horizontal. Walls are thus drawn on the stereonet plots as straight lines passing through the center of the plot, while the rim of the stereonet represents a horizontal excavation roof (Figure 2.2). The method is effective for identifying the forms of simple rock wedges that could fall or slide from the walls or roof of an underground opening. These wedges can then be sized from the excavation dimensions or by engineering judgment for subsequent analysis. However, inclined excavation surfaces such as may occur between the roof and springline of a tunnel were not treated by Cartney.

The next development in generalized approaches for identifying keyblocks in tunnels was published by Priest (1980). The Inclined Hemisphere Projection Method can identify pyramidal blocks and their translational modes of failure from given discontinuity and excavation surface orientations. The method uses stereographic projection techniques similar to those of the Ubiquitous Joint Method. However, Priest's approach overcomes Cartney's constraints on excavation surface orientations by rotating the stereographic projection plane to coincide with the excavation surface. Although effective, this requires construction of a new rotated projection for each excavation surface being examined (Figure 2.3).

The most generalized approach available for identifying blocks is the Keyblock Method of Goodman and Shi (1981), which is based on Block Theory (Goodman and Shi, 1985). The method uses stereographic

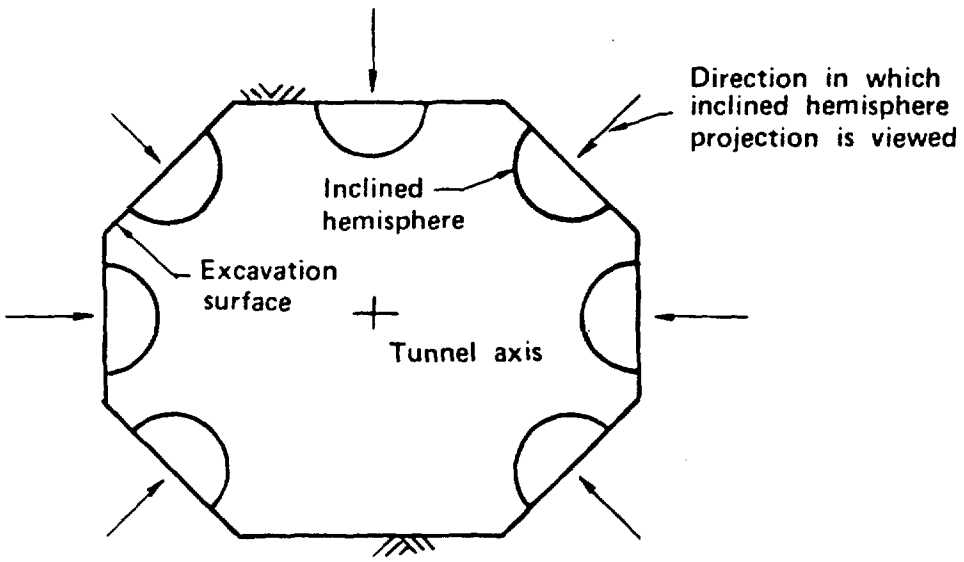

Figure 2.3 Repeated stereographic constructions needed for the Inclined Hemisphere Projection Method (after Priest, 1980).

construction techniques, and has also been implemented with vector analysis principles for expedient solutions using a computer. The excavation surface limitations of Cartney's method and the repeated graphical constructions of Priest's method are avoided by using what is known as a whole stereographic projection. In the example plot of Figure 2.1c, the region within the reference circle represents a conventional upper hemisphere stereonet plot, while the area outside the reference circle is the remainder of the sphere. By including both upper and lower hemispheres on one construction, the intersection of planar discontinuity sets and excavation surfaces of any orientation can be examined for potential keyblocks and their failure modes. Because of its versatility, the method was used to analyze the field observations presented in Chapter 4 for modes of failure. Some of the procedures of the method are summarized in the next part of this chapter.

Chan and Goodman (1983) developed an application of the Keyblock Method that incorporates variations in discontinuity spacings and sizes. This new approach, like the methods described above, requires that discontinuity set orientations be defined. In addition, though, distributions of discontinuity spacings and extents are needed. These statistical parameters are used to construct hypothetical discontinuity trace maps that represent the intersections of fractures with an excavation surface. The constructions are scanned using principles from graph theory for trace patterns indicative of keyblocks or of combinations of keyblocks. Once the keyblocks are located, they can be individually analyzed for stability. Acquisition

of the statistical data needed for the method may, however, impede its early use during site exploration and excavation design. The method was not used in this work because all of the keyblocks encountered in the field observations were of simple pyramidal shapes, and because the necessary statistical data were not available.

Block Theory and Keyblock Identification

The Keyblock Method allows an investigator to examine the intersections of discontinuity sets and excavation surfaces for plane combinations creating blocks that are kinematically able to fail. The method has been applied to surface excavations (Goodman and Shi, 1981) and to underground excavations (Shi and Goodman, 1981). Graphical methods for block identification are outlined below; ways to assess kinematic modes of failure, computer implementations of the methods, and other applications of Block Theory are covered in a book by Goodman and Shi (1985).

Figure 2.4 indicates the types of blocks that might be expected to occur in a discontinuous rock mass. Of these block types, the removable blocks are of primary interest in excavation design. As explained by Goodman and Shi (1985), the other types of blocks are stable as long as the removable blocks do not fail. Of the three categories of removable blocks, the methods for stability analysis developed in Chapter 3 are particularly relevant for keyblocks and potential keyblocks.

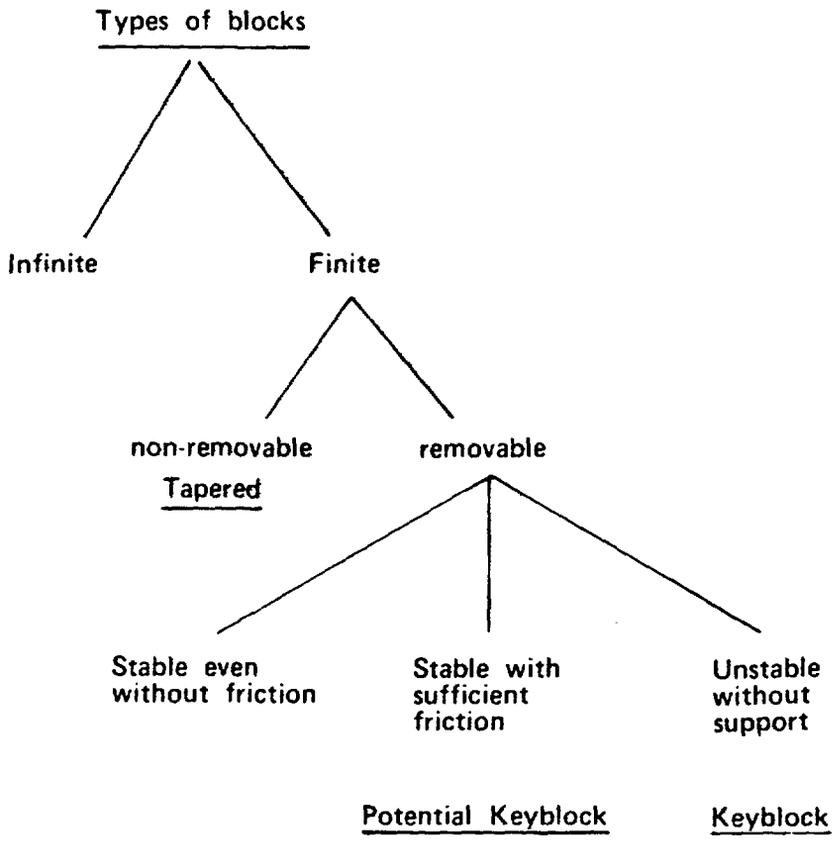

Figure 2.4 Types of blocks in a discontinuous rock mass (after Goodman and Shi, 1985).

Keyblock identification requires that certain assumptions be made about the discontinuities that form removable blocks; they are taken to be planar, extensive, and of known orientation. These assumptions are also required by the methods of Cartney and of Priest which were described previously. Planar discontinuity surfaces are reasonable to assume unless a discontinuity surface has a significant curvature at the problem scale of interest. Even then, an average representation of the surface can be used until specific blocks are singled out for stability analysis. Discontinuities are considered to extend far enough to intersect one another so as to form removable blocks. If this is not true in a given instance, then rock bridges exist between discontinuities that would to some degree stabilize potential keyblocks. This is a separate problem that is not treated here. Discontinuity orientations must be known for possible blocks to be defined by the stereographic constructions or the numerical procedures of the Keyblock Method. If adequate orientation data is available, an identification analysis can be repeated for widely dispersed (fringe) members of the discontinuity sets, or for unique geologic features that do not belong to a set.

Given the assumptions described above, the Keyblock Method enables an investigator to identify removable blocks from a whole stereographic projection. The data needed for such an analysis consist of the orientations of discontinuities present at the excavation site and orientations of the excavation surfaces to be examined. These planes are plotted on the whole stereographic projection; Figure 2.1 compares the way in which a discontinuity plane

is represented on a conventional lower hemisphere stereonet with its appearance on an upper hemisphere whole projection. Note that the great circle of the discontinuity plane that appears within the reference circle is reversed between the two projections. This is because the conventional plot is a lower hemisphere projection while the whole stereographic projection of Figure 2.1 uses an upper hemisphere. In other words, the projections have opposite focal points, which makes one a mirror image of the other. The other difference between the projections is that the whole projection includes the entire great circle of each plane whereas the conventional projection shows only the portion of the great circle that falls within the reference circle. A single graphical construction can be made for the discontinuities of interest and then examined for any number of excavation surfaces without having to rotate or redraw the discontinuities.

When discontinuity planes are plotted on a stereographic projection, they are shifted through space so as to pass through the center of the three-dimensional sphere that is represented in two dimensions by the projection. Conceptually, the planes divide the sphere into pyramids of rock, where each pyramid apex is at the center of the sphere, and each pyramid base is part of the surface of the sphere. These pyramids are called "joint pyramids" by Goodman and Shi (1985). An excavation surface passing through the center of the sphere divides the sphere into two regions (or half-spaces) that correspond to the excavation opening and to the adjacent rock. Joint pyramids that have their base in the rock mass side of the excavation

surface are tapered such that they get larger with distance into the rock mass, away from their apex. These pyramids represent blocks that cannot move into the excavation. Conversely, joint pyramids that have their base in the free space provided by the excavation must be tapered such that they get smaller with distance into the rock, away from their base. These correspond to blocks that can move into the excavation and are therefore kinematically capable of failure.

It is difficult to represent the three-dimensional situation described above on a two-dimensional diagram. The whole stereographic projection enables the user to make such a representation in a way that allows the removable blocks to be identified. Figure 2.5 shows three example discontinuities that will be intersected by tunnel excavation surfaces. The regions of the projection that are defined by the plotted discontinuities are actually the bases of the pyramids described in the preceding paragraph, projected onto the stereographic plane. Once these regions are established, excavation surfaces of any orientation can be added to the projection to be examined for potentially unstable blocks created by these discontinuities.

Identification of removable blocks is accomplished by looking for regions that are located entirely within the opening indicated by the plotted excavation surface (Figure 2.6). Once the removable blocks associated with an excavation surface have been identified, each discontinuity making up the block can be checked to see if the block is on the upper or lower side of the discontinuity. Procedures published by Goodman (1976) and by Goodman and Shi (1985) can then be

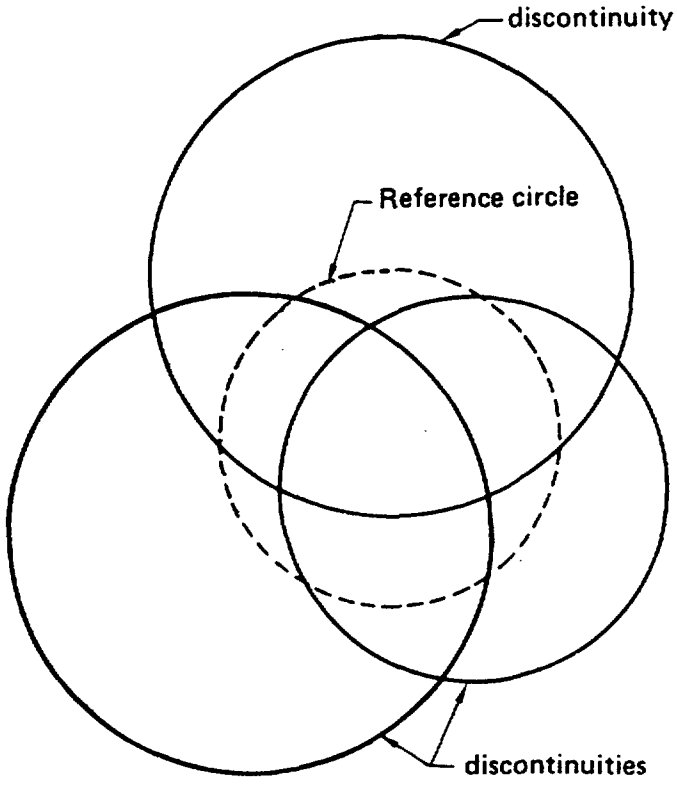

Figure 2.5 Typical plot of discontinuities on a whole stereographic projection.

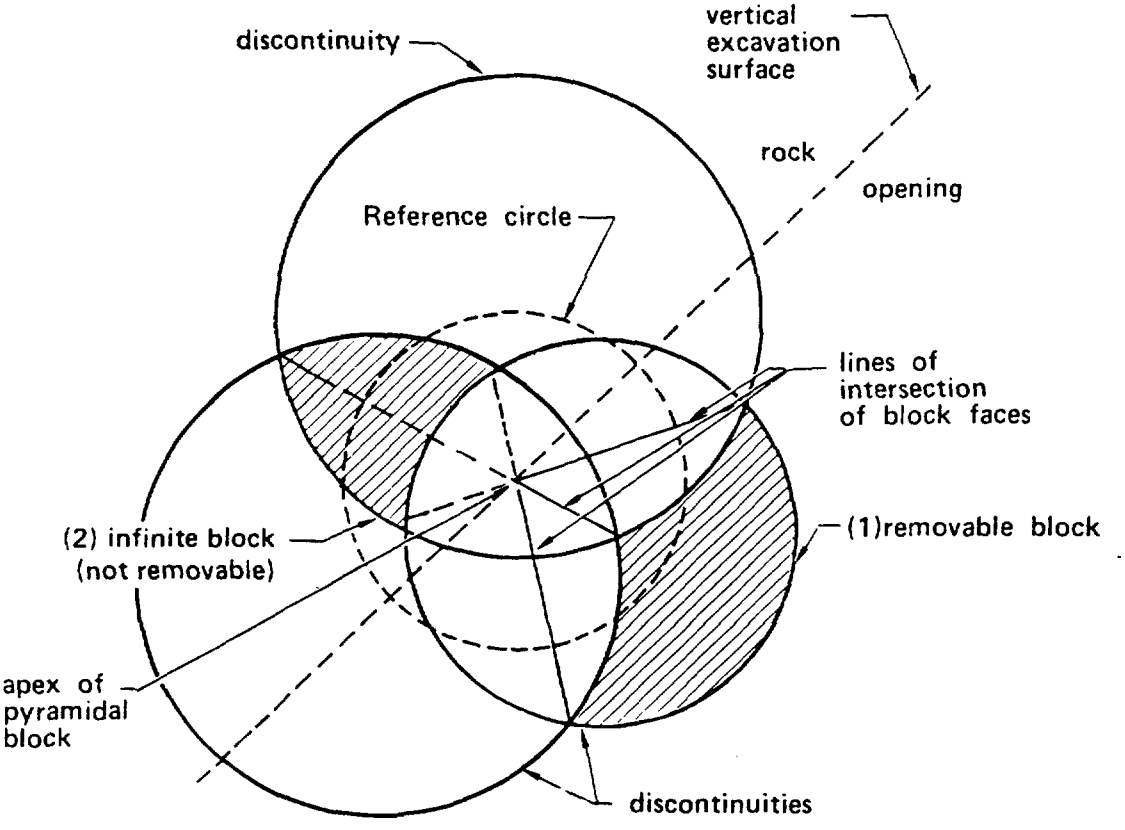

Figure 2.6 Identification of blocks from whole stereographic projection. Hatched area one indicates a block that is removable into the excavation (a potential keyblock). Area two indicates a block that is infinite and is not removable.

used to discern potential failure modes, and to calculate the maximum size that the block could have while still being able to fail into the excavation.

CHAPTER 3 KEYBLOCK STABILITY ANALYSIS METHODS

Once a removable block (keyblock or potential keyblock) has been identified, its stability must be evaluated so that the excavation design can include any ground support measures that are needed to maintain the integrity of the opening. In addition to solving specific problems, methods for assessing the stability of a keyblock can be used profitably in a parametric sense to examine a range of conditions which may affect block behavior. An analytical model with which keyblock stability and displacement behavior may be evaluated is developed in this chapter, and can be applied to two-dimensional and three-dimensional cases. Computer models for these two cases are given in the Appendices. The models are used in subsequent chapters to back-analyze field observations and physical model investigations of keyblock failures.

Approaches for Evaluating Keyblock Stability

Keyblock displacement and stability pose a fully three-dimensional problem, just as block identification poses a three-dimensional problem. In general, block behavior is influenced by the shear strength of the discontinuities forming the keyblock, the initial stresses acting on the block faces, the changes in stresses that occur as the block displaces, and the block geometry. Stress changes are a function of discontinuity dilatancy, normal and shear stiffness, and block displacement. Keyblock geometry includes block height and width, block location around the excavation perimeter, displacement

direction, and block size with respect to the size of the opening. Inspection of Table 3.1, which lists previous analytical approaches, reveals that not all of these factors that influence keyblock stability have been addressed by earlier models.

Different approaches have been taken by the models listed in Table 3.1 in the ways in which they evaluate keyblock behavior. Beyond whether a model treats keyblocks in two dimensions or in three dimensions, there is a significant difference in whether or not a model provides for adjustments in stresses as the block moves towards failure. Models that do not include stress changes typically do not include discontinuity stiffnesses or dilatancy, or keyblock displacement. Since some displacement is usually required in order to mobilize shear stresses along a dilatant discontinuity to help resist block failure, these models do not evaluate keyblock behavior under realistic shear stress conditions. Such models are conservative in their approach to ground support needs. Analytic models that do account for stiffness use different methods of solution; some calculate keyblock displacement corresponding to a specified set of stress conditions, while others calculate the stresses and resultant forces caused by a specified displacement. In either case, the problem is examined parametrically to see if equilibrium will be reached under in situ conditions.

Table 3.1 Analytic Models for Keyblock Stability

Investigator	Block Geometry	Initial Stresses[1]	Discontinuity Dilatancy	Discontinuity Stiffness
Benson et al, 1971	2D	not used	no	no
Cording et al, 1971	2D	assumed[2]	no	no
Goodman, 1976	3D	not used	no	no
Hoek, 1977	3D	not used	no	no
Croney et al, 1978	3D	assumed[2]	no	no
Bray, 1979[3]	2D	tangent to opening	no	linear
Coric, 1979	3D	assumed[2]	no	no
Hoek & Brown, 1980	3D	not used	no	no
Warburton, 1981	3D	not used	no	no
Crawford, 1982	2D	tangent to opening	no	linear
Goodman et al, 1982	3D	tangent to opening	yes	linear
Zhu & Zhizhong, 1982	2D	assumed[2]	no	no
Crawford & Bray, 1983	2D	tangent to opening	no	linear
Elsworth, 1983[4]	2D	2D hydrostatic	yes	linear
Zhifa, 1983	3D	assumed[2]	no	no
Belytschko et al, 1983	2D	assumed[2]	no	no
Boyle, work in progress	3D	tangent to opening	yes	linear
Yow, this work	3D	3D	yes	linear or non-linear

NOTES: (1) Initial stresses are those affecting block before displacement. All models include friction and block weight.

(2) Initial stresses on block faces assumed from separate stress analysis.

(3) Unpublished notes by John Bray.

(4) Elsworth, D., 1983, "Wedge Stability in the Roof of a Circular Cross Section Underground Opening - Plane Strain Condition," 20 pp. Unpublished report, Department of Civil Engineering (Geological Engineering), University of California, Berkeley.

Stability Analysis Assumptions

Figure 1.1d illustrated in two dimensions some of the assumptions that are needed for the methods of analysis developed in this chapter. A tunnel or excavation, circular in section, is sited in a rigid rock mass that contains planar discontinuities. The discontinuities themselves are unhealed and are extensive enough that they intersect to form simple, pyramidal keyblocks. Figure 3.1 shows a typical pyramidal block in three dimensions. The circular tunnel section is appropriate for tunnels excavated by boring machines, and is in some cases a reasonable approximation for tunnels of other shapes.

The circular tunnel section allows the use of the Kirsch solution (Goodman, 1980) for calculating initial stresses in two-dimensional analyses. A solution by Amadei (1982) can be used for initial stresses in three-dimensional analyses. The solutions are based on elastic theory; these procedures can be used in numerical models for an expedient estimate of initial stresses around the excavation prior to any displacements along discontinuities. Other investigators have used finite element codes to calculate initial stress values (e.g., Croney et al., 1978), but this makes the analysis more cumbersome to use in evaluating a range of in situ conditions.

Finally, in order to be able to define discontinuity deformation behavior, the rock mass is assumed to deform as a system of springs of varying stiffnesses. The rock that forms the keyblock and its

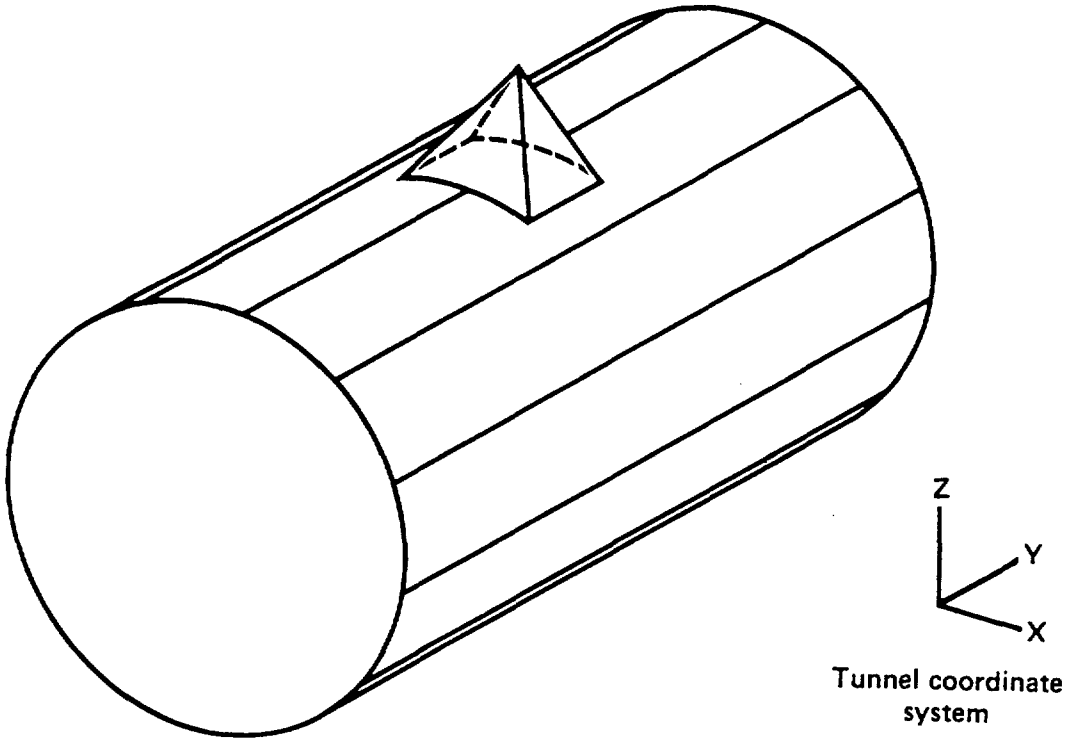

Figure 3.1 Typical geometry of pyramidal keyblock.

surroundings is taken to be very stiff in comparison to the discontinuities. All displacement is thus assumed to occur along discontinuities. A spring system is illustrated in Figure 3.2 for deformation of a jointed rock in one dimension. Such a conceptual approach is described by Goodman (1976 and 1980); its application in keyblock behavior models will be developed below in the discussion of discontinuity characteristics.

Keyblock Instability and Displacement

As sketched in Figure 3.3, keyblocks can fail in a translational mode either by falling or by sliding. Rotational block failure such as toppling is beyond the scope of this work. If a keyblock falls, separation occurs on all of the keyblock faces simultaneously. Alternatively, sliding can occur on either one or two block faces, and allows these faces to remain in contact during failure.

There are practical limits on the displacement that can be expected of a keyblock before either a condition of stability is reached under prevailing conditions, or the keyblock completely fails. These limits can be used as a practical check on the performance of the keyblock behavior model to detect unrealistic results caused by errors in the data or the computations. The lower limits of keyblock displacement correspond to the elastic deformation calculated for a similar excavation in continuous rock. Two-dimensional plane strain equations for computing radial deformation of a circular tunnel in an elastic rock without

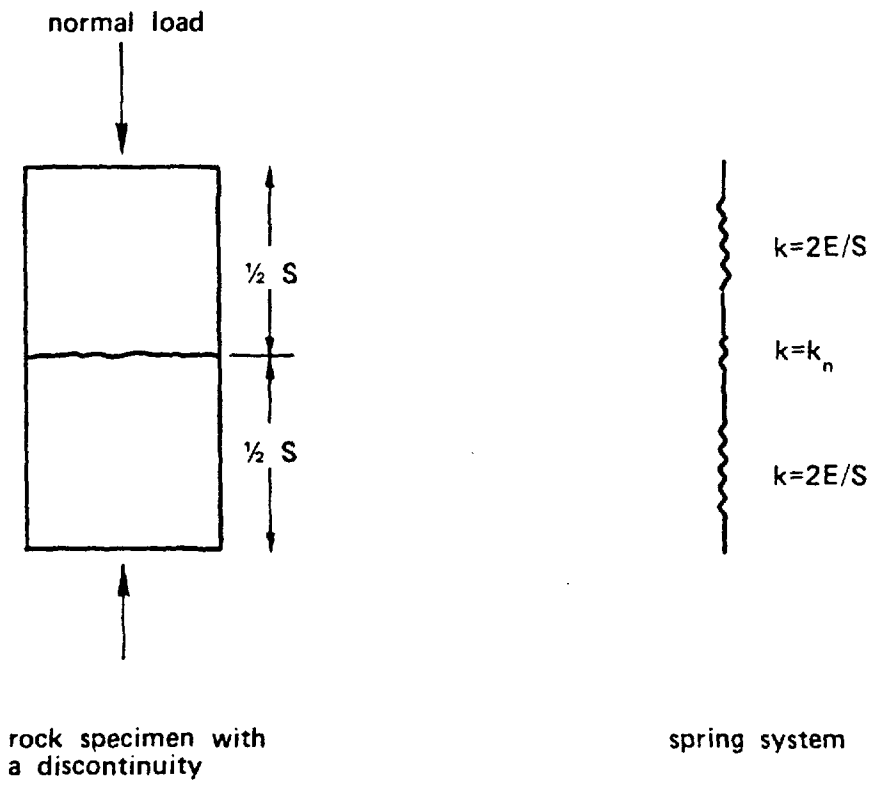

Figure 3.2 Representation of rock mass by system of springs of varying stiffness. The discontinuities in the rock mass are assumed to have spacing S and normal stiffness k_n. The intact rock has an elastic modulus E.

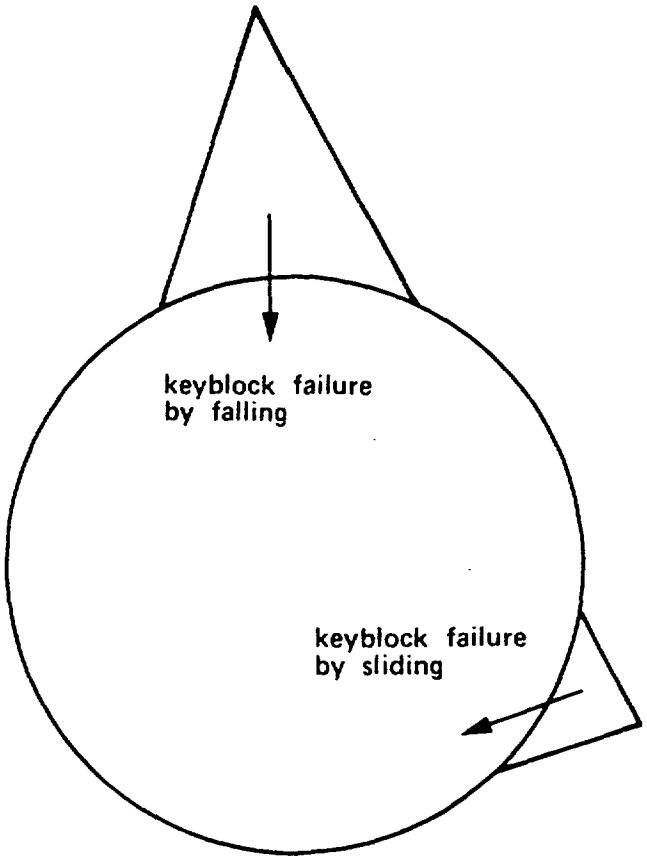

Figure 3.3 Keyblock failure by free fall (all faces separate) and by sliding (one or two faces remain in contact).

discontinuities can be found in texts by Goodman (1980) and by Obert and Duval (1967). The equation given by Goodman is:

$$u_r = \frac{S_H + S_V}{4G} R + \frac{S_H - S_V}{4G} R \, [4(1 - \nu) - 1] \cos 2\theta \qquad (3.1)$$

where: u_r = radial displacement of the tunnel wall

S_H = horizontal stress, unperturbed by the tunnel

S_V = vertical stress, unperturbed by the tunnel

G = shear modulus

ν = Poisson's ratio

R = radius of the tunnel

θ = tangential coordinate

Conversely, upper limits on keyblock displacement magnitude can be approximated from estimates of the displacement necessary to mobilize the peak shear strengths of the discontinuities that bound the block. This presumes that the keyblock fails once all available peak shear strength has been surpassed. Barton and Choubey (1977) have suggested that peak strength is reached after a shear displacement of about one percent of the discontinuity length as measured in the direction of sliding. Since discontinuity length will depend on keyblock and excavation geometry, an average length based on the height from the excavation to the block apex should suffice for estimating displacement magnitudes.

Discontinuity Shear Strength

Two discontinuity characteristics, strength and stiffness, must be considered in order to properly calculate the stability of a keyblock. The discontinuity shear strengths limit the shear stresses which can act on block surfaces in contact with adjacent rock, and ultimately govern whether or not the keyblock can be stable as situated. The normal and shear stiffnesses in turn control the changes in discontinuity stresses that are induced by keyblock displacement.

The shear strength of an unhealed discontinuity can be represented as a combination of a friction angle (ϕ^o) for a smooth rock surface and a dilatancy angle (i^o) for the discontinuity surface roughness. If the shear strength is assumed to vary linearly with the normal stress, it can be calculated as:

$$\tau_a = \sigma_n \tan (i + \phi) \tag{3.2}$$

In this expression τ_a is the available shear strength and σ_n is the normal stress on the discontinuity. Dilatancy also affects changes in normal stress during displacement, as will be explained below.

Barton and Choubey (1977) have given an expression that represents a nonlinear variation of discontinuity shear strength as a function of normal stress, surface strength, and surface roughness:

$$\tau_a = \sigma_n \tan(JRC \log_{10} (\frac{JCS}{\sigma_n}) + \phi_r) \tag{3.3}$$

JRC is the joint roughness coefficient, which is a measure of surface roughness. JCS is the joint compressive strength, which is a measure of the strength of the asperities that make the discontinuity surface rough. ϕ_r is a residual friction angle that Barton and Choubey relate empirically to ϕ. Note that the nonlinear equation can be divided into a dilatancy component and a friction component. The dilatancy component becomes smaller as the normal stress increases, reflecting failures of asperities during shear.

Figure 3.4 plots shear strength as a function of normal stress for both the linear and nonlinear strength equations for typical rock discontinuity properties. Both approaches are available in the keyblock stability models. A choice can be made between the approaches based on the data available for analysis, or based on the magnitude of the expected changes in normal stresses. Normal stresses along the discontinuity planes that form the keyblock will vary from their initial values to zero as discontinuity separation occurs during block failure. The nonlinear strength option can then be selected if indicated by a large magnitude of stress change.

Discontinuity Stiffness

The normal stiffness k_n of a discontinuity can be defined as the change in normal stress that occurs with a given change in

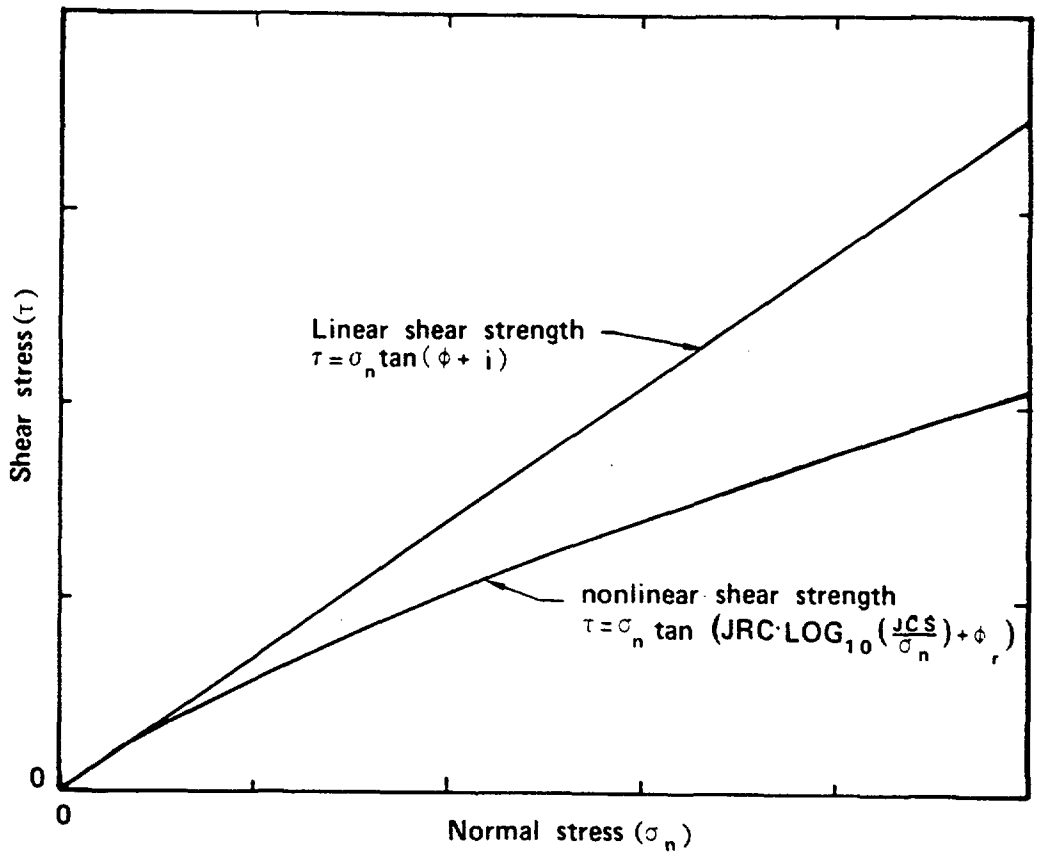

Figure 3.4 Shear strength calculated using linear and nonlinear approaches.

discontinuity thickness (aperture opening or closure). Similarly, shear stiffness k_s is the change of shear stress that results from an incremental amount of shear displacement.

If a load is applied normal to a discontinuity contained in a rock specimen (Figure 3.2) the resulting deformation in one dimension represents the sum of the deformation of the intact rock and the deformation of the discontinuity (Figure 3.5). A jointed rock mass can thus be thought of in a one-dimensional sense as a sequence of springs that act in series. Assuming isotropic, linear elastic rock, the rock is represented by very stiff, linear spring behavior while discontinuities are represented by initially softer, highly nonlinear springs. Correspondingly, the total rock mass deformability and its components are:

$$\frac{1}{E_m} = \frac{1}{E} + \frac{1}{k_n S} \tag{3.4}$$

In this equation, E_m is the modulus of deformation curve of the rock mass, E is the elastic modulus of the intact rock, k_n is the normal stiffness of a discontinuity, and S is the average discontinuity spacing.

Inspection of the discontinuity deformation plotted in Figure 3.6 reveals that the curve asymptotically approaches a vertical slope as the normal load increases. The vertical line has been designated by Goodman (1976) as the maximum closure of the discontinuity. Although the nonlinear deformation curve can be represented with a hyperbolic

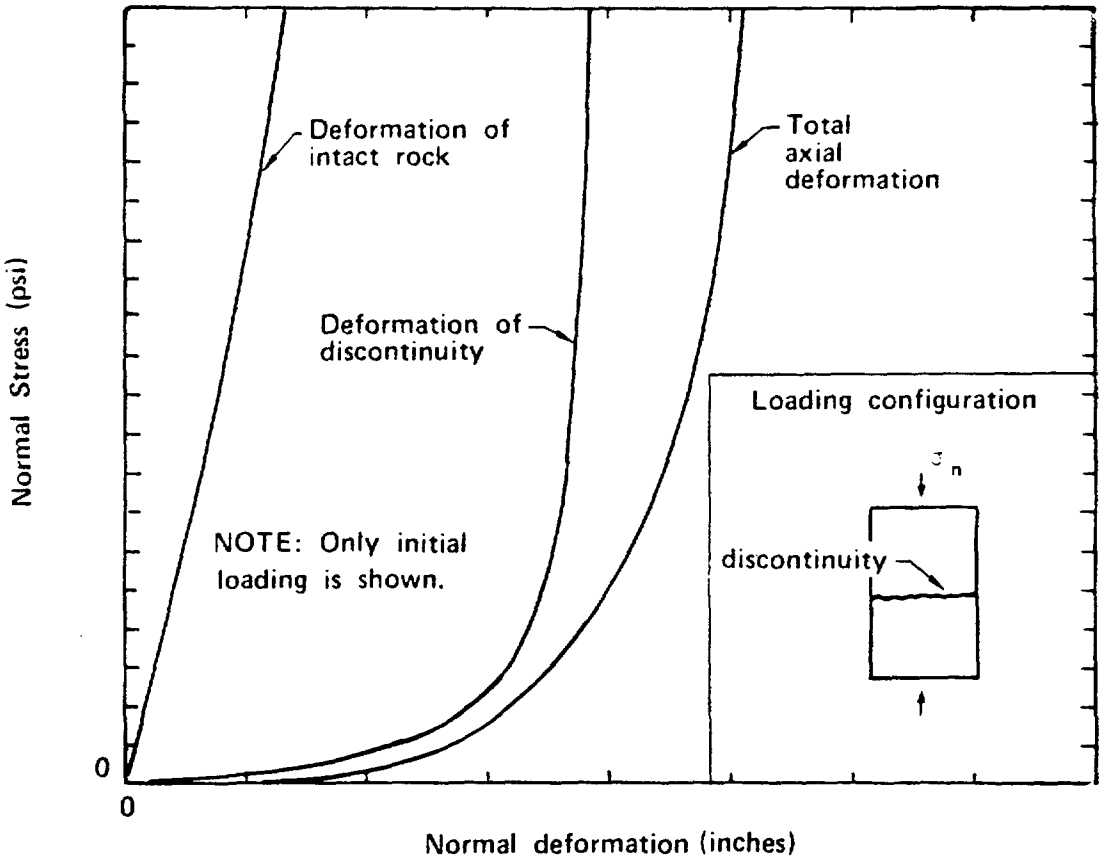

Figure 3.5 Typical form of normal deformations resulting from axial loading of a rock sample containing a discontinuity.

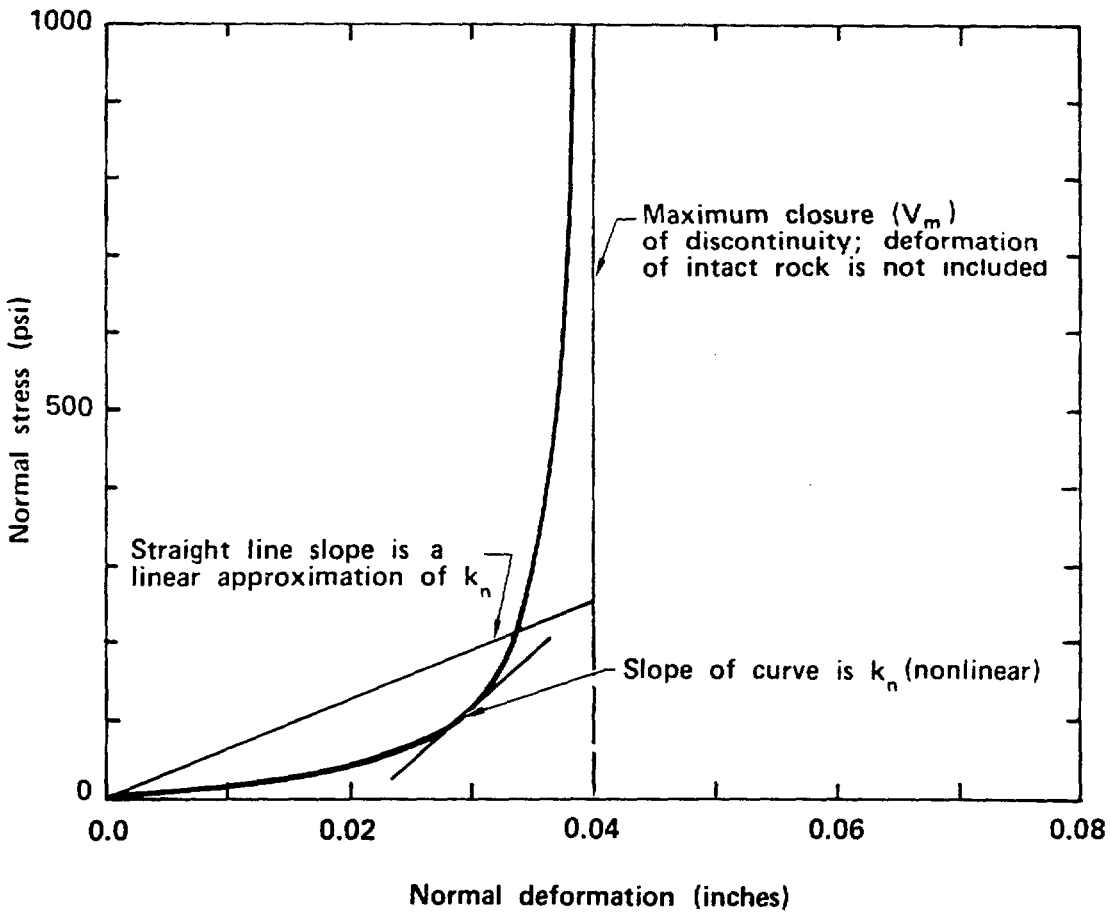

Figure 3.6 Linear and nonlinear representations of discontinuity normal stiffness.

equation, Figure 3.6 shows how the normal stiffness can be approximated with two straight line segments. This useful engineering approximation is available in the keyblock stability models and requires as input a single value for k_n. A more correct approach that is described below is also available (as an option) in the keyblock behavior models.

Bandis et al (1983) compared mathematical models that have been suggested for the nonlinear normal stiffness of joints with the results of stiffness tests conducted on discontinuity samples from different rock types. They propose a hyperbolic model for nonlinear behavior in the following form:

$$\sigma_n = \frac{\Delta V}{a - b\Delta V} \tag{3.5}$$

where σ_n = normal stress on the discontinuity, and

ΔV = discontinuity closure.

The coefficients a and b can be obtained by rewriting equation 3.5 and considering the limiting extremes of discontinuity closure at very large and very small normal stresses:

$$\sigma_n = \frac{1}{\frac{a}{\Delta V} - b} = \frac{1/a}{\frac{1}{\Delta V} - \frac{b}{a}} \tag{3.6}$$

Large normal stresses imply that the discontinuity closure ΔV approaches the maximum closure V_m. Therefore, as the normal stress

goes to infinity, $a/b = V_m$. Conversely, low normal stresses imply that ΔV goes to zero. In this case $1/\Delta V$ becomes much larger than b/a, and the latter term can be dropped. Thus, $1/a = k_{ni}$, where k_{ni} is the initial normal stiffness.

Once the coefficients a and b in equations 3.5 and 3.6 are defined, equation 3.6 can be changed into an expression for discontinuity closure:

$$\Delta V = \frac{\sigma_n \quad V_m}{k_{ni} V_m + \sigma_n} \tag{3.7}$$

The slope of the deformation curve (Figure 3.6) represents the normal stiffness of the discontinuity. Since the stiffness varies nonlinearly with normal stress, it can be found from the derivative of equation 3.5 with respect to joint closure:

$$k_n = \frac{k_{ni}}{\left(1 - \frac{\Delta V}{V_m}\right)^2} \tag{3.8}$$

The preceding hyperbolic model for discontinuity normal stiffness (equations 3.5 through 3.8) was developed by Bandis et al (1983). These equations can, however, be used with equation 3.4 to derive an estimate of k_n under in situ stress conditions before the excavation is created. This estimate can then be used with the hyperbolic stiffness equation, enabling nonlinear discontinuity deformation to be included in the keyblock stability model. In the following equations the maximum discontinuity closure V_m is replaced by the

discontinuity aperture under no-load conditions (negligible normal stress), a_o.

Equation 3.8 can be rewritten to solve for k_{ni} as follows:

$$k_{ni} = k_n - \frac{2k_n \Delta V}{a_o} + k_n \frac{\Delta V^2}{a_o^2} \tag{3.9}$$

Equation 3.7 can be rearranged and k_{ni} can be substituted from 3.9 to obtain an expression relating normal stress, normal stiffness, discontinuity no-load aperture, and discontinuity closure:

$$\Delta V(a_o k_n - 2\Delta V k_n + \frac{\Delta V^2}{a_o} k_n + \sigma_n) = \sigma_n a_o \tag{3.10}$$

Finally, equation 3.10 can be modified into a third degree polynomial which can be solved for the ratio of discontinuity closure to no-load aperture under ambient in situ conditions:

$$k_n(\frac{\Delta V}{a_o})^3 - 2k_n(\frac{\Delta V}{a_o})^2 + (\frac{\sigma_n}{a_o} + k_n)(\frac{\Delta V}{a_o}) - \frac{\sigma_n}{a_o} = 0 \tag{3.11}$$

The non-trivial solutions of equation 3.11 include two possible values for the discontinuity closure as a fraction of total maximum closure. Inspection of a representative curve (Figure 3.6) for discontinuity normal deformation reveals that aperture closure will typically be greater than 50% for most initial in situ stresses of interest. If the smaller closure value is selected, k_{ni} must be very close to the in situ k_n, implying that either the in situ stresses are very low

(low k_n) or that the discontinuity is very stiff (high k_{ni}). The larger of the two closure values is arbitrarily used in the stability models to represent the condition of the discontinuity before the underground opening is excavated or keyblock displacement occurs.

Once equation 3.11 has been solved, the ratio of closure to aperture can be used in equation 3.9 to calculate k_{ni}. The coefficients a and b can then be determined, and equation 3.6 can be used to obtain normal stresses as the discontinuity forming the keyblock face opens or closes.

Figure 3.6 includes a typical nonlinear curve that relates normal load and displacement. This curve was generated with equation 3.6, which completely defines the curve from values of a, b, and k_{ni}. This is implemented as an optional alternative to the linear approximation for normal stiffness in the keyblock behavior models. It should be noted that the discontinuity aperture used as a reference for joint opening or closing during block displacement is calculated from equation 3.7 using the modified in situ stresses around the underground opening, as explained in the final section of this chapter.

The use of equation 3.11 requires values for the normal stress on the discontinuity, discontinuity normal stiffness at the given stress level, and initial (no-load) discontinuity aperture. Principal stresses that affect the discontinuity can be estimated from overburden depth, or may be available from site investigation measurements. The stresses can then be rotated to find normal and

shear stresses on each discontinuity plane using procedures outlined by Goodman (1980). Initial discontinuity apertures can be assumed, or estimated from an empirical equation provided by Bandis et al (1983). However, the normal stiffness of the discontinuity under the ambient stress conditions is difficult to estimate because of its variability.

If we treat the discontinuities that create keyblocks as members of sets, examine only one set at a time, and assume that the discontinuities of a set have an average spacing, we can rearrange equation 3.4 as follows to obtain an estimate of k_n:

$$k_n = \frac{E/S}{(E/E_m) - 1} \tag{3.12}$$

Such an estimate represents an average k_n for the discontinuity set under the stress conditions that exist before the underground opening is excavated. Values are required for the average discontinuity spacing, the modulus of the intact rock, and the ratio of the rock mass deformability to the intact rock deformability. Discontinuity spacings and the modulus of deformation for intact rock can be measured during site investigations, but now the difficulty lies in estimating the ratio of the deformation moduli. Heuze (1980) has suggested that the ratio of rock mass to intact rock deformation moduli can often be assumed as 0.4. Alternatively, the in situ modulus can be estimated from correlations with rock mass classification schemes. With estimates or with field measurements, the nonlinear normal stiffness of each block face can now be quantified. As an aside, the nonlinear behavior of k_n as a function

of stress implies that the rock mass becomes increasingly stiff with depth as long as its behavior is elastic. This is because the discontinuities are more tightly closed with higher confining stresses. This effect is itself nonlinear, so that the change in rock mass stiffness should be most noticeable as one excavates downward from the ground surface, and should become imperceptible at great depth. Destressed zones around excavations would mask these observations.

Discontinuity shear stiffness is used in the keyblock behavior model to modify the shear stresses acting on the keyblock faces that are created by discontinuities. Before any block displacement occurs, the stresses on the block faces are determined by the stress field around the underground opening. When keyblock displacement commences, the shear stresses increase on each bounding discontinuity in accord with its shear stiffness until the maximum available shear strength is reached. However, the normal stress is usually dropping as displacement occurs, and so the peak available strength may be reached almost immediately. Either of two approaches can be used to represent the shear stiffness, corresponding to the linear and nonlinear definitions of normal stiffness developed above.

For the linear representation, a constant ratio of shear stiffness to normal stiffness can be used in the model. This approximation for shear deformation is a constant stiffness model (Figure 3.7) that assumes elastic behavior as described by Goodman (1976). Goodman et al (1982) examined a range of linear stiffness ratios in an analysis

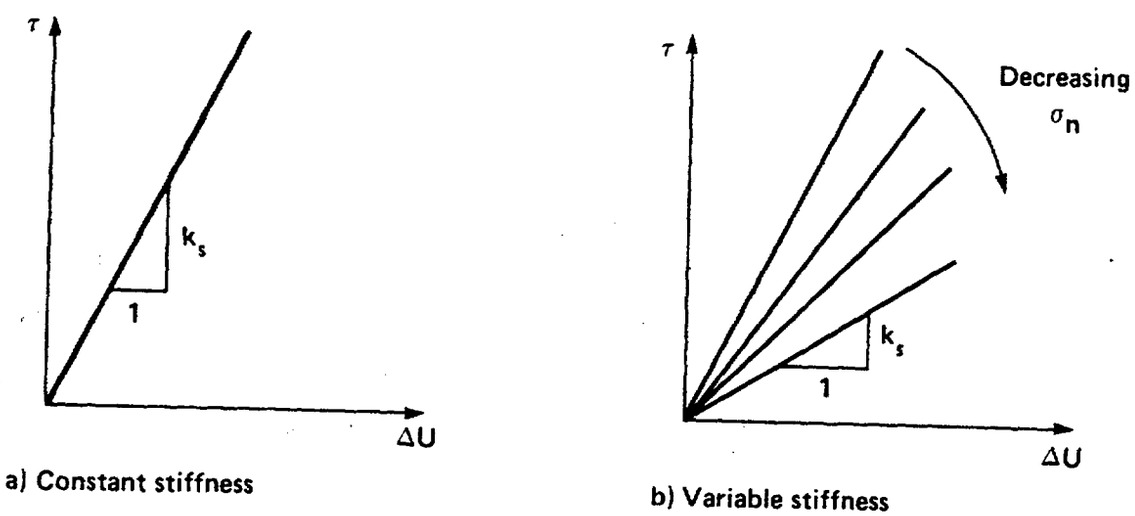

Figure 3.7 Constant stiffness and peak displacement (variable stiffness) representations of shear stiffness.

of a keyblock subjected to a tangential stress field in a planar excavation roof. They found that the stability of the keyblock was less sensitive to the stiffness ratio than to other parameters such as shear strength.

Barton and Choubey (1977) have suggested the following equation for calculation of shear stiffness (k_s) from some of the same parameters that are used in the nonlinear representations of discontinuity shear strength and normal stiffness:

$$k_s = \frac{100}{L} \sigma_n \tan \left(JRC \log_{10} \left(\frac{JCS}{\sigma_n}\right) + \phi_r \right) \tag{3.13}$$

This equation is based on observations by Barton and Choubey that peak shear strength is reached when shear displacement has reached about one percent of the discontinuity length (L) measured in the direction of sliding. Discontinuity length will of course depend on block and excavation geometry. Equation 3.13 is used in the keyblock behavior models in conjunction with the nonlinear normal stiffness and shear strength equations.

Before leaving this discussion of normal and shear stiffness, it should be pointed out that discontinuity surfaces can apparently suffer irreversible changes during repeated cycles of normal loading if the stresses are sufficiently high. This is seen as hysteresis in plots of load versus deformation in the work of Bandis et al (1983). Damage to discontinuity surfaces at high stresses causes some of the joint closure to be unrecoverable as indicated by Figure 3.8. If an

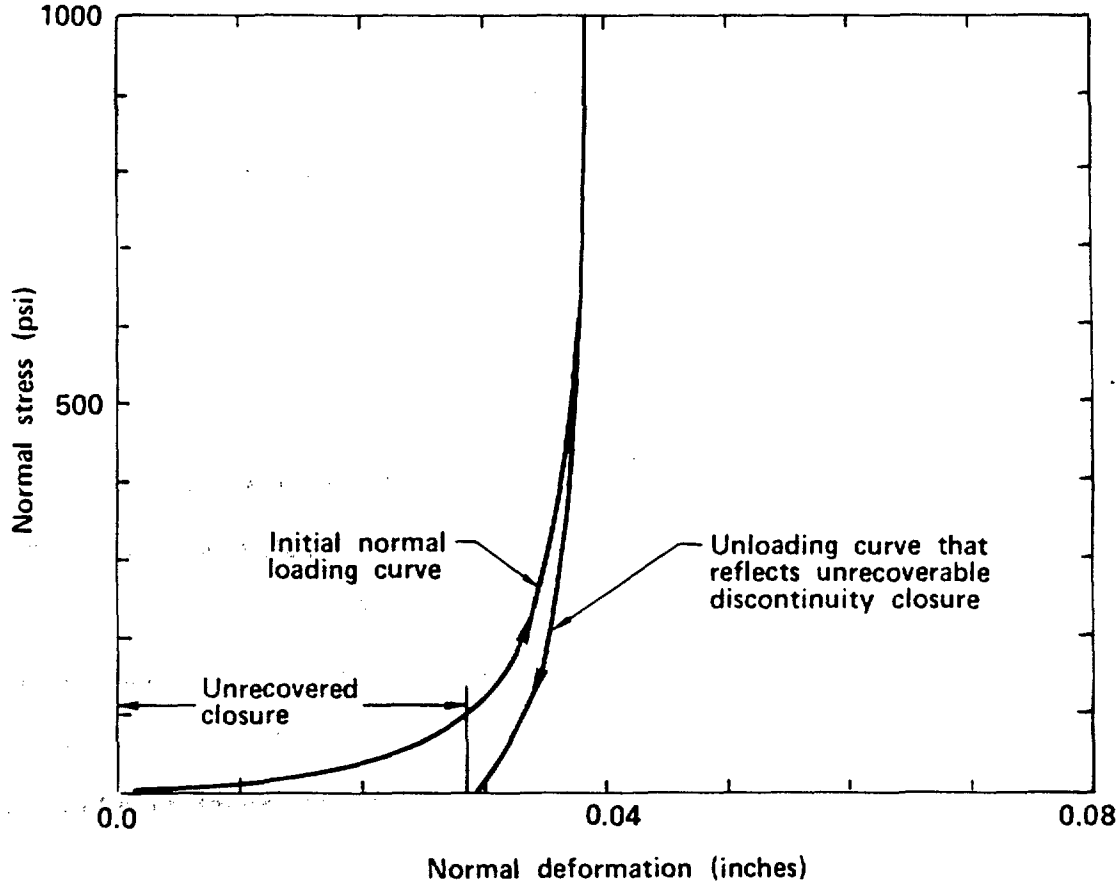

Figure 3.8 Effect of unrecoverable closure on discontinuity normal stiffness.

estimate of damage can be quantified, it could be incorporated in the nonlinear normal stiffness computations by shifting the stiffness curve. This technique is not used in the keyblock behavior models because compressive stresses that are high enough to cause such a significant alteration of discontinuity behavior are also high enough that the assumption regarding the relative deformation of the intact rock and the discontinuities is no longer valid.

Load and Stress Conditions

Three different types of stresses and forces that influence keyblock stability are included in the keyblock behavior models. These are the stresses in situ as modified by the presence of the underground opening, the changes in the stress field around the opening that result from temperature changes, and the weight of the block itself. The block weight is a matter of rock density and the block volume calculated from the geometry of a given problem, and so will be discussed below as part of the summation of forces acting on the block. Fluid pressures within the discontinuities are not included in this analysis, but can be added using either assumed or calculated pressure distributions for each block face. Ground support forces can also be added to the force summation equations; they are not included here because they do not enter into the more fundamental problem of the behavior of an unsupported keyblock.

Stress in situ around an underground circular opening can be calculated using closed form expressions from elastic theory. In two

dimensions, the stresses at a point can be computed as a function of location using the Kirsch solution:

$$\sigma_r = \frac{S_V + S_H}{2}\left(1 - \frac{R^2}{r^2}\right) + \frac{S_H - S_V}{2}\left(1 - 4\frac{R^2}{r^2} + 3\frac{R^4}{r^4}\right) \cos 2\theta + P\frac{R^2}{r^2} \tag{3.14}$$

$$\sigma_\theta = \frac{S_V + S_H}{2}\left(1 + \frac{R^2}{r^2}\right) - \frac{S_H - S_V}{2}\left(1 + 3\frac{R^4}{r^4}\right) \cos 2\theta + P\frac{R^2}{r^2} \tag{3.15}$$

$$\tau_{r\theta} = \frac{S_V - S_H}{2}\left(1 + 2\frac{R^2}{r^2} - 3\frac{R^4}{r^4}\right) \sin 2\theta \tag{3.16}$$

where r, θ = radial and tangential coordinates

R = hole radius

S_H = horizontal stress, unperturbed by tunnel

S_V = vertical stress, unperturbed by tunnel

P = internal pressure

σ_r, σ_θ, $\tau_{r\theta}$ = radial, tangential, and shear stress at point r, θ

Daemen (1983) rotated these two-dimensional stresses into the normal and shear stresses affecting a discontinuity that passes through the point (see Figure 3.9 for the problem geometry):

$$\sigma = \frac{\sigma_r + \sigma_\theta}{2} - \frac{\sigma_r - \sigma_\theta}{2} \cos 2(\beta - \theta) - \tau_{r\theta} \sin 2(\beta - \theta) \quad (3.17)$$

$$\tau = - \frac{\sigma_\theta - \sigma_r}{2} \sin 2(\beta - \theta) - \tau_{r\theta} \cos 2(\beta - \theta) \quad (3.18)$$

Equations 3.14 through 3.18 are used in the two-dimensional keyblock behavior model to calculate the stresses that initially act on the block at a series of points along each face. The way in which these stresses are adjusted for displacement is discussed in the next section of this chapter. Elsworth (1983) extended two-dimensional keyblock stability methods to include a hydrostatic stress field around a circular underground opening; however, he used a stress solution from elastic theory for thick-walled cylinders rather than the Kirsch solution.

For three-dimensional problems, most previous investigators have assumed that the block under analysis is located in a planar excavation surface, and that the stresses are tangential to the opening (see Table 3.1). A generalized plane strain solution developed by Amadei (1982) is available that allows the three-dimensional stress tensor to be calculated as a function of location around a cylindrical opening in an arbitrary in situ stress field. This solution has been modified for the three-dimensional keyblock behavior model, and is used to compute the stresses acting on a grid of points representing each block face. These initial stresses are then adjusted for the effects of keyblock displacement as described below.

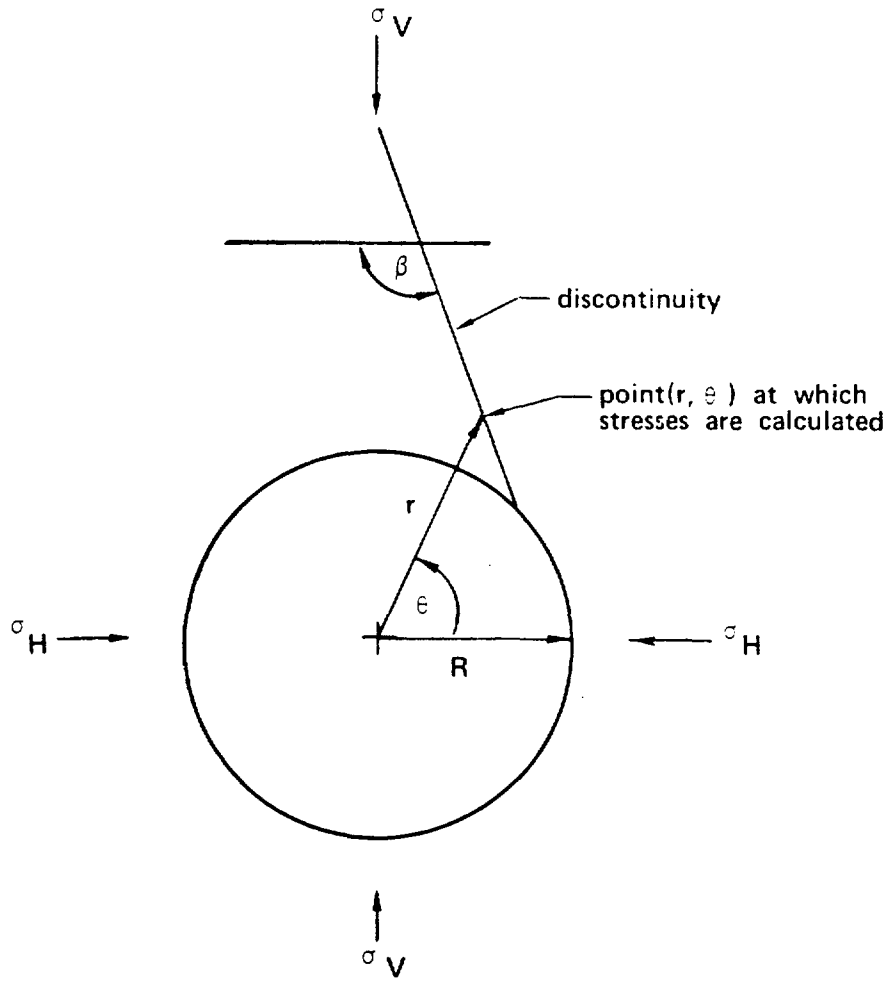

Figure 3.9 Geometry used in Kirsch two-dimensional solution for stresses around a circular hole.

The stresses around an underground opening may change significantly during the operational life of an opening due to variations in rock mass temperature (examples are given in Chapter 6). These stress changes are induced by the thermal expansion or contraction of the rock. This was recognized and examined in the context of its effects on stress measurements by Stephens and Voight (1982), but their emphasis was primarily on stresses in a borehole wall. Zudans et al (1965) have published equations based on theories of elasticity with which components of stress changes caused by thermal loading or unloading within a thick-walled cylinder may be calculated. These equations are for steady state heat transfer, where the temperature is constant at some outer radius b. This represents an extreme case which would bound transient temperature conditions.

$$\sigma_r = \frac{E\,\alpha\,\Delta T}{2(1-\nu)\ \ln\frac{b}{R}}\left[\ln\frac{b}{r} + \frac{R^2}{b^2-R^2}\left(1-\frac{b^2}{r^2}\right)\ln\frac{b}{R}\right] \qquad (3.19)$$

$$\sigma_\theta = \frac{E\,\alpha\,\Delta T}{2(1-\nu)\ \ln\frac{b}{R}}\left[-1 + \ln\frac{b}{r} + \frac{R^2}{b^2-R^2}\left(1+\frac{b^2}{r^2}\right)\ln\frac{b}{R}\right] \qquad (3.20)$$

$$\sigma_Z = \frac{E\,\alpha\,\Delta T}{2(1-\nu)\ \ln\frac{b}{R}}\left[-1 + 2\ln\frac{b}{r} + \frac{2R^2}{b^2-R^2}\ \ln\frac{b}{R}\right] \qquad (3.21)$$

where: r, θ = radial and tangential coordinates as before

Z = direction parallel to tunnel axis

E = modulus of elasticity

α = coefficient of linear thermal expansion

ΔT = temperature difference between tunnel wall at radius R and rock at radius b

ν = Poisson's ratio

As implemented in the two-dimensional and three-dimensional keyblock stability models, the approximation of thermal stresses arbitrarily assumes that the radius b at which temperature is constant is ten times the excavation radius R. This factor of ten can be readily changed if better temperature distribution data are available.

Formulation of Keyblock Stability Equations

Evaluation of the behavior and stability of a keyblock requires that the forces affecting the block be summed into a resultant that can be evaluated for magnitude and direction. The factors that enter into such a force summation have been described in preceding sections of this chapter. The forces included are the weight of the keyblock and the normal and shear stresses numerically integrated over each block face that they act upon. These normal and shear stresses are a function of their location on the block surfaces, the initial stresses, keyblock weight, keyblock displacement, and temperature changes. Procedures for computing most of these quantities have been outlined above; they will now be combined to formulate a method for stability analysis. Block weight is brought into the calculation when the stresses are summed into resulting forces; this is not strictly correct. The error that it causes is discussed in the second section of Chapter 5, below.

Only the three-dimensional model will be described since the two-dimensional model represents a simpler application of the same principles. The method calculates a total resultant force in the tunnel coordinate system as a function of keyblock displacement, instead of the opposite approach of finding the displacement that results from a combination of forces. This resultant force can then be examined for a number of specified displacements (1) to see if equilibrium is reached as the block slips, and (2) to see if any excess resisting forces are available to provide a margin of safety against failure for stable blocks.

To begin an analysis of keyblock behavior, the initial (pre-displacement) stresses on the keyblock faces must be calculated. Three sets of coordinate systems are needed as listed in Table 3.2 and shown in Figure 3.10. The unperturbed in situ stresses that exist prior to construction are referenced at first to the global coordinate system, but are rotated into the tunnel coordinate system in which the keyblock resides using Goodman's (1980) procedures. Since the stresses are not uniformly distributed over each block face once the opening is excavated, a grid of points (or nodes) is set up for each discontinuity face of the keyblock (Figure 3.11) in order to allow numerical integration of the stresses into forces. The stresses as modified elastically by the cylindrical excavation are calculated for the grid points using the tunnel coordinate system. Each face has a coordinate system of its own, though, which is based on the normal to the discontinuity that creates the face and the projection of the displacement vector onto the face (Table 3.2). The stress tensor at

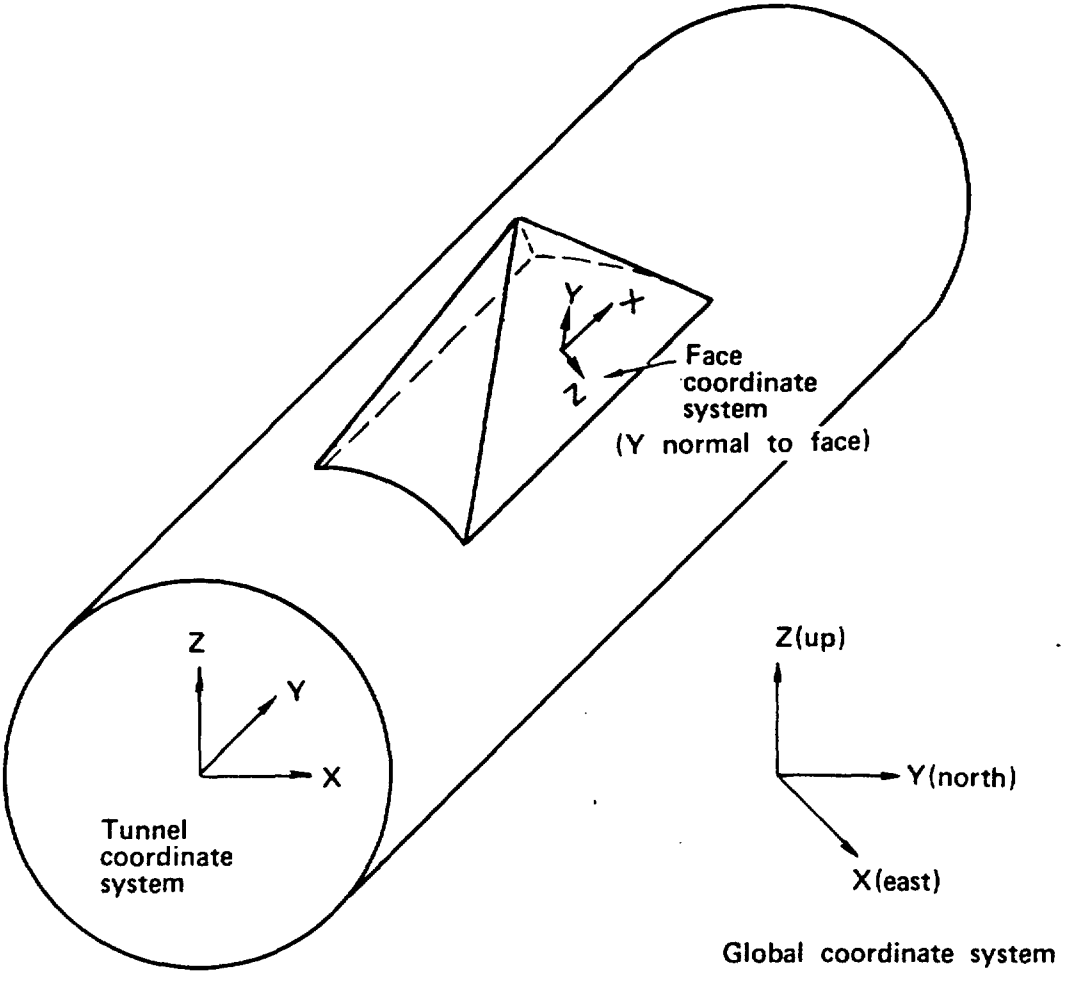

Figure 3.10 Coordinate systems used in three-dimensional block analyses.

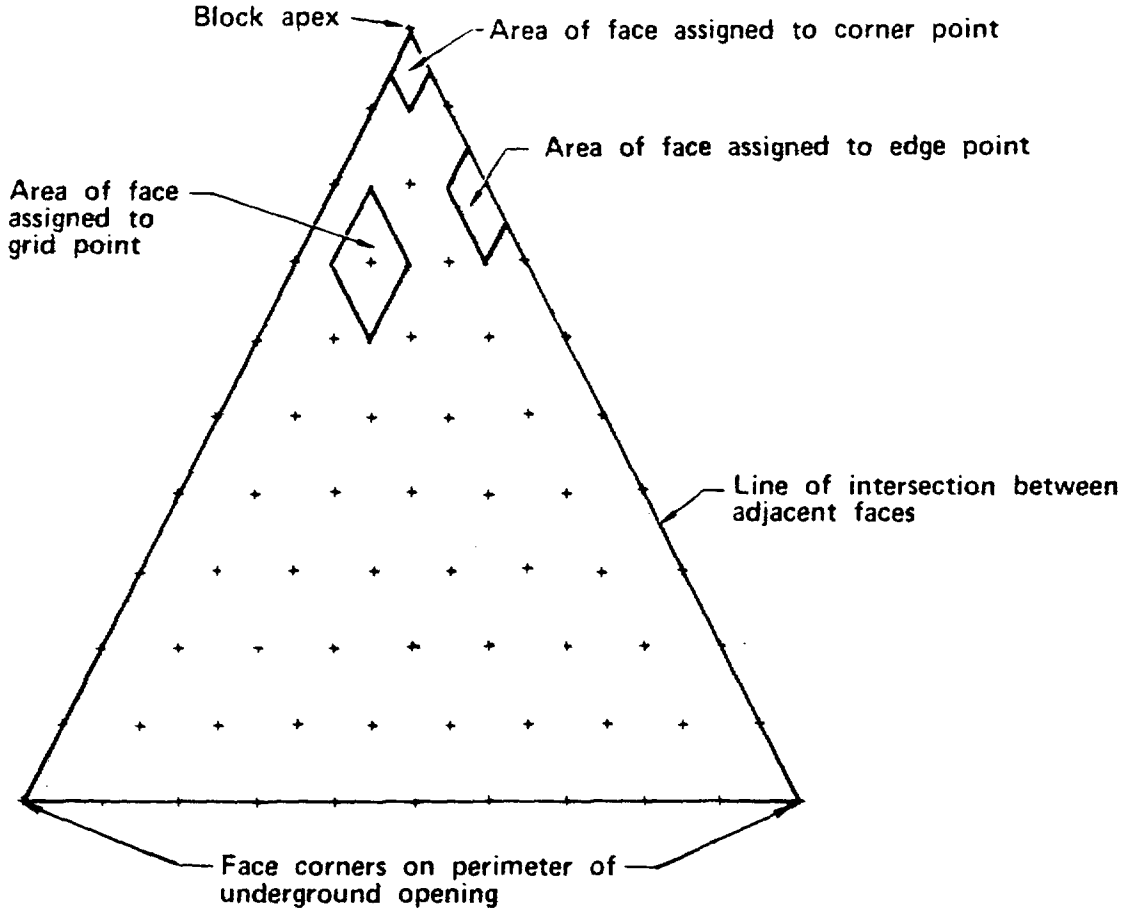

Figure 3.11 Typical grid of points used to calculate initial stresses for each keyblock face.

Table 3.2 Coordinate Systems Used in Three-Dimensional Keyblock Behavior Analysis

System	+X axis	+Y axis	+Z axis
Global	East	North	Vertical up
Tunnel	Horizontal Through Springline	Tunnel Axis	Through Back Perpendicular to X and Y
Keyblock(1) Face	Transverse to Projected Displacement Direction in Face	Normal to Face	Parallel to Projected Displacement Direction

NOTE: (1) One face system is used for each keyblock face that is not an excavation surface.

each grid point is rotated from the tunnel coordinate system to the face coordinate system, and any stress changes caused by thermal effects are rotated and imposed on these initial stresses at this time. Once these computations are complete, the initial normal stress and initial shear stress (for zero block displacement) are available for each grid point.

If nonlinear discontinuity deformation is to be accounted for, some intermediate calculations are needed. Once the face grids are set up, but before the in situ stresses are adjusted for the effects of the excavation, the normal stresses on the discontinuities are found and used with equation 3.11 to obtain estimates of aperture closures. These closures represent average values for each discontinuity under ambient in situ stresses, and are used in equation 3.9 to compute initial normal stiffnesses. The initial normal stiffnesses are used to set up a hyperbolic equation for normal stiffness for each discontinuity. The effects of the underground opening on the stress field are then calculated as mentioned above; the stresses usually increase because of the stress concentrations around the tunnel. These increases in normal stress are used with the hyperbolic equations to adjust the normal stiffness and aperture value at each grid point prior to the start of keyblock displacement. Note that each part of the calculational grid may be at a different point on the hyperbolic curve for that discontinuity, and that even though the rock is assumed to be "rigid," the discontinuity is at slightly varying degrees of closure along its length prior to block displacement because of the distribution of normal stresses.

The next step in the process is to adjust the initial stresses for an increment of displacement in a specified direction. This is done in a sequence of operations: First, the displacement is resolved into its net effect on each discontinuity grid point in terms of an aperture change (normal) component and a sliding (shear) component. If the angle between the displacement vector and the discontinuity plane is β, and the face has a dilatancy angle (i^o), then the amount of aperture opening ΔV that occurs with displacement D is:

$$\Delta V = D\ (\sin \beta - \cos \beta \tan i) \tag{3.22}$$

In this equation the $\sin \beta$ term represents the movement of the block away from the average discontinuity surface, while the $\cos \beta \tan i$ term is a dilatancy effect that reduces the opening of the surface. Aperture opening is positive and closure is negative in this equation. The dilatancy angle is specified for each face for linear analyses, and is extracted from the shear strength equation (Equation 3.3) for nonlinear analyses.

Similarly, shear slip along each average discontinuity surface is given by:

$$\Delta U = D \cos \beta \tag{3.23}$$

The next operation in the sequence is to adjust the normal stresses at each grid point. For the nonlinear analysis, this is done by entering the hyperbolic stiffness equations with the adjusted aperture values

and calculating new normal stresses for each grid point. For a linear analysis, the initial normal stress (σ_{ni}) for each point is modified as follows:

$$\sigma_n = \sigma_{ni} - k_n \Delta V \tag{3.24}$$

With increasing keyblock displacement, the normal stiffness and normal stress follow an unloading path as the block separates from the surrounding rock. The available shear strength also drops because of its relationship to the normal stress, while the shear stresses increase until they reach the level of shear strength that is mobilized. Equation 3.3 or 3.4 is therefore used with the adjusted values for normal stress to determine the available shear strength at each grid point. The shear stress at each point is then set equal to the available shear strength, or the shear stress calculated from shear stiffness and displacement, whichever is less. The shear stress calculated from the initial shear stress τ_i and the displacement is:

$$\tau = \tau_i + k_s \Delta U \tag{3.25}$$

During the calculations of block geometry necessary for setting up the grids for each face, the block volume is computed and used to obtain the weight of the keyblock. Face areas are also assigned to each grid point to allow numerical integration of stresses into forces acting normal and parallel to each face. These forces are then rotated into the global coordinate system and summed. Under the

convention of positive being upward in the tunnel Z axis direction, the keyblock weight (W) is a negative force. If the final resultant force (F) is oriented upward, it represents an excess of shear force that must be overcome in order to pull the keyblock out of the surrounding rock mass to the specified level of displacement. If, conversely, F is negative (acting downward) it represents a force which must be resisted by support for the block to be at equilibrium at the given displacement.

The resultant force F can be normalized by dividing by weight W; the expression F/W is a ratio of resultant force to keyblock weight. The sign of the ratio can also be switched so that a positive F/W indicates a support that must be supplied for stability, while a negative F/W implies a negative support, or pullout force. Using this sign convention, the F/W ratio can be related to a factor of safety (FS) by the following equation:

$$FS = 1.0 - F/W \tag{3.26}$$

It must be remembered that each F/W value for a given keyblock has a specific displacement associated with it. Figure 3.12 plots F/W against displacement for a typical keyblock that might fail by falling. This convention is used because it is conceptually similar to a ground reaction curve.

Inspection of the block reaction curve of Figure 3.12 reveals several interesting points about the displacement behavior of a stable

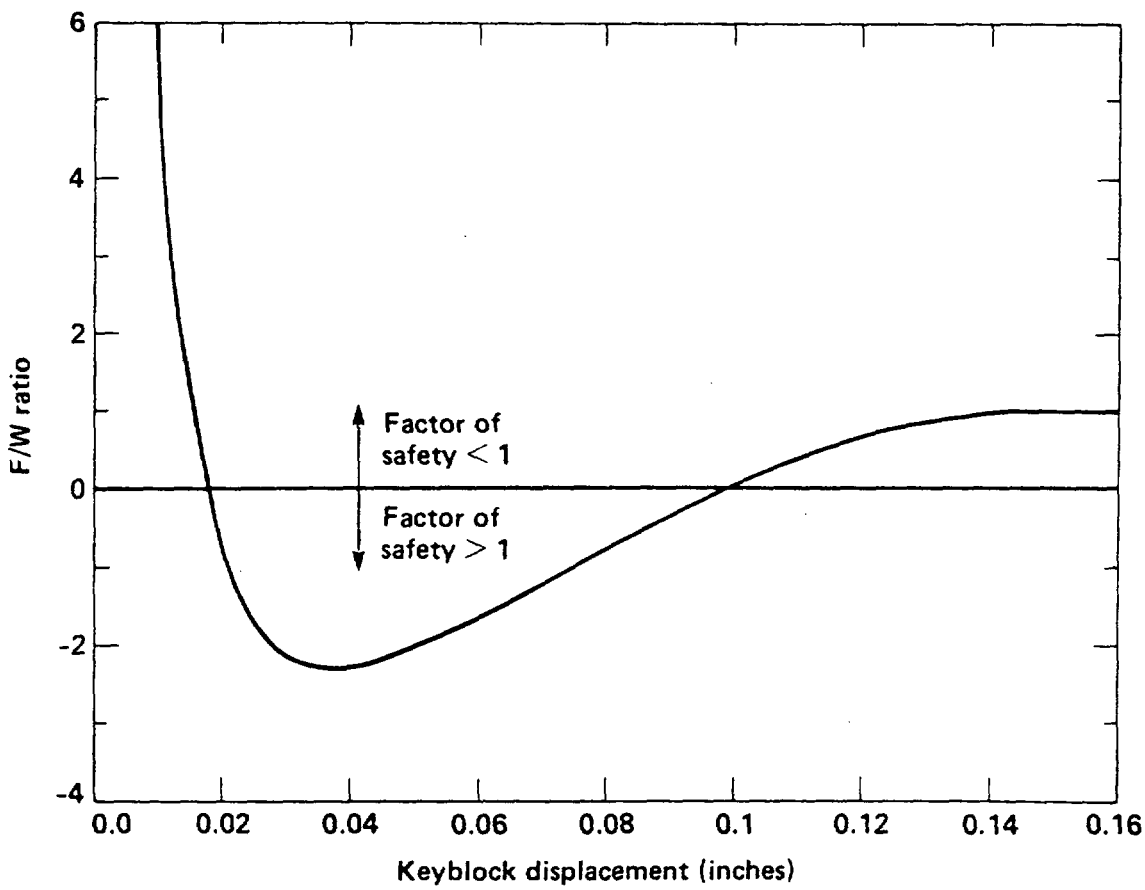

Figure 3.12 F/W ratio as function of displacement (block reaction curve) for falling keyblock.

keyblock. As the block starts to displace, the block reaction curve (F/W ratio vs displacement) starts out above, rather than at, unity. This reflects an elastic unloading of the discontinuities that occurs during excavation of the opening, and indicates that a force much greater than the block weight would be needed if the block were to be shoved back into a zero displacement condition. Second, F/W drops with increased displacement, and the keyblock reaches equilibrium and presumably stops moving once F/W reaches zero. If additional displacement is specified or allowed, however, the curve continues down until a minimum is reached. After this the peak shear strength of the discontinuities has been exceeded at all points by the mobilized shear stresses, and the curve trends upward until F/W equals unity. At this and larger values of displacement, the block faces have lost all shear strength and are likely to be entirely separated from the surrounding rock, and the entire block weight must be supported.

A plot of F/W versus displacement for a marginally unstable keyblock has a form similar to that of Figure 3.12, except that F/W remains positive for all displacement values. This indicates that the block never reaches a stable condition without support. Completely unstable keyblocks present a curve that never goes below unity, while safe keyblocks cease moving at an F/W ratio of zero or less (factor of safety greater than one). Figure 3.13 shows typical block reaction curves for all three types of blocks for comparison.

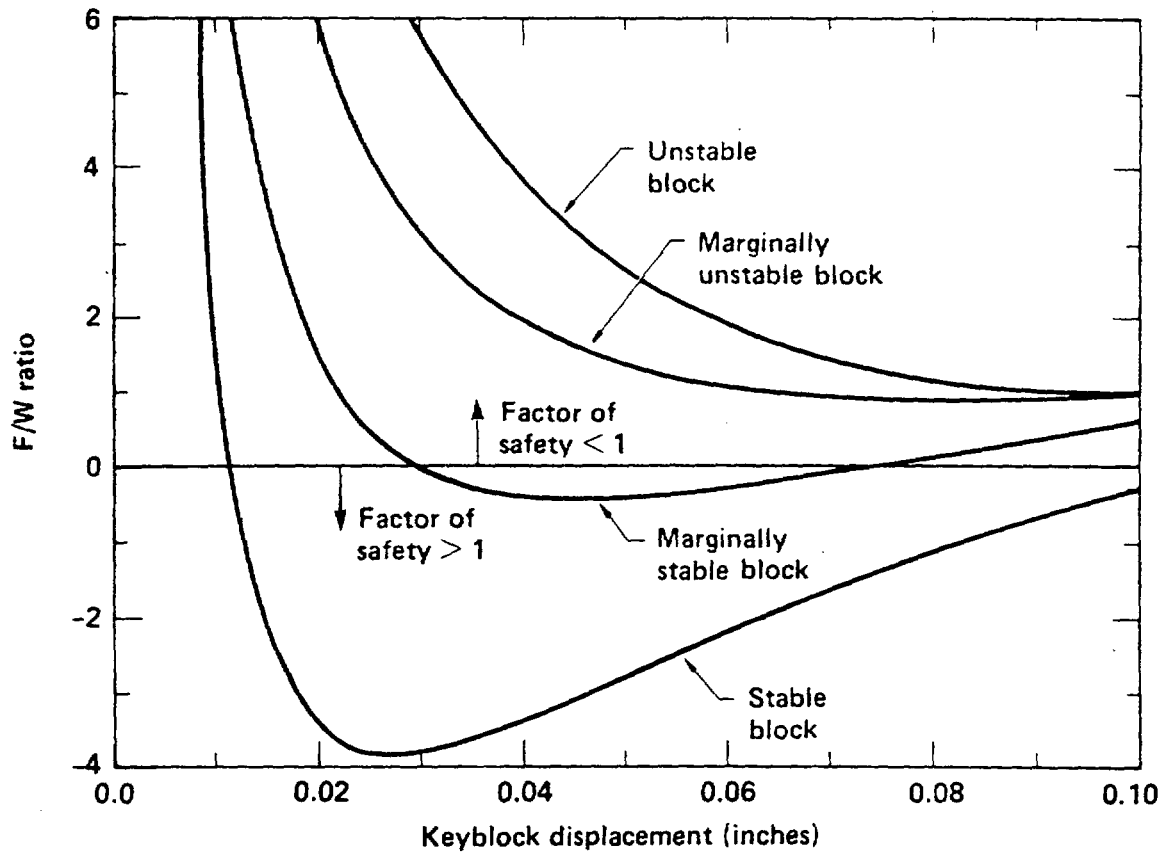

Figure 3.13 Block reaction curves for stable, marginal and unstable falling keyblocks.

CHAPTER 4 FIELD OBSERVATIONS OF KEYBLOCKS

The methods developed in Chapter 3 for evaluating the stability and displacement behavior of keyblocks have been implemented in numerical models that are presented in Appendices 1 and 2. Field observations of keyblock disposition (fallen or apparently stable) have been back-analyzed with the three-dimensional model; the field observations and the results of their analyses are described in this chapter. A suite of laboratory studies of blocks performed by Crawford and Bray (1983) with physical models were back-analyzed with the two-dimensional model; these results are also described. These observations and tests were back-analyzed in order to check the validity of the numerical models.

Observations at the Nevada Test Site

Keyblock observations were made in two tunnel complexes at the Nevada Test Site. Figure 4.1 provides a location map for the area. Observations were made in tunnels in a granitic rock mass, the Climax stock, and in welded tuff, under Rainier Mesa. The tunnels in granite were the Spent Fuel Test-Climax (SFT-C) drifts and the Piledriver event access drift (Figure 4.2), while the tunnels in tuff were part of the G-Tunnel complex.

The ribs and crown of over 800 linear feet of tunnel were inspected in the Climax stock. Nine relatively large keyblocks were observed in a one hundred foot long segment of the Piledriver access

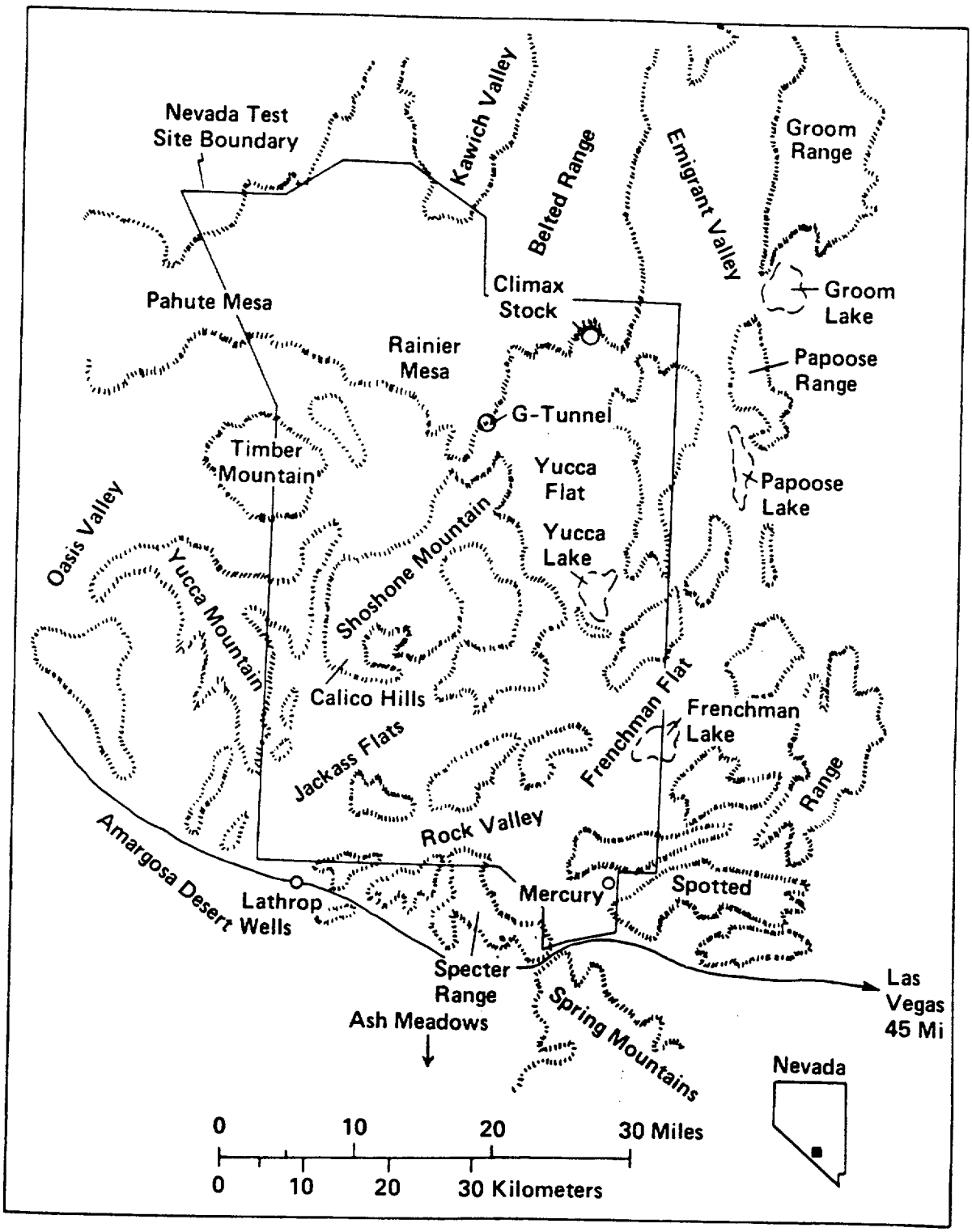

Figure 4.1 Location map for the Nevada Test Site (after Langkopf and Eshom, 1982).

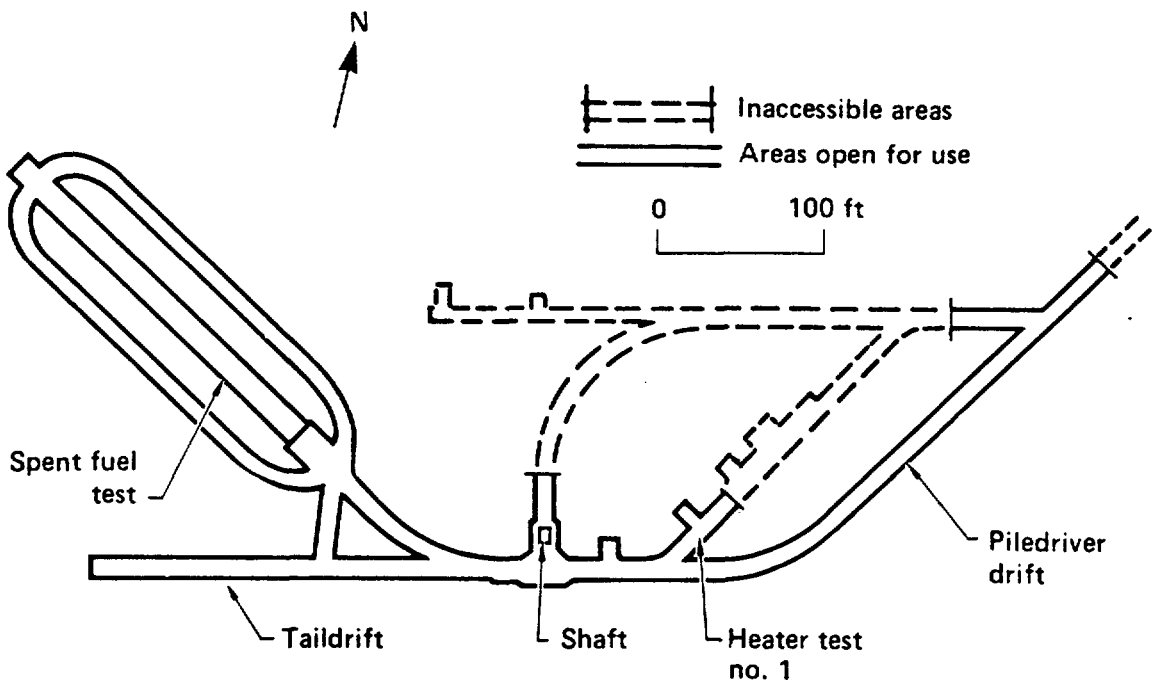

Figure 4.2 Layout of drifts at 420 meter level of Climax stock, NTS.

drift, but only four were found in six hundred feet of the Spent Fuel Test-Climax drifts. These four were obscured by steel mesh which hampered measurements as described below; these four blocks were therefore not back-analyzed for stability. Many other keyblocks were seen that were too small to be measured, but the relative frequency of blocks between the two drift settings remained about the same. This variation in keyblock frequency is a direct result of drift orientation; the SFT-C drifts were oriented essentially parallel and perpendicular to the steeply-dipping joint sets (Wilder and Yow, 1984) and thus did not encounter very many pyramid-shaped blocks. In contrast, the Piledriver drift intersected the sets at more oblique angles, and consequently experienced many more failures of pyramidal blocks per hundred feet of drift. This variation in block occurrence is discussed further below.

It should be noted at this point that the Piledriver drifts were excavated prior to the Piledriver weapons effects test, whereas the SFT-C drifts were not. However, both sets of drifts have since been subjected to ground shaking caused by other tests without consequent block falls; keyblocks that were marginally stable were removed during construction or during the Piledriver experiment. The Piledriver drift has apparently been stable for over ten years.

The blocks in the Piledriver drift generally had one of two typical pyramidal shapes based on their location around the drift perimeter. Blocks that occurred at the tunnel springline were of the

form shown in Figure 4.3; these are called shoulder blocks by Ward (1978). Other blocks occurred in the crown (Figure 4.4) or rib of the tunnel. Of these, two of the blocks in the ribs were noticeably truncated (i.e., a stub of the keyblock remained in the apex of the pyramidal cavity).

Over 6000 feet of tunnel in tuff in the NTS G-Tunnel complex were similarly inspected (Figure 4.5). However, most of this footage had been heavily shotcreted or was supported with steel ribs and continuous timber lagging, and only one fallen keyblock was mapped (Figure 4.6) in about 300 feet of open tunnel that was in welded tuff. Block face orientations in G-Tunnel were determined from geometric measurements rather than compass readings because of remnant magnetism within the welded tuff units.

Techniques Used for Field Observations

A total of fourteen relatively large keyblocks, some fallen and some yet in place, were thus observed in tunnels at the Nevada Test Site (Table 4.1). Four of the fallen blocks were in excavation surfaces that were covered with steel chain link mesh anchored by rock bolts. The heavy steel mesh effectively prevented measurement of block dimensions and orientations, and back-analysis of these blocks was thus not possible. Of the remaining ten keyblocks, one was still in place but had apparently displaced slightly. Since the block had not fallen, its dimensions had to be estimated.

Figure 4.3 Typical keyblock at springline (shoulder) of Piledriver drift.

Figure 4.4 Typical keyblocks in crown of Piledriver drift.

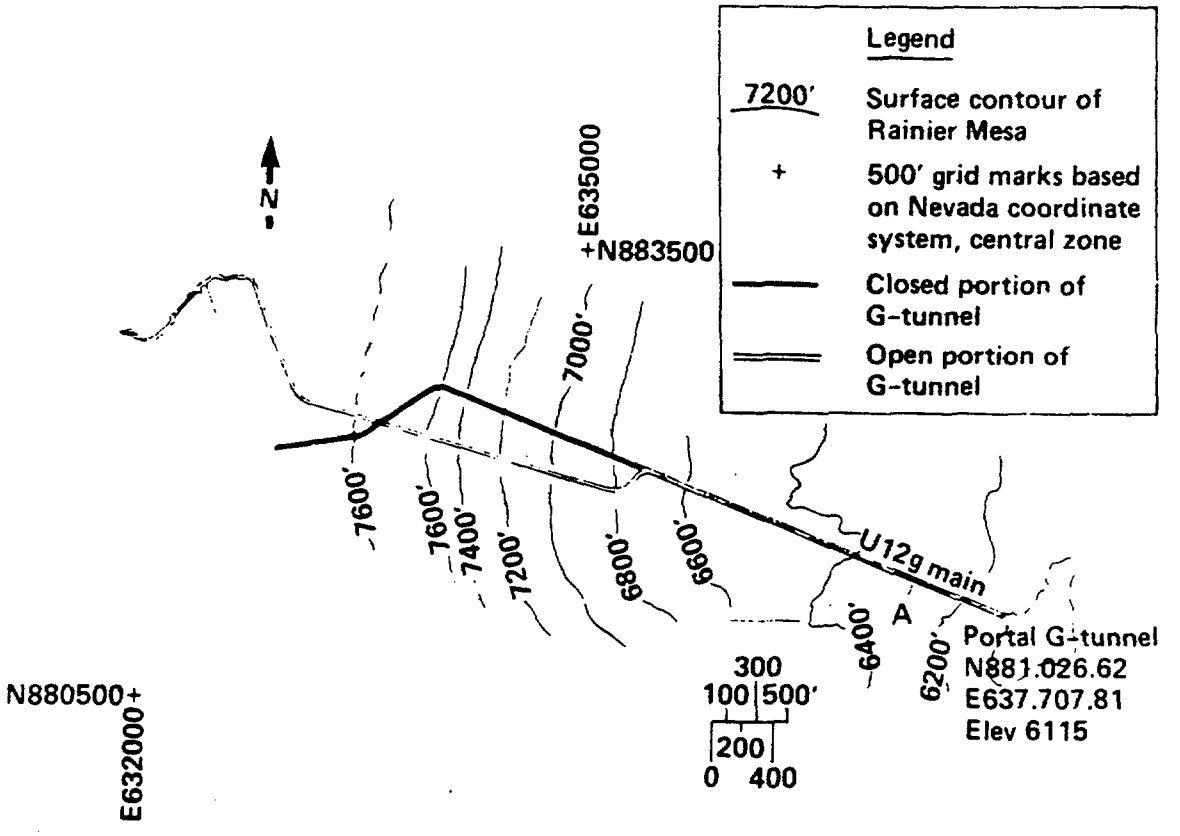

Figure 4.5 Location of observations in G-tunnel (map after Langkopf and Eshom, 1982.

Figure 4.6 Keyblock in rib of G tunnel.

Table 4.1 Summary of Field Observations of Keyblocks

Location[1]	Inspected Length of Tunnel	Mapped Keyblocks[2]
Piledriver Drift	100 feet	9
Spent Fuel Test-Climax	700 feet	4[3]
G-Tunnel	300 feet[4]	1

NOTES: (1) All tunnels are at the Nevada Test Site (Figure 4.1).

(2) Many keyblocks were seen that were too small to obtain measurements needed for back-analysis of stability.

(3) Complete measurements precluded by steel mesh on rock surface.

(4) Most of the remainder of G-Tunnel was obscured by steel sets, timber lagging, or shotcrete.

The nine keyblocks which had fallen and were accessible were measured in several ways (Table 4.2). The orientations of the block faces (formed by discontinuities) were measured with a Brunton compass. In some cases the location of the block prevented compass measurement of one or more face orientations, so a large adjustable triangle was used to measure angles between adjacent faces. These angular measurements were used to determine missing face orientations using stereonet constructions. A steel tape was used to measure the dimensions of each block face, and each block was photographed from several perspectives. The location of each block was recorded by tunnel survey station, and the height of each block above the tunnel floor was noted. Finally, a carpenter's contour gauge was used to obtain a typical roughness profile of a sample length of each discontinuity in the direction of block displacement, and a Schmidt hammer was used to obtain hammer rebound readings from which the joint compressive strength could be estimated.

Of the various types of measurements made for each block, the most difficult were the face orientation and hammer rebound measurements. This was because the work was often overhead, and because the cavities left by the fallen keyblocks had to be relatively large to allow measurements of face orientation and Schmidt hammer rebound. The latter was especially true because the hammer had to be perpendicular to the face being measured. Many smaller keyblocks necessarily had to be ignored because of their size, and of the accessible keyblocks, complete data sets were obtained for only six. Three other blocks

Table 4.2 Keyblock Measurements

Measurement	Technique
Keyblock face orientations	Brunton compass and adjustable triangle
Keyblock face dimensions	Steel tape measure
JRC	Carpenter's profile gauge
JCS	Estimated from Schmidt hammer readings
ϕ_r	Estimated from rock core tilt test results

required shear strength estimates from nearby discontinuities of the same set, and one block proved to be in too awkward of an overhead location to allow adequate measurements. Even though some of the blocks could not be back-analyzed because of a lack of data, keyblock occurrence in itself was important because of its relationship to the excavation orientation.

The roughness profiles and Schmidt hammer readings were used to estimate discontinuity shear behavior with procedures suggested by Barton and Choubey (1977). The roughness profiles were visually compared with profiles published by Barton and Choubey to estimate joint roughness coefficient (JRC). The JRC values were used with joint compressive strength values derived from the Schmidt hammer readings in equation 3.3 for shear strength and equation 3.13 for shear stiffness in the back-analysis work. No-load aperture values were estimated from the JRC values with a procedure suggested by Bandis et al (1983).

Deere and Miller (1966) correlated Schmidt hammer readings with several different rock properties in an extensive study. However, the work by Deere and Miller used the Schmidt hammer in a vertical downward loading direction. All of the readings obtained in the field work had to be corrected to this common basis because hammer orientation varied according to which face was being tested. Figure 4.7 was therefore prepared from Barton and Choubey's table of hammer reading correction values to make these adjustments. In the Nevada Test Site field work, hammer readings on the keyblock cavity faces and

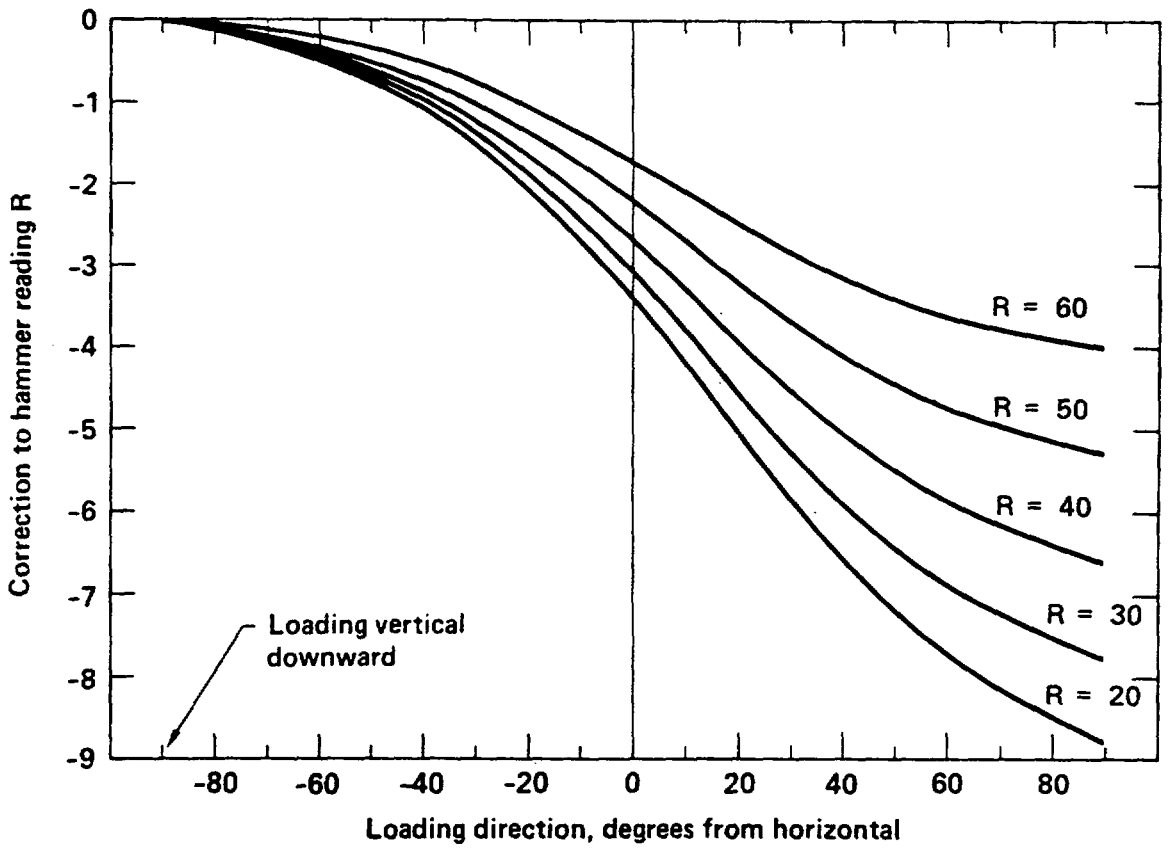

Figure 4.7 Correction curves for Schmidt hammer orientation.

on freshly sawn rock surfaces were used to estimate the compressive strengths of the discontinuities and the rock matrix, respectively. The joint compressive strength (JCS) suggested by Barton and Choubey (1977) represents the strength of discontinuity surfaces.

In some cases the keyblock geometry would not allow the hammer to be used perpendicular to a block cavity face. In these situations JCS values were estimated from adjacent parts of the same discontinuity, or from nearby members of the same discontinuity set. Interestingly, the Schmidt hammer readings on clean, freshly cut rock surfaces indicated a compressive strength for the Climax granite matrix of 33,000 psi (dry); testing of laboratory specimens found the strength to be 29,000 $\pm$ 4000 psi (Carlson et al, 1980).

Field Observations of Keyblock Occurrences

Figure 4.8 contours the lower hemisphere poles of discontinuities mapped in the Spent Fuel Test drifts with the poles of keyblock faces superimposed as asterisks. Figure 4.10 presents similar contours of data for the G-Tunnel rock mechanics drift from Langkopf and Eshom (1982). In most cases the block face orientations measured in this work agree with discontinuity orientations from previous mapping. This indicates that block identification techniques listed in Chapter 2 can be used to define the general forms (Figure 4.9, for example) of most blocks that would be encountered by an excavation. However, some mapped blocks were created by fringe members of the joint sets. Block identification should therefore be done with caution during design.

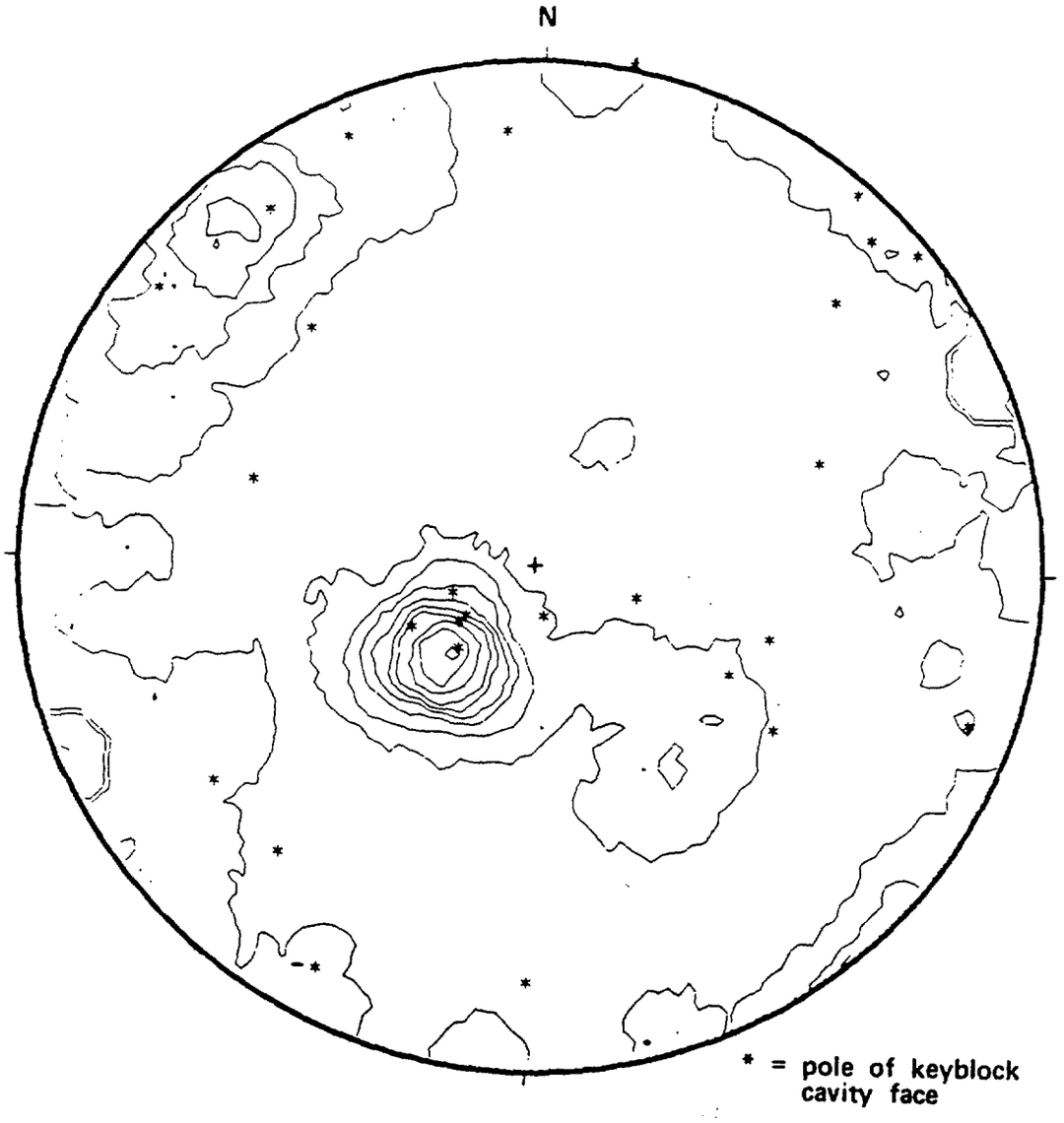

Figure 4.8 Lower hemisphere concentrations of poles of fractures mapped in Spent Fuel Test-Climax drifts. 1% contour interval.

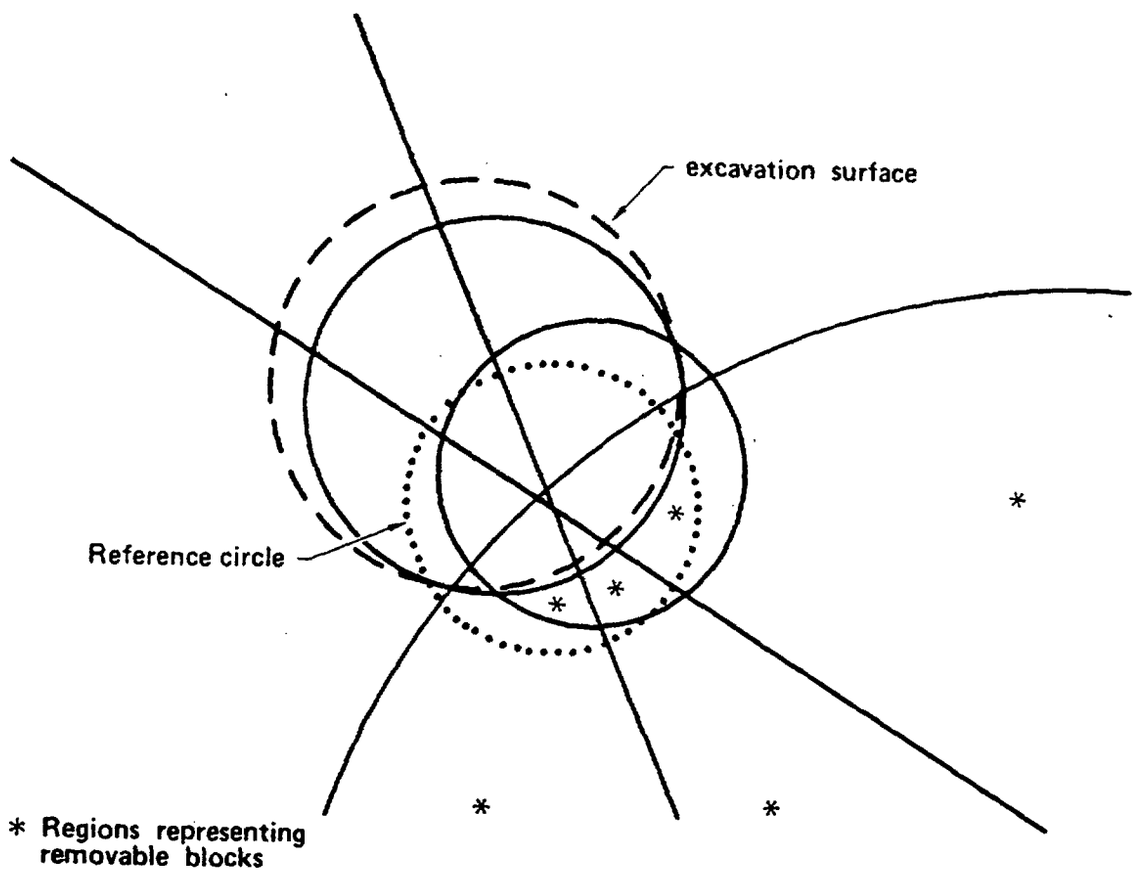

Figure 4.9a Keyblock analysis for north shoulder of Piledriver drift.

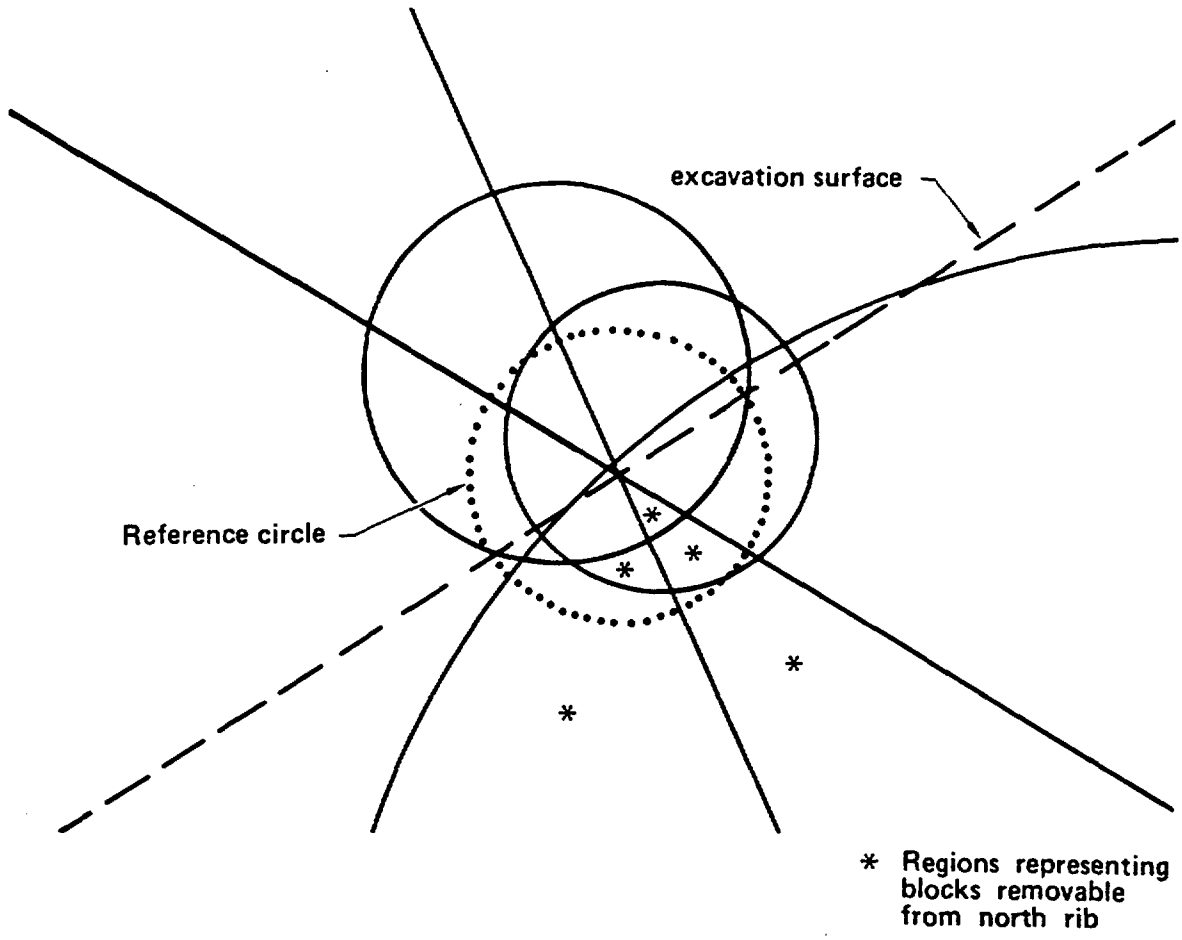

Figure 4.9b Keyblock analysis for rib of Piledriver drift.

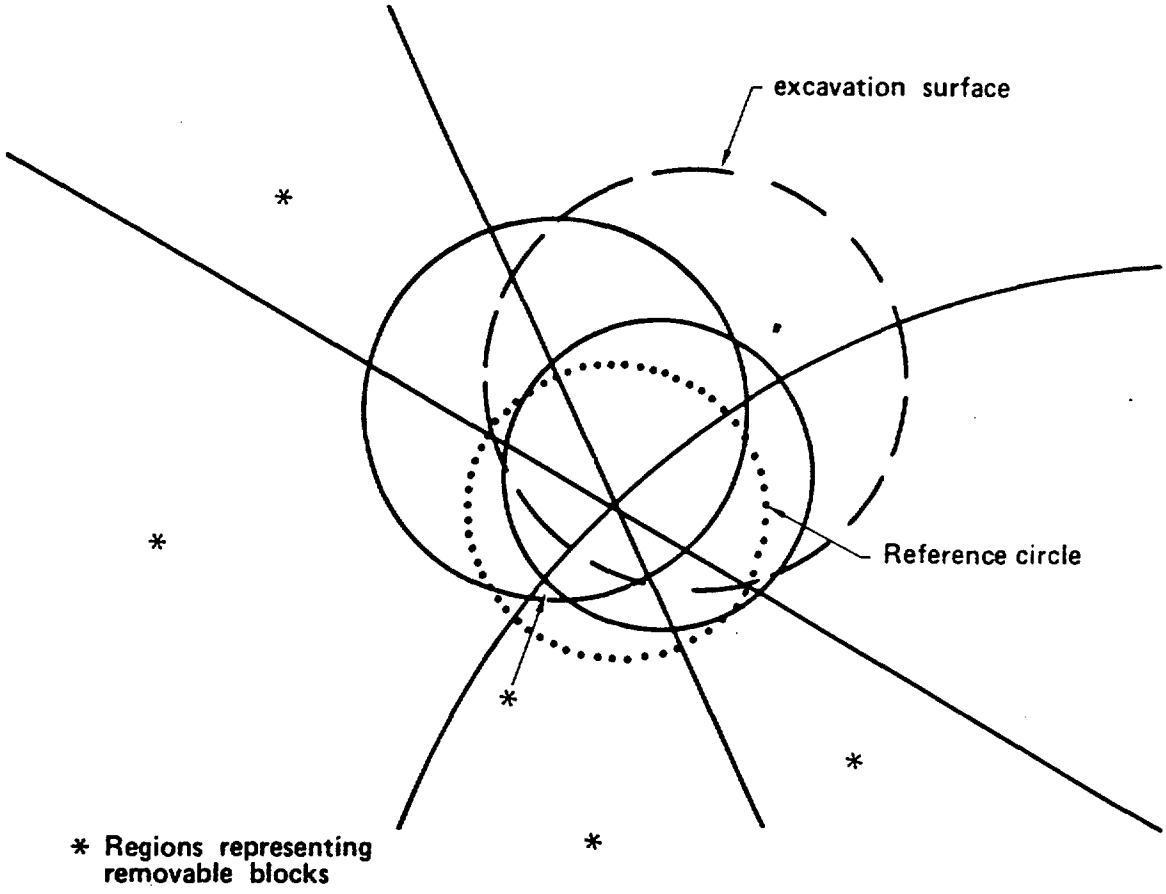

Figure 4.9c Keyblock analysis for north shoulder of Spent Fuel Test canister drift.

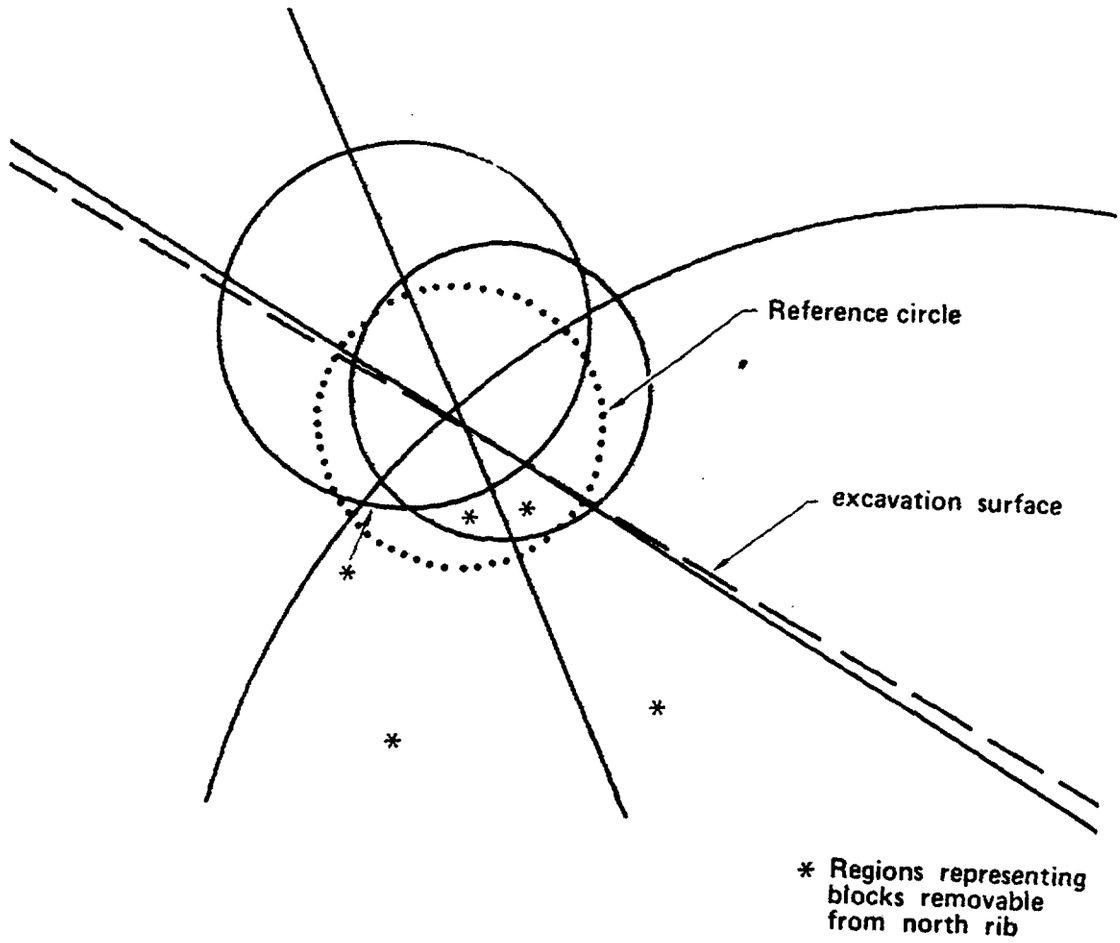

Figure 4.9d Keyblock analysis for rib of Spent Fuel Test canister drift.

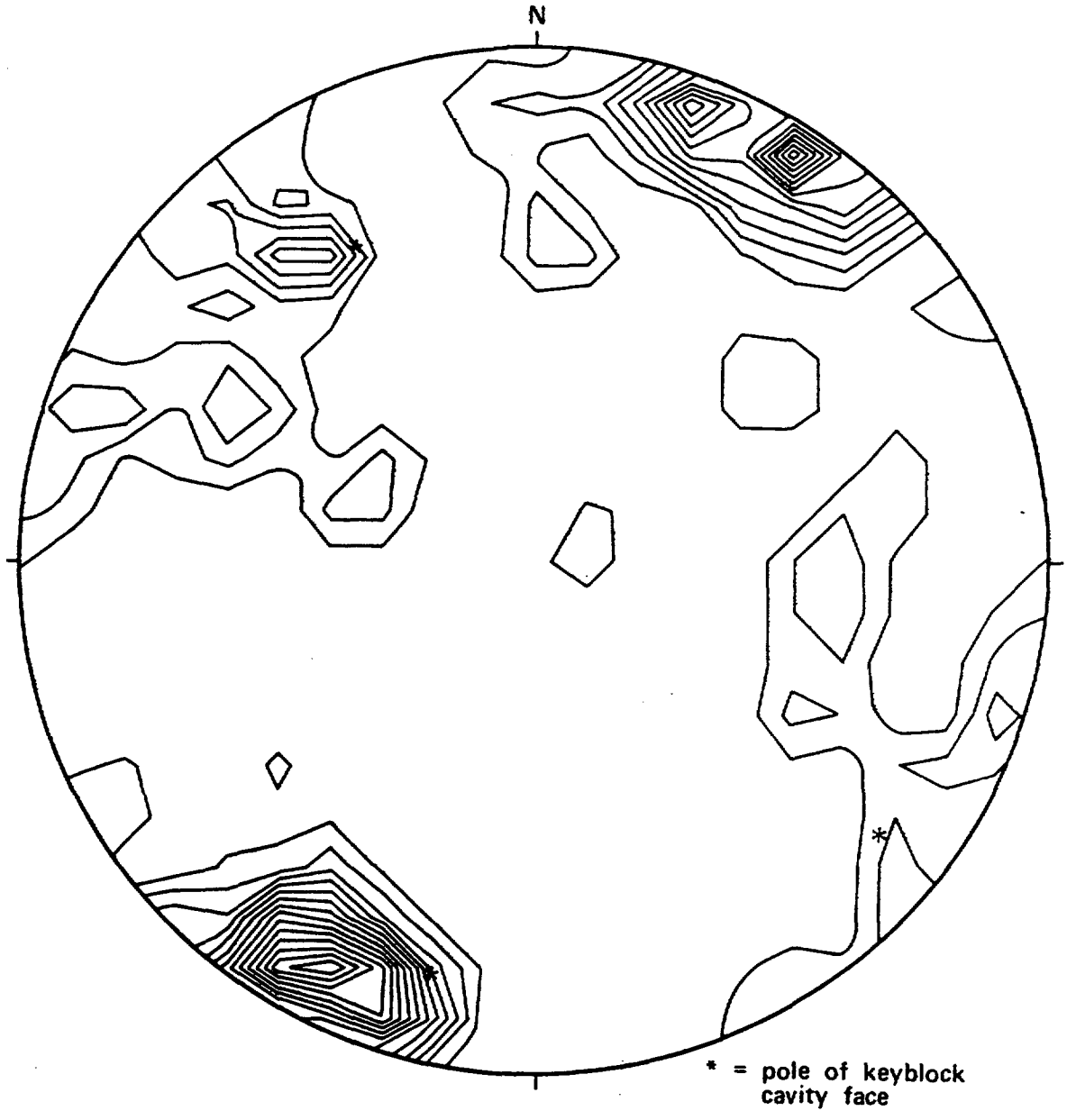

Figure 4.10 Lower hemisphere concentrations of poles of fractures mapped in G-tunnel rock mechanics drift (after Langkopf and Eshom, 1982). 1% contour interval.

Much of the difference in keyblock frequency between the Climax stock and G-Tunnel is apparently due to the difference in jointing between the two sites. At the Climax stock, Wilder and Yow (1984) identified four pervasive joint sets, four less prominent joint sets, and three shear sets. In contrast, Langkopf and Eshom (1982) identified only steeply dipping sets at Sandia National Laboratories' rock mechanics drift in G-Tunnel, near where the keyblock was mapped. Table 4.3 summarizes the nature of the keyblocks mapped in each setting. It will be noted that three discontinuities intersect to create each observed keyblock. In most cases in the Climax granite, a low angle (shallow dip angle) joint combined with two steeply-dipping features to form and release the block. Inspection of Figure 4.10 reveals that the G-Tunnel tuff has no such set of low angle discontinuities to provide block release, and the one keyblock mapped in G-Tunnel indeed was formed by three steeply-dipping fractures. However, fracturing does change from unit to unit within the tuff, and a considerable amount of scatter can be seen in Figure 4.10. Identification of keyblocks from the tuff discontinuity data may thus not be as straightforward as for the granite, where the jointing is more completely defined.

The contrast in keyblock frequency between the SFT-C drifts and the Piledriver drifts is important because it illustrates the effect of tunnel orientation on keyblock occurrence. As listed in Table 4.1, the SFT-C drift observations included four keyblocks in 700 feet of drift, while the Piledriver drift observations included nine keyblocks in less than 100 feet of drift. Both sets of excavations are located

Table 4.3 Summary Descriptions of Measured Keyblocks

Tunnel	Station/Location	Description of Keyblock
Piledriver Drift	2 + 22/shoulder of north rib	formed by one low angle and two near-vertical discontinuities; block fallen
Piledriver Drift	2 + 45/shoulder of north rib	formed by one low angle and two near-vertical discontinuities; block fallen
Piledriver Drift	2 + 05/south side of tunnel crown	formed by one low angle and two steeply-dipping discontinuities; block fallen
Piledriver Drift	2 + 22/in crown	formed by three steeply-dipping discontinuities; block fallen from sagging rock beam
Piledriver Drift	2 + 22/in crown	formed by three steeply-dipping discontinuities; block still in place
Piledriver Drift	2 + 55/south rib	formed by one low angle and two near-vertical discontinuities; block fallen but truncated
Piledriver Drift	2 + 60/south rib at springline	formed by three steeply-dipping discontinuities; located in intensely fractured zone
Piledriver Drift	2 + 80/south rib	formed by one low angle and two steeply-dipping discontinuities; block fallen but truncated
G-Tunnel	north rib of extensometer drift	formed by three steeply dipping discontinuities; block fallen(1)

NOTES: (1) not back-analyzed because large included angle of apex made failure inevitable.

within the Climax stock, and both encountered essentially the same geologic structure (Wilder and Yow, 1984). The excavations were in all cases made with drill and blast techniques. The remaining primary source of block frequency variation is the orientation of the openings with respect to the geologic structure.

Figure 4.9a shows a whole stereographic projection of the four predominant joint sets found by geologic mapping at the 420 meter level in the Climax stock, along with a fifth less dominant set that was observed to form one face of some of the keyblocks. The reference circle for this upper hemisphere projection is shown as a dotted circle. Superimposed as a dashed line on the plot is a plane representing an excavation surface dipping at 45° to form the north shoulder of the drift. The area within the dashed circle represents the rock mass forming the shoulder of the drift, while the area of the plot falling outside the dashed circle represents the free space created by the excavation. Blocks are delineated by regions (joint pyramids) formed by the intersection of discontinuities (solid lines) on the projection. The blocks that are shaped such that they can displace into the excavation are designated by asterisks on the drawing. Figure 4.9b is a similar projection with the dashed line indicating a vertical rib of the Piledriver drift. The asterisks in 4.9b indicate potential keyblocks in the north rib of the drift. Figure 4.9c represents the north shoulder of the SFT-C canister drift and heater drifts, and Figure 4.9d represents the vertical ribs of these SFT-C drifts. In 4.9c the asterisks mark potential keyblocks in

the north shoulder of the drifts, and in 4.9d they mark keyblocks potentially removable from the north rib of these drifts.

Inspection of the four whole stereographic projections of Figure 4.9 reveals the cause of the differences in keyblock frequency between the SFT-C and Piledriver drifts. Comparing first the plots that represent the north shoulders of the drifts (Figures 4.9a and 4.9c), it is seen that the Piledriver drift encounters six geometric forms of potential keyblocks, while the SFT-C drifts encounter only five. Since small regions on the stereographic projection represent slender keyblocks, one of the possible keyblock forms in the SFT-C drift shoulders is relatively insignificant in size, leaving four main keyblock forms for this excavation surface. This implies that the north shoulder of the Piledriver drift can encounter about half again as many geometric keyblock forms as the north shoulder of the SFT-C drifts. A similar comparison for keyblocks potentially removable from the north ribs of the two drift settings defines five block types for the Piledriver drift, and five for the SFT-C drifts. Again, however, one of the SFT-C keyblock regions is particularly small, leaving four block types for the SFT-C drift north ribs and five for the Piledriver drift north rib.

A second criteria suggested by Shi and Goodman (1982) can also be used to compare keyblock forms in the two drift settings. If corners of the regions indicating blocks come close to the excavation surface, this implies that corresponding lines of intersection between block faces are nearly parallel to the excavation. Such blocks are

relatively thin and do not impose unusually severe requirements on the excavation ground support system, and may in fact fail immediately upon exposure as part of the excavation overbreak. If the four parts of Figure 4.9 are reconsidered in light of this criteria, the north shoulder of the Piledriver drift has two significant keyblock forms and the north shoulder of the SFT-C drifts also has two significant forms. The Piledriver drift north rib has three significant keyblock forms, while the SFT-C drift north ribs have one significant geometric keyblock form. The Piledriver drifts can thus encounter more geometric forms of keyblocks created by the intersecting discontinuities than the SFT-C drifts can, using either criteria for the assessment.

An important aspect of analyzing potentially unstable keyblocks is the size of the block with respect to the tunnel. Whole stereographic projection techniques such as used in Figure 4.9 to identify keyblocks provide only an indication of the geometric shape of each block, and no quantitative definition of keyblock size. Keyblock size is limited by the dimensions of the excavation into which a block can displace. This concept is illustrated by Figures 4.11, 4.12, and 4.13. Figures 4.11a, 4.12a, and 4.13a show a whole stereographic projection for a Piledriver drift shoulder block, crown block, and rib block, respectively. Figures 4.11b, 4.12b, and 4.13b show the corresponding drift sections, maximum possible keyblock sizes, and actual encountered keyblock sizes for these cases. The fact that no keyblocks were encountered having the maximum possible size may be a

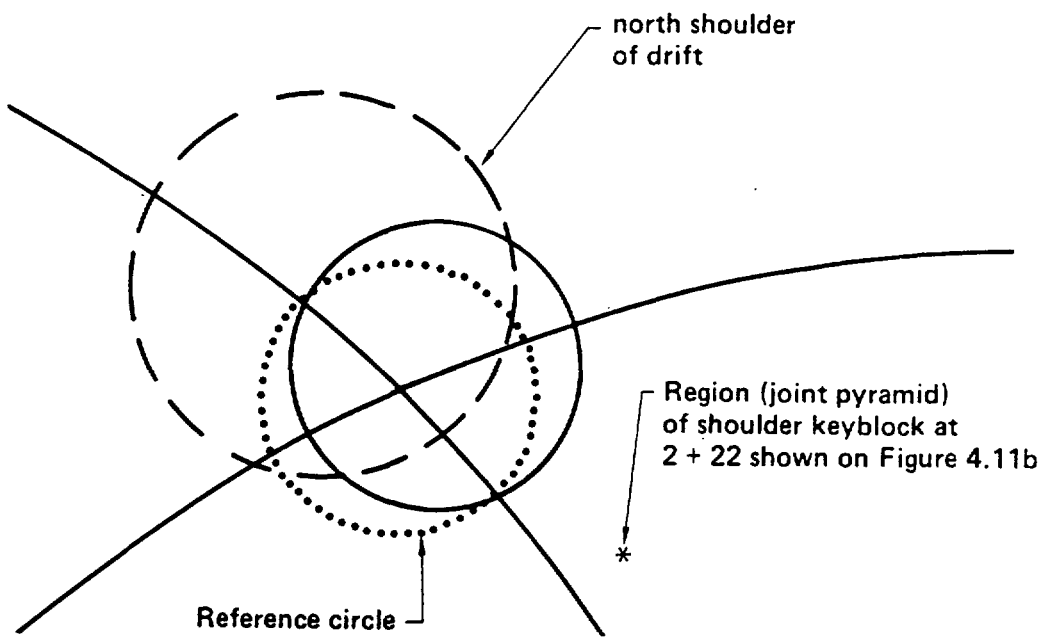

Figure 4.11a Keyblock in north shoulder of Piledriver drift.

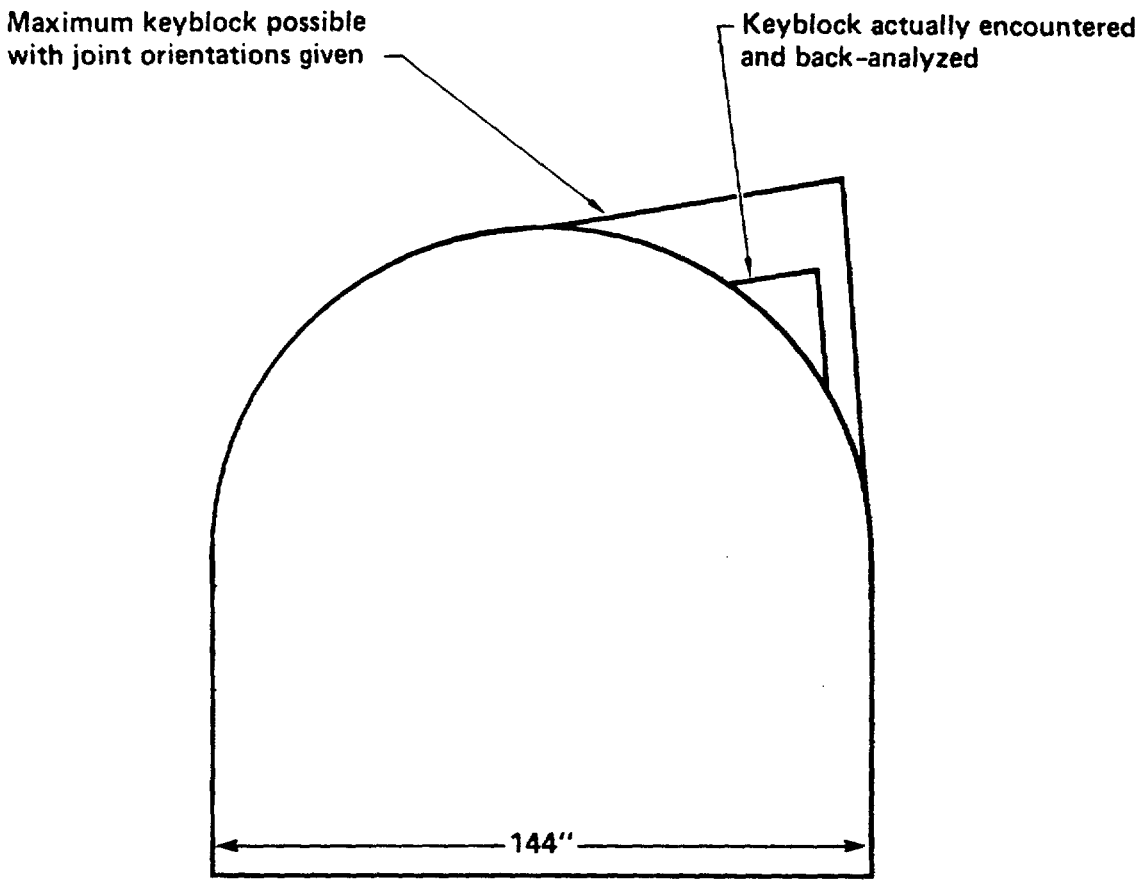

Note: View is looking S56W
along tunnel axis

Figure 4.11b Keyblock in north shoulder of Piledriver drift.

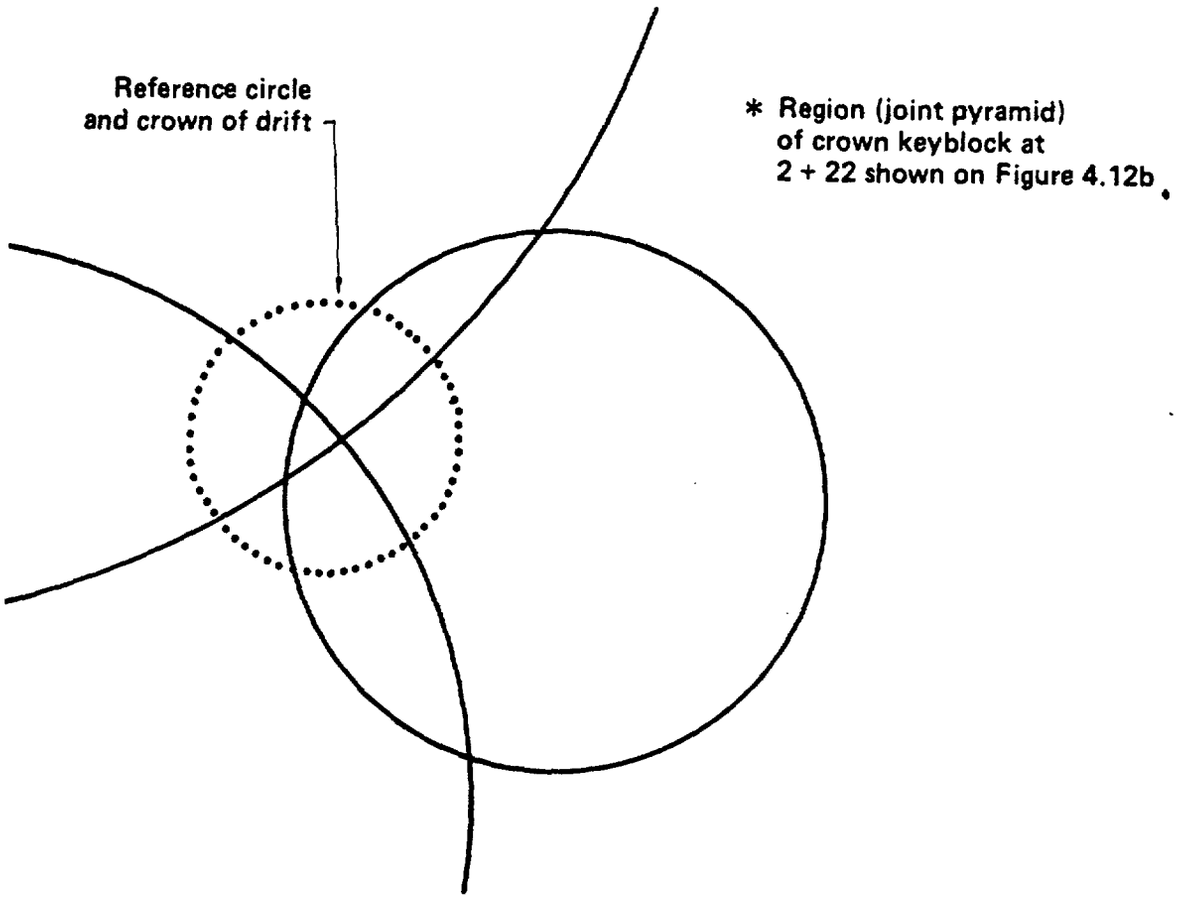

Figure 4.12a Keyblock in crown of Piledriver drift.

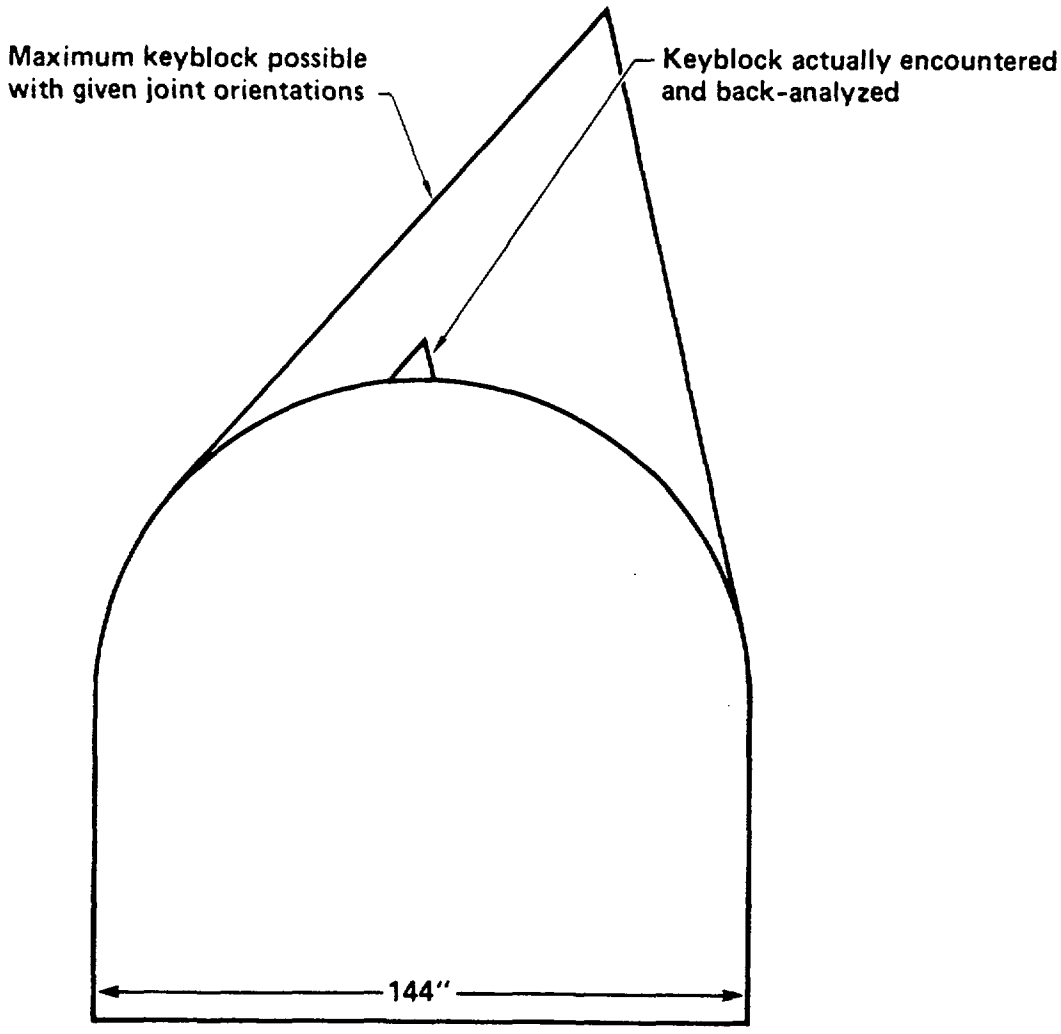

Note: View is looking N56E
along tunnel axis

Figure 4.12b Keyblock in crown of Piledriver drift.

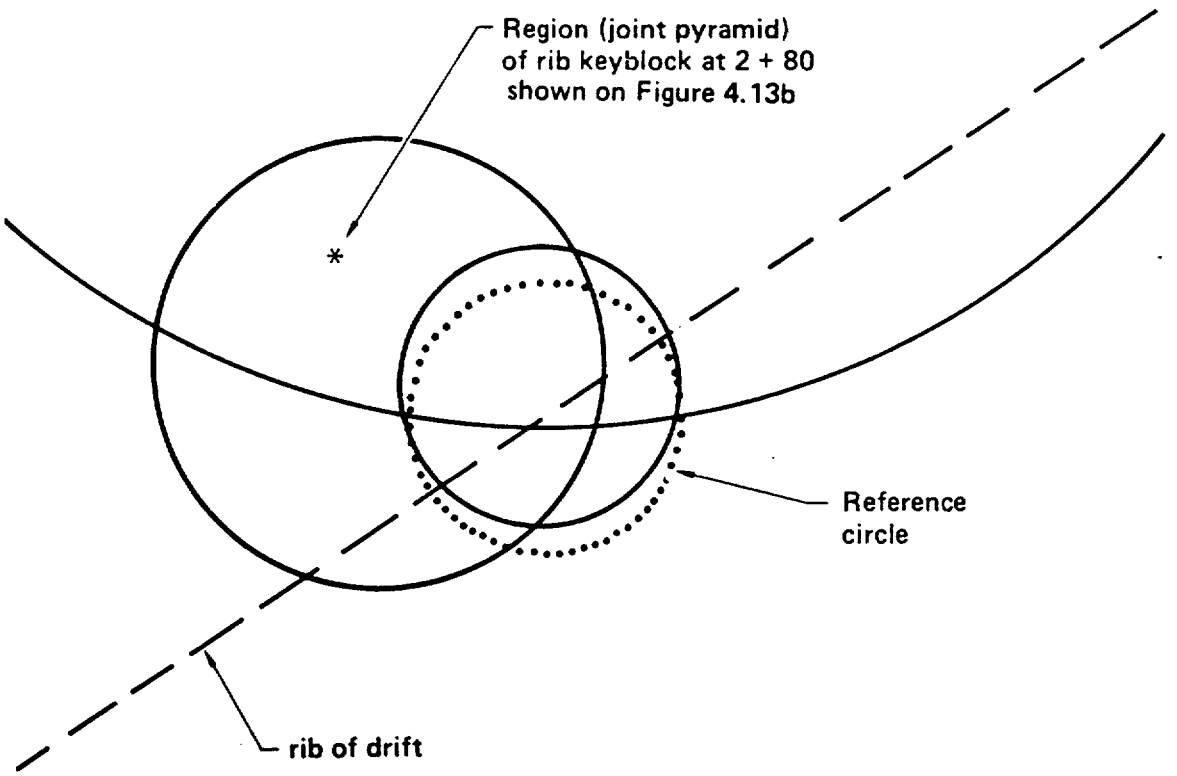

Figure 4.13a Keyblock in south rib of Piledriver drift.

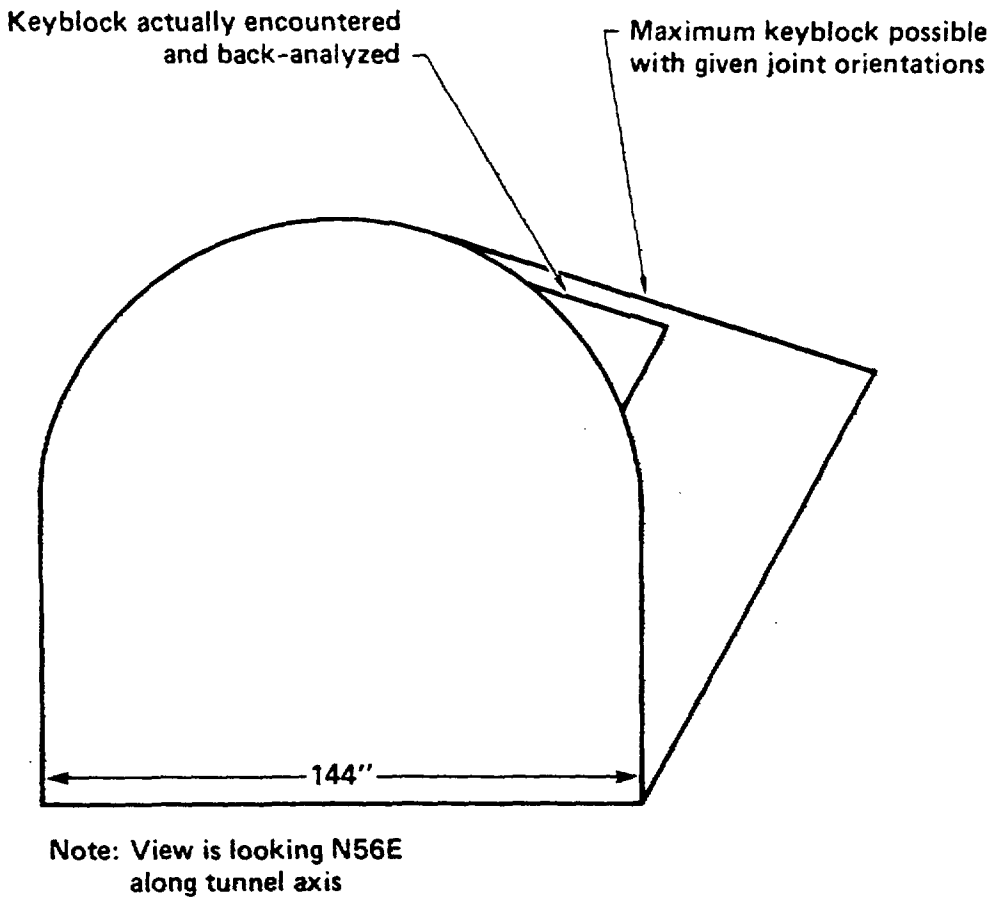

Figure 4.13b Keyblock in south rib of Piledriver drift.

result of a limited length of drift checked for keyblocks, or it may be related to the fact that actual discontinuities are not infinite in extent.

Analyses of Keyblock Stability

Table 4.4 summarizes data (from eight keyblocks in the Piledriver drift) used in the back-analyses done with the three-dimensional block behavior model of Appendix 2, and Table 4.5 summarizes the results. Since all that is known of the behavior of the observed blocks is whether or not they have fallen, and no displacement data is available from development of the failure, the analysis focused on evaluating the block stability at the maximum available resistance to failure. In addition to discontinuity properties, an uncertainty in each calculation was the direction of block displacement. A failure mode analysis was therefore performed for each block using procedures published by Goodman and Shi (1985). The results of the failure mode analysis were used for an initial estimate of displacement direction, because some blocks apparently slid on one plane, some slid on two planes, and some separated on all planes during failure. Once the minimum F/W support ratio was found for the initial displacement direction, the direction was varied in order to locate higher and lower minimum F/W ratios. The block was deemed unstable from the model results if all F/W ratios for the range of displacement directions were greater than zero (factor of safety less than unity). Conversely, the block was indicated to be stable if the F/W ratio went

Table 4.4 Summary of Data Used in Back-Analysis of Keyblocks

Keyblock	Face	Face Strike	Face Dip	JRC	JCS(2) (psi)
2 + 22, north shoulder	1	N65E	85SE	4	8300
	2	N45W	85SW	6	4900
	3	N40W	20NE	5	5000
2 + 45, north shoulder	1	N65E	85SE	6	9800
	2	N50W	88SW	4	7400
	3	N40W	22NE	3	10400
2 + 05, south side of crown	1	N40W	88SW	2	12100
	2	N35E	60NW	3	12100
	3	N40W	20NE	3	9600
2 + 22, crown	1	N15E	60SE	2(1)	5000 (1)
	2	N52E	82NW	2	5000
	3	N42W	76NW	2	5000
2 + 22, crown	1	N15E	60SE	2(1)	5000 (1)
	2	N52E	82NW	2	5000
	3	N45W	85SW	2	5000
2 + 55, south rib	1	N63W	85NE	1	7700
	2	N20E	85NW	3	10100
	3	N50W	26NE	4	17200
2 + 60, south rib	1	N30E	48NW	3(1)	7500 (1)
	2	N50W	75NE	1	7500
	3	N80E	66S	3	7500
2 + 80, south rib	1	N80E	80N	4	10500
	2	N18E	52NW	4	10500
	3	N80E	13N	4	6100

NOTES: (1) Assumed from nearby discontinuity segments.
(2) ϕ_r assumed as 30° from tilt tests on core; in situ stresses after Creveling et al (1984)

Table 4.5 Results of Back-Analysis of Keyblocks

Keyblock	Keyblock Status	Failure Mode	Analysis Result
2 + 22, north shoulder	fallen	slide on one plane	unstable
2 + 45, north shoulder	fallen	slide on one plane	unstable
2 + 05, south side of crown	fallen	slide on two planes	unstable
2 + 22, crown	fallen	free fall	stable(1)
2 + 22, crown	in place	free fall	stable
2 + 55, south rib	fallen	slide on two planes	unstable
2 + 60, south rib	fallen	free fall	stable(2)
2 + 80, south rib	fallen	slide on one plane	unstable

NOTES: (1) This block is at the edge of a sagging slab of rock; the stress assumptions of the analysis may not be valid, or the assumed properties may be wrong.

(2) This block is in a zone of intensely fractured rock; the stress and stiffness assumptions of the analysis may not be valid, or the assumed properties may be wrong.

below zero, since a negative F/W represents a force needed to pull the block out (factor of safety greater than unity).

Table 4.5 lists two cases where the numerical model erroneously predicted a fallen keyblock to be stable. As noted in the table, one block was in the edge of a sagging slab of granite, and the rock may well have experienced a significant drop in confining stress. A similar but larger block at the same tunnel station was stable, but was located somewhat back from the edge of the slab. The model assumptions regarding initial stresses were thus probably incorrect for the block at the slab edge. In the second case, the block was in a very intensely fractured zone, and the stiffness assumptions may have been at fault. Both cases also involved assumed shear strength values, which may have been in error.

In general, Table 4.5 indicates a good correlation between numerical model results and field observations, except for the two special cases that were described above. However, these back-calculations provide only a check on the ability of the keyblock behavior model to evaluate block stability. Physical model studies performed and published by Crawford and Bray (1983) were therefore back-analyzed with the two-dimensional model as a check on its ability to calculate pullout forces necessary to destabilize a block.

Analyses of Physical Models

Figure 4.14a shows the geometry of the plaster model used by Crawford and Bray (1983). The tests modeled two-dimensional wedges subjected to a tangential stress field in the flat roof of an underground excavation. Plaster wedges were fit into slots or cavities in a slab of plaster that represented the rock over the excavation. Horizontal stresses paralleling the excavation surface were then applied to the edges of the slab, and the block was slowly pulled out of place to simulate failure. A proving ring assembly measured the force required to "fail" the block. Blocks of various apex angles were tested by Crawford and Bray at a range of horizontal stress values.

Figure 4.14b shows the approximation of the test geometry that was used with the two-dimensional numerical model of Appendix 1. The numerical model requires a circular excavation, and so a circular opening of very large radius was used along with far-field stress values necessary to create the required pre-displacement stress regime around the block. The initial horizontal stress distribution in the physical model was uniform; the corresponding distribution of tangential stresses in the numerical model varied by less than 2.5 percent from the uniform distribution. Linear discontinuity behavior was assumed with $\phi = 32°$, and $i = 0°$, based on shear strength properties published by Crawford and Bray. Linear stiffness assumptions affect the magnitude of block displacement at failure much

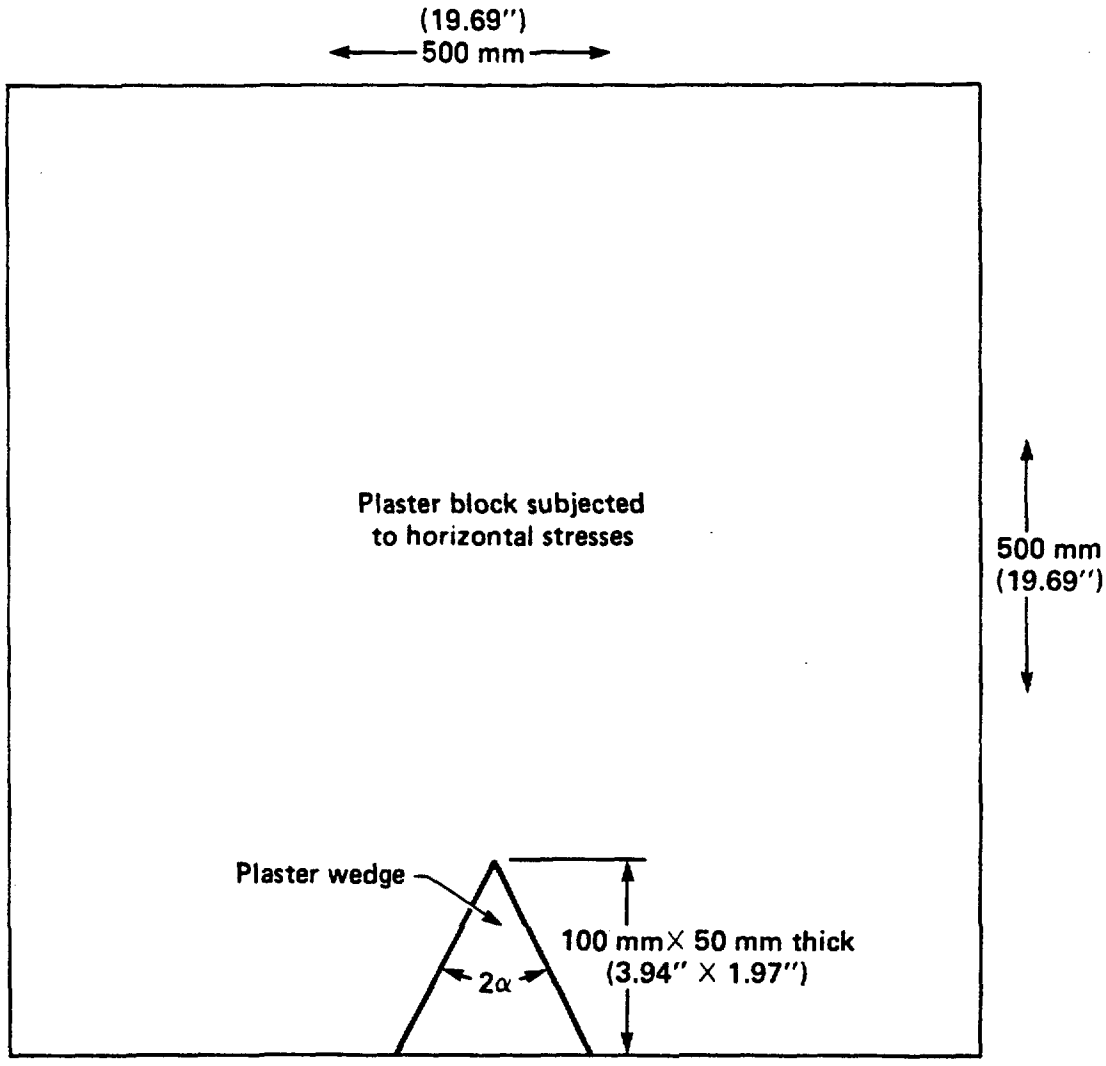

Figure 4.14a Geometry of physical model tested by Crawford and Bray (1983)

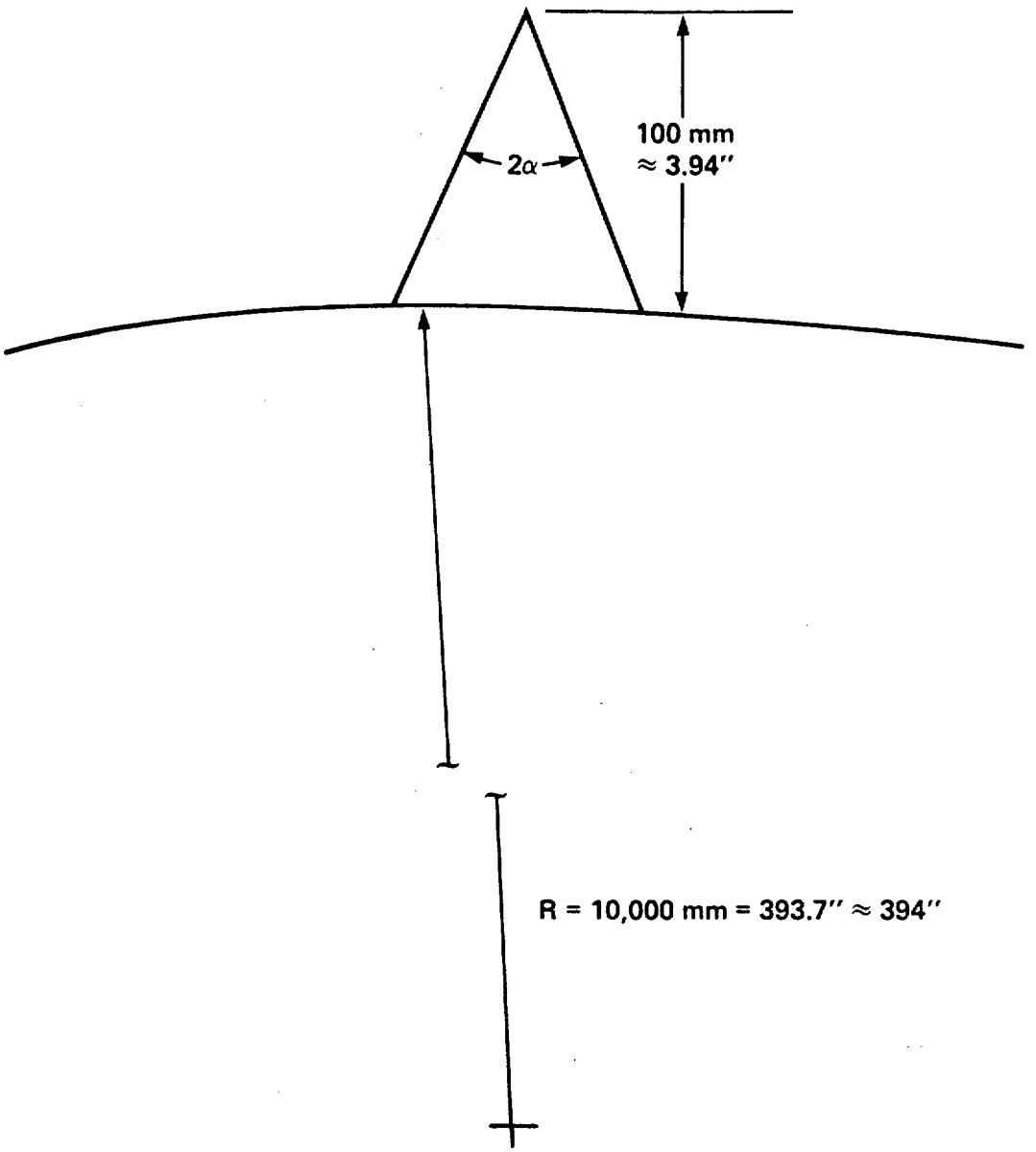

Figure 4.14b Geometry used with 2D code to back-analyze model

more strongly than they do the pullout force; these values were assumed as k_n = 10,000 psi/inch and k_s = 100 psi/inch.

Symmetric wedges with included apex angles of 60°, 50°, and 40° were back-analyzed; these correspond to models tested by Crawford and Bray (1983). Typical resulting pullout forces are plotted in Figure 4.15 for numerical model results and physical model tests for the 60° included angle. The slope of the line representing the numerical model results matches well the slope of a line drawn through the physical model results. However, the latter is offset downward, indicating a pullout stress at zero confining pressure of about -0.5 MPa (-72.5 psi). Pullout stress is the pullout force divided by the area of the excavation surface formed by the keyblock; in this case the negative sign indicates a required amount of support pressure. The offset indicates a problem with the physical model since the maximum support force for a completely failed block should be the block weight. This equates to a minimum pullout stress of about -0.006 MPa (-1 psi). Crawford and Bray noted that there were problems with the seating of the wedge in the surrounding "rock mass" for each test and this may be the source of the offset. Similar offsets were seen in the test results of the physical models for other apex angles. If the data points and line are shifted upward to correct the offset, the back-analyzed line matches the test data nicely.

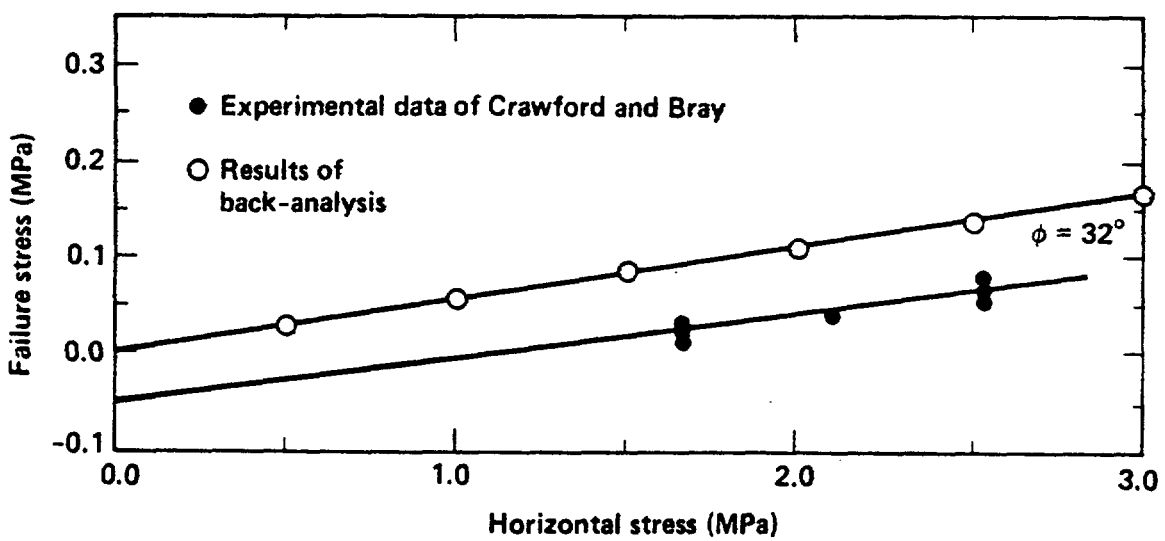

Figure 4.15 Back-analysis of pullout force measured in physical model by Crawford and Bray (1983).

CHAPTER 5 PARAMETER EFFECTS ON KEYBLOCK STABILITY

Back-analysis of field observations of fallen and stable keyblocks indicates that the three-dimensional numerical model can be used to estimate keyblock stability. Back-analysis of laboratory tests of block pullout force under various confining pressures indicates that the two-dimensional numerical model can be used to estimate pullout force, which is a different way of expressing block stability. Both numerical models use the same representations of discontinuity strength and deformation, and both apparently can be used to evaluate the stability of keyblocks if appropriate information is available or can be estimated for block geometry, in situ stresses, and discontinuity properties. This chapter describes the results of parametric studies that were used to examine the ways in which stresses, discontinuity stiffness and shear strength, block geometry, and displacement affect stability. Some inherent limitations of the stability analysis methods are discussed before presenting the results of the scoping calculations.

Description of Keyblocks Used for Studies

Figure 5.1 shows the symmetrical two-dimensional and three-dimensional keyblocks used for most of the parametric studies. A horizontal tunnel with a radius of 72 inches (1.8 m) was modeled; the radius from the tunnel centerline to the block apex was 96 inches (2.4 m). Each discontinuity forming a block face dips at 60° below horizontal, and joint apertures for negligible normal stress are 0.04

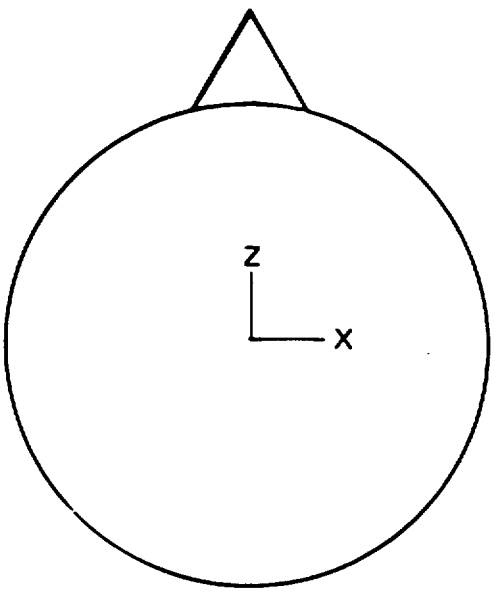

Figure 5.1a Typical symmetric keyblock used for two-dimensional studies.

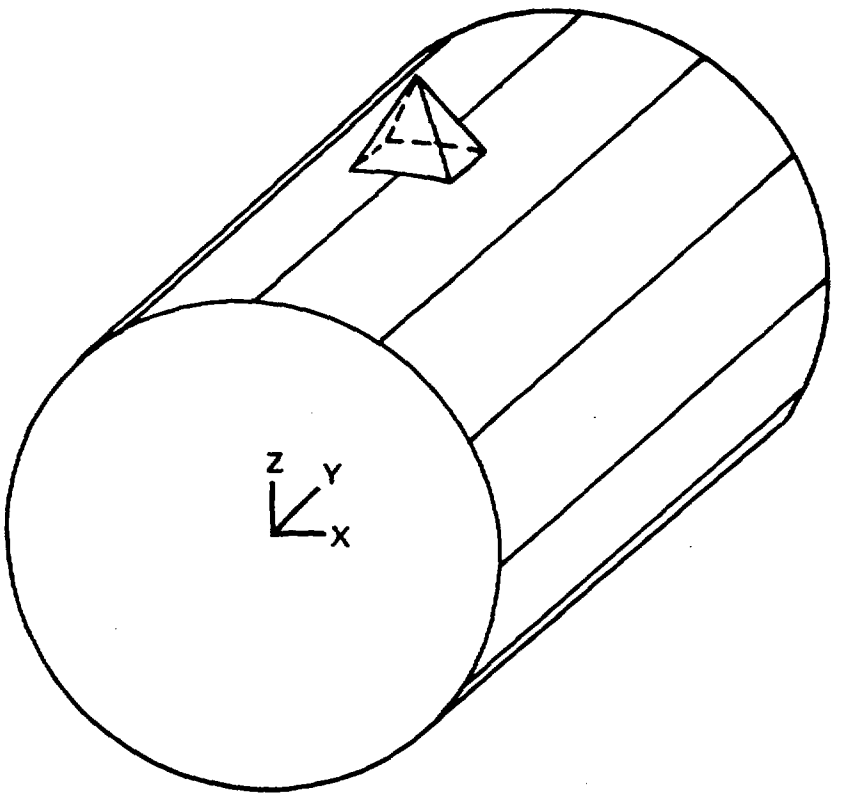

Figure 5.1b Typical symmetric keyblock used for three-dimensional studies.

inches (0.001 m). In situ principal stresses prior to excavation of the tunnel are assumed to act vertically and, in a horizontal plane, at 45° angles from the tunnel axis.

Table 5.1 lists in three categories the parameters that were studied for their effect on keyblock stability. In addition to the parameters listed in Table 5.1, a comparison was made of two-dimensional versus three-dimensional model results and of linear and nonlinear representations of discontinuity behavior. Block stability is a function of all of these parameters, but some parameters influence stability more strongly than do others. In the studies below, only one parameter was varied at a time. The results were plotted on similar scales so that the relative significance of a given parameter in a design problem could be judged from its expected variability and from the gradients of the curves plotted from the parametric studies (Figures 5.2 through 5.15).

Table 5.1 Parameters Examined for Effect on Keyblock Stability

Discontinuity Behavior	Stresses	Keyblock Geometry
shear strength	stress magnitude	block acuteness
deformation stiffness	lateral stress ratio	block size (tunnel size constant)
	thermal loading	block and tunnel size (scale)

All combinations of parameters that were studied used symmetric blocks in the tunnel crown. This was because the stability solution is sensitive to whether or not the selected displacement direction is correct. In a design analysis several different directions of displacement would be examined in a searching sequence that is similar to the way in which a soil mechanics slope stability analysis searches for critical circles along which slope failure would most likely occur. Use of a symmetric crown block allowed the displacement direction to be specified as vertically downward so as to find the results of an analysis as quickly as possible.

Limitations of Stability Analysis Method

The stability solutions provided by the numerical models which implement the equations of Chapter 3 are subject to certain limitations in accuracy because of the sequence in which forces are summed. The selection of two-dimensional versus three-dimensional analysis procedures makes a difference in the results, although it is one that can be anticipated. These factors are in addition to the assumptions about geometry, stiffness, and stresses that were used in developing the equations in Chapter 3.

As described previously, the sequence of operations in evaluating block stability for a given amount of displacement is to first calculate the effect of the displacement on the stresses affecting each block face, and then sum those stresses with the block weight into a resultant force. A possible error that can arise in this

sequence of calculations is the place in the procedure at which the block weight is brought into the equations. An increment of displacement is used to compute a change in normal stress and shear stress on a block face; the shear stress is then constrained by the available shear strength, which is a function of normal stress. A component of the block weight should ideally be included in the normal and shear stress at each grid point. In the analysis models the weight is not brought into the calculations for each displacement increment until the stresses are summed at the end of that increment. This is because of the difficulty of apportioning a component of the block weight to each block face in a generalized solution procedure. For a typical two-dimensional analysis of the block shown in Figure 5.1a this would make a difference of less than 2% in the normal stress at failure, and a difference of about 3% in the shear stress. Investigators do not usually know shear strength to within 3%, for example, and so the effects of the force summation sequence are overshadowed by uncertainties of the input data.

Another source of small errors in the analysis procedures is the iterative approach used in determining a dilation angle for calculating aperture changes in the nonlinear discontinuity behavior equations. In the linear representation the dilation angle (i) is always a constant, but in the nonlinear representation the dilation angle is:

$$i = JRC \log_{10} \left(\frac{JCS}{\sigma_n}\right) \tag{5.1}$$

from equation 3.3. Since σ_n is a function of aperture closure (Figure 3.6), and closure is partly a function of dilatancy, the numerical models use equivalent dilatancy angles from the previous displacement increment rather than iterating to find "current" values of dilatancy angles for use in computing aperture changes. Again, this produces an error in the computed resultant force that is typically of the order of two or three percent. This is not significant for most stability calculations for parametric studies, particularly since the error is systematic.

Recall that F/W is the ratio of resultant support force to block weight. The support force is the force needed to hold the block at equilibrium at the specified level of displacement. Positive F/W ratios thus indicate that an actual supporting force must be applied for the block to be at equilibrium at that displacement, while a negative F/W indicates a pullout force that must be applied to pull the block out to that displacement. Recalling equation 3.26, if $F/W > 0$ then the factor of safety is less than unity, while if $F/W < 0$ the factor of safety is greater than unity.

An unsupported block in a constant stress field could be expected to displace under its own weight until either it fails completely or it reaches a condition of equilibrium at a displacement where $F/W = 0$. Negative F/W values therefore indicate a reserve of stabilizing shear resistance against block failure that can be mobilized by increasing displacements. This presumes that discontinuity properties and loading conditions are constant with time. If displacement continues

past the minimum F/W point, the peak resisting force is surpassed, and the block fails catastrophically as soon as F/W becomes positive. If the block is supported, displacement can continue until the entire block weight is carried by the support (F/W = 1) or equilibrium is reached at an intermediate point.

The selection of two-dimensional versus three-dimensional analysis procedures makes a decided difference in the stability solutions obtained. Figure 5.2 compares block reaction curves for three-dimensional and two-dimensional blocks of the form shown in Figure 5.1. All discontinuities dip at 60° below horizontal, and the problems are equivalent in terms of stiffness, initial stress, and shear strength parameters. Nevertheless, it can be seen that the 2D approach underestimates the stability of the block in comparison to the 3D approach. This is apparently caused by the block confinement and additional strength available in the geometry of the 3D approach. Most parametric studies of this chapter were made with 3D analyses because they are more realistic than 2D calculations.

Keyblock Displacement

As the keyblock of Figure 5.1a displaces from the position that it occupied prior to opening of the excavation, the stresses acting on each block face change continually until the block either fails or becomes stable. Equations for treating these stress changes in either a nonlinear way or as a linear approximation were developed in Chapter 3. Figure 5.3 shows block reaction curves for typical

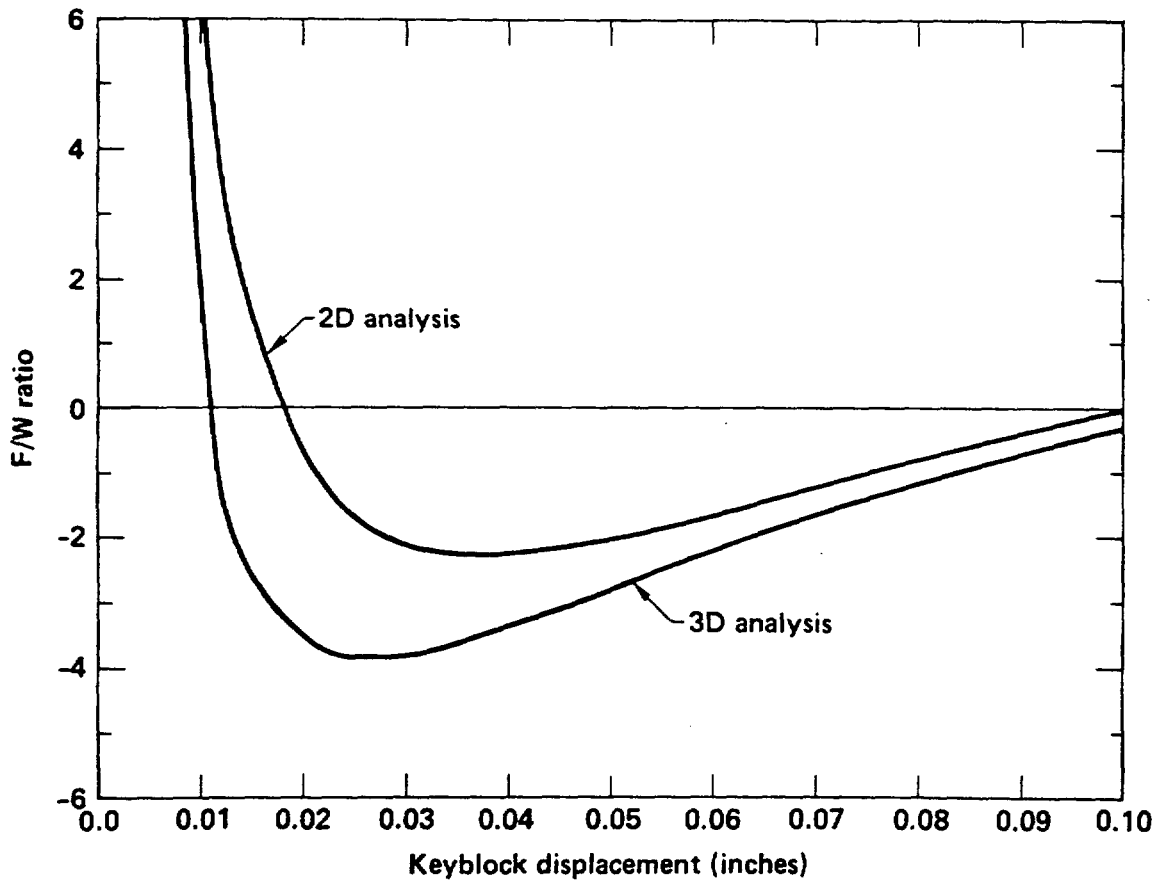

Figure 5.2 Block reaction curves for 2D and 3D analyses. Other parameters same in both cases.

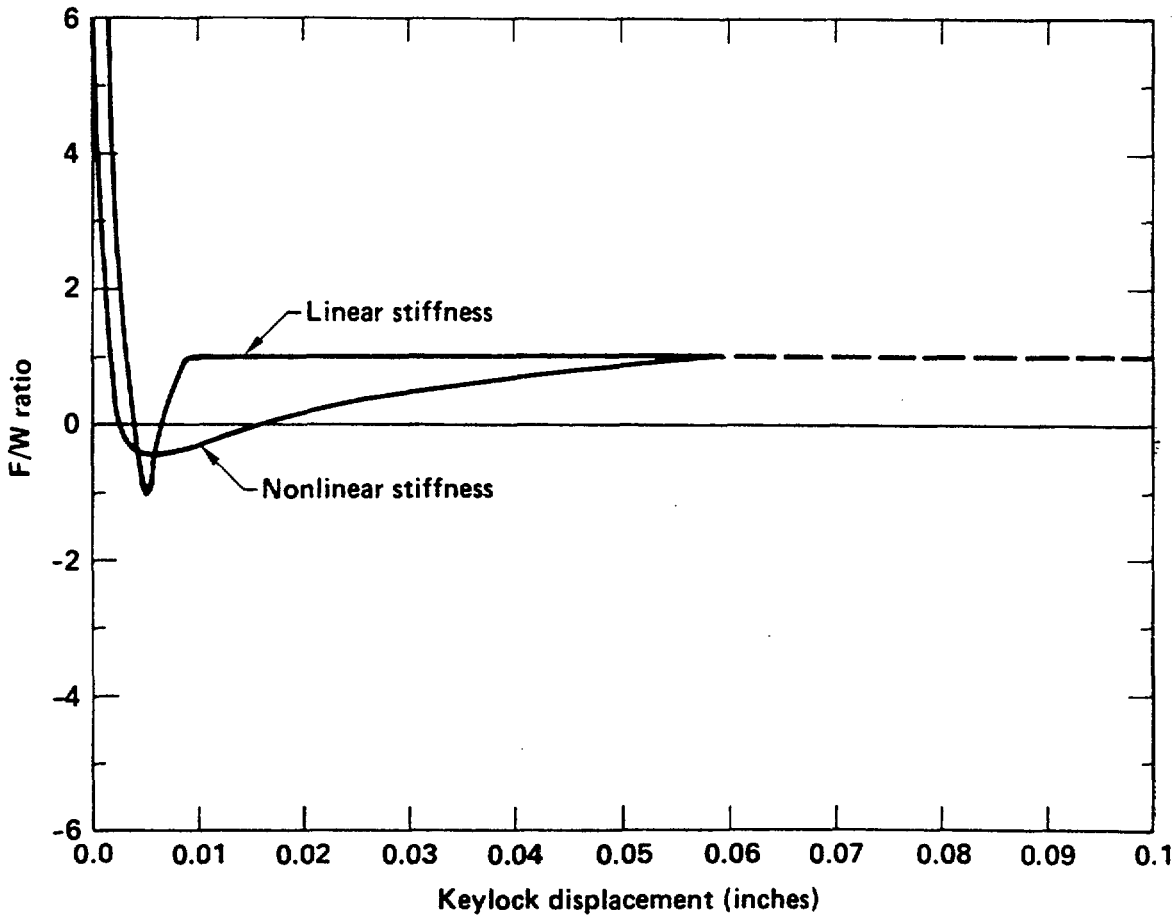

Figure 5.3 Block reaction curves of 3D keyblock for linear and nonlinear discontinuity models.

nonlinear and linear analyses of geometrically identical blocks. It is difficult to estimate properties for linear stiffness and shear strength to perfectly match the results of a nonlinear analysis, so the minimum F/W values seen in the two curves do not quite agree.

Two important results can be seen in the general shapes of these curves, however. First, the block reaction curve descends to a minimum F/W ratio somewhat more quickly for the linear behavior. In other words, the linear approximation results in a faster "unloading" of the block towards equilibrium than does the nonlinear model. Second, and more importantly, once the minimum F/W has been passed the linear model indicates a rapid upward trend to where F/W becomes positive and the block fails. The nonlinear model shows a more gradual rise in F/W once the minimum is surpassed, indicating greater possible keyblock displacement before failure occurs. The nonlinear model is more accurate and is used for most of these parametric studies, but the linear approximation is more conservative for design use <u>if</u> the assumed linear stiffness values are good estimates.

In general, properties used in either type of analysis affect the block reaction curve in two ways. The shear strength values limit the shear stress on the block faces and thus control the minimum F/W value that can be obtained with block displacement, other things being equal. The stiffness properties in turn control the stress changes that occur with displacement, and hence determine the magnitude of displacement that is necessary to get to the minimum F/W, other things again being equal. In other words, the shear strength affects the

lower limit of the curve, while the stiffness affects the magnitude of permissible block displacement.

Figure 5.4 shows the variation of normal stress and shear stress along the face of the two-dimensional block as displacement occurs. A nonlinear discontinuity model was used and a hydrostatic stress field was assumed for this particular analysis. The stress values at minimum displacement gradually drop and become more evenly distributed as block displacement progresses. The leveling of the distributions reflects the initial variation of stresses with distance away from the tunnel, and the modifying influence of the discontinuity strengths and stiffnesses as displacement occurs. This analysis showed the block to be stable, even though the normal and shear stresses dropped continually with displacement. Such a result is possible because the contribution of the normal stresses to forces that drive the block to failure decrease faster than the shear stresses do. This can be seen in the slopes of the curves of Figure 5.4c, and in the following discussion.

Neglecting keyblock weight for the moment, and examining only one face of a pyramidal keyblock that is subject to falling, the stress on the face that contributes to the forces driving the block towards failure is $\sigma_n \sin \beta$. β is the angle between the block face and vertical downward. The forces resisting failure are limited by the available shear strength: $\sigma_n \tan \phi \cos \beta$. If the keyblock is stable, $\sigma_n \tan \phi \cos \beta$ must be sufficiently larger than

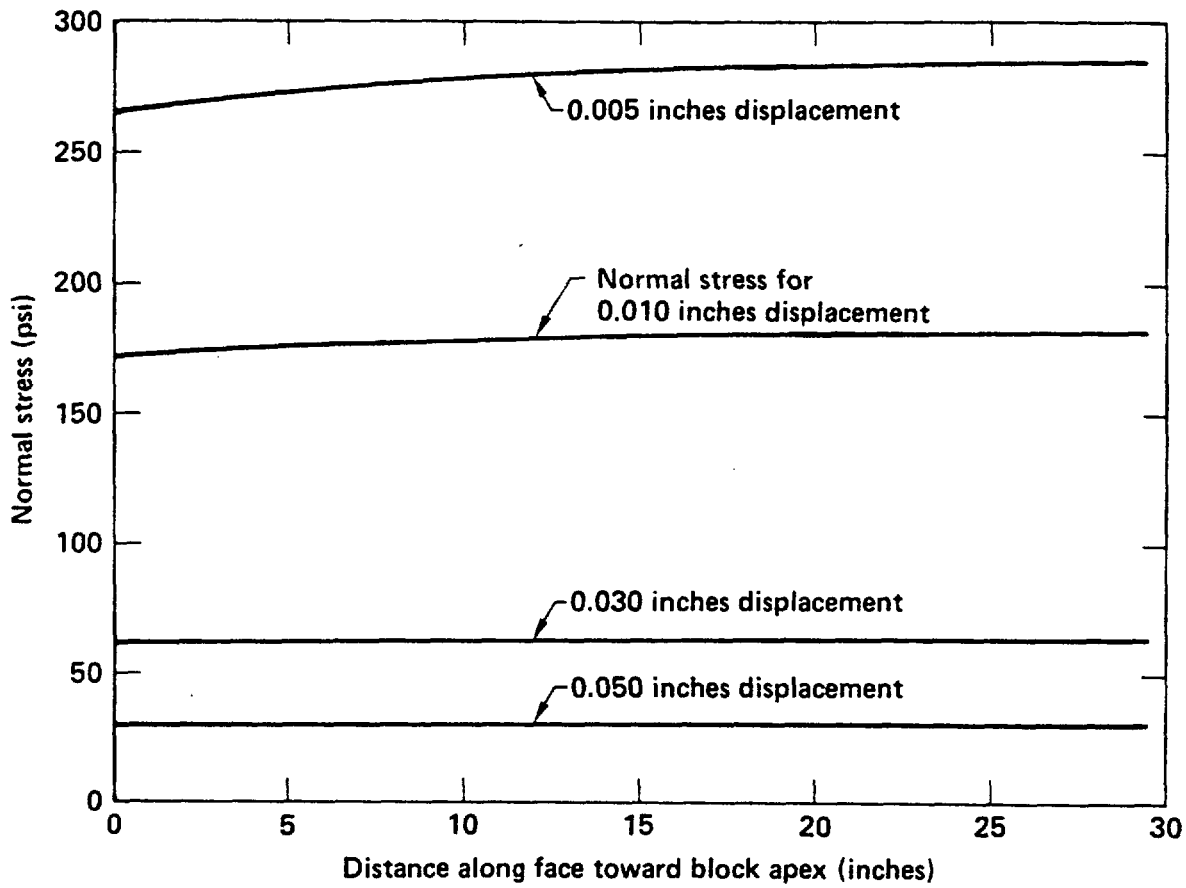

Figure 5.4a Variation of normal stress along face with increasing block displacement.

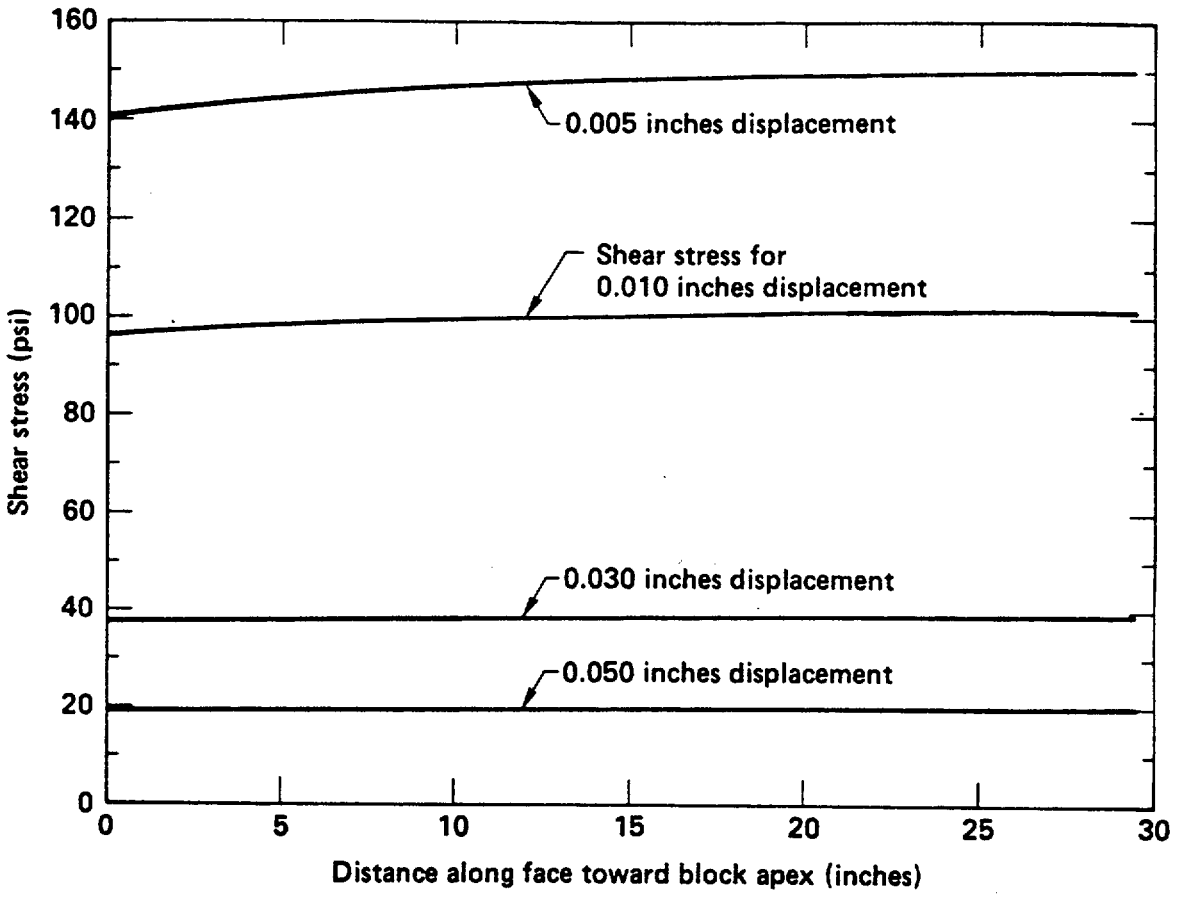

Figure 5.4b Variation of shear stress along face with increasing block displacement.

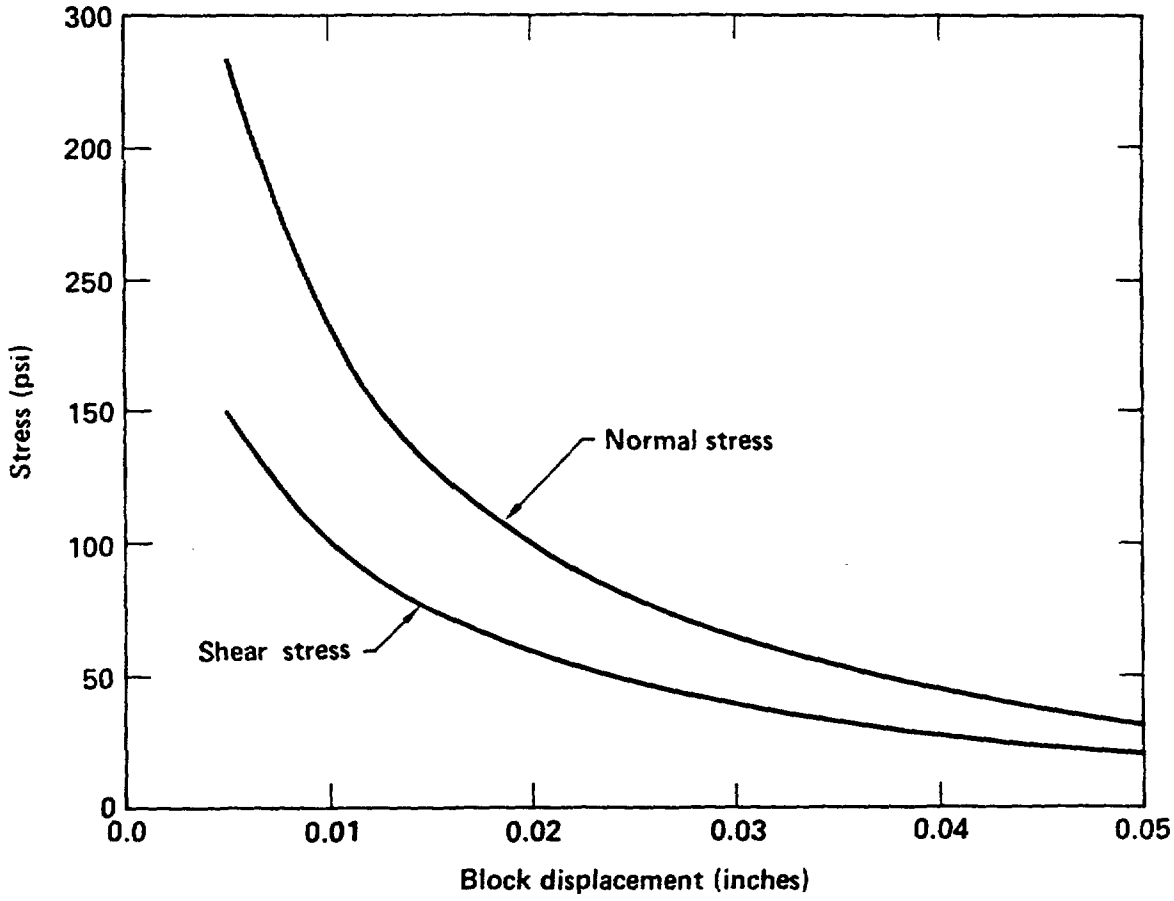

Figure 5.4c Variation in stress at a point on block face near apex during displacement.

$\sigma_n \sin \beta$ to resist a component of the block weight as well as the $\sigma_n \sin \beta$ component. Rearranging, for the block to be stable:

$$\tan \phi > \tan \beta \tag{5.2}$$

Dilatancy and block weight are not included in this equation, but the general trend is apparent.

Discontinuity Shear Strength

The shear strength of each discontinuity making up the keyblock contains a dilatancy component and a friction component. Friction is represented by an angle ϕ_r, while dilatancy is represented by equation 5.1 for nonlinear behavior. These quantities define the shear strength that is available under a given normal stress using equation 3.3. Figure 5.5 shows the ways in which changes in these three parameters affect keyblock stability.

In Figure 5.5a, the minimum F/W ratio that can be achieved for the pyramidal block of Figure 5.1a is plotted as a function of joint roughness coefficient (JRC). This plot assumes a hydrostatic stress field prior to excavation, with a stress magnitude of 500 psi in compression. Joint compressive strength (JCS) is 3000 psi and ϕ_r is 25°. The nonlinear curve indicates that block stability is strongly dependent on dilatancy; this becomes more evident mathematically if equation 5.1 is rearranged slightly so that the exponential effect of JRC can be seen:

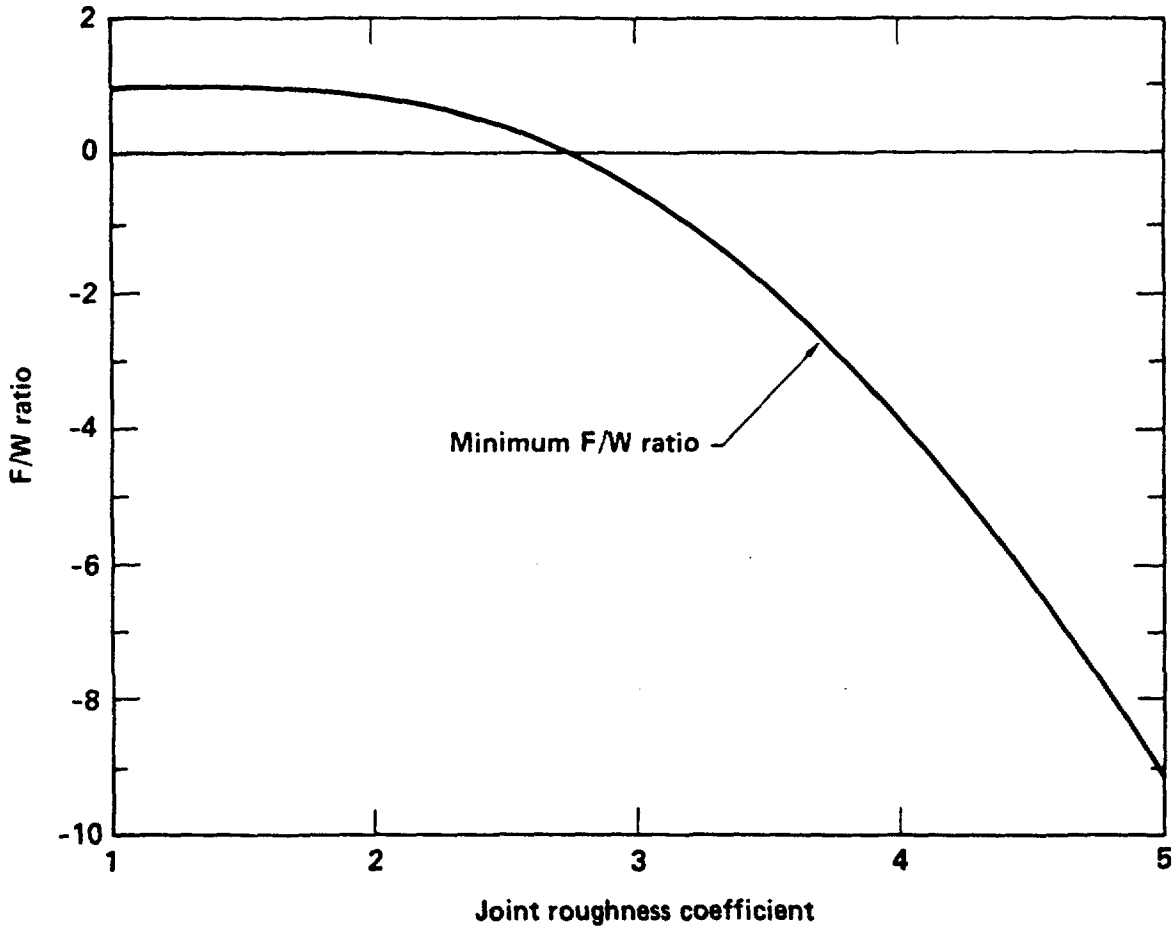

Figure 5.5a Variation of minimum F/W ratio with Joint Roughness Coefficient (JRC).

$$i = \log_{10}\left(\left(\frac{JCS}{\sigma_n}\right)^{JRC}\right) \tag{5.3}$$

Increases in JRC then imply that the discontinuity surface is rougher. This in turn makes the available shear strength larger, and also increases the shear stiffness.

Figure 5.5b shows how the minimum F/W is affected by another variable in the nonlinear formulation for dilatancy. JRC is held at 4 in this case, and $\phi_r = 25°$. F/W ratio is plotted as a function of JCS, and the plot shows that block stability increases as the joint compressive strength increases, although the effect is not as strong as that of JRC. JCS reflects the strength of the asperities that make the discontinuity dilatant; a higher JCS value implies that fewer asperities fail during shear and that correspondingly more must be overridden. Increases in JRC or JCS thus increase the shear strength and slow the decrease in normal stress as the keyblock displaces.

Finally, Figure 5.5c plots the change in minimum F/W ratio as a function of ϕ_r. As expected, increased residual friction makes the keyblock more stable. However, the trend is not quite as pronounced as that of JRC because ϕ_r affects only the available shear strength while dilatancy affects both shear strength and the changes in normal stress brought about by aperture opening or closure.

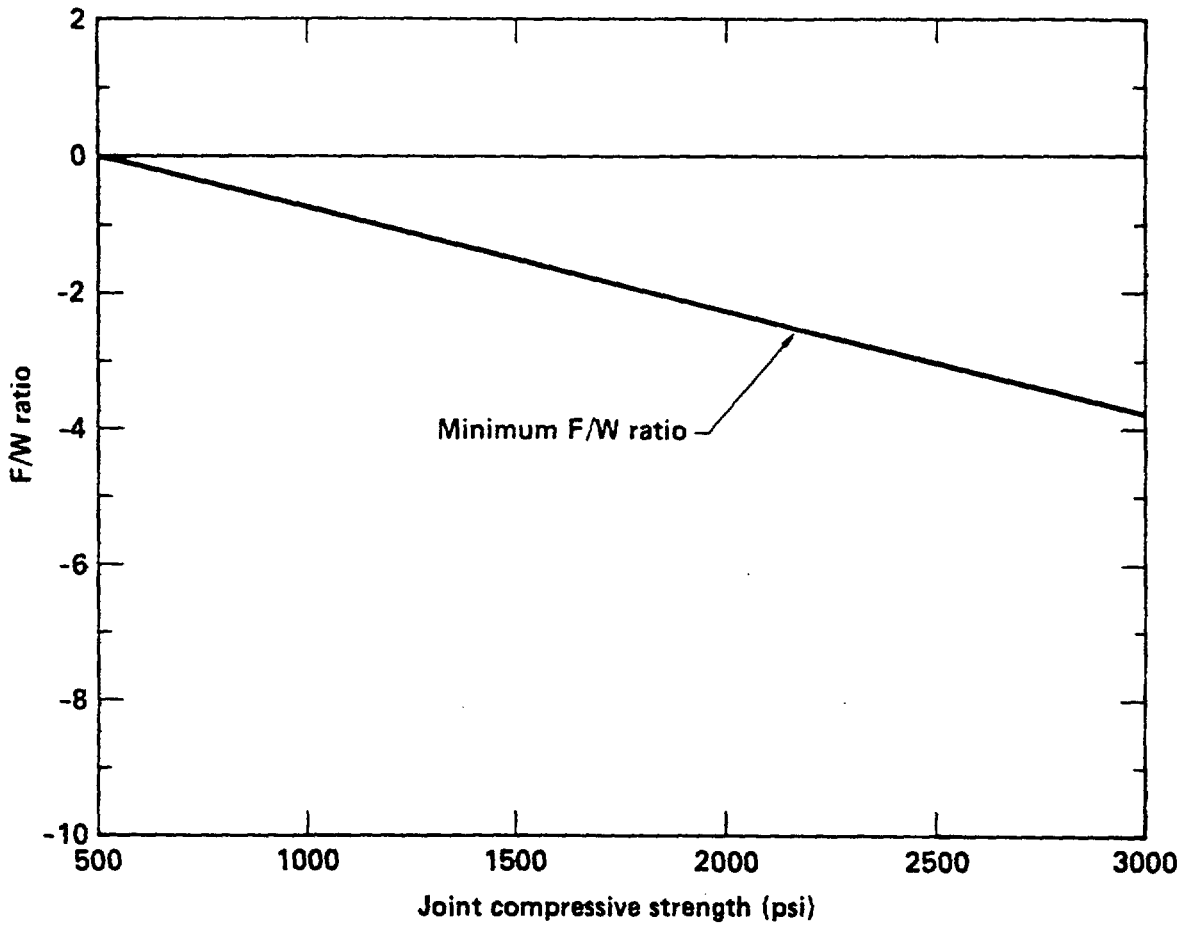

Figure 5.5b Variation of minimum F/W ratio with Joint Compressive Strength (JCS).

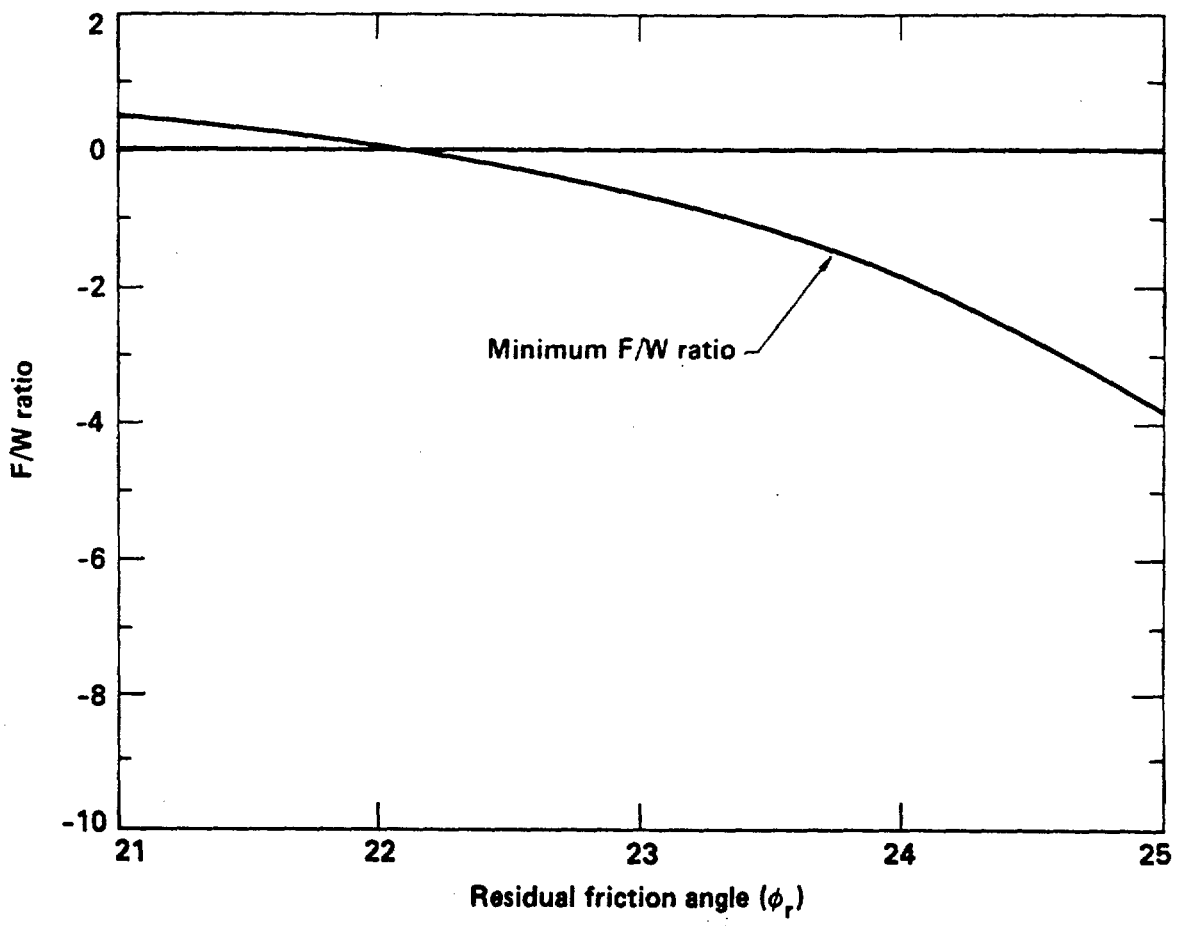

Figure 5.5c Variation of minimum F/W ratio with residual friction angle (ϕ_r).

Discontinuity Stiffness

It was shown in Chapter 3 that discontinuity normal stiffness is related to the initial aperture of the fracture under negligible normal load, and to the given normal stress acting on the fracture in situ. Conversely, the stiffness must affect the changes in stress that are generated by block displacement. The load-deformation relation has been defined by the maximum possible aperture closure and the initial normal stiffness. Figure 5.6 shows how the initial normal stiffness of a discontinuity would be affected by changes in initial aperture (or maximum closure), as defined by equations 3.11 and 3.9 if the normal stress and normal stiffness are held constant. Smaller apertures mean smaller attainable maximum closures, which imply that load-deformation curves such as that in Figure 3.6 must initially slope upward more steeply for tighter discontinuities.

Figure 5.7 shows the variation of minimum F/W ratio with a range of initial normal stiffnesses. Block stability is seen to decrease as normal stiffness increases. This is because the normal stresses decrease more quickly on discontinuities experiencing a given increment of keyblock displacement. The drop in normal stress brings down the available shear strength before the shear stresses can become large enough to support the block. Although this effect is present, it does not appear to be as pronounced as the shear strength effects on keyblock stability discussed above.

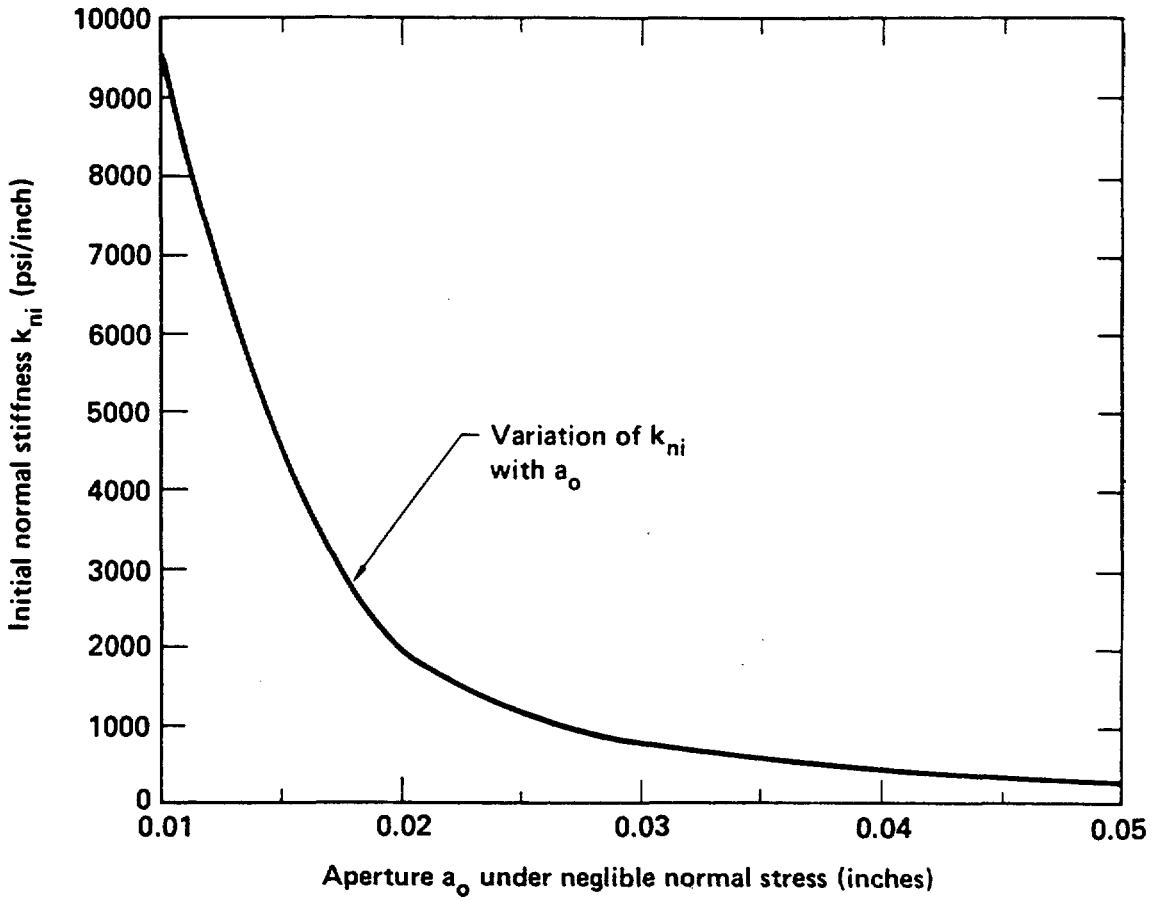

Figure 5.6 Initial normal stiffness versus no-load aperture.

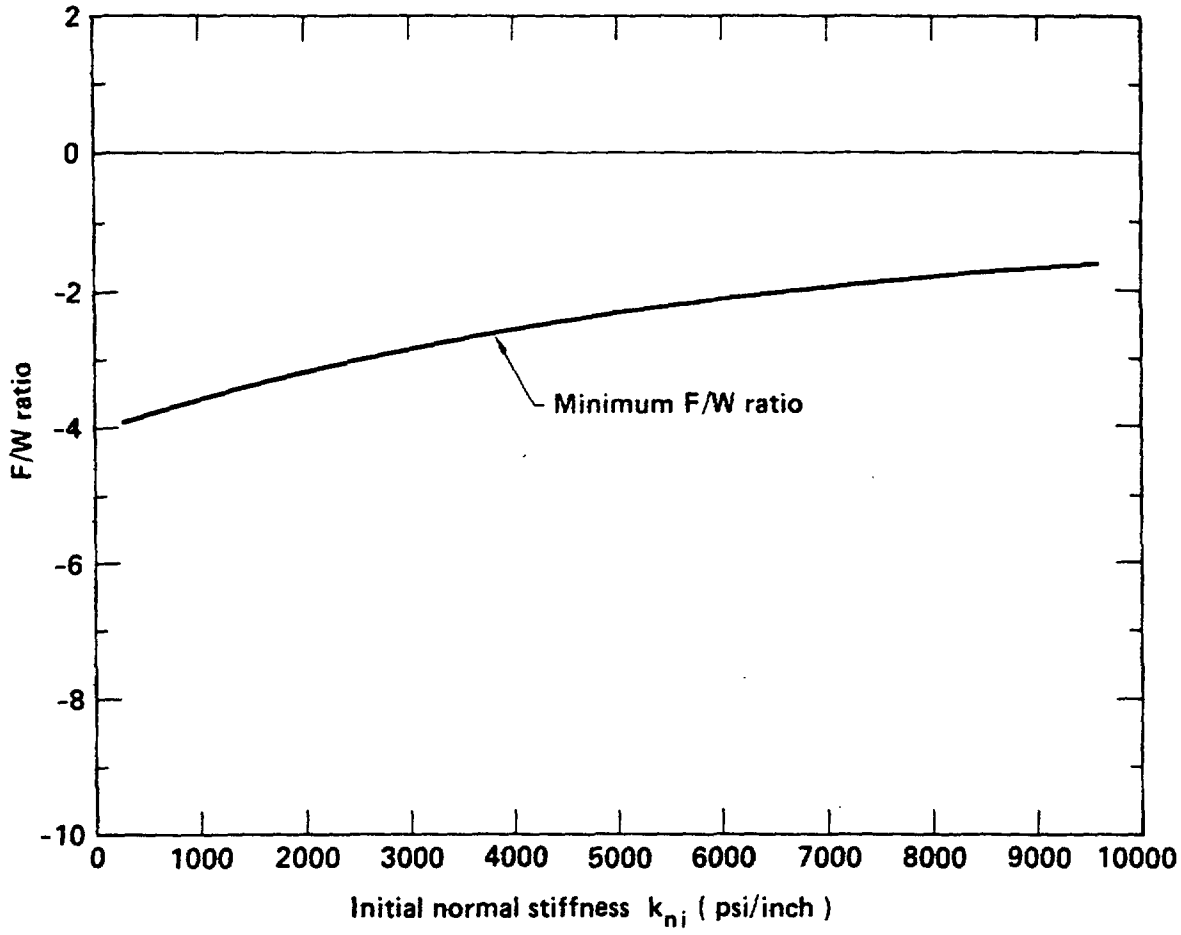

Figure 5.7 Minimum F/W ratio versus initial normal stiffness.

Stresses and Loads

Aside from discontinuity shear strength, the most critical condition affecting the stability of a given keyblock is the stress environment in which it is located. This cannot be studied by simply plugging different stress values into the model and looking at the results because of the effect of normal stiffness variations in situ. As explained in Chapter 3, normal stiffness is a function of normal stress and can be expected to increase as stress magnitudes increase. Conceptually, this should make a rock mass stiffer with depth (Figure 5.8). Discontinuity stiffnesses were adjusted for stress magnitude using the hyperbolic equations of Chapter 3 for single fractures under normal loading, and the E_m values in Figure 5.8 were then calculated using equation 3.4 for various stresses. The plot has a distorted S shape; the early curvature indicates the predominance of discontinuity deformation at low in situ stresses, while the high-stress asymptote is the 1×10^7 psi elastic modulus of the intact rock. The curve approaches this limit gradually as the discontinuities reach maximum closure in this one-dimensional conceptual model.

Different E_m values corresponding to different levels of confining stress were used in the 3D block behavior model to represent overall stiffness changes so that block stability could be examined for the effects of in situ stress magnitude. Figure 5.9 plots the change in minimum F/W ratio that occurs with stress magnitudes varying from 1000 psi to 5 psi, with other parameters (including lateral stress ratio) held constant at 0.5. The trend is for the block to

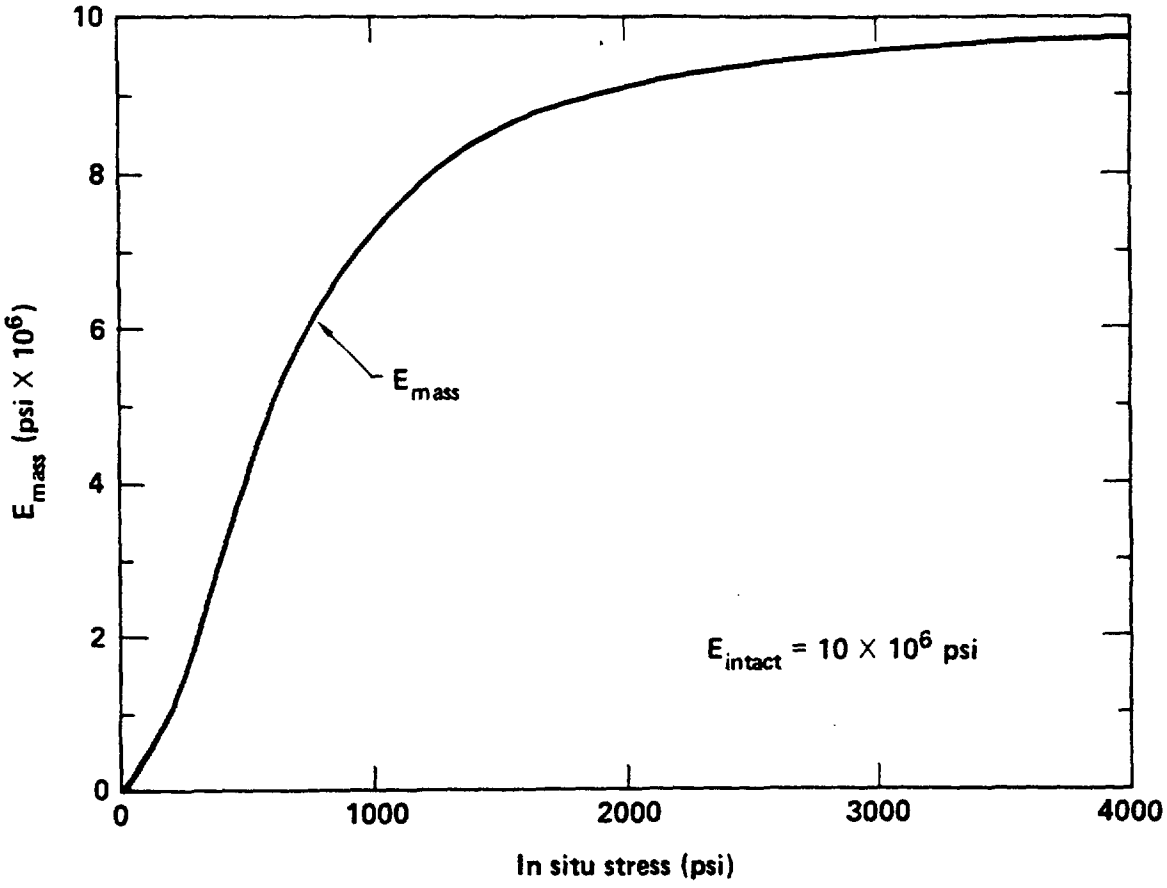

Figure 5.8 Variation of E_{mass} with in situ stress.

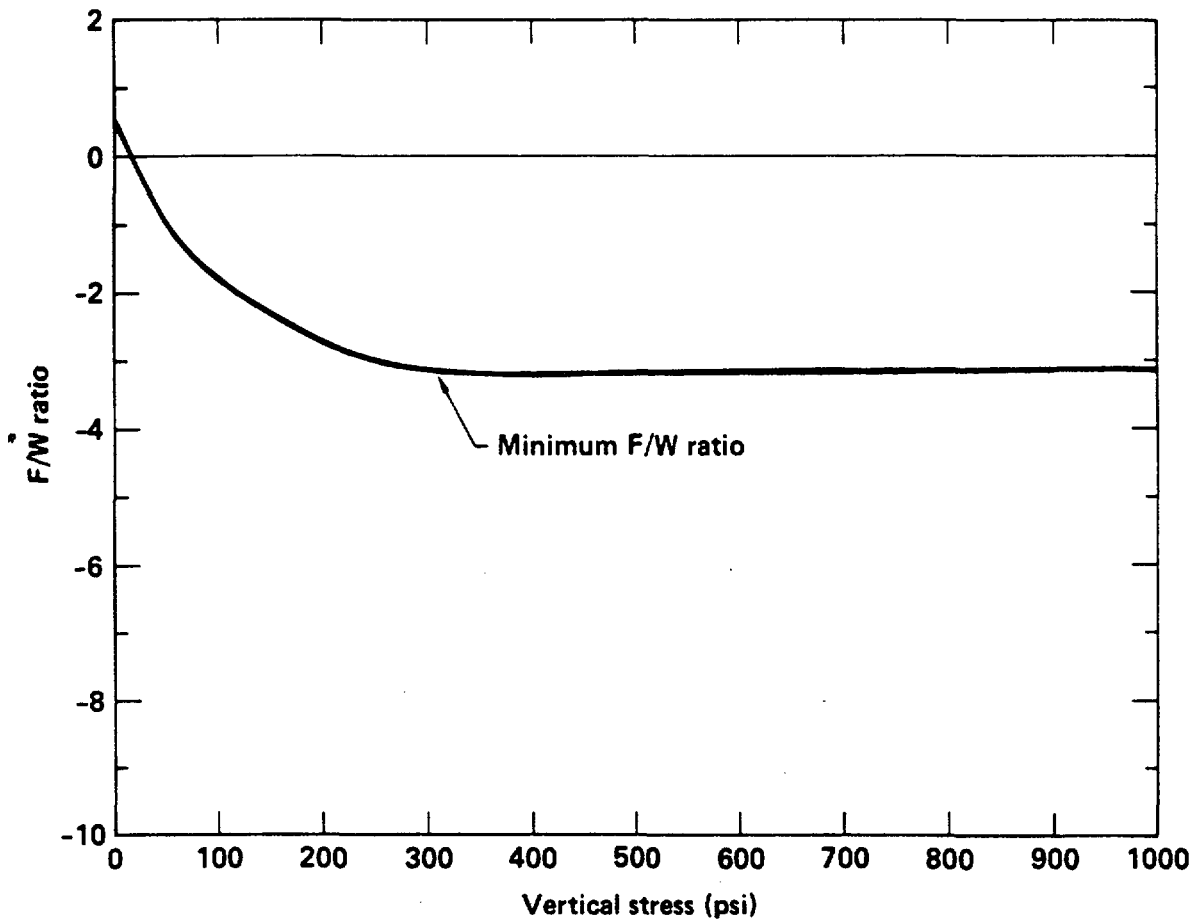

Figure 5.9 Minimum F/W ratio versus in situ vertical stress magnitude with 0.5 lateral stress ratio.

become less stable as the initial confining stresses decrease, and the trend accelerates as the stress magnitudes become very small.

Figure 5.10 shows the changes in minimum F/W ratio that result from differing lateral stress ratios at a constant vertical stress of 500 psi. The lateral stresses before excavation are assumed to be equal in magnitude and to act in a horizontal plane. Stability can be seen to decrease as lateral stress ratio decreases; again the trend accelerates as the lateral stress ratio goes below about one-half. Similar calculations were made for horizontal stress anisotropy, with average horizontal stresses being kept constant. Since all four block faces have identical strength and stiffness and the problem geometry was symmetric, the minimum F/W ratios were not affected.

Because confining stresses are so important to block stability, factors that affect the stress magnitudes over the design life of an excavation can become important design considerations. One such factor is stress changes induced by heating or cooling of the rock around an excavation. Equations for evaluating the stress changes caused by temperature variations in an elastic material were given in Chapter 3. Figure 5.11 shows the effect of temperature changes on the stability of the pyramidal block used in the previous calculations. Temperature increases above ambient cause an increase in compressive stresses that have a very slight stabilizing effect on the block. However, temperatures below the pre-excavation ambient conditions have a destabilizing effect that accelerates just as the effects of stress magnitude and stress ratio accelerated in Figures 5.9 and 5.10.

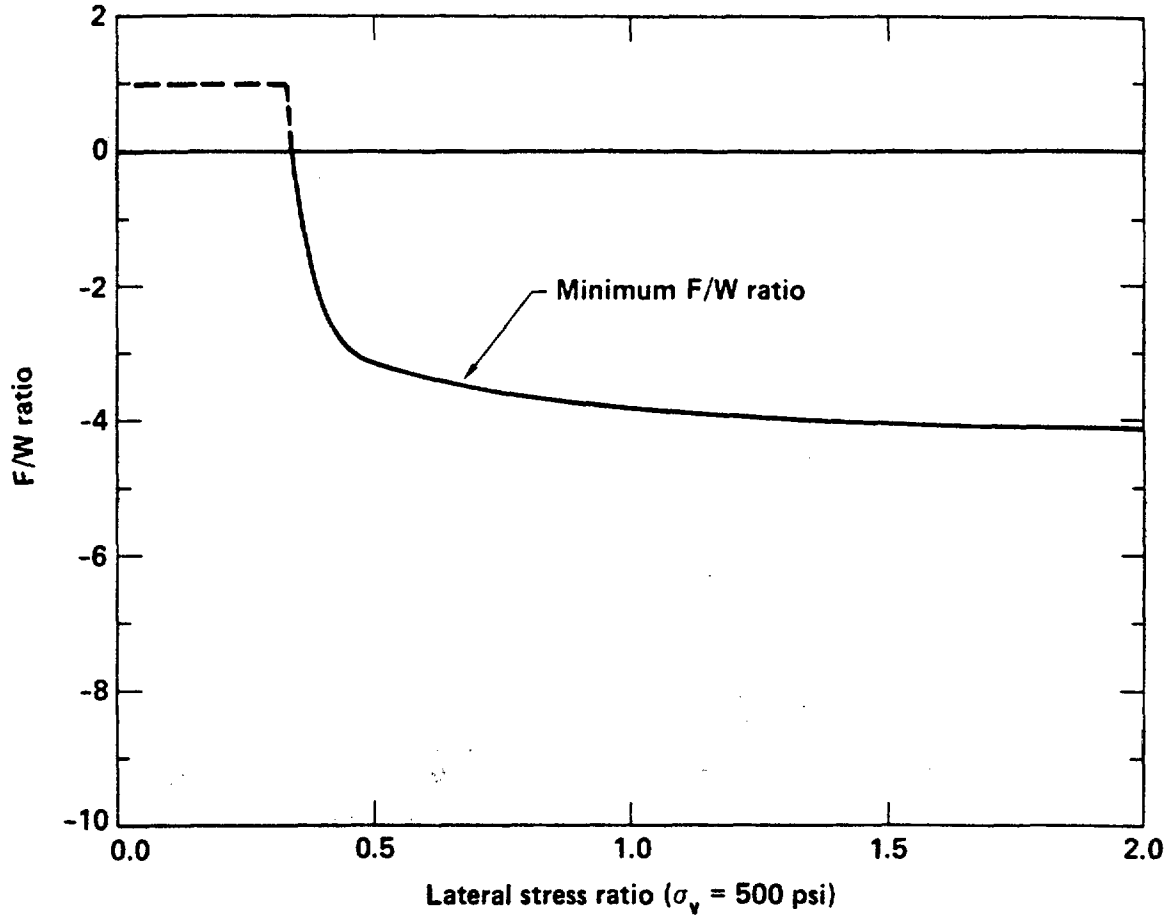

Figure 5.10 Minimum F/W ratio versus lateral stress ratio at constant in situ vertical stress.

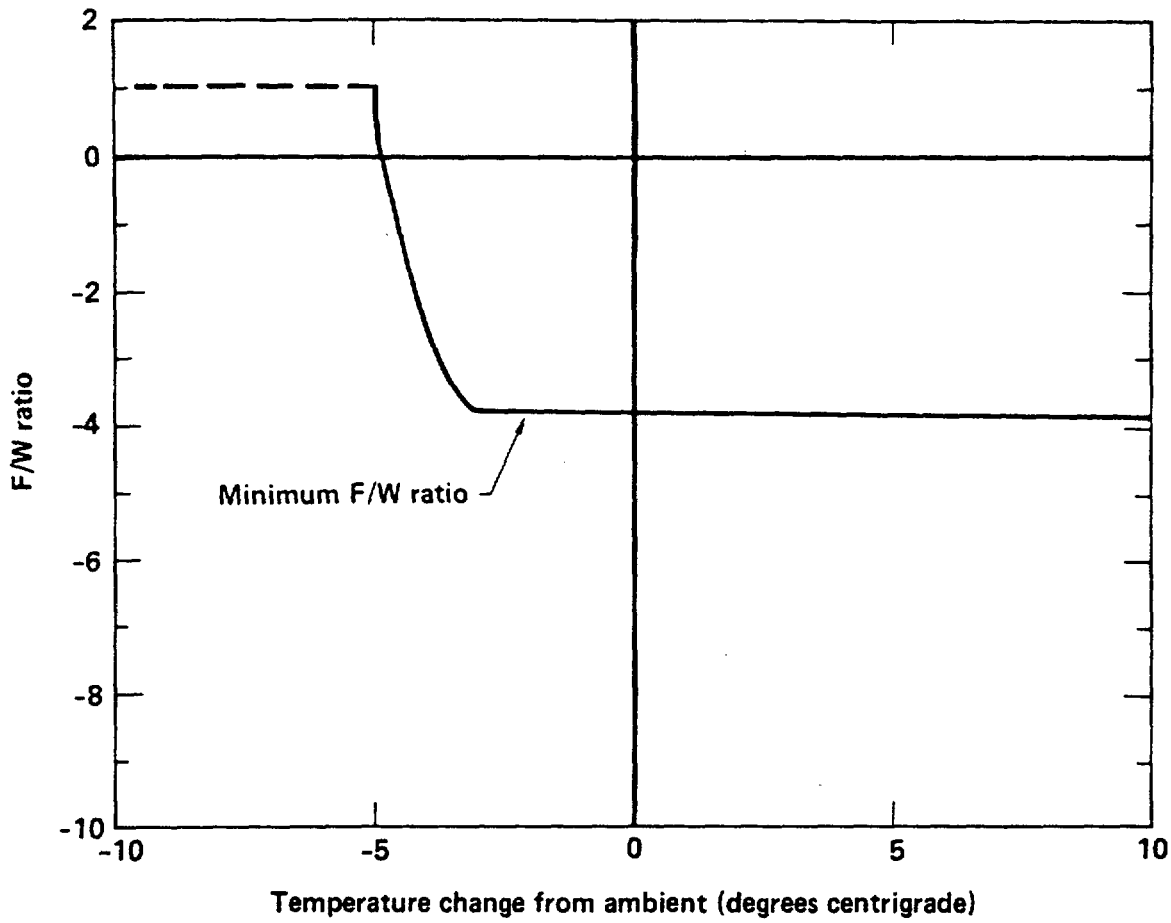

Figure 5.11 Variation of minimum F/W ratio caused by temperature change in tunnel.

Block Geometry

So far the parametric studies have involved a keyblock having the geometry shown in Figure 5.1. The tunnel radius, block size, and discontinuity orientations have been constant while properties such as strength and stiffness have been varied. The effects of block geometry on F/W ratio are now examined by varying the geometry of the pyramidal block while holding strengths, stiffnesses, and the in situ stress field constant.

Figure 5.12 shows the effect of keyblock narrowness or slenderness (expressed in terms of included apex angles) on block stability. The radius of the tunnel and the height of the block are constant, and the dips of the discontinuities below horizontal were varied from their values of 60° used in the preceding calculations. The 60° dips resulted in an included angle of 60° at the block apex between opposite block faces. Block slenderness can be seen to have an effect similar in significance to that of changing the discontinuity shear strength. The minimum F/W ratio becomes more negative (more stable) as the block becomes narrower and becomes more positive (less stable) as it becomes broader. This reflects the increased confinement of the block and corresponding increased ability to mobilize shear strength.

Figure 5.13 shows the effect of keyblock size on F/W ratio. In this case the block height was varied while the discontinuity dips and the tunnel radius were constant. Larger blocks are apparently less stable than smaller blocks for two reasons: First, since this block

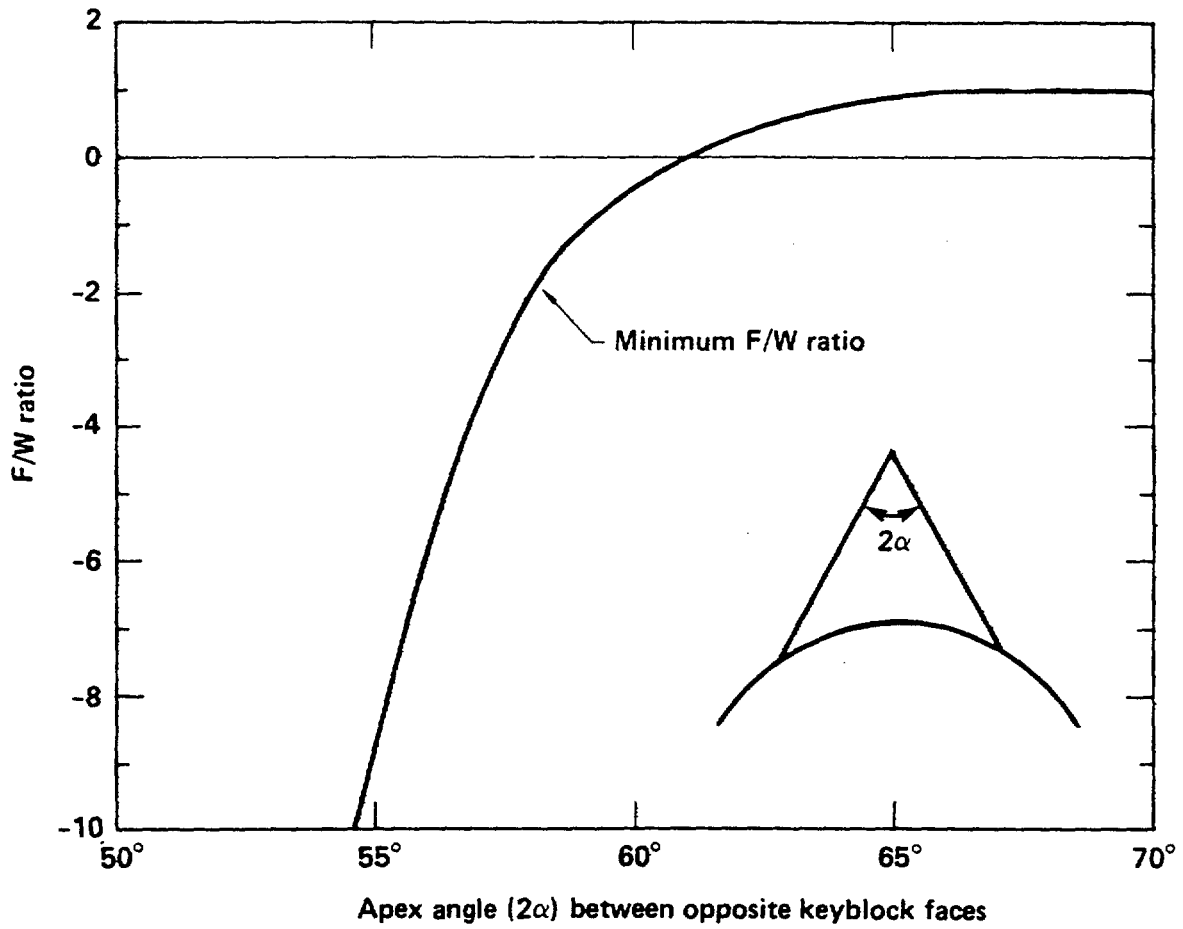

Figure 5.12 Minimum F/W ratio versus acuteness of apex.

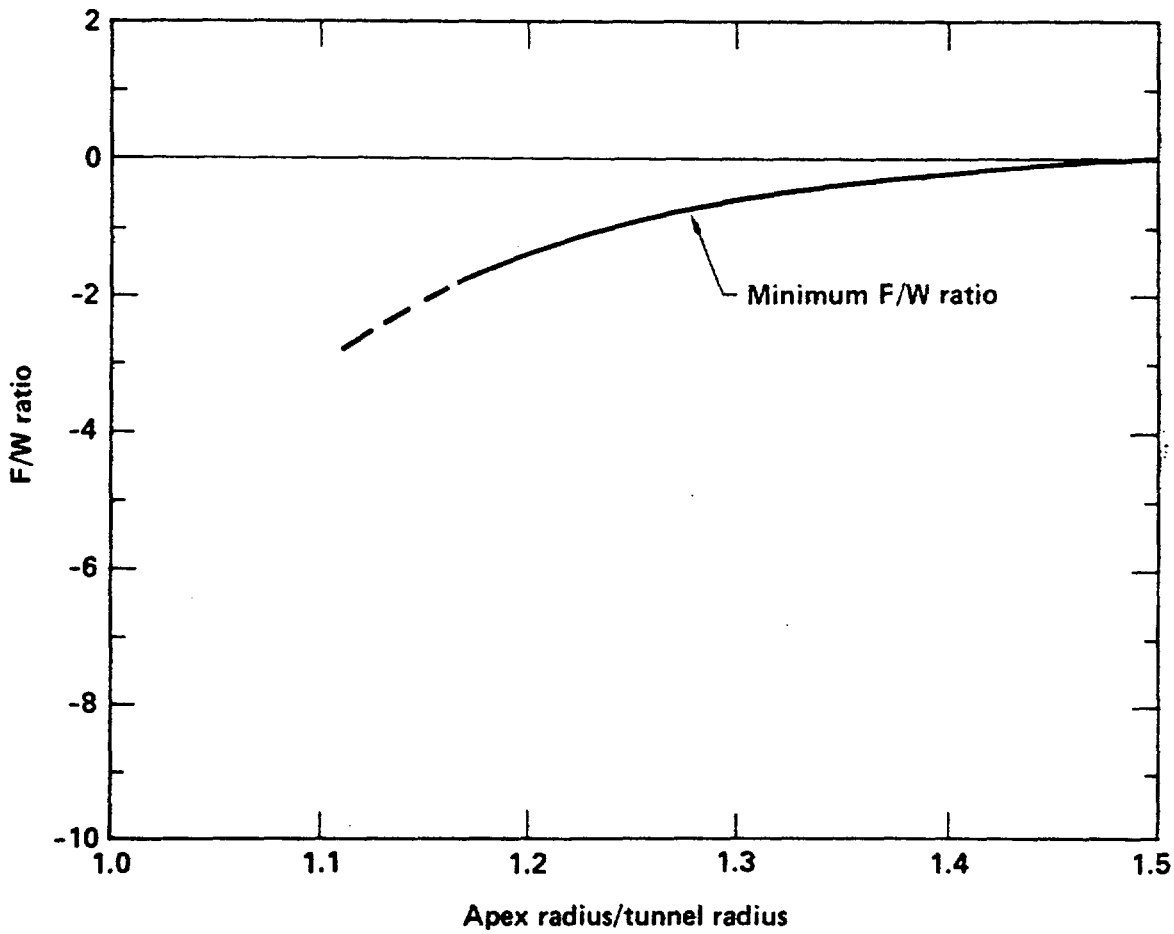

Figure 5.13 Minimum F/W ratio versus keyblock size (ratio of distance between tunnel axis and block apex to the radius of tunnel).

behavior model does not provide for a stress-relieved (damaged) zone of reduced stiffness around the excavation perimeter, smaller blocks are subjected to larger average confining stresses (tangent to the opening) than are larger blocks. Second, and speaking in general terms, the weight of a block increases roughly with the cube of the block height, while the surface area increases in approximate proportion to the square of the height. Since the weight is what moves a block towards failure, and the restraining forces are generated by stresses acting on the block surface area, large keyblocks should be (and are) less stable than small ones.

Figure 5.14 shows how keyblock stability is expected to change as the scale of a problem changes. In these calculations the tunnel radius was varied but the ratio of block height to tunnel radius was kept constant, as were the other parameters. The observed decrease in block stability with increased scale seems to bear out the second reason for size effects outlined in the previous paragraph. The block faces are, in this set of calculations, all subjected to the same initial stress distributions regardless of size because of the form of the elastic stress solution.

Finally, since some fallen keyblocks have been observed to have left a truncated stub of rock in the apex of the cavity which once contained the block, an analysis was performed to see if a mechanism could be found by which block truncation could occur. Figure 5.15 plots tensile stress as a function of radial distance from the tunnel axis at which the pyramidal block was truncated. The apex of the

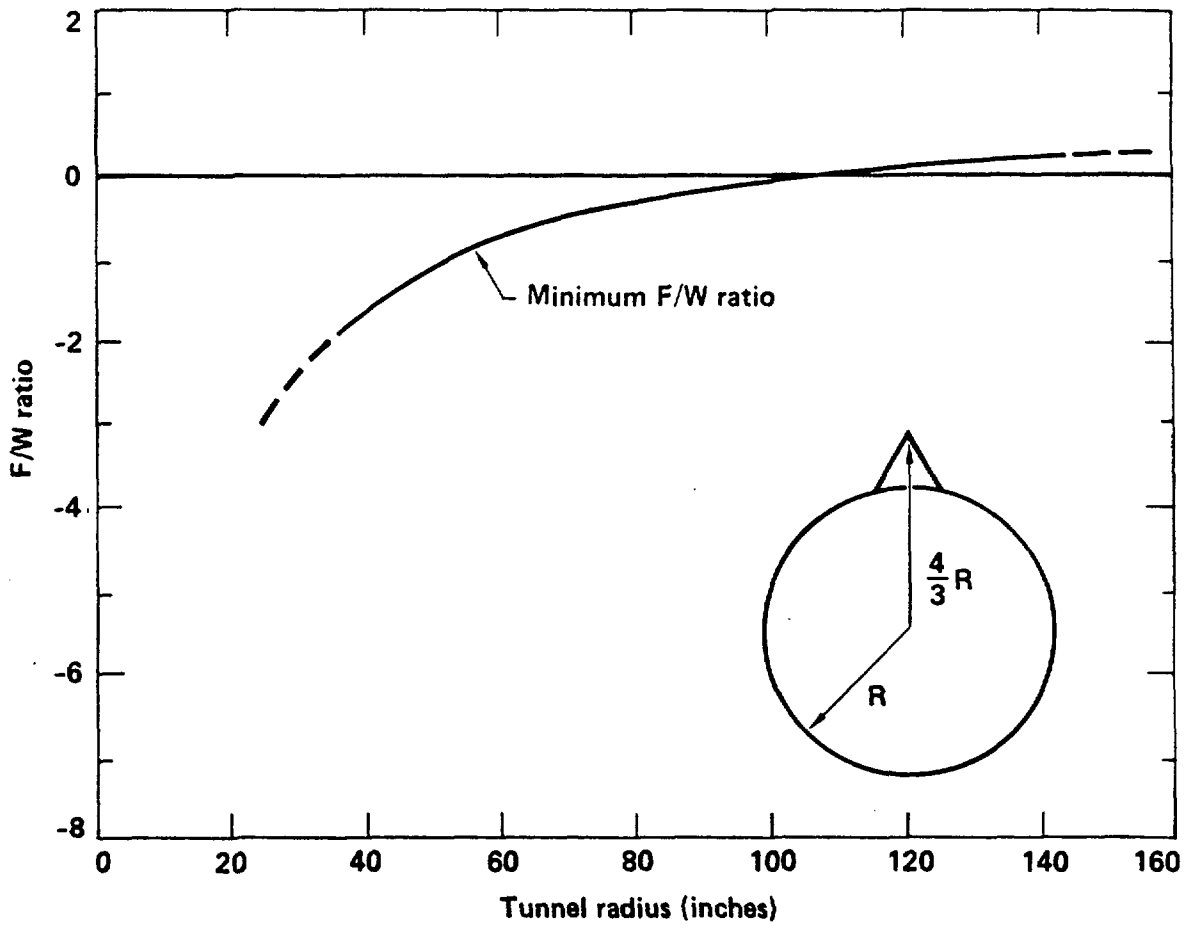

Figure 5.14 Minimum F/W ratio versus scale of keyblock and tunnel (radius to block apex = 4/3 radius of tunnel).

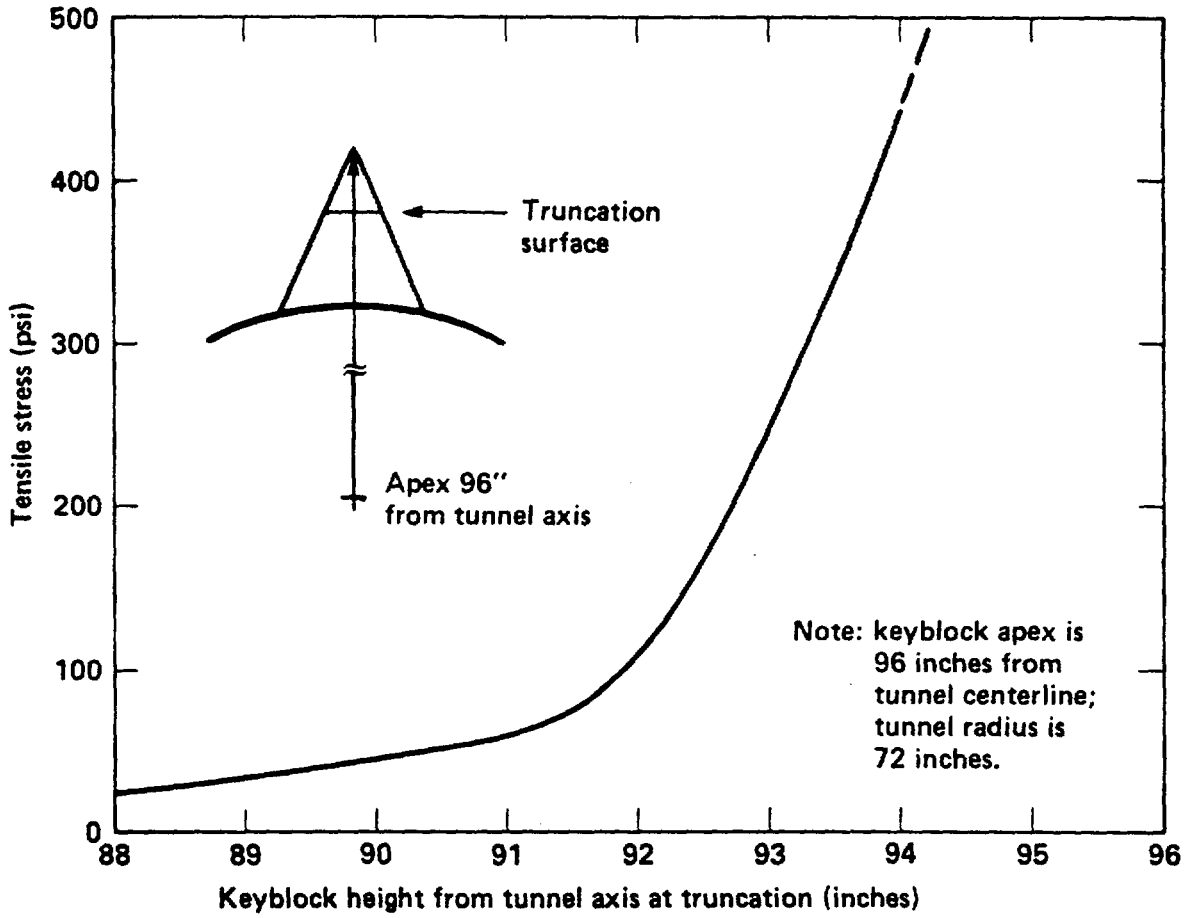

Figure 5.15 Tensile stress on possible truncated surface near apex of keyblock.

block before truncation occurred was 96 inches from the tunnel axis for this calculation. The plotted curve shows the tensile stress that would be needed on the plane of truncation for this particular block to be stable, even with the shear stresses on faces below the truncation accounted for. The stress would act on a plane at the indicated distance from the tunnel axis, and perpendicular to a line of symmetry running from the tunnel axis to the block apex. Since such a plane becomes smaller as the apex is approached, the stresses become larger with distance from the tunnel axis as shown. If the stub of rock remaining between the truncation and the apex could resist pullout sufficiently, tensile failure would occur at the point along this curve where the tensile strength of the intact rock was exceeded. This explains conceptually why many blocks observed in the field have been truncated.

CHAPTER 6 CONCLUSIONS AND APPLICATIONS

Chapter 1 described the significance of keyblock stability in underground excavation performance, and broke the problem into two parts: block identification and block stability analysis. Chapter 2 outlined techniques developed by others with which the block identification part of the problem may be solved. Procedures were formulated in Chapter 3 for analyzing the combinations of forces that define keyblock stability as a function of displacement. These procedures contribute to the science of rock mechanics by making advances over previous techniques in two ways: arbitrary, fully three-dimensional in situ stress fields and nonlinear discontinuity deformation behavior can both now be properly treated in an analysis of block stability. These procedures define a reaction curve for block behavior which describes how stability and support requirements change with block displacement.

The procedures of Chapter 3 were implemented in two-dimensional and three-dimensional numerical models for block behavior that are presented in Appendices 1 and 2, respectively. Field observations of keyblocks in tunnels were then described in Chapter 4. These field observations of block stability as well as laboratory tests (by Crawford and Bray, 1983) of keyblock pullout force were back-analyzed to check the validity of the block behavior models. Once the validity of the models was established, sensitivity studies were run to evaluate the effects of parameter changes on keyblock stability. The results of these studies were presented in Chapter 5 for a symmetric

pyramidal block; a relatively simple block was modeled because block geometry itself has an important effect on stability. The intent of this chapter, then, is to draw conclusions about keyblock stability from the work presented in the preceding chapters.

Design Use of Keyblock Behavior Models

The use of a keyblock stability analysis in designing underground openings is not necessary if the rock mass to be excavated contains no discontinuities. However, if the rock contains discontinuities, a keyblock analysis may be employed to advantage in design, during construction, or to evaluate certain aspects of post-construction performance. Hammett and Hoek (1981) described how the failure mechanisms to be considered in excavation design change with depth and in various geologic settings. Important factors included the stress field, strength of intact rock, and nature of discontinuities within the rock mass. These considerations help determine what types of analysis are appropriate for a given design.

The keyblock analysis can be used during the design process with discontinuity set orientations and excavation orientations to evaluate the possibility of encountering potentially unstable rock blocks. Discontinuity set orientations may be estimated from site exploratory drilling using procedures summarized by Yow and Wilder (1983). However, as was shown in Chapter 4, fringe members of joint sets can form keyblocks, and so the observed range of joint orientations of a dispersed set should be checked. The methods outlined in Chapter 2

will identify possibly unstable blocks, and the block behavior models can then evaluate the stability of these blocks from either assumed or measured data for a given excavation size and orientation. The quality of the stability calculation is obviously related to the quality of the data; however, this relationship allows the accuracy needed in the stability calculation to determine the required accuracy of the data.

During construction of an underground opening, structural features such as faults or shears are sometimes encountered unexpectedly. If such structural features apparently intersect to create keyblocks, block stability can be quickly evaluated using the block behavior models. If the trace of the keyblock perimeter has been completely exposed in the excavation surface and block faliure has not occurred, the question of stability may or may not be moot, since parameters that may change over the useful life of the excavation could allow a stable block to become unstable. Alternatively, if the keyblock is large, only part of the block may be exposed at first, and a quick analysis may be sufficient before proceeding with the excavation. This would allow the need for additional ground support to be evaluated and remedied before further excavation allowed the block to become unstable.

An analysis of post-construction keyblock stability may be needed in some cases if rock mass temperature or stress condition changes are expected over the life of the excavation. The rock several meters away from the Spent Fuel Test-Climax drifts, for example, experienced

a temperature decrease of over 2°C below ambient in a matter of a few months solely because of the cooling effect of the ventilation airflow. Excavation of adjacent openings can also be important in cases where the stresses would be affected.

Table 6.1 gives a qualitative assessment of the relative significance of various parameters in terms of their influence on the stability of a keyblock in an underground opening. These assessments were developed from the sensitivity studies of Chapter 5, and give a preliminary indication of the importance of each parameter. Following sections amplify some aspects of these parameter influences that may not have been obvious in the figures of Chapter 5.

Excavation Depth and Keyblock Stability

The sensitivity studies of Chapter 5 show that stability of a keyblock in an underground excavation is influenced by the stress magnitudes and lateral stress ratios, among other things. Figure 5.9 illustrated how variations in magnitude of vertical stress affect stability with constant lateral stress ratio, and Figure 5.10 plotted changes in stability caused by changes of lateral stress ratio with constant vertical stress magnitude. In each case, a transition from stable to unstable block behavior is seen where the minimum F/W ratio (support force ratio) goes from negative to positive. At F/W = 0 the block is marginally at equilibrium without any excess forces resisting failure.

Table 6.1 Relative Influence of Parameters[1] Affecting Stability of Keyblock in Crown of Tunnel

Parameter[1]	Relative Influence on Stability
discontinuity shear strength	strong
discontinuity stiffness	weak[2]
in situ stress magnitude	strong
lateral stress ratio	strong influence at low stress magnitudes; weak influence otherwise
temperature changes	strong influence if temperatures decrease; weak influence otherwise
block slenderness[3]	strong
block size with respect to constant excavation size	moderate
block and excavation size, dimensions kept in same proportion	moderate

NOTES: (1) The analyses of Chapter 5 did not include dynamic loads, fluid pressures in the discontinuities, or creep or plasticity effects.
(2) Stiffness affects keyblock displacement much more strongly than it does stability.
(3) Block slenderness is the smallest included angle between opposite block faces at the apex.

Similar analyses can be done for many combinations of vertical stress magnitude and lateral stress ratio to determine what stress conditions allow a block to be stable and what conditions lead to failure. Since stability is also heavily influenced by discontinuity shear strength, this type of calculation was run for two blocks having different shear strengths to see if strength changes would make a qualitative difference in the stress effects. Figure 6.1 plots the combinations of vertical stress magnitude and lateral stress ratio necessary for these two blocks to each be at equilibrium with an F/W ratio of zero.

The curves plotted in Figure 6.1 for pyramidal blocks having the two different discontinuity shear strengths are qualitatively the same. A block is stable at relatively low lateral stress ratios if the vertical stress magnitude is large enough. At lower stress magnitudes a larger lateral stress ratio is needed for stability to be attainable, and the effect accelerates as the vertical stress magnitude becomes very small. If vertical stress is converted to excavation depth by dividing by the unit weight of the overburden, the curves agree with observations of tunnel stability in blocky ground. At shallow depths block instability is a problem, but at greater depths the larger in situ stresses make the opening more stable, until stresses are high enough to induce failure of intact rock.

Curves similar to those of Figure 6.1 can be constructed for other combinations of block geometry, shear strength, and in situ stress, but the general trends will be the same. These trends rationally

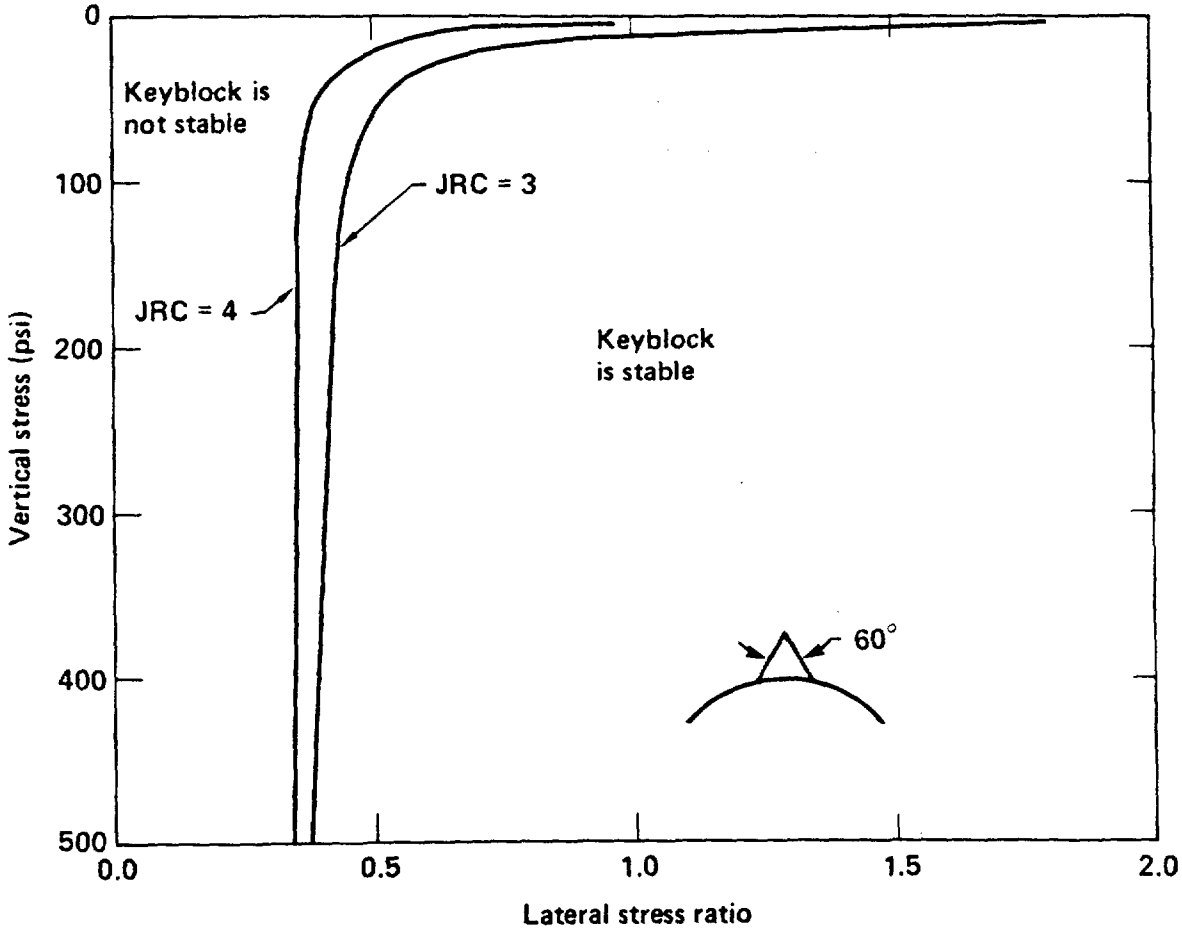

Figure 6.1 Lateral stress ratio required in situ for F/W ratio of zero.

support the intuition and experience of excavation designers. As an aside, most previous investigators (e.g., Crawford, 1982, and Crawford and Bray, 1983) have examined keyblock behavior only at relatively low horizontal stress magnitudes with zero or negligible vertical stress. These analyses would plot in the upper right-hand corner of Figure 6.1.

Thermal Effects

Since stresses play such an important role in keyblock stability, the importance of stress changes induced by thermal loading or unloading is not surprising. Figure 6.2 shows the stress changes that would be induced in the rock at the middle of the block of Figure 5.1 by temperature changes in the adjacent tunnel. This plot assumes that steady-state heat flow conditions have been reached, and thus is a limiting case for transient temperature conditions.

Figure 5.11 showed the effect of temperature changes on a particular hypothetical keyblock. In a general sense, temperature increases result in stress increases caused by thermal expansion of the rock, while temperature decreases have the opposite effect. A rise in temperature in an underground excavation, then, would move the stresses affecting a keyblock to the right and down on Figure 6.1, as all normal compressive stresses would increase. Lower temperatures would move the stresses up and to the left on Figure 6.1, allowing the block to fail once the confining stresses become low enough.

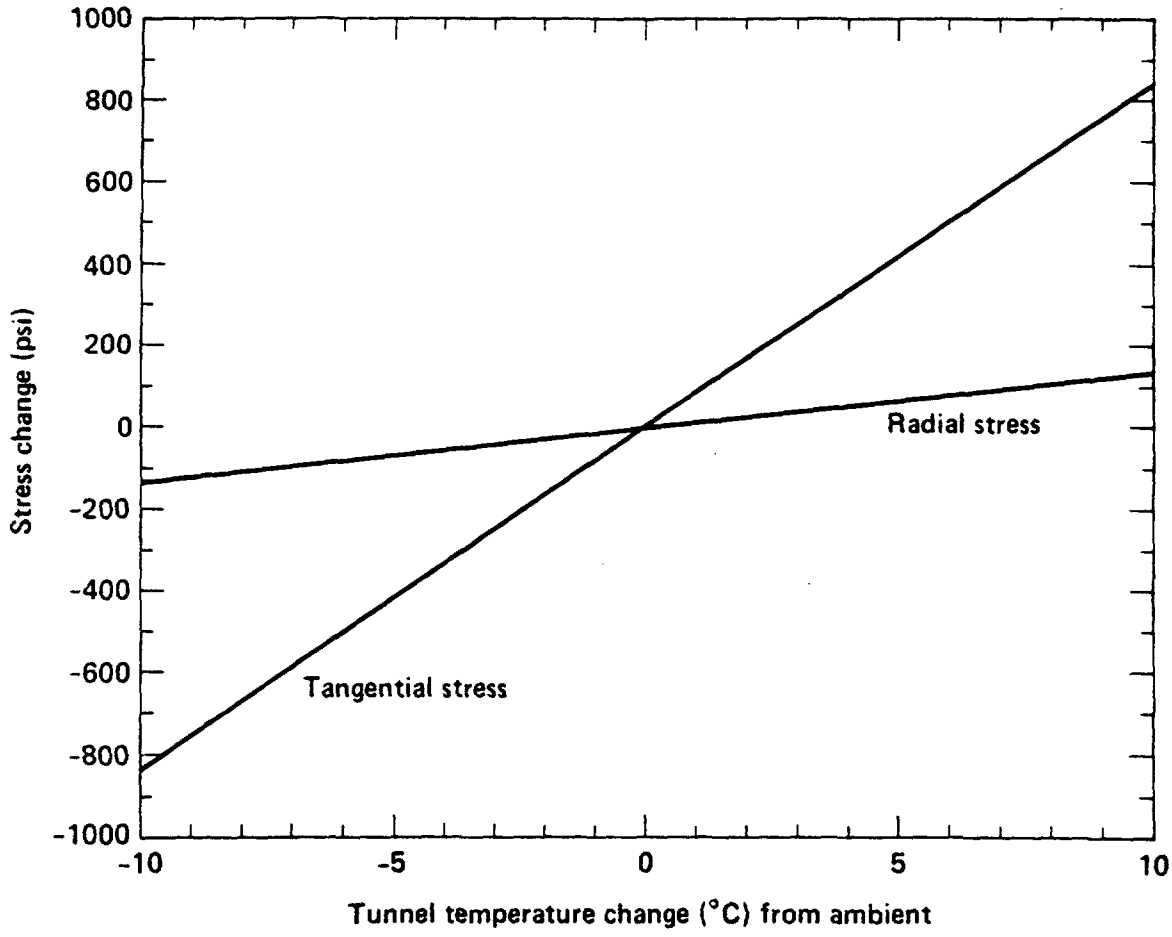

Figure 6.2 Typical linear stress changes around circular tunnel caused by temperature changes within tunnel (compression positive).

Analysis of thermal effects on keyblock stability has obvious application for situations in which excavation ventilation is expected to cool the rock mass, or in which temperature changes will be induced by refrigeration or storage of cold or hot materials in the underground opening. Cold materials such as liquified gaseous hydrocarbons have been stored in underground excavations, but published case histories have not been sufficiently detailed to identify block instability caused by the drop in temperature. Two additional factors that complicate this class of problems, though, are that such extreme cold freezes water in the discontinuities, and that the storage caverns are usually pressurized. Less extreme cases, such as cold food storage, have involved bedded sedimentary rocks in which keyblocks are not formed by the discontinuities. A case of the opposite sort was described by Rehbinder (1984) in which a cavern for hot water storage has been cycled several times between 40°C and 95°C. No block stability problems have been encountered; the temperature never dropped below what it was at the time of excavation and so no thermally-induced keyblock instability would be expected.

This latter situation of temperatures above ambient has particular significance for application to underground openings for nuclear waste disposal. Heat generated by the radionuclide decay of emplaced waste will cause the temperature of the openings to rise; the temperatures will gradually return to pre-emplacement conditions as the waste decay continues. Unless the thermally-induced compressive stresses damage the discontinuity asperities as described in Chapter 3, or cause failure of intact rock, the thermal cycle caused by the radioactive

waste should not by itself cause long term keyblock instability. Stability during construction of the underground openings may be a different matter, though, particularly if the ventilation air cools rock that contains marginally stable keyblocks.

Keyblock Geometry and Discontinuity Strength

The relationship of block geometry to keyblock stability has been considered for a selection of two-dimensional cases by Cording and Mahar (1974) and in a much more generalized three-dimensional sense by Goodman and Shi (1985). The sensitivity studies of Chapter 5 examined the geometric effects of block slenderness, size, and scale for the stability of a simple pyramidal keyblock. Block slenderness can be considered in terms of the angle between opposite block faces where they intersect at the apex, size refers to the block height and volume with respect to a constant excavation size, and scale refers to the size of a block and excavation when the dimensions of the two are maintained in the same proportions.

Increases in size and scale result in a decrease of keyblock stability, other things being equal. This implies that a design for an underground opening should consider first the maximum keyblock size allowed by the excavation dimensions. However, block slenderness has a more pronounced effect on stability than does either size or scale. Basically, if the smallest included apex angle between two opposite faces is larger than the sum of the friction angles and dilatancy angles of the two faces, the block will fail immediately upon

excavation of the opening. If the included apex angle is smaller than the sum of the friction and dilatancy angles, the keyblock is potentially stable, but an analysis should be performed as a check on its behavior. If the block is extremely narrow, though, it may be assumed as stable unless exceptional circumstances such as extremely low in situ stresses prevail. Consideration of block narrowness and discontinuity shear strength must include uncertainties in the data. A 5° error in block face orientation, for example, can potentially affect calculated block stability in a way that is similar to a 5° error in friction angle.

Excavation Sequence and Techniques

The relationship between keyblock stability and the stresses around an underground excavation suggests that construction sequences or techniques that affect the stress field can also affect block stability. Examples of this can be found in the changing pattern of stresses behind an advancing excavation face, and in the way that excavation technique can affect the rock mass.

As an excavation advances, the tunnel behind the advancing face deforms to a position of equilibrium with any support system that is installed (e.g., Panet and Guenot, 1982). Depending on the initial in situ stress conditions, the circumferential compressive stresses (hoop stresses) around the tunnel perimeter may increase behind the advancing face to reach static conditions as the rock around the tunnel deforms elastically. Conceptually then, a keyblock in the

perimeter of a cylindrical tunnel would experience its lowest confining stresses directly behind the advancing face. A potentially unstable block in the crown would displace into the excavation either until it failed or until its F/W ratio reached zero. As the working face moved onward, any increase in hoop stresses around the tunnel would increase the confinement of the block and thus drive the F/W ratio to a negative value, indicating an excess of forces resisting failure. If other factors (such as loss of strength with time) do not subsequently affect the stability of the block, the most critical time in the deformation history of the block may be when it has initially been released by the advancing excavation face.

Excavation technique can also affect keyblock stability, even if dynamic loads from blast effects are not involved. Deere (1981) and Hattrup (1981) have both described situations where rock blocks have been dislodged behind the advancing cutterhead of a tunnel boring machine (TBM). The force applied to thrust the cutterhead of a TBM forward is usually provided by hydraulic cylinders acting against shoes or pads that contact the tunnel perimeter. These pads typically are pushed radially outward with stresses up to several hundred pounds per square inch, and must affect the stress field around the tunnel. This perturbance, even though temporary, may aggravate the problems with block stability by reducing confining stresses enough to allow blocks to fall.

Possible Stabilization Measures

The use of shotcrete to support keyblocks in blocky ground has been described by Fernandez-Delgado et al (1979), and the use of rockbolts to stabilize blocks has been described in the papers by Goodman and others (see references). However, other stabilization measures suggest themselves, at least conceptually, because of the impact of stress conditions on keyblock stability. If the thrust of TBM bearing plates against a tunnel perimeter can lower the hoop stresses and allow blocks to become unstable, then artificially induced increases in hoop stresses should increase the stability of the rock. This stabilization of fractured rock has in fact been observed in the effect of tensioned rock bolts on blocky ground (Lang, 1957), where the stresses induced by tensioned bolts create a stabilizing zone of compression around the roof of an opening. Other techniques that could be used in special circumstances to increase compressive stresses for stabilization purposes might include pressurized flat jacks inserted adjacent to a critical keyblock, or temperature increases induced by electrical resistance heaters. The stress changes thus created can be included in the block stability analysis to see if the expected improvements in stability are adequate.

Keyblock Displacement Without Failure

Most of the preceding discussion has been directed towards evaluating keyblock stability. However, keyblock displacement can be important even if failure does not occur. It was shown in Chapter 3

that block displacement increases the shear stresses along the block faces until either the available shear strength is exceeded at all points and the block fails, or enough stress has been mobilized to support the block. Two other phenomena occur simultaneously though, as the keyblock displaces: the normal stress and the normal stiffness on each discontinuity both decrease, and each discontinuity opens. The discontinuity opening may be either slight, because of shear deformation and dilatancy, or somewhat larger, due to a combination of shear deformation, dilatancy, and normal deformation. Block movement thus produces a local zone of increased permeability (caused by increased average discontinuity aperture) and reduced stiffness (caused by decreased discontinuity normal stiffness) in the perimeter of the underground opening. Both phenomena have been observed in the field, and each can be important even if block failure is avoided.

REFERENCES

Amadei, B., 1982, The Influence of Rock Anisotropy on Measurement of Stresses In Situ, PhD Dissertation, University of California, Berkeley.

Bandis, S. C., A. C. Lumsden, and N. R. Barton, 1983, "Fundamentals of Rock Joint Deformation," International Journal of Rock Mechanics and Mining Sciences & Geomechanics Abstracts Volume 20, pp. 249-268.

Barton, N. and V. Choubey, 1977, "The Shear Strength of Rock Joints in Theory and Practice," Rock Mechanics and Rock Engineering Volume 10, pp. 1-54.

Belytschko, T., M. Plesha, and C. H. Dowding, 1983, "A Computer Method for the Stability Analysis of Jointed Rock Masses", in Proceedings of International Conference, Constitutive Laws for Engineering Materials, Tucson, AZ, pp. 333-339.

Benson, R. P., R. J. Conlon, A. H. Merritt, P. Joli-Coeur, and D. U. Deere, 1971, "Rock Mechanics at Churchill Falls," in Proceedings of the ASCE Symposium on Underground Rock Chambers, Pheonix, AX, pp. 407-486.

Brekke, T. L., 1968, "Blocky and Seamy Rock in Tunneling," in Bulletin of the Association of Engineering Geologists, Volume 5, pp. 23-26.

Carlson, R. C., W. C. Patrick, D. G. Wilder, W. G. Brough, D. N. Montan, P. E. Harben, L. B. Ballou, H. C. Heard, 1980, Spent Fuel Test-Climax: technical measurements interim report, FY1980, Lawrence Livermore National Laboratory Report UCRL 53064.

Cartney, S. A., 1977, "The Ubiquitous Joint Method. Cavern Design at Dinorwic Power Station," in Tunnels & Tunneling Volume 9, pp. 54-57.

Chan, L. and R. E. Goodman, 1983, "Prediction of Support Requirements for Hard Rock Excavations using Keyblock Theory and Joint Statistics," in Proceedings of the 24th U.S. Symposium on Rock Mechanics, College Station, TX, pp. 557-576.

Cording, E. J., A. J. Hendron, Jr., and D. U. Deere, 1971, "Rock Engineering for Underground Caverns," in Proceedings of the Symposium on Underground Rock Chambers, Phoenix, AZ, pp. 567-600.

Cording, E. J. and J. W. Mahar, 1974, "The Effects of Natural Geologic Discontinuities on Behavior of Rock in Tunnels," in Proceedings of the 1974 Rapid Excavation and Tunneling Conference, San Francisco, CA, Volume 1, pp. 107-138.

Coric, S., 1979, "Stability Analysis of Underground Cavities in Fissured Rock Masses," in Proceedings of the 4th International Congress on Rock Mechanics, Montreux, Switzerland, Volume 3, pp. 475-479.

Crawford, A. M., 1982, "Rock Wedge Stability," in Proceedings of the 23rd U.S. Symposium on Rock Mechanics, Berkeley, CA, pp. 1057-1064.

Crawford, A. M. and J. W. Bray, 1983, "Influence of the In Situ Stress Field and Joint Stiffness on Rock Wedge Stability in Underground Openings," Canadian Geotechnical Journal, Volume 20, pp. 276-287.

Creveling, J. B., F. S. Shuri, K. M. Foster, and S. V. Mills, 1984, In Situ Measurements at the Spent Fuel Test--Climax, Lawrence Livermore National Laboratory Contractor's Report UCRL 15628.

Croney, P., T. F. Legge, and A. Dhalla, 1978, "Location of Block Release Mechanisms in Tunnels from Geologic Data and the Design of Associated Support," in Proceedings of the Conference on Computer Methods in Tunnel Design, London, U.K., pp. 97-119.

Daemen, J. J. K., 1983, "Slip Zones for Discontinuities Parallel to Circular Tunnels or Shafts," International Journal of Rock Mechanics and Mining Sciences & Geomechanics Abstracts, Volume 20, pp. 135-148.

Deere, D. U., 1981, "Adverse Geology and TBM Tunneling Problems," in Proceedings of the 1981 Rapid Excavation and Tunneling Conference, San Francisco, CA, Volume 1, pp. 574-586.

Deere, D. U. and R. P. Miller, 1966, Engineering Classification and Index Properties for Intact Rock, University of Illinois Technical Report AFWL-TR-65-116.

Douglas, T. H., L. R. Richards, and L. J. Arthur, 1979, "Dinorwic Power Station - Rock Support of the Underground Caverns," in Proceedings of the 4th International Congress on Rock Mechanics, Montreux, Switzerland, Volume 1, pp. 361-369.

Fernandez-Delgado, G., E. J. Cording, J. W. Mahar, and M. L. Van Sint Jan, 1979, "Thin Shotcrete Linings in Loosening Rock," in Proceedings of the 1979 Rapid Excavation and Tunneling Conference, Atlanta, GA, Volume 1, pp. 790-813.

Goodman, R. E., 1967, Analysis of Structures in Jointed Rock, Report of Investigations for U.S. Army Corps of Engineers, Omaha District, Contract DACA 45-67-C-0015.

Goodman, R. E., 1976, Methods of Geological Engineering in Discontinuous Rocks, West Publishing Company, St. Paul, MN.

Goodman, R. E., 1980, Introduction to Rock Mechanics, John Wiley & Sons, New York, NY.

Goodman, R. E. and G. Shi, 1981, "Geology and Rock Slope Stability - Application of the Keyblock Concept for Rock Slopes," in Proceedings of the 3rd International Conference on Stability in Surface Mining, Vancouver, Canada, pp. 347-373.

Goodman, R. E. and G. Shi, 1985, Block Theory and Its Application to Rock Engineering, Prentice Hall, Englewood Cliffs, NJ.

Goodman, R. E., G. Shi, and W. Boyle, 1982, "Calculation of Support for Hard, Jointed Rock using the Keyblock Principle," in Proceedings of the 23rd U.S. Symposium on Rock Mechanics, Berkeley, CA, pp. 883-898.

Hammett, R. D. and E. Hoek, 1981, "Design of Large Underground Caverns for Hydroelectric Projects with Particular Reference to Structurally Controlled Failure Mechanisms," in Proceedings of the ASCE International Convention: Recent Developments in Geotechnical Engineering for Hydro Projects, New York, NY, pp. 192-206.

Hattrup, J. S., 1981, "Development of Tunnel Boring Machine Systems for Ground Control,: in Proceedings of the 1981 Rapid Excavation and Tunneling Conference, San Francisco, CA, Volume 1, pp. 587-598.

Heuze, F. E., 1980, "Scale Effects in the Determination of Rock Mass Strength and Deformability," Rock Mechanics, Volume 12, pp. 167-192.

Heuze, F. E., W. C. Patrick, T. R. Butkovich, J. C. Peterson, R. V. de la Cruz, and C. F. Voss, 1982, "Rock Mechanics Studies of Mining in the Climax Granite," International Journal of Rock Mechanics and Mining Sciences & Geomechanics Abstracts, Volume 19, pp. 167-183.

Hoek, E., 1977, "Structurally Controlled Instability in Underground Excavations," in Proceedings of the 18th U.S. Symposium on Rock Mechanics, Keystone, CO, pp. 5A6-1 through 5A6-5.

Hoek, E. and E. T. Brown, 1980, Underground Excavations in Rock, The Institution of Mining and Metallurgy, London, U.K.

Lang, T. A., 1957, "Rock Behavior and Rock Bolt Support in Large Excavations," in Proceedings of Symposium on Underground Power Stations, New York, N.Y.

Langkopf, B. S. and E. Eshom, 1982, Site Exploration for Rock Mechanics Field Tests in the Grouse Canyon Member, Belted Range Tuff, U12g Tunnel Complex, Nevada Test Site, Sandia National Laboratories Report SAND81-1897.

Lucas, J. M., 1980, "A General Stereographic Method for Determining the Possible Mode of Failure of Any Tetrahedral Rock Wedge," International Journal of Rock Mechanics and Mining Sciences & Geomechanics Abstracts Volume 17, pp. 57-61.

Obert, L. and W. I. Duvall, 1967, Rock Mechanics and the Design of Structures in Rock, John Wiley & Sons, New York, NY.

Panet, M. and A. Guenot, 1982, "Analysis of Convergence Behind the Face of a Tunnel," in Proceedings of the 3rd International Symposium: Tunneling '82, Institution of Mining & Metallurgy, London, U.K., pp. 197-204.

Priest, S. D., 1980, "The Use of Inclined Hemisphere Projection Methods for the Determination of Kinematic Feasibility, Slide Direction and Volume of Rock Blocks," International Journal of Rock Mechanics and Mining Sciences & Geomechaics Abstracts Volume 17, pp. 1-23.

Rehbinder, G., 1984, "Strains and Stresses in the Rock Around an Unlined Hot Water Cavern," Rock Mechanics and Rock Engineering Volume 17, pp. 129-145.

Shi, G. and R. E. Goodman, 1981, "A New Concept for Support of Underground and Surface Excavations in Discontinuous Rocks Based on a Keystone Principle," in Proceedings of the 22nd U.S. Symposium on Rock Mechanics, Boston, MA, pp. 290-296.

Stephens, G. and B. Voight, 1982, "Hydraulic Fracturing Theory for Conditions of Thermal Stress," International Journal of Rock Mechanics and Mining Sciences & Geomechanics Abstracts Volume 19, pp. 279-284.

Warburton, P. M., 1981, "Vector Stability Analysis of an Arbitrary Polyhedral Rock Block with any Number of Free Faces," International Journal of Rock Mechanics and Mining Sciences & Geomechanics Abstracts Volume 18, pp. 415-427.

Ward, W. H., 1978, "Ground Supports for Tunnels in Weak Rocks," Geotechnique Volume 28, pp. 133-171.

Wilder, D. G. and J. L. Yow, Jr., 1984 "Structural Geology of the Spent Fuel Test-Climax, Nevada Test Site," Lawrence Livermore National Laboratory Report UCRL 53381.

Yow, J. L., Jr. and D. G. Wilder, 1983, "Planning Exploratory Drilling: The Effect of Blind Zones and Level of Logging Effort," in Proceedings of the 24th U.S. Symposium on Rock Mechanics, College Station, TX, pp. 807-812.

Zhifa, Y., 1983, "Application of the Method of Projection on Coordinate Planes to Designing an Underground Opening within Discontinuous Rock Mass," in Proceedings of International Symposium on Engineering Geology and Underground Construction, Lisbon, Portugal, pp. I.15-I.24.

Zhu, J. and Zhizhong Xiao, 1982, "The Method of Evaluation for the Stability of Karst Caverns," in Rock Mechanics: Caverns and Pressure Shafts, Volume 1, pp. 519-528.

Zudans, Z., T. C. Yen, and W. H. Steigelmann, 1965, Thermal Stress Techniques in the Nuclear Industry, American Elsevier, New York, NY, pp. 232-236.

APPENDIX 1 Two-dimensional keyblock stability analysis program BSTB2D

The equations developed in Chapter 3 have been implemented into a numerical two-dimensional solution for the stability of a keyblock as a function of block displacement. This solution has been coded in the BASIC computer language as an interactive program named BSTB2D that can be run on a Hewlett-Packard 9816 computer. The user is prompted by the program for data needed for the analysis in a series of queries that are answered from the keyboard. Figure A1.1 illustrates the problem geometry used in the solution; other aspects of the use of the program are stated in the interactive prompts provided to the user.

BSTB2D uses a routine named SILJAK (which is copyrighted by the Hewlett-Packard Company) to solve equation 3.11 of Chapter 3. SILJAK finds all roots of a polynomial to within a specified tolerance without needing the derivative of the equation or an initial guess for a solution. SILJAK is contained in a file named HPBSTAB2D (not included here), which is automatically loaded when BSTB2D is executed. The routine can be purchased from Hewlett Packard, or the user can substitute a similar routine. The steps performed by BSTB2D to analyze keyblock stability are listed below:

1. Prompt user for input data. This data must be in a consistent system of units, and includes:
    - -- printing options and a problem header

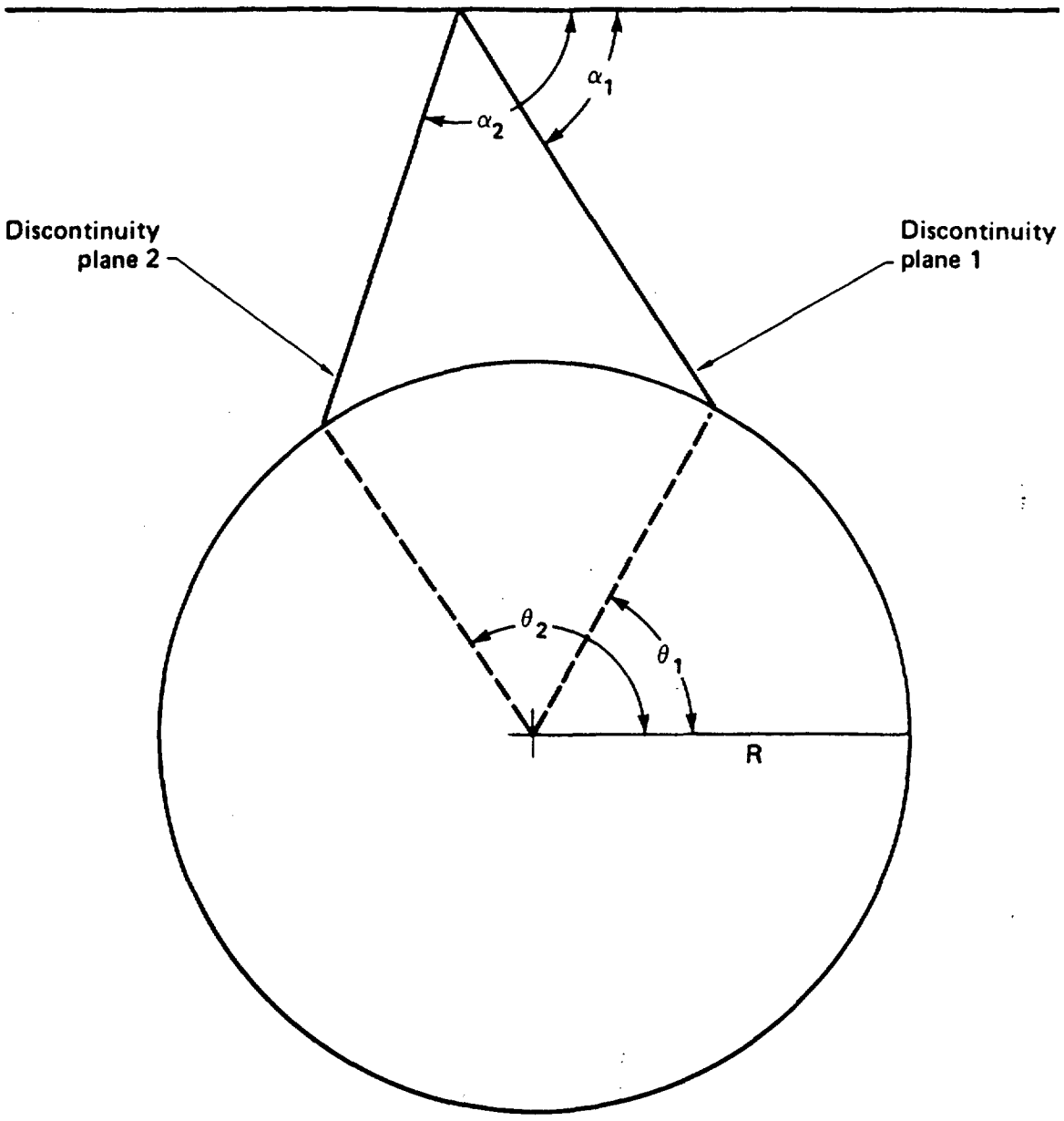

Figure A1.1 Geometry used in two-dimensional keyblock stability model.

- -- rock unit weight, tunnel radius, displacement increment, and number of increments to be solved
- -- vertical stress, lateral stress ratio, and internal pressure within tunnel
- -- modulus of intact rock, rock mass modulus, Poisson's ratio, and coefficient of thermal expansion
- -- temperature change
- -- choice of linear or nonlinear joint behavior
- -- discontinuity plane locations and orientations

If linear behavior is selected, the following is needed:

- -- friction angle, dilatancy angle, and residual friction angle
- -- normal stiffness and k_s/k_n ratio

If nonlinear behavior is selected, then the following is required:

- -- joint roughness coefficient (JRC), joint compressive strength (JCS), and residual friction angle
- -- average spacing and no-load aperture

2. After prompting for input, BSTB2D calculates the volume and weight of the block, assuming unit thickness. The two planes that form the keyblock boundaries are each divided into 20 segments.

3. The Kirsch solution is used to calculate the initial stresses at each of the 21 segment end points on each plane. If the nonlinear stiffness option has been chosen, the initial normal stiffness and aperture closure are computed from pre-excavation stresses and then adjusted for the stress concentrations around the opening.

4. At this time, the user is prompted for the displacement direction as an angle from vertical downward. BSTB2D prints the problem header and echoes the input data. The keyblock is then displaced the specified number of increments; the horizontal and vertical resultant forces and F/W ratio are displayed for each increment.

5. After the specified number of displacement increments have been completed, the user is offered the following options:

   -- specify a new displacement magnitude, direction, or both
   -- change discontinuity strengths or stiffnesses
   -- specify a tunnel temperature change
   -- change the far-field vertical and horizontal stresses
   -- truncate the block at a selected height
   -- entirely restart the program

A listing of BSTB2D follows.

```
10    PRINT "BSTB2D                    VERSION 1.0                    12/12/84"
20    PRINT " "
30    PRINT "NOTES:"
40    PRINT "1. ALL UNITS MUST BE CONSISTENT."
50    PRINT "2. PLANE 1 IS CW AROUND OPENING FROM BLOCK CENTER; PLANE 2 IS CCW."
60    PRINT "3. ALL THETA(PLANE 2) > THETA(APEX) > ALL THETA(PLANE 1)."
70    PRINT " "
80    ! ************************************************************************
90    !
100   !       THIS 2-D PROGRAM CALCULATES SUPPORT FORCES NEEDED TO BRING A BLOCK
110   ! SUBJECTED TO GRAVITATIONAL LOADING INTO LIMIT EQUILIBRIUM WITH A
120   ! FACTOR OF SAFETY OF UNITY.  THE RESULTS CAN BE EXPRESSED AS A
130   ! RATIO OF SUPPORT FORCE TO BLOCK WEIGHT; NEGATIVE VALUES INDICATE
140   ! THE FORCE REQUIRED TO DESTABILIZE AN OTHERWISE STABLE BLOCK.  CIRCULAR
150   ! OPENINGS ARE ASSUMED.
160   !
170   ! VALUES USED IN THE ANALYSIS:
180   !
190   ! BLOCK DISPLACEMENT (L)
200   ! ROCK UNIT WEIGHT (FL^-3)
210   ! NORMAL STIFFNESS OF DISCONTINUITY PLANE (FL^-3)
220   ! SHEAR STIFFNESS OF DISCONTINUITY PLANE (FL^-3)
230   ! FRICTION ANGLE OF DISCONTINUITY PLANE
240   ! DILATENCY ANGLE OF DISCONTINUITY PLANE
250   ! PLANE DIPS AND INTERSECTIONS WITH THE TUNNEL
260   ! HORIZONTAL AND VERTICAL STRESSES IN SITU (FL^-2)
270   ! BLOCK HEIGHT PERPENDICULAR TO EXCAVATION SURFACE (L)
280   !
290   ! Theta1 IS THE ANGLE CCW FROM RIGHT HORIZONTAL AT WHICH A PLANE
300   ! INTERSECTS THE TUNNEL; Theta2 IS THE ANGLE AT WHICH THE PLANE
310   ! ENDS AT THE APEX OR TRUNCATED END OF THE BLOCK.
320   !
330   ! ************************************************************************
340   ! BSTAB2D REVISIONS:
350   ! 1.0  12/12/84  ORIGINAL CODE BY JESSE L. YOW, JR.
360   !************************************************************************
370   !
380   DEG
390   OPTION BASE 1
400   INTEGER I,J,K
410   !
420   COM Theta1(2),Theta2(2),Phi(2),Dilang(21,2),Normal(2),Nf(2),Shear(2),Sf(2)
430   COM Kn(2),Ks(2),Length(2),Alph(2),Dip(2),Dd(2),Head$[80],Phires(2)
440   COM Ninc(21,2),Sinc(21,2),Linc(21,2),Tinc(21,2),Strength(21,2),Rinc(21,2)
450   COM Initns(21,2),Initss(21,2),Gamma,Radius,Disincd,Sv,Sh,Emass,El,Mu,Talph
460   COM Jrc(2),Jcs(2),Weight,Sigratio,Kratio,F$[1],Finc$[1],F$[1],Flin$[1]
470   COM Aperture(2),Space(2),Incl(21,2),Kin(2),Mud
480   COM Root(1:3),Iroot(1:3),Cof(0:3),Icof(0:3)
490   !
500   LOADSUB ALL FROM "HPBSTAB2D" ! LOAD HP PROPIETARY SUBROUTINES
```

```
510   !
520   Mudp=1
530   Nlines=6
540   F$=" "
550   !
560   ! INPUT PARAMETERS
570   !
580   INPUT "PUT RESULTS ON PRINTER AS WELL AS SCREEN ?",F$
590   INPUT "PRINT INCREMENTAL STRESSES ALONG PLANES ?",Pinc$
600   INPUT "PROBLEM HEADER (80 CHARACTERS MAX) ?",Head$
610   INPUT "ROCK UNIT WEIGHT,TUNNEL RADIUS, DISPLACEMENT INC, AND NO. INCS ?",G
amma,Radius,Disincd,Mud
620   INPUT "VERTICAL STRESS, LATERAL STRESS RATIO, AND INTERNAL PRESSURE ?",Sv,
Sigratio,Pressure
630   Sh=Sv*Sigratio
640   IF F$="S" THEN 1060
650   INPUT "MODULUS, MASS MODULUS, POISSON'S RATIO, AND EXPANSION COEF ?",E1,Em
ass,Mu,Talph
660   INPUT "DELTA T ?",Tdelt
670   IF F$="H" THEN 1060
680   !
690   Nplanes=2            ! FOR 2-D BLOCKS
700   !
710   INPUT "NONLINEAR JOINT BEHAVIOR ?",Flin$
720   FOR I=1 TO Nplanes
730     IF F$="F" THEN 800
740     !
750     DISP "INPUT THETA CCW ABOVE RIGHT HORIZONTAL FOR PLANE";I;
760     INPUT " ",Theta1(I)
770     DISP "INPUT 'DIP' CW BELOW RIGHT HORIZONTAL FOR PLANE";I;
780     INPUT " ",Dip(I)
790     !
800     IF Flin$<>"Y" THEN 890
810     DISP "JRC, JCS, RESIDUAL PHI FOR PLANE";I;
820     INPUT " ",Jrc(I),Jcs(I),Phires(I)
830     DISP "AVERAGE SPACING AND APERTURE FOR PLANE";I;
840     INPUT " ",Space(I),Aperture(I)
850     MAT Phi= (0)
860     MAT Dilang= (0)
870     GOTO 970
880     !
890     DISP "INPUT FRICTION ANGLE, DILATANCY ANGLE, & RESIDUAL PHI FOR PLANE";I
;
900     INPUT " ",Phi(I),Dilang(1,I),Phires(I)
910     FOR J=2 TO 21
920       Dilang(J,I)=Dilang(1,I)
930     NEXT J
940     DISP "INPUT NORMAL STIFFNESS KN AND KS/KN STIFFNESS RATIO FOR PLANE";I;
950     INPUT " ",Kn(I),Kratio
960     Ks(I)=Kratio*Kn(I)
970   NEXT I
980   !
990   IF F$="F" THEN 1220
1000  IF F$="T" THEN INPUT "BLOCK HEIGHT ?",Height
```

```
1010  !
1020  ! BEGIN CALCULATIONS
1030  !
1040  GOSUB 2450  ! CALCULATE BLOCK GEOMETRY
1050  !
1060  Cavg=(Sv+Sh)/2.0
1070  Cdev=(Sv-Sh)/2.0
1080  !
1090  FOR I=1 TO Nplanes
1100    GOSUB 3220  !    CALCULATE THE INITIAL FORCES
1110  NEXT I
1120  !
1130  IF Flin$="Y" THEN GOSUB 4690 ! CALCULATE INITIAL JOINT CLOSURE
1140  !
1150  IF F$="S" OR F$="H" THEN 1220
1160  !
1170  ! FIND MAXIMUM PULLOUT FORCE
1180  !
1190  INPUT "DISPLACEMENT ALPHA CCW FROM VERTICAL DOWNWARD ?",Alphad
1200  Dd(1)=180-Alph(1)+Alphad
1210  Dd(2)=Alph(2)-Alphad
1220  IF (90-Dd(1))<Dilang(1,1) THEN 1270
1230  IF (90-Dd(2))<Dilang(1,2) THEN 1270
1240  GOTO 1300
1250  !
1260  PRINTER IS 1
1270  PRINT "BLOCK IS MOVING INTO PLANE; SOLUTION WILL NOT CONVERGE"
1280  GOTO 1190
1290  !
1300  Dis=Disincd
1310  Headflag=0
1320  FOR Increment=1 TO Mud
1330    FOR J=1 TO Nplanes
1340      GOSUB 1780! CALCULATE SHEAR AND NORMAL FORCES
1350    NEXT J
1360    GOSUB 2230  ! CALCULATE RESULTANT FORCE
1370    GOSUB 3800  ! PRINT RESULTS
1380    Headflag=1
1390    Dis=Dis+Disincd
1400  NEXT Increment
1410  GOTO 1540
1420  !
1430  INPUT "DISPLACEMENT ?",Dis
1440  Deldisp=Dis/10
1450  FOR Incdis=1 TO 10
1460    Dis=Deldisp*Incdis
1470    FOR J=1 TO Nplanes
1480      GOSUB 1780
1490    NEXT J
1500    GOSUB 2230
```

```
1510  NEXT Incdis
1520  GOSUB 3800     ! PRINT RESULTS
1530  !
1540  INPUT "OPTION ?",F$
1550  IF F$="D" THEN 1430
1560  IF F$="E" THEN 1760
1570  IF F$="F" THEN 690
1580  IF F$="H" THEN 660
1590  IF F$="M" THEN 1190
1600  IF F$="R" THEN 550
1610  IF F$="S" THEN 620
1620  IF F$="T" THEN 1000
1630  !
1640  PRINT " "
1650  PRINT "OPTIONS AVAILABLE ARE:"
1660  PRINT "D  SPECIFY DISPLACEMENT AND DIRECTION"
1670  PRINT "E  END"
1680  PRINT "F  CHANGE JOINT PLANE PARAMETERS"
1690  PRINT "H  TEMPERATURE CHANGE DELTA T"
1700  PRINT "M  FIND MAXIMUM PULLOUT FORCE"
1710  PRINT "R  RESTART PROGRAM"
1720  PRINT "S  CHANGE IN SITU STRESSES"
1730  PRINT "T  TRUNCATE BLOCK"
1740  GOTO 1540
1750  !
1760  STOP
1770  ! ******************************************************
1780  ! CALCULATE NORMAL AND SHEAR FORCES FOR GIVEN DISPLACEMENT
1790  ! ******************************************************
1800  IF Flin$="Y" THEN 1950
1810  !
1820  FOR K=1 TO 21
1830    Ninc(K,J)=Initns(K,J)-(Kn(J)*Dis*(COS(Dd(J))-SIN(Dd(J))*TAN(D
))
1840    IF Ninc(K,J)<0 THEN Ninc(K,J)=0.
1850    Strength(K,J)=Ninc(K,J)*TAN(Phi(J)+Dilang(K,J))  ! CALC AVAILA
N
1860    Sinc(K,J)=Initss(K,J)+Ks(J)*Dis*SIN(Dd(J))  ! CALC DISP GENERA
1870    IF Dis=0. THEN 1910
1880    IF Sinc(K,J)<Strength(K,J) THEN 1910
1890    Strength(K,J)=Ninc(K,J)*TAN(Phires(J))
1900    Sinc(K,J)=Strength(K,J)
1910  NEXT K
1920  !
1930  GOTO 2160
1940  !
1950  FOR K=1 TO 21
1960    IF Ninc(K,J)<1 THEN Ninc(K,J)=1
1970    Dilang(K,J)=Jrc(J)*LGT(Jcs(J)/Ninc(K,J))
1980  NEXT K
1990  !
2000  FOR K=1 TO 21
```

```
2010    D=Dis*(COS(Dd(J))-SIN(Dd(J))*TAN(Dilang(K,J))) ' JOINT OPENING
2020    X=Incl(K,J)-D
2030    IF X<=0 THEN 2060
2040    Ninc(K,J)=Kin(J)/((1/(X))-(1/Aperture(J)))
2050    GOTO 2080
2060    Ninc(K,J)=0
2070  !
2080    D=Dis*SIN(Dd(J)) ' JOINT SHEAR DISPLACEMENT
2090    Strength(K,J)=Ninc(K,J)*TAN(Dilang(K,J)+Phires(J))
2100    Sinc(K,J)=Initss(K,J)+Strength(K,J)*100*D/Length(J)
2110    IF Dis=0 THEN 2140
2120    IF Sinc(K,J)<Strength(K,J) THEN 2140
2130    Sinc(K,J)=Strength(K,J)
2140  NEXT K
2150  !
2160  GOSUB 3670
2170  '
2180  Nf(J)=Nsum
2190  Sf(J)=Ssum
2200  '
2210  RETURN
2220  ! ***************************
2230  ' CALCULATE RESULTANT FORCES
2240  ' ***************************
2250  A1=Dip(1)
2260  A2=180-Dip(2)
2270  '
2280  Fh=Nf(2)*SIN(A2)+Sf(2)*COS(A2)-Nf(1)*SIN(A1)-Sf(1)*COS(A1)
2290  Fh=-Fh
2300  '
2310  Fv=Nf(2)*COS(A2)-Sf(2)*SIN(A2)+Nf(1)*COS(A1)-Sf(1)*SIN(A1)+Weight
2320  !
2330  Alf=90.0-ATN(Fh/Fv)
2340  !
2350  Fr=SGN(Fv)*SQR(Fv*Fv+Fh*Fh)
2360  !
2370  Tense=0.
2380  IF Truncw=0. THEN 2420
2390  Tense=Fr*COS(Tpeak-Alf)/Truncw
2400  Tense=SGN(Fr)*SQR(Tense*Tense)
2410  !
2420  Fw=Fr/Weight
2430  RETURN
2440  ! ************************
2450  ! CALCULATE BLOCK GEOMETRY
2460  ! ************************
2470  Alph(1)=180-Dip(1)
2480  Alph(2)=180-Dip(2)
2490  !
2500  Beta1=180-Alph(1)+Theta1(1)
```

```
2510  Beta2=180-Theta1(2)+Alph(2)
2520  IF Beta1>180 OR Beta1<90 THEN PRINT "POSSIBLE PLANE 1 GEOMETRY ERROR"
2530  IF Beta2>180 OR Beta2<90 THEN PRINT "POSSIBLE PLANE 2 GEOMETRY ERROR"
2540  !
2550  Length(2)=TAN(Alph(1))*(COS(Theta1(2))-COS(Theta1(1)))
2560  Length(2)=Radius*(SIN(Theta1(2))-SIN(Theta1(1))-Length(2))
2570  Length(2)=Length(2)/(COS(Alph(2))*TAN(Alph(1))-SIN(Alph(2)))
2580  !
2590  Length(1)=Radius*(SIN(Theta1(2))-SIN(Theta1(1)))
2600  Length(1)=(Length(1)+Length(2)*SIN(Alph(2)))/SIN(Alph(1))
2610  !
2620  Hmax=Length(1)*Length(1)+Radius*Radius
2630  Hmax=Hmax+2*Radius*Length(1)*COS(Alph(1)-Theta1(1))
2640  Hmax=SQR(Hmax)
2650  Hbmax=Hmax-Radius
2660  !
2670  Tpeak=Theta1(1)+ASN((Length(1)/Hmax)*SIN(Alph(1)-Theta1(1)))
2680  Theta2(1)=Tpeak
2690  Theta2(2)=Tpeak
2700  !
2710  Area=Length(1)*SIN(Alph(1)-Theta1(1))
2720  Area=Area+Length(2)*SIN(Theta1(2)-Alph(2))
2730  Area=Area-Radius*PI*(Theta1(2)-Theta1(1))/180
2740  Area=Area*Radius/2.0
2750  !
2760  IF F$="T" THEN 2830      ! CHECK IF BLOCK IS DEFINED AS TRUNCATED
2770  !
2780  Height=Hbmax
2790  Trunch=0.
2800  Truncw=0.
2810  GOTO 2940
2820  !
2830  H=Height+Radius
2840  Trunch=Hmax-Radius-Height
2850  Truncw=Trunch*(TAN(Alph(1)-Tpeak)+TAN(Tpeak-Alph(2)))
2860  Area=Area-Trunch*Truncw/2.0
2870  !
2880  Length(1)=Length(1)-Trunch/COS(Alph(1)-Tpeak)
2890  Length(2)=Length(2)-Trunch/COS(Tpeak-Alph(2))
2900  !
2910  Theta2(1)=Tpeak-ATN(Trunch*TAN(Alph(1)-Tpeak)/H)
2920  Theta2(2)=Tpeak+ATN(Trunch*TAN(Tpeak-Alph(2))/H)
2930  !
2940  FOR I=1 TO Nplanes ! GENERATE INCREMENTS FOR INITIAL STRESSES
2950    Linc(1,I)=0.
2960    Tinc(1,I)=Theta1(I)
2970  NEXT I
2980  !
2990  FOR I=1 TO Nplanes
3000    Dln=Length(I)/20.0
```

```
3010    FOR J=2 TO 21
3020      Linc(J,I)=Linc(J-1,I)+Dln
3030    NEXT J
3040  NEXT I
3050  '
3060  FOR J=1 TO 21
3070    Rinc(J,1)=2*Linc(J,1)*Radius*COS(Alph(1)-Theta1(1))
3080    Rinc(J,1)=SQR(Rinc(J,1)+Radius*Radius+Linc(J,1)*Linc(J,1))
3090    Rinc(J,2)=2*Linc(J,2)*Radius*COS(Theta1(2)-Alph(2))
3100    Rinc(J,2)=SQR(Rinc(J,2)+Radius*Radius+Linc(J,2)*Linc(J,2))
3110  NEXT J
3120  '
3130  FOR J=1 TO 21
3140    Tinc(J,1)=Theta1(1)+ASN((Linc(J,1)/Rinc(J,1))*SIN(Alph(1)-Theta1(1)))
3150    Tinc(J,2)=Theta1(2)-ASN((Linc(J,2)/Rinc(J,2))*SIN(Theta1(2)-Alph(2)))
3160  NEXT J
3170  '
3180  Weight=Gamma*Area*1.0
3190  '
3200  RETURN
3210  ' ****************************
3220  ' SOLVE FOR THE INITIAL FORCES
3230  ' ****************************
3240  FOR J=1 TO 21
3250  '
3260    Rat=Radius/Rinc(J,I)
3270    Sigr=Cavg*(1-Rat^2)
3280    Sigr=Sigr-Cdev*(1-4*Rat^2+3*Rat^4)*COS(2*Tinc(J,I))
3290    Sigr=Sigr+Pressure*Rat^2
3300  '
3310    Sigt=Cavg*(1+Rat^2)
3320    Sigt=Sigt+Cdev*(1+3*Rat^4)*COS(2*Tinc(J,I))
3330    Sigt=Sigt-Pressure*Rat^2
3340    IF Tdelt=0 THEN 3450
3350  '
3360    Lna=LOG(10)
3370    C1=-E1*Talph*Tdelt/(2*(1-Mu)*Lna)
3380    C2=1/99
3390    C3=10*Rat
3400    Lnr=LOG(C3)
3410  '
3420    Sigr=Sigr+C1*(-Lnr-C2*(1-C3*C3)*Lna)
3430    Sigt=Sigt+C1*(1-Lnr-C2*(1+C3*C3)*Lna)
3440  '
3450    Tau=Cdev*(1+2*Rat^2-3*Rat^4)*SIN(2*Tinc(J,I))
3460  '
3470    Ninc(J,I)=(Sigr+Sigt)/2
3480    Ninc(J,I)=Ninc(J,I)-((Sigr-Sigt)/2)*COS(2*(Alph(I)-Tinc(J,I)))
3490    Ninc(J,I)=Ninc(J,I)-Tau*SIN(2*(Alph(I)-Tinc(J,I)))
3500  '
```

```
3510    Sinc(J,I)=((Sigr-Sigt)/2)*SIN(2*(Alph(I)-Tinc(J,I)))
3520    Sinc(J,I)=Sinc(J,I)-Tau*COS(2*(Alph(I)-Tinc(J,I)))
3530    IF I=1 THEN Sinc(J,I)=-Sinc(J,I)
3540  !
3550    Initns(J,I)=Ninc(J,I)
3560    Initss(J,I)=Sinc(J,I)
3570  !
3580  NEXT J
3590  !
3600  J=I
3610  GOSUB 3670
3620  Normal(J)=Nsum
3630  Shear(J)=Ssum
3640  !
3650  RETURN
3660  ! ********************************
3670  ! TRAPEZOIDAL SUMMATION OF STRESSES
3680  ! ********************************
3690  Nsum=0.
3700  Ssum=0.
3710  FOR K=1 TO 21
3720    Nsum=Nsum+Ninc(K,J)
3730    Ssum=Ssum+Sinc(K,J)
3740  NEXT K
3750  Nsum=(Nsum-Ninc(1,J)/2-Ninc(21,J)/2)*Length(J)/20
3760  Ssum=(Ssum-Sinc(1,J)/2-Sinc(21,J)/2)*Length(J)/20
3770  !
3780  RETURN
3790  ! *************
3800  ! PRINT RESULTS
3810  ! *************
3820  IMAGE 4X,D.5D,X,5D,X,6D.D,3(7D.D),2(X,MD.DDE)
3830  IMAGE 5X,DDD.D,X,MD.DDE,5(3X,4D.2D)
3840  !
3850  IF F$="D" OR F$="H" OR F$="M" THEN 4060
3860  !
3870  IF Headflag=1 THEN 4060
3880  PRINT " "
3890  PRINT Head$
3900  PRINT " "
3910  PRINT "UNIT WEIGHT, VERT STRESS, HORZ STRESS",Gamma,Sv,Sh
3920  PRINT "TUNNEL RADIUS, INTERNAL PRESSURE      ",Radius,Pressure
3930  PRINT "BLOCK HEIGHT, MAXIMUM HEIGHT, WEIGHT ",DROUND(Height,4),DROUND(Hbma
x,4),DROUND(Weight,4)
3940  PRINT "E, E MASS, POISSON'S RATIO, EXP COEF ",E1,Emass,Mu,Talph
3950  !
3960  PRINT " "
3970  PRINT "PLANE 'DIP' THETA  LENGTH (JRC)PHI   (JCS)I  RES PHI    LIN Kn    L
IN Ks"
3980  FOR I=1 TO Nplanes
3990    IF Flin$="Y" THEN PRINT USING 3820;I,Dip(I),Theta1(I),Length(I),Jrc(I),J
cs(I),Phires(I),kn(I),ks(I)
4000    IF Flin$="Y" THEN GOTO 4020
```

```
4010    PRINT USING 3820;I,Dip(I),Theta1(I),Length(I),Phi(I),Dilang(1,I),Phires(
I),Kn(I),Ks(I)
4020  NEXT I
4030  !
4040  PRINT " "
4050  PRINT "   DELTA T     DISP.     VERT F    HORZ F  RESULT F   TENSILE
F/W"
4060  PRINT USING 3830;Tdelt,Dis,Fv,Fh,Fr,Tense,Fw
4070  !
4080  IF F$<>"Y" THEN RETURN
4090  PRINTER IS 701
4100  !
4110  IF Nlines>45 THEN PRINT CHR$(12)
4120  IF Nlines>45 THEN Nlines=6
4130  IF F$="D" OR F$="H" OR F$="M" OR Headflag=1 THEN 4350
4140  !
4150  PRINT " "
4160  PRINT Head$
4170  PRINT " "
4180  PRINT "UNIT WEIGHT, VERT STRESS, HORZ STRESS",Gamma,Sv,Sh
4190  PRINT "TUNNEL RADIUS, INTERNAL P, DISP ALPHA",Radius,Pressure,Alphad
4200  PRINT "BLOCK HEIGHT, MAXIMUM HEIGHT, WEIGHT ",DROUND(Height,4),DROUND(Hbma
x,4),DROUND(Weight,4)
4210  PRINT "MODULUS, POISSON'S RATIO, EXP COEF   ",E1,Mu,Talph
4220  !
4230  PRINT " "
4240  PRINT "PLANE 'DIP' THETA  LENGTH (JRC)PHI   (JCS)I  RES PHI    LIN Kn    L
IN Ks"
4250  FOR I=1 TO Nplanes
4260    IF Flin$="Y" THEN PRINT USING 3820;I,Dip(I),Theta1(I),Length(I),Jrc(I),J
cs(I),Phires(I),Kn(I),Ks(I)
4270    IF Flin$="Y" THEN GOTO 4290
4280    PRINT USING 3820;I,Dip(I),Theta1(I),Length(I),Phi(I),Dilang(1,I),Phires(
I),Kn(I),Ks(I)
4290  NEXT I
4300  !
4310  PRINT " "
4320  PRINT "   DELTA T     DISP.     VERT F    HORZ F  RESULT F   TENSILE
F/W"
4330  Nlines=Nlines+13
4340  !
4350  PRINT USING 3830;Tdelt,Dis,Fv,Fh,Fr,Tense,Fw
4360  Nlines=Nlines+1
4370  !
4380  IF Pinc$<>"Y" THEN 4660
4390  !
4400  PRINT " "
4410  PRINT "  LENGTH 1  N STRESS  S STRESS  STRENGTH   NS/DISP   F ANGLE"
4420  FOR I=1 TO 21
4430    Fang=0
4440    IF Dis=0 THEN 4470
4450    X=Ninc(I,1)/Dis
4460    GOTO 4480
4470    X=0
4480    IF Ninc(I,1)=0 THEN 4500
4490    Fang=ATN(Strength(I,1)/Ninc(I,1))
4500    PRINT USING "7D.2D";Linc(I,1),Ninc(I,1),Sinc(I,1),Strength(I,1),X,Fang
```

```
4510  NEXT I
4520  !
4530  PRINT " "
4540  PRINT "  LENGTH 2  N STRESS  S STRESS  STRENGTH   NS/DISP   F ANGLE"
4550  FOR I=1 TO 21
4560    Fang=0
4570    IF Dis=0 THEN 4600
4580    X=Ninc(I,2)/Dis
4590    GOTO 4610
4600    X=0
4610    IF Ninc(I,2)=0 THEN 4630
4620    Fang=ATN(Strength(I,2)/Ninc(I,2))
4630    PRINT USING "7D.2D";Linc(I,2),Ninc(I,2),Sinc(I,2),Strength(I,2),X,Fang
4640  NEXT I
4650  Nlines=66
4660  PRINTER IS 1
4670  '
4680  RETURN
4690  ! ************************
4700  ! INITIAL JOINT STIFFNESS
4710  ! ************************
4720  FOR I=1 TO Nplanes
4730    Sig=Sv*ABS(COS(Dip(I)))+Sh*SIN(Dip(I))
4740    Kin(I)=(E1/Space(I))/(E1/Emass-1)
4750    X=Sig/(Aperture(I)*Kin(I))
4760    IF X<=.25 THEN GOTO 4810
4770    PRINTER IS 1
4780    PRINT "APERTURE SOLUTION WILL NOT CONVERGE"
4790    PAUSE
4800  !
4810    Cof(0)=-Sig/Aperture(I)
4820    Cof(1)=Kin(I)-Cof(0)
4830    Cof(2)=-2*Kin(I)
4840    Cof(3)=Kin(I)
4850    MAT Icof= (0)
4860    MAT Root= (0)
4870    MAT Iroot= (0)
4880  !
4890    CALL Siljak(3,Cof(*),Icof(*),1.E-12,1.E-12,50,Root(*),Iroot(*))
4900  !
4910    MAT SORT Root(*)
4920    Dva=Root(2)
4930    Kin(I)=Kin(I)*(1-Dva)*(1-Dva)
4940  !
4950  NEXT I
4960  !
4970  FOR I=1 TO Nplanes
4980    FOR J=1 TO 21
4990      Incl(J,I)=Initns(J,I)*Aperture(I)/(Kin(I)*Aperture(I)+Initns(J,I))
5000    NEXT J
```

```
5010  NEXT I
5020  '
5030  RETURN
5040  END !*****************************************************************
```

APPENDIX 2 Three-dimensional keyblock stability analysis program BSTB3D

The equations developed in Chapter 3 have been implemented into a numerical three-dimensional solution for the stability of keyblocks as a function of displacement. This solution has been coded in the BASIC computer language as an interactive program named BSTB3D that can be run on a Hewlett-Packard 9816 computer. The user is prompted by the program for data needed for the analysis in a series of queries that are answered from the keyboard. Figure 5.1 illustrated the problem geometry used in the solution; other aspects of the use of the program are stated in the interactive prompts provided to the user.

The steps performed by BSTB3D to analyze keyblock stability are listed below:

1. Load necessary subroutines from files named "HPBSTAB3D" and "STRESS3DB." File STRESS3DB is listed following the listing of BSTB3D, and contains the coded solutions for three-dimensional stresses at a point near a cylindrical underground excavation. File HPBSTAB3DB contains proprietary subroutines to which the Hewlett-Packard Company holds copyright. Similar subroutines can be substituted by the user, or these codes can be obtained from Hewlett-Packard. These proprietary subroutines are:

   LUDSHT - solves a linear system of equations using triangular decomposition

CMULT - multiplication of two complex numbers

CDIVID - complex number division

CABS - absolute value of a complex number

CSQRT - square root of a complex number

CINV - inverse of a complex number

SILJAK - finds roots of a polynomial without initial guess or derivative of the equation

2. Prompt user for input data. This data must be in a consistent system of units, and includes:

   -- printing options and a problem header
   -- number of discontinuity planes, rock mass modulus, modulus of intact rock, Poisson's ratio, and coefficient of linear thermal expansion
   -- tunnel radius, tunnel axis rise and azimuth, distance from tunnel axis to block apex, clockwise angle of line between tunnel axis and apex from vertical upward, and internal pressure within tunnel
   -- displacement vector dip, azimuth, and increment, number of increments, rock unit weight, and changes in tunnel temperature
   -- principal stress magnitudes, dips, and azimuths
   -- choice of linear or nonlinear joint behavior

   If linear behavior is selected, the following is needed for each discontinuity forming a block face:

-- dip, dip azimuth, normal stiffness, and shear stiffness
-- friction angle, dilatancy angle, and residual friction angle

If nonlinear behavior is selected, then the following is required:

-- dip, dip azimuth, average spacing, and average aperture at negligible normal stress
-- joint roughness coefficient (JRC), joint compressive strength (JCS), and residual friction angle

3. After prompting for input, BSTB3D echoes the parameters to provide a check to the user.

4. BSTB3D sets up the coordinate systems for the tunnel and rotates the 3D in situ stress tensor into the tunnel system. The rotated stress tensor is listed for inspection.

5. Equations are set up for each discontinuity face of the keyblock, and coordinates are calculated in the tunnel system for the block corners. If the block is subsequently truncated, corners of the truncation surface are also calculated.

6. The block is partitioned into segments and the volume and weight of the block are computed. Each face is then divided into a grid of points for stress calculations. Face coordinate systems are

set up for rotation of stresses into components acting parallel and perpendicular to the displacement direction.

7. If nonlinear deformation behavior has been chosen for the discontinuities the initial normal stiffnesses are computed using pre-excavation stresses, and subsequently are adjusted for stress concentrations around the tunnel.

8. Stresses are calculated for each of the face grid points and rotated from the tunnel coordinate system into the face coordinate systems.

9. Grid point stresses are adjusted for successive increments of displacement. The stresses are summed into resultant forces affecting the block; these forces and the F/W ratio are printed for each increment.

Once the specified number of displacement increments has been examined, the user is given several options:

-- truncate the block near the apex
-- impose a temperature change in the tunnel
-- specify a new displacement magnitude to be checked
-- specify a new displacement direction
-- change the discontinuity shear parameters
-- restart the program for a new analysis

A listing of BSTB3D follows.

```
10    PRINT "BSTB3D                    VERSION 1.3                    1/18/85"
20    PRINT " "
30    PRINT "VALUES USED IN THE ANALYSIS:"
40    PRINT " "
50    PRINT "BLOCK DISPLACEMENT (L) AND DISPLACEMENT DIP AND AZIMUTH"
60    PRINT "ROCK UNIT WEIGHT (FL^-3)"
70    PRINT "NORMAL AND SHEAR STIFFNESSES OF DISCONTINUITY PLANE (FL^-3)"
80    PRINT "FRICTION ANGLE AND DILATENCY ANGLE OF DISCONTINUITY PLANE"
90    PRINT "DISCONTINUITY PLANE DIPS AND DIP AZIMUTHS"
100   PRINT "IN SITU STRESSES AND STRESS ORIENTATIONS (FL^-2)"
110   PRINT "TEMPERATURE CHANGES AND COEF OF THERMAL EXPANSION"
120   PRINT "*****************************************************************
************"
130   PRINT "BSTAB3D REVISIONS:"
140   PRINT "1.3    1/18/85  ORIGINAL CODE BY JESSE L. YOW, JR."
150   PRINT "*****************************************************************
************"
160   !
170   DEG
180   OPTION BASE 1
190   INTEGER Dcnt,Dvd,I,J,K,L,Kc1,Kc2,Ke1,Ke2
200   !
210   COM /Data1/ Jtin(7,2),Phi(7),Dilang(7,66),Kn(7),Ks(7),Nplanes
220   COM /Data2/ Stin(6),Stindir(3,2),E1,E2,E3,Mu1,Mu2,Mu3,G1,G2,G3
230   COM /Data3/ Radius,Apexr,Apext,Trise,Tar,Tundir(3,2),Head$[80]
240   COM /Data4/ Disp,Dispdir(2),Dispinc,Farea(7),Gamma,Talph,Tdelt
250   COM /Data5/ Phires(7),Jrc(7),Jcs(7),Pressure,Viewvec(3),Viewcos(3,3)
260   COM /Data6/ Vol,Weight,Emass,Aperture(7),Space(7),Plin$[1]
270   COM /Dircos1/ Jtcos(7,3),Tuncos(3,3),Refcos(3,3),Deta(7)
280   COM /Dircos2/ Stigcos(3,3),Ddcos(3),Slider(7,3,3),Slirot(7,6,6)
290   COM /Eqns1/ Jteqn(7,4),Apex(3),Apecos(3),Linter(7,6),Corner(7,6)
300   COM /Flags/ Fprinter$[1],Froot,Nlines,Npages,Fheader,Foption$[1],Loaded
310   COM /Nonlin/ Closure(7,66),Kin(7),Sin(7),Ninc
320   COM /Sigseq/ Facexyz(7,66,4),Initial(7,66,3),Final(7,66,2),Force(7,2)
330   COM /Stress/ Stig(6),Stpt(6),Mu(3),Imu(3),Fb(3),Fr(3),Beta(6,6),Ae(6,6)
340   COM /Trunc/ Tcorn(7,3),Tapexr,Tarea
350   !
360   DIM Rot(6,6),D33a(3,3),D33b(3,3),D33c(3,3),D3a(3),Df(3)
370   DIM D7(7),D76(7,6),I7(7),D6(6),D31a(3,1),Lab1$[10]
380   DIM Cof(0:3),Icof(0:3),Root(3),Iroot(3)
390   !
400   IMAGE 8X,DD.2(6X,4D),2(X,MD.DDE),3(2X,6D.D)
410   IMAGE 6(X,MD.DDE)
420   IMAGE 10A,DD,XXXX,MD.DDE,2(6X,4D)
430   IMAGE 3D.D,X,MD.DDE,3D.D,5D,3(X,MD.DDE),X,5D.DD,4D.D,X,MD.DDE
440   !
450   IF Loaded=1 THEN 500
460   LOADSUB ALL FROM "HPBSTAB3D" ! LOAD HP PROPRIETARY SUBROUTINES
470   LOADSUB ALL FROM "STRESS3DB" ! LOAD SUBROUTINES FOR STRESS CALCULATIONS
480   Loaded=1
490   !
500   Lab1$="SIGMA" ! LABEL FOR PRINTING STRESS INPUT
```

```
510   Fprinter$=" "        ! FLAG FOR LINE PRINTER
520   Fzz=1.E-6      ! FUZZ FOR ROUNDING TO INTEGER
530   Foption$=" "      ! FLAG FOR OPTIONS
540   !
550   GOSUB 1310 ! PROMPT USER FOR DATA
560   !
570   IF Foption$="F" THEN 670
580   G1=E1/(2*(1+Mu1))
590   !
600   GOSUB 2230 ! INITIALIZE ARRAYS
610   GOSUB 2390 ! CALCULATE DIRECTION COSINES WRT REFERENCE COORDINATE SYSTEM
620   GOSUB 2650 ! ROTATE STRESS FIELD INTO TUNNEL REFERENCE SYSTEM
630   GOSUB 2880 ! SET UP PLANE EQNS AND CORNER COORDINATES
640   GOSUB 4130 ! PARTITION BLOCK AND COMPUTE VOLUME AND WEIGHT
650   GOSUB 5140 ! PARTITION BLOCK FACES INTO GRID FOR STRESS COMPUTATIONS
660   GOSUB 6110 ! ROTATE DISPLACEMENT DIRECTION ONTO FACES
670   IF Flin$="Y" THEN GOSUB 6810 ! CALCULATE INITIAL JOINT STIFFNESSES
680   IF Foption$="F" THEN GOTO 850
690   GOSUB 7060 ! CALCULATE STRESSES AT POINTS & ROTATE INTO DISP DIRECTION
700   GOTO 850
710   !
720   INPUT "DISPLACEMENT DIP AND AZIMUTH ?",Dispdir(*)
730   GOSUB 2590
740   GOSUB 6110
750   GOTO 850
760   !
770   INPUT "TRUNCATED APEX RADIUS ?",Tapexr
780   GOSUB 3790
790   GOSUB 4130
800   GOSUB 5140
810   GOTO 850
820   !
830   INPUT "DELTA TEMPERATURE ?",Tdelt
840   GOSUB 7120 ! CALCULATE THERMAL STRESSES
850   GOSUB 7480 ! INITIALIZE STRESS MATRICES
860   !
870   Disp=0.
880   Fheader=0
890   !
900   FOR Increment=1 TO Ninc
910     Disp=Disp+Dispinc
920     GOSUB 7600! ADJUST STRESSES FOR DISPLACEMENT
930     GOSUB 8150! FIND RESULTANT FORCES
940     GOSUB 8460! PRINT RESULTS
950   NEXT Increment
960   GOTO 1090
970   !
980   INPUT "DISPLACEMENT ?",Disp
990   Deldisp=Disp/10
1000  GOSUB 7480 ! INITIALIZE STRESS MATRICES
```

```
1010  FOR Incdisp=1 TO 10
1020    Disp=Deldisp*Incdisp
1030    GOSUB 7600  ! ADJUST STRESSES FOR DISPLACEMENT
1040    GOSUB 8150  ! FIND RESULTANT FORCES
1050  NEXT Incdisp
1060  !
1070  GOSUB 8460 ! PRINT RESULTS
1080  !
1090  INPUT "TYPE ONE-LETTER CHOICE OF OPTION '",Foption$
1100  IF Foption$="C" THEN 770
1110  IF Foption$="D" THEN 980
1120  IF Foption$="E" THEN 1290
1130  IF Foption$="F" THEN 550
1140  IF Foption$="R" THEN 530
1150  IF Foption$="S" THEN 720
1160  IF Foption$="T" THEN 830
1170  !
1180  PRINT " "
1190  PRINT "C  TRUNCATE BLOCK NEAR APEX"
1200  PRINT "D  SPECIFY DISPLACEMENT"
1210  PRINT "E  END"
1220  PRINT "F  CHANGE JOINT PLANE SHEAR PARAMETERS"
1230  PRINT "R  RESTART PROGRAM"
1240  PRINT "S  SPECIFY NEW DISPLACEMENT DIRECTION"
1250  PRINT "T  SPECIFY TEMPERATURE CHANGE"
1260  PRINT " "
1270  GOTO 1090
1280  !
1290  STOP '-----------------------------------------------------------------
1300  ! ************************
1310  ! INPUT AND ECHO PARAMETERS
1320  ! ************************
1330  PRINTER IS 1
1340  IF Foption$="F" THEN 1530
1350  !
1360  INPUT "ECHO RESULTS ON PRINTER ?",Fprinter$
1370  INPUT "PROBLEM HEADER (80 CHARACTERS MAX) ?",Head$
1380  INPUT "NUMBER OF PLANES, E MASS, E INTACT, POISSON'S RATIO, AND EXPANSION
COEF ?",Nplanes,Emass,E1,Mu1,Talph
1390  INPUT "TUNNEL RADIUS, CENTERLINE RISE, AZIMUTH, APEX DISTANCE, THETA, INTE
RNAL P ?",Radius,Trise,Taz,Apexr,Apext,Pressure
1400  Tapexr=Apexr
1410  INPUT "DISPLACEMENT DIP, AZIMUTH, INCREMENT, # INCS, ROCK UNIT WEIGHT, AND
 DEL T ?",Dispdir(*),Dispinc,Ninc,Gamma,Tdelt
1420  !
1430  ! INPUT IN SITU STRESSES
1440  !
1450  FOR I=1 TO 3
1460    DISP "INPUT MAGNITUDE, DIP, AND AZIMUTH OF SIGMA";I;
1470    INPUT " ",Stin(I),Stindir(I,1),Stindir(I,2)
1480  NEXT I
1490  !
1500  ! INPUT DISCONTINUITY PLANE DATA
```

```
1510  !
1520  INPUT "NONLINEAR JOINT BEHAVIOR (Y/N) ?",Flin$
1530  FOR I=1 TO Nplanes
1540    IF Flin$="Y" THEN 1620
1550  !
1560    DISP "INPUT DIP, DIP AZIMUTH, NORMAL STIFFNESS, & SHEAR STIFFNESS FOR PL
ANE";I;
1570    INPUT " ",Jtin(I,1),Jtin(I,2),Kn(I),Ks(I)
1580    DISP "INPUT PHI ANGLE, DILATANCY ANGLE, & RESIDUAL PHI ANGLE FOR PLANE";
I;
1590    INPUT " ",Phi(I),Dilang(I,1),Phires(I)
1600    GOTO 1670
1610  !
1620    DISP "INPUT DIP, DIP AZIMUTH, SPACING, AND APERTURE FOR PLANE";I;
1630    INPUT " ",Jtin(I,1),Jtin(I,2),Space(I),Aperture(I)
1640    DISP "INPUT JRC, JCS, AND RESIDUAL PHI ANGLE FOR PLANE";I;
1650    INPUT " ",Jrc(I),Jcs(I),Phires(I)
1660  !
1670  NEXT I
1680  !
1690  ! ECHO INPUT DATA
1700  !
1710  PRINT Head$
1720  PRINT " "
1730  PRINT "NUMBER OF DISCONTINUITY PLANES   ",Nplanes
1740  PRINT "E MASS, E INTACT, POISSON'S RATIO",Emass,E1,Mu1
1750  PRINT "EXPANSION COEF, INTERNAL PRESS   ",Talph,Pressure
1760  PRINT "TUNNEL RADIUS, RISE, & AZIMUTH   ",Radius,Trise,Taz
1770  PRINT "MAX RADIUS & THETA TO BLOCK APEX ",Apexr,Apext
1780  PRINT "DISP INCREMENT & ROCK UNIT WEIGHT",Dispinc,Gamma
1790  PRINT " "
1800  PRINT "                MAGNITUDE        DIP    AZIMUTH"
1810  FOR I=1 TO 3
1820    PRINT USING 420;Lab1$,I,Stin(I),Stindir(I,1),Stindir(I,2)
1830  NEXT I
1840  PRINT " "
1850  PRINT "     PLANE        DIP    DIP AZ    LIN Kn    LIN Ks  (JRC)PHI    (JC
S)I   RES PHI"
1860  FOR I=1 TO Nplanes
1870    IF Flin$="Y" THEN PRINT USING 400;I,Jtin(I,1),Jtin(I,2),Kn(I),Ks(I),Jrc(
I),Jcs(I),Phires(I)
1880    IF Flin$="Y" THEN 1900
1890    PRINT USING 400;I,Jtin(I,1),Jtin(I,2),Kn(I),Ks(I),Phi(I),Dilang(I,1),Phi
res(I)
1900  NEXT I
1910  !
1920  IF Fprinter$<>"Y" THEN 2200
1930  !
1940  PRINTER IS 701
1950  !
1960  PRINT CHR$(12)
1970  PRINT Head$
1980  PRINT " "
1990  PRINT "NUMBER OF DISCONTINUITY PLANES   ",Nplanes
2000  PRINT "E MASS, E INTACT, POISSON'S RATIO",Emass,E1,Mu1
```

```
2010  PRINT "EXPANSION COEF, INTERNAL PRESS   ",Talph,Pressure
2020  PRINT "TUNNEL RADIUS, RISE, & AZIMUTH   ",Radius,Trise,Taz
2030  PRINT "RADIUS AND THETA TO BLOCK APEX   ",Apexr,Apext
2040  PRINT "DISP INCREMENT & ROCK UNIT WEIGHT",Dispinc,Gamma
2050  PRINT " "
2060  PRINT "                    MAGNITUDE        DIP   AZIMUTH"
2070  FOR I=1 TO 3
2080    PRINT USING 420;Lab4$,I,Stin(I),Stindir(I,1),Stindir(I,2)
2090  NEXT I
2100  PRINT " "
2110  PRINT "     PLANE        DIP    DIP AZ    LIN Kn    LIN Ks  (JRC)PHI    (JC
S)I   RES PHI"
2120  FOR I=1 TO Nplanes
2130    IF Flin$="Y" THEN PRINT USING 400;I,Jtin(I,1),Jtin(I,2),Kn(I),Ks(I),Jrc(
I),Jcs(I),Phires(I)
2140    IF Flin$="Y" THEN 2160
2150    PRINT USING 400;I,Jtin(I,1),Jtin(I,2),Kn(I),Ks(I),Phi(I),Dilang(I,1),Phi
res(I)
2160  NEXT I
2170  Nlines=21+Nplanes
2180  Npages=1
2190  !
2200  PRINTER IS 1
2210  RETURN
2220  ! ********************************
2230  ! INITIALIZE ARRAYS FROM INPUT DATA
2240  ! ********************************
2250  MAT Linter= (0)
2260  MAT Corner= (0)
2270  MAT Refcos= IDN
2280  !
2290  !
2300  Tundir(1,1)=90
2310  Tundir(1,2)=Taz+90
2320  Tundir(2,1)=90-Trise
2330  Tundir(2,2)=Taz
2340  Tundir(3,1)=ABS(Trise)
2350  IF Trise<=0 THEN Tundir(3,2)=Taz
2360  IF Trise>0 THEN Tundir(3,2)=Taz+180
2370  RETURN
2380  ! ************************************************
2390  ! DIRECTION COSINES WRT REFERENCE COORDINATE SYSTEM
2400  ! ************************************************
2410  FOR I=1 TO 3 ! DIRECTION COSINES OF THE TUNNEL SYSTEM
2420    Tuncos(I,1)=FNDircosl(Tundir(I,1),Tundir(I,2))
2430    Tuncos(I,2)=FNDircosm(Tundir(I,1),Tundir(I,2))
2440    Tuncos(I,3)=FNDircosn(Tundir(I,1))
2450  NEXT I
2460  !
2470  FOR I=1 TO 3 ! DIRECTION COSINES OF THE PRINCIPAL STRESSES
2480    Stigcos(I,1)=FNDircosl(Stindir(I,1)+90,Stindir(I,2))
2490    Stigcos(I,2)=FNDircosm(Stindir(I,1)+90,Stindir(I,2))
2500    Stigcos(I,3)=FNDircosn(Stindir(I,1)+90)
```

```
2510  NEXT I
2520  !
2530  FOR I=1 TO Nplanes ! DIRECTION COSINES OF THE JOINTS
2540    Jtcos(I,1)=FNDircosl(Jtin(I,1),Jtin(I,2))
2550    Jtcos(I,2)=FNDircosm(Jtin(I,1),Jtin(I,2))
2560    Jtcos(I,3)=FNDircosn(Jtin(I,1))
2570  NEXT I
2580  !
2590  Ddcos(1)=FNDircosl(Dispdir(1)+90,Dispdir(2))
2600  Ddcos(2)=FNDircosm(Dispdir(1)+90,Dispdir(2))
2610  Ddcos(3)=FNDircosn(Dispdir(1)+90)
2620  !
2630  RETURN
2640  ! ******************************************
2650  ! ROTATE STRESSES INTO TUNNEL COORDINATE SYSTEM
2660  ! ******************************************
2670  MAT D33a= TRN(Stigcos)
2680  MAT D33b= Tuncos*D33a
2690  CALL Transf(D33b(*),Rot(*))
2700  MAT Stig= Rot*Stin
2710  !
2720  PRINT " "
2730  PRINT "   SIGMA 1   SIGMA 2   SIGMA 3    TAU 23    TAU 31    TAU 12"
2740  PRINT USING 410;Stin(*) ! PRINT OLD STRESS ARRAY ON CRT
2750  PRINT USING 410;Stig(*) ! PRINT NEW STRESS ARRAY ON CRT
2760  !
2770  IF Fprinter$<>"Y" THEN 2870
2780  !
2790  PRINTER IS 701
2800  PRINT " "
2810  PRINT "   SIGMA 1   SIGMA 2   SIGMA 3    TAU 23    TAU 31    TAU 12"
2820  PRINT USING 410;Stin(*) ! PRINT OLD STRESS ARRAY
2830  PRINT USING 410;Stig(*) ! PRINT NEW STRESS ARRAY
2840  Nlines=Nlines+4
2850  PRINTER IS 1
2860  !
2870  RETURN
2880  ! ********************************
2890  ! PLANE EQNS AND CORNER COORDINATES
2900  ! ********************************
2910  MAT Apecos= (0)
2920  MAT Apex= (0)
2930  MAT Corner= (0)
2940  MAT Jteqn= (0)
2950  MAT Linter= (0)
2960  !
2970  Apecos(1)=FNDircosl(Apext,90) ! APEX DIRECTION COSINES
2980  Apecos(2)=FNDircosm(Apext,90)
2990  Apecos(3)=FNDircosn(Apext)
3000  !
```

```
3010  FOR I=1 TO 3
3020    Apex(I)=Apecos(I)*Ape r' APEX COORDINATES
3030  NEXT I
3040  !
3050  FOR I=1 TO Nplanes ! JT EQNS IN TUNNEL COORDINATE SYSTEM
3060    FOR K=1 TO 3
3070      Jteqn(I,K)=Tuncos(K,1)*Jtcos(I,1)+Tuncos(K,2)*Jtcos(I,2)+Tuncos(K,3)*J
tcos(I,3)
3080    NEXT K
3090    Jteqn(I,4)=Apex(1)*Jteqn(I,1)+Apex(2)*Jteqn(I,2)+Apex(3)*Jteqn(I,3)
3100  NEXT I
3110  !
3120  FOR I=1 TO Nplanes ! LINES OF INTERSECTION BETWEEN FACES
3130    J=I+1
3140    IF I=Nplanes THEN J=J-Nplanes
3150    Linter(I,1)=Jteqn(I,2)*Jteqn(J,3)-Jteqn(J,2)*Jteqn(I,3)    ! L DIRCOS
3160    Linter(I,2)=Jteqn(J,1)*Jteqn(I,3)-Jteqn(I,1)*Jteqn(J,3)    ! M DIRCOS
3170    Linter(I,3)=Jteqn(I,1)*Jteqn(J,2)-Jteqn(J,1)*Jteqn(I,2)    ' N DIRCOS
3180  !
3190    C=SQR(Linter(I,1)*Linter(I,1)+Linter(I,3)*Linter(I,3))
3200    X=ACS((Linter(I,1)*Apecos(1)/C)+(Linter(I,3)*Apecos(3)/C))! ANGLE IN XZ
PLANE BETWEEN INTERSECTION LINE AND LINE THRU APEX
3210    IF X>90 THEN X=180-X
3220    Y=ASN(SIN(X)*Apexr/Radius)-X ' THETA DIFF BETWEEN APEX AND INT LINE
3230  !
3240    Linter(I,4)=Y
3250    Linter(I,5)=I      ! FIRST FACE
3260    Linter(I,6)=J      ' SECOND FACE
3270  NEXT I
3280  !
3290  FOR I=Nplanes+1 TO 7
3300    Linter(I,4)=Apext+180
3310  NEXT I
3320  !
3330  FOR I=1 TO Nplanes ! CALCULATE CORNER COORDINATES
3340    J=Linter(I,5)
3350    K=Linter(I,6)
3360    X=Apext+Linter(I,4)
3370    Test=0
3380  !
3390    D33c(1,1)=Jteqn(J,1) ! EQN OF FACE J
3400    D33c(1,2)=Jteqn(J,2)
3410    D33c(1,3)=Jteqn(J,3)
3420    D31a(1,1)=Jteqn(J,4)
3430  !
3440    D33c(2,1)=Jteqn(K,1) ! EQN OF FACE K
3450    D33c(2,2)=Jteqn(K,2)
3460    D33c(2,3)=Jteqn(K,3)
3470    D31a(2,1)=Jteqn(K,4)
3480  !
3490    D33c(3,1)=FNDircosl(X,90) ! PLANE TANGENT TO TUNNEL
3500    D33c(3,2)=FNDircosm(X,90)
```

```
3510    D33c(3,3)=FNDircosn(X)
3520    D31a(3,1)=Radius
3530  !
3540    CALL Ludsht(D33c(*),D31a(*),3,1) ! SOLVE FOR X,Y,Z OF CORNER
3550  !
3560    D3a(1)=D31a(1,1)
3570    D3a(2)=D31a(2,1)
3580    D3a(3)=D31a(3,1)
3590  !
3600    IF ABS(1-SQR(D3a(1)*D3a(1)+D3a(2)*D3a(3))/Radius)<.01 THEN 3690
3610  !
3620    X=Apext-Linter(I,4)
3630    Test=Test+1
3640    IF Test>2 THEN 3390
3650  !
3660    PRINT "PROBLEM WITH CORNER",J,K
3670    PAUSE
3680  !
3690    Corner(I,1)=D3a(1) ! X COORDINATE
3700    Corner(I,2)=D3a(2) ! Y COORDINATE
3710    Corner(I,3)=D3a(3) ! Z COORDINATE
3720    Corner(I,4)=J ! FIRST FACE
3730    Corner(I,5)=K ! SECOND FACE
3740    Corner(I,6)=0 ! PLANE TANGENT TO TUNNEL
3750    Linter(I,4)=X ! CHANGE TO THETA ANGLE ALONG TUNNEL SURFACE
3760  NEXT I
3770  RETURN
3780  ! ***********************************
3790  ! CALCULATE CORNERS OF TRUNCATED APEX
3800  ! ***********************************
3810  FOR I=1 TO Nplanes
3820    J=Linter(I,5)
3830    K=Linter(I,6)
3840    X=Apext
3850  !
3860    D33c(1,1)=Jteqn(J,1) ! EQN OF FACE J
3870    D33c(1,2)=Jteqn(J,2)
3880    D33c(1,3)=Jteqn(J,3)
3890    D31a(1,1)=Jteqn(J,4)
3900  !
3910    D33c(2,1)=Jteqn(K,1) ! EQN OF FACE K
3920    D33c(2,2)=Jteqn(K,2)
3930    D33c(2,3)=Jteqn(K,3)
3940    D31a(2,1)=Jteqn(K,4)
3950  !
3960    D33c(3,1)=FNDircosl(X,90) ! PLANE TANGENT TO TUNNEL
3970    D33c(3,2)=FNDircosm(X,90)
3980    D33c(3,3)=FNDircosn(X)
3990    D31a(3,1)=Tapexr
4000  !
```

```
4010    CALL Ludsht(D33c(*),D31a(*),3,1) ! SOLVE FOR X,Y,Z OF CORNER
4020  !
4030    D3a(1)=D31a(1,1)
4040    D3a(2)=D31a(2,1)
4050    D3a(3)=D31a(3,1)
4060  !
4070    Tcorn(I,1)=D3a(1) ! X COORDINATE
4080    Tcorn(I,2)=D3a(2) ! Y COORDINATE
4090    Tcorn(I,3)=D3a(3) ! Z COORDINATE
4100  NEXT I
4110  RETURN
4120  ! ******************************************
4130  ! PARTITION BLOCK AND COMPUTE VOLUME AND WEIGHT
4140  ! ******************************************
4150  MAT D76= Linter
4160  !
4170  FOR I=1 TO 7 ! GROUP THETA INTERCEPTS AROUND Apext
4180    IF D76(I,4)>180+Apext THEN D76(I,4)=D76(I,4)-360
4190    D76(I,4)=D76(I,4)-Apext
4200  NEXT I
4210  !
4220  MAT SORT D76(*,4) TO D7 ! FIND ORDER OF THETA VALUES
4230  MAT D76= Linter
4240  MAT REORDER D76 BY D7 ! ORDER INTERSECT LINES BY THETA
4250  !
4260  FOR I=1 TO 7
4270    I7(I)=D76(I,4)      ! FIND THETA FROM APEX
4280  NEXT I
4290  !
4300  Orb=2*Radius*SIN(.05) ! "WIDTH" OF A 0.1 DEGREE ARC (SEGMENT BASE WIDTH)
4310  Itmin=MIN(I7(*))
4320  Itmax=MAX(I7(*))
4330  J=INT(D76(1,5)+Fzz)   ! INITIAL PLANES BOUNDING SEGMENT
4340  K=INT(D76(1,6)+Fzz)   ! INITIAL PLANES BOUNDING SEGMENT
4350  L=2
4360  Vol=0
4370  !
4380  FOR Iv=Itmin TO Itmax STEP .1      ! COMPUTE BLOCK VOLUME BY SEGMENTS
4390    IF Iv>=180 THEN 4730 ! CHECK IF DONE WITH VOLUME
4400    IF Iv<I7(L) THEN 4570 ! CHECK IF PASSED INTERSECT LINE L
4410  !
4420    IF J<>D76(L,5) THEN 4450 ! REVISE J
4430    J=INT(D76(L,6)+Fzz)
4440    GOTO 4470
4450    IF J<>D76(L,6) THEN 4470
4460    J=INT(D76(L,5)+Fzz)
4470    IF K<>D76(L,5) THEN 4500 ! REVISE K
4480    K=INT(D76(L,6)+Fzz)
4490    GOTO 4520
4500    IF K<>D76(L,6) THEN 4520
```

```
4510    K=INT(D76(L,5)+Fzz)
4520    L=L+1
4530    IF L>Nplanes THEN 4730
4540    IF J<>K THEN 4400 ! IF J=K THEN VOLUME CALCULATION IS FINISHED
4550    GOTO 4710
4560  !
4570    A=SIN(Iv+Apext)                    ! EQN OF PLANE TANGENT TO TUNNEL
4580    C=COS(Iv+Apext)
4590    D=Radius
4600  !
4610    X=A*D ! X,Y,Z COORDINATES OF TANGENT PLANE FORMING SEGMENT BASE
4620    Z=C*D
4630  !
4640    Y1=(Jteqn(J,1)*X+Jteqn(J,3)*Z-Jteqn(J,4))/Jteqn(J,2)
4650    Y2=(Jteqn(K,1)*X+Jteqn(K,3)*Z-Jteqn(K,4))/Jteqn(K,2)
4660    Dely=ABS(Y1-Y2) ! LENGTH OF SEGMENT BASE ALONG TUNNEL
4670    Bs=Dely*Ork ! AREA OF SEGMENT BASE
4680    Ht=ABS((A*Apex(1)+C*Apex(3)-D)/SQR(A*A+C*C))        ! HEIGHT OF SEGMENT
4690    Dvol=Bs*Ht/3 ! VOLUME OF SEGMENT
4700    Vol=Vol+Dvol ! VOLUME OF BLOCK
4710  NEXT Iv
4720  !
4730  IF Foption$<>"C" THEN 4990
4740  !
4750  Tarea=0
4760  FOR I=3 TO Nplanes
4770    Dx=Tcorn(1,1)-Tcorn(I-1,1)
4780    Dy=Tcorn(1,2)-Tcorn(I-1,2)
4790    Dz=Tcorn(1,3)-Tcorn(I-1,3)
4800    L1=SQR(Dx*Dx+Dy*Dy+Dz*Dz)
4810  !
4820    Dx=Tcorn(1,1)-Tcorn(I,1)
4830    Dy=Tcorn(1,2)-Tcorn(I,2)
4840    Dz=Tcorn(1,3)-Tcorn(I,3)
4850    L2=SQR(Dx*Dx+Dy*Dy+Dz*Dz)
4860  !
4870    Dx=Tcorn(I,1)-Tcorn(I-1,1)
4880    Dy=Tcorn(I,2)-Tcorn(I-1,2)
4890    Dz=Tcorn(I,3)-Tcorn(I-1,3)
4900    L3=SQR(Dx*Dx+Dy*Dy+Dz*Dz)
4910  !
4920    S=(L1+L2+L3)/2
4930    Tarea=Tarea+SQR(S*(S-L1)*(S-L2)*(S-L3))
4940  NEXT I
4950  !
4960  Tvol=Tarea*(Apexr-Tapexr)/3
4970  Vol=Vol-Tvol
4980  !
4990  Weight=Vol*Gamma
5000  !
```

```
5010  PRINT " "
5020  PRINT "BLOCK VOLUME & WEIGHT:",DROUND(Vol,6),DROUND(Weight,4)
5030  !
5040  IF Fprinter$<>"Y" THEN 5120
5050  !
5060  PRINTER IS 701
5070  PRINT " "
5080  PRINT "BLOCK VOLUME & WEIGHT:",DROUND(Vol,6),DROUND(Weight,4)
5090  Nlines=Nlines+2
5100  PRINTER IS 1
5110  !
5120  RETURN
5130  ! ******************************************************
5140  ! PARTITION BLOCK FACES INTO GRID FOR STRESS COMPUTATIONS
5150  ! ******************************************************
5160  MAT Farea= (0)
5170  FOR I=1 TO Nplanes
5180    Trad=Apexr+1.E-6
5190  !
5200    FOR K=1 TO Nplanes! FIND EDGES AND CORNERS OF FACE
5210      IF Corner(K,4)<>I THEN 5230
5220      Kc1=K
5230      IF Corner(K,5)<>I THEN 5250
5240      Kc2=K
5250      IF Linter(K,5)<>I THEN 5270
5260      Ke1=K
5270      IF Linter(K,6)<>I THEN 5290
5280      Ke2=K
5290    NEXT K
5300  !
5310    Bet=ACS(Linter(Ke1,1)*Linter(Ke2,1)+Linter(Ke1,2)*Linter(Ke2,2)+Linter(K
e1,3)*Linter(Ke2,3))! INCLUDED ANGLE IN FACE AT APEX
5320  !
5330    Dx1=(Corner(Kc1,1)-Apex(1))/10
5340    Dy1=(Corner(Kc1,2)-Apex(2))/10
5350    Dz1=(Corner(Kc1,3)-Apex(3))/10
5360    Dx2=(Corner(Kc2,1)-Apex(1))/10
5370    Dy2=(Corner(Kc2,2)-Apex(2))/10
5380    Dz2=(Corner(Kc2,3)-Apex(3))/10
5390  !
5400    IF Foption$<>"C" THEN 5450
5410    X=(Tcorn(Kc1,1)+Tcorn(Kc2,1))/2
5420    Z=(Tcorn(Kc1,3)+Tcorn(Kc2,3))/2
5430    Trad=SQR(X*X+Z*Z)
5440  !
5450    FOR K=1 TO 10! COMPUTE COORDINATES OF EDGE POINTS
5460      Facexyz(I,K,1)=Corner(Kc1,1)-Dx1*(K-1)
5470      Facexyz(I,K,2)=Corner(Kc1,2)-Dy1*(K-1)
5480      Facexyz(I,K,3)=Corner(Kc1,3)-Dz1*(K-1)
5490      Facexyz(I,K+11,1)=Corner(Kc2,1)-Dx2*(K-1)
5500      Facexyz(I,K+11,2)=Corner(Kc2,2)-Dy2*(K-1)
```

```
5510      Facexyz(I,K+11,3)=Corner(Kc2,3)-Dz2*(K-1)
5520    NEXT K
5530  !
5540    FOR K=1 TO 3
5550      Facexyz(I,11,K)=Apex(K)
5560    NEXT K
5570  !
5580    L=21
5590    FOR J=1 TO 9 ! ASSIGN COORDINATES TO POINTS WITHIN FACE EDGES
5600      Dvd=11-J
5610      Dx=(Facexyz(I,J,1)-Facexyz(I,J+11,1))/Dvd
5620      Dy=(Facexyz(I,J,2)-Facexyz(I,J+11,2))/Dvd
5630      Dz=(Facexyz(I,J,3)-Facexyz(I,J+11,3))/Dvd
5640      FOR K=1 TO Dvd-1
5650        L=L+1
5660        Facexyz(I,L,1)=Facexyz(I,J,1)-Dx*K
5670        Facexyz(I,L,2)=Facexyz(I,J,2)-Dy*K
5680        Facexyz(I,L,3)=Facexyz(I,J,3)-Dz*K
5690      NEXT K
5700    NEXT J
5710  !
5720    Dh=0 ! CALCULATE AREAS FOR FACE SEGMENTS
5730    Dw=0
5740    FOR J=1 TO 3
5750      Dh=Dh+(Facexyz(I,1,J)-Facexyz(I,2,J))^2
5760      Dw=Dw+(Facexyz(I,2,J)-Facexyz(I,22,J))^2
5770    NEXT J
5780    Dh=SQR(Dh)
5790    Dw=SQR(Dw)
5800  !
5810    Ar1=Dh*Dw*SIN(Bet)
5820    Ar2=Ar1/2
5830    Ar4=Ar1/4
5840  !
5850    Facexyz(I,1,4)=Ar4 ! AREAS FOR SEGMENTS AT CORNERS AND APEX
5860    Facexyz(I,11,4)=Ar4
5870    Facexyz(I,12,4)=Ar4
5880  !
5890    FOR J=2 TO 10 ! AREAS FOR SEGMENTS ALONG FACE EDGES
5900      Facexyz(I,J,4)=Ar2
5910      Facexyz(I,J+11,4)=Ar2
5920      Facexyz(I,J+20,4)=Ar2
5930    NEXT J
5940  !
5950    FOR J=31 TO 66 ! AREAS FOR SEGMENTS WITHIN FACE EDGES
5960      Facexyz(I,J,4)=Ar1
5970    NEXT J
5980  !
5990    FOR J=1 TO 66 ! SET AREA TO ZERO IF WITHIN TUNNEL OR TRUNCATED
6000      R=SQR(Facexyz(I,J,1)^2+Facexyz(I,J,3)^2)
```

```
6010      IF R>Radius-Fzz THEN Facexyz(I,J,4)=0
6020      IF R>Trad THEN Facexyz(I,J,4)=0
6030    NEXT J
6040  !
6050    FOR J=1 TO 66 ! AREA OF FACES
6060      Farea(I)=Farea(I)+Facexyz(I,J,4)
6070    NEXT J
6080  NEXT I
6090  RETURN
6100  ! ********************************
6110  ! SET UP DISP DIRECTIONS FOR FACES
6120  ! ********************************
6130  MAT D3a= Ddcos          ! ROTATE DISP DIRCOS INTO TUNNEL COORDINATE SYSTEM
6140  MAT Ddcos= Tuncos*D3a
6150  !
6160  FOR I=1 TO Nplanes                  ! PROJECT ONTO FACES (DOUBLE X PRODUCT)
6170    Slider(I,1,1)=Jteqn(I,2)*Ddcos(3)-Ddcos(2)*Jteqn(I,3)                ! XL
6180    Slider(I,1,2)=Ddcos(1)*Jteqn(I,3)-Jteqn(I,1)*Ddcos(3)                ! XM
6190    Slider(I,1,3)=Jteqn(I,1)*Ddcos(2)-Ddcos(1)*Jteqn(I,2)                ! XN
6200  !
6210    C=SQR(Slider(I,1,1)*Slider(I,1,1)+Slider(I,1,2)*Slider(I,1,2)+Slider(I,1
,3)*Slider(I,1,3))
6220  !
6230    FOR J=1 TO 3                                          ! NORMALIZE VECTOR
6240      Slider(I,1,J)=-Slider(I,1,J)/C
6250    NEXT J
6260  !
6270    Slider(I,2,1)=Jteqn(I,1)                                             ! YL
6280    Slider(I,2,2)=Jteqn(I,2)                                             ! YM
6290    Slider(I,2,3)=Jteqn(I,3)                                             ! YN
6300  !
6310    Slider(I,3,1)=Slider(I,1,2)*Jteqn(I,3)-Jteqn(I,2)*Slider(I,1,3)      ! ZL
6320    Slider(I,3,2)=Jteqn(I,1)*Slider(I,1,3)-Slider(I,1,1)*Jteqn(I,3)      ! ZM
6330    Slider(I,3,3)=Slider(I,1,1)*Jteqn(I,2)-Jteqn(I,1)*Slider(I,1,2)      ! ZN
6340  !
6350    C=SQR(Slider(I,3,1)*Slider(I,3,1)+Slider(I,3,2)*Slider(I,3,2)+Slider(I,3
,3)*Slider(I,3,3))
6360  !
6370    FOR J=1 TO 3                                          ! NORMALIZE VECTOR
6380      Slider(I,3,J)=Slider(I,3,J)/C
6390    NEXT J
6400  NEXT I
6410  !
6420  FOR I=1 TO Nplanes   ! SEE IF PROJECTED DISP DIRECTION IS IN PLANE OF FACE
6430    Check=0
6440    FOR J=1 TO 3
6450      Check=Check+Jteqn(I,J)*Slider(I,3,J)
6460    NEXT J
6470    IF ABS(Check)<Fzz THEN 6500
6480    PRINT "DISP DIRECTION IS NOT IN PLANE FOR FACE",I
6490    PAUSE
6500  NEXT I
```

```
6510  !
6520  FOR I=1 TO Nplanes     ' FIND ANGLE BETWEEN FACE AND DISPLACEMENT DIRECTION
6530    X=0
6540    FOR J=1 TO 3
6550      X=X+Slider(I,3,J)*Ddcos(J)
6560    NEXT J
6570    Deta(I)=ACS(X)
6580    IF Deta(I)>90 THEN Deta(I)=180-Deta(I)
6590  NEXT I
6600  '
6610  FOR I=1 TO Nplanes              ' SET UP STRESS ROTATION MATRIX FOR EACH FACE
6620    FOR J=1 TO 3
6630      FOR K=1 TO 3
6640        D33a(J,K)=Slider(I,J,K)
6650      NEXT K
6660    NEXT J
6670  '
6680    CALL Transf(D33a(*),Rot(*))  ! CREATE ROTATION MATRIX FOR PLANE I
6690  '
6700    MAT D6= Rot*Stig
6710    Sin(I)=D6(2)                  ' NORMAL STRESS ON PLANE BEFORE EXCAVATION
6720  '
6730    FOR J=1 TO 6
6740      FOR K=1 TO 6
6750        Slirot(I,J,K)=Rot(J,K)
6760      NEXT K
6770    NEXT J
6780  NEXT I
6790  RETURN
6800  ' ********************************
6810  ! COMPUTE INITIAL JOINT STIFFNESSES
6820  ! ********************************
6830  FOR I=1 TO Nplanes
6840    Kin(I)=(E1/Space(I))/(E1/Emass-1)
6850    X=Sin(I)/(Aperture(I)*Kin(I))
6860    IF X<=.25 THEN GOTO 6920
6870  !
6880    PRINTER IS 1
6890    PRINT "APERTURE SOLUTION WILL NOT CONVERGE"
6900    PAUSE
6910  !
6920    Cof(0)=-Sin(I)/Aperture(I)
6930    Cof(1)=Kin(I)-Cof(0)
6940    Cof(2)=-2*Kin(I)
6950    Cof(3)=Kin(I)
6960    MAT Icof= (0)
6970  !
6980    CALL Siljak(3,Cof(*),Icof(*),1.E-12,1.E-12,50,Root(*),Iroot(*))
6990  !
7000    MAT SORT Root(*)
```

```
7010    Dva=Root(2)
7020    Kin(I)=Kin(I)*(1-Dva)*(1-Dva)
7030  NEXT I
7040  RETURN
7050  ! ******************************************
7060  ! COMPUTE STRESSES AT GRID POINTS ON EACH FACE
7070  ! ******************************************
7080  MAT Initial= (0)
7090  MAT Closure= (0)
7100  Froot=0 ! FLAG FOR FIRST USE OF STRESS3D
7110  !
7120  FOR I=1 TO Nplanes
7130    FOR J=1 TO 66
7140      DISP I,J
7150      IF Facexyz(I,J,4)=0 THEN 7430 ! POINT IS WITHIN TUNNEL
7160  !
7170      Ra=SQR(Facexyz(I,J,1)^2+Facexyz(I,J,3)^2)/Radius ! RADIUS FOR AMADEI
7180      IF Facexyz(I,J,1)=0 THEN 7210
7190      X=ATN(Facexyz(I,J,3)/Facexyz(I,J,1))
7200      GOTO 7230
7210      X=90
7220  !
7230      X=90-X
7240      IF Facexyz(I,J,1)<0 THEN X=X+180
7250      X=X-90
7260      Tet=360-X
7270      IF Tet>360 THEN Tet=Tet-360
7280  !
7290      CALL Stress3d(Ra,Tet) ! COMPUTE STRESSES IN TUNNEL SYSTEM AT POINT
7300  !
7310      FOR K=1 TO 6
7320        FOR L=1 TO 6
7330          Rot(K,L)=Slirot(I,K,L)
7340        NEXT L
7350      NEXT K
7360  !
7370      MAT D6= Rot*Stpt ! ROTATE STRESSES ONTO FACE I OF BLOCK
7380  !
7390      Initial(I,J,1)=D6(2) ! NORMAL STRESS (Y)
7400      Initial(I,J,2)=D6(4) ! SHEAR STRESS ALONG DISPLACEMENT DIRECTION (YZ)
7410      Initial(I,J,3)=D6(6) ! SHEAR STRESS ACROSS DISPLACEMENT DIRECTION (XY)
7420  !
7430    NEXT J
7440  NEXT I
7450  DISP " "
7460  RETURN
7470  ! ************************************
7480  ! INITIALIZE STRESS AND CLOSURE MATRICES
7490  ! ************************************
7500  FOR I=1 TO Nplanes
```

```
7510    FOR J=1 TO 66
7520      IF Flin$<>"Y" THEN 7540
7530      Closure(I,J)=Initial(I,J,1)*Aperture(I)/(Kin(I)*Aperture(I)+Initial(I,
J,1))                          ! JOINT CLOSURE DUE TO EXCAVATION-INDUCED STRESSES
7540      Final(I,J,1)=Initial(I,J,1)
7550      Final(I,J,2)=Initial(I,J,2)
7560    NEXT J
7570  NEXT I
7580  RETURN
7590  ! ********************************
7600  ! ADJUST STRESSES FOR DISPLACEMENT
7610  ! ********************************
7620  D=Disp
7630  DISP Disp
7640  IF Flin$="Y" THEN 7870       ! CHECK FOR NON-LINEAR JOINT BEHAVIOR
7650  '
7660  FOR I=1 TO Nplanes  ! LINEAR JOINT BEHAVIOR
7670    FOR J=1 TO 66
7680  '
7690      IF Facexyz(I,J,4)=0 THEN 7830 ! POINT IS WITHIN TUNNEL
7700  !
7710      X=Kn(I)*D*(SIN(Deta(I))-COS(Deta(I))*TAN(Dilang(I,1)))
7720      Final(I,J,1)=Initial(I,J,1)-X ! NORMAL STRESS CHANGED BY DISPLACEMENT
7730      IF Final(I,J,1)<0 THEN Final(I,J,1)=0 ! DISALLOW TENSION
7740  '
7750      X=Ks(I)*D*COS(Deta(I))
7760      Final(I,J,2)=Initial(I,J,2)-X ! SHEAR STRESS CHANGED BY DISPLACEMENT
7770  '
7780      X=Final(I,J,1)*TAN(Phi(I)+Dilang(I,1)) ! COMPUTE MAXIMUM FRICTION
7790      IF ABS(Final(I,J,2))<X THEN 7830
7800  !
7810      X=Final(I,J,1)*TAN(Phires(I)) ! COMPUTE RESIDUAL FRICTION
7820      Final(I,J,2)=X*SGN(Final(I,J,2))
7830    NEXT J
7840  NEXT I
7850  GOTO 8120
7860  '
7870  FOR I=1 TO Nplanes ! NON-LINEAR JOINT BEHAVIOR
7880    FOR J=1 TO 66
7890      X=Final(I,J,1)
7900      IF X<1 THEN X=1
7910      Dilang(I,J)=Jrc(I)*LGT(Jcs(I)/X)
7920  !
7930      Dope=D*(SIN(Deta(I))-COS(Deta(I))*TAN(Dilang(I,1))) ! JOINT OPENING
7940      X=Closure(I,J)-Dope                                 ! NEW VALUE FOR CLOSURE
7950      IF X<=Closure(I,J) THEN 8000
7960  !
7970      DISP "OVER CLOSURE LIMIT FOR JOINT NODE",I,J
7980      X=Closure(I,J)
7990  '
8000      IF X<=0 THEN 8030
```

```
8010      Final(I,J,1)=Kin(I)/((1/(X))-(1/Aperture(I)))
8020      GOTO 8050
8030      Final(I,J,1)=0
8040  !
8050      Dear=D*COS(Deta(I))
8060      Strength=Final(I,J,1)*TAN(Dilang(I,J)+Phires(I))
8070      Final(I,J,2)=Initial(I,J,2)-Strength*100*Dear*COS(Deta(I))/(Apex-Radi
us)
8080      IF ABS(Final(I,J,2))<Strength THEN 8100
8090      Final(I,J,2)=Strength*SGN(Final(I,J,2))
8100    NEXT J
8110  NEXT I
8120  DISP " "
8130  RETURN
8140  ! ************************************
8150  ! SUM RESULTANT FORCES ACTING ON BLOCK
8160  ! ************************************
8170  MAT Force= (0)
8180  !
8190  FOR I=1 TO Nplanes ! SUM STRESSES INTO FORCES ON PLANE I
8200    FOR J=1 TO 66
8210      Force(I,1)=Force(I,1)+Final(I,J,1)*Facexyz(I,J,4)
8220      Force(I,2)=Force(I,2)+Final(I,J,2)*Facexyz(I,J,4)
8230    NEXT J
8240  NEXT I
8250  !
8260  MAT Fb= (0)
8270  !
8280  FOR I=1 TO Nplanes ! SUM FORCES IN BLOCK COORDINATE SYSTEM
8290    FOR J=1 TO 3
8300      Fb(J)=Fb(J)-Force(I,1)*Slider(I,2,J)-Force(I,2)*Slider(I,3,J)
8310    NEXT J
8320  NEXT I
8330  !
8340  MAT D33b= TRN(Tuncos)
8350  MAT Fr= D33b*Fb ! ROTATE FORCE VECTORS INTO REFERENCE SYSTEM
8360  Fr(3)=Fr(3)-Weight ! ADD WEIGHT TO FORCE IN Z DIRECTION
8370  Fw=SQR(Fr(1)*Fr(1)+Fr(2)*Fr(2)+Fr(3)*Fr(3))
8380  Fw=-Fw*SGN(Fr(3))/Weight
8390  !
8400  Tense=0
8410  IF Tarea<=0 THEN RETURN
8420  IF Foption$="C" THEN Tense=Fr(3)*COS(Apext)/Tarea
8430  !
8440  RETURN
8450  ! ****************
8460  ! PRINT OUT RESULTS
8470  ! ****************
8480  IF Foption$="D" OR Foption$="T" OR Foption$="S" OR Fheader=1 THEN 8510
8490  PRINT " "
8500  PRINT "DEL T     DISP.  DIP   AZ        Fx        Fy        Fz     Fr/W
 HT   TENSILE"
```

```
8510  PRINT USING 430;Tdelt,Disp,Dispdir(*),Fr(*),Fw,Tapexr,Tense
8520  !
8530  IF Fprinter$<>"Y" THEN 8660
8540  !
8550  PRINTER IS 701
8560  IF Foption$="D" OR Foption$="T" OR Foption$="S" OR Fheader=1 THEN 8610
8570  PRINT " "
8580  PRINT "DEL T      DISP.   DIP    AZ          Fx          Fy          Fz      Fr/W
 HT   TENSILE"
8590  Fheader=1
8600  Nlines=Nlines+2
8610  PRINT USING 430;Tdelt,Disp,Dispdir(*),Fr(*),Fw,Tapexr,Tense
8620  Nlines=Nlines+1
8630  IF Nlines<(Npages*66-6) THEN 8660
8640  PRINT CHR$(12)
8650  Npages=Npages+1
8660  PRINTER IS 1
8670  !
8680  RETURN
8690  END !*****************************************************************
8700  DEF FNDircosl(Alph,Bet) ! DIRECTION COSINE L
8710    Dcl=SIN(Alph)*SIN(Bet)
8720    RETURN Dcl
8730  FNEND !****************************************************************
8740  DEF FNDircosm(Alph,Bet) ! DIRECTION COSINE M
8750    Dcm=SIN(Alph)*COS(Bet)
8760    RETURN Dcm
8770  FNEND !****************************************************************
8780  DEF FNDircosn(Alph) ! DIRECTION COSINE N
8790    Dcn=COS(Alph)
8800    RETURN Dcn
8810  FNEND !****************************************************************
8820  SUB Transf(A(*),B(*)) ! CONSTRUCT 6X6 ROTATION MATRIX
8830    OPTION BASE 1
8840    INTEGER I,J
8850    FOR I=1 TO 3
8860      FOR J=1 TO 3
8870        B(I,J)=A(I,J)*A(I,J)
8880      NEXT J
8890      B(I,4)=2*A(I,2)*A(I,3)
8900      B(I,5)=2*A(I,3)*A(I,1)
8910      B(I,6)=2*A(I,1)*A(I,2)
8920    NEXT I
8930    FOR J=1 TO 3
8940      B(4,J)=A(2,J)*A(3,J)
8950      B(5,J)=A(3,J)*A(1,J)
8960      B(6,J)=A(1,J)*A(2,J)
8970    NEXT J
8980    B(4,4)=A(2,2)*A(3,3)+A(3,2)*A(2,3)
8990    B(4,5)=A(2,3)*A(3,1)+A(3,3)*A(2,1)
9000    B(4,6)=A(2,1)*A(3,2)+A(3,1)*A(2,2)
```

```
9010    B(5,4)=A(1,2)*A(3,3)+A(3,2)*A(1,3)
9020    B(5,5)=A(1,3)*A(3,1)+A(3,3)*A(1,1)
9030    B(5,6)=A(1,1)*A(3,2)+A(3,1)*A(1,2)
9040    B(6,4)=A(1,2)*A(2,3)+A(2,2)*A(1,3)
9050    B(6,5)=A(1,3)*A(2,1)+A(2,3)*A(1,1)
9060    B(6,6)=A(1,1)*A(2,2)+A(2,1)*A(1,2)
9070  SUBEND !*************************************************************
```

```
10    SUB Stress3d(Ra,Tet)
20    !
30    ! CODED BY JESSE YOW IN NOVEMBER, 1984
40    !
50    ! PART OF THIS CODING IS MODIFIED FOR USE ON AN hp9816 COMPUTER FROM
60    ! A PROGRAM CALLED BERNI2 IN BERNARD AMADEI'S THESIS (1982)
70    !
80    ! THE THERMAL STRESSES ARE CALCULATED WITH EQNS 3.88 FROM ZUDANS, YEN,
90    ! AND STEIGELMANN (1965)
100   !
110     OPTION BASE 1
120     INTEGER I,J
130   !
140     COM /Data2/ Stin(*),Stindir(*),E1,E2,E3,Mu1,Mu2,Mu3,G1,G2,G3
150     COM /Data3/ Radius,Apexr,Apext,Trise,Ta2,Tundir(*),Head$
160     COM /Data4/ Disp,Dispdir(*),Dispinc,Farea(*),Gamma,Talph,Tdelt
170     COM /Data5/ Fhires(*),Jrc(*),Jcs(*),Pressure,Viewvec(*),Viewcos(*)
180     COM /Flags/ Fprinter$,Froot,Nlines,Npages,Fheader,Foption$,Loaded
190     COM /Stress/ Stig(*),Stpt(*),Mu(*),Imu(*),Fb(*),Fr(*),Beta(*),Aa(*)
200   !
210     DIM Hp(6,6),Ts(6,6),Tts(6,6),Th(6,6),Te(6,6),Tte(6,6),Ah(3,3),Sfo(6)
220     DIM T1(6,6),T2(6,6),T3(6,6),A(3,3),Heat(6),T6(6)
230     DIM Fx(6,6),Fqx(6),Aaa(7),T5(6),T4(6),Root(6),Iroot(6)
240     DIM L4(3),I14(3),Landa(3),Ilanda(3),L2(3),I12(3),L3(3),I13(3)
250     DIM Dum(0:6),Idum(0:6),Dumr(6),Idumr(6),Sol(6),Rsol(6),Isol(6)
260   !
270   ! INITIALIZE MATRICES
280   !
290     MAT Heat= (0)
300   !
310     Sfo(1)=Stig(1)
320     Sfo(2)=Stig(3)
330     Sfo(3)=Stig(2)
340     Sfo(4)=Stig(4)
350     Sfo(5)=Stig(6)
360     Sfo(6)=Stig(5)
370   !
380     IF Froot=1 THEN 1370
390   !
400     MAT A= (0)
410     MAT Ah= (0)
420     MAT Hp= (0)
430   !
440   ! SET UP COMPLIANCE MATRIX HP
450   !
460     FOR I=1 TO 3
470       Hp(I,I)=1/E1
480       Hp(I+3,I+3)=1/G1
490     NEXT I
500     Hp(1,2)=-Mu1/E1
```

```
510     Hp(1,3)=-Mu1/E1
520     Hp(2,3)=-Mu1/E1
530     Hp(2,1)=Hp(1,2)
540     Hp(3,1)=Hp(1,3)
550     Hp(3,2)=Hp(2,3)
560   !
570   ! SET UP TRANSFORMATION MATRICES
580   !
590     CALL Orien2(Trise,Taz,A(*))
600     CALL Transf(A(*),Ts(*))
610     MAT Tts= TRN(Ts)
620   !
630     CALL Orienh(Trise,Taz,Ah(*))
640     CALL Transf(Ah(*),Th(*))
650     FOR I=1 TO 6
660       FOR J=1 TO 6
670         Te(I,J)=Th(I,J)
680         IF ((I<=3) AND (J>3)) THEN Te(I,J)=.5*Th(I,J)
690         IF ((I>3) AND (J<=3)) THEN Te(I,J)=2*Th(I,J)
700       NEXT J
710     NEXT I
720     MAT Tte= TRN(Te)
730   !
740   ! CALC STRAIN-STRESS MATRIX AA IN TUNNEL COORDINATE SYSTEM
750   !
760     MAT T1= Te*Tts
770     MAT T2= T1*Hp
780     MAT T3= T2*Ts
790     MAT Aa= T3*Tte
800   !
810   ! CALC COEFFICIENTS IN BETA MATRIX
820   !
830     FOR I=1 TO 6
840       FOR J=1 TO 6
850         Beta(I,J)=Aa(I,J)-Aa(I,3)*Aa(J,3)/Aa(3,3)
860       NEXT J
870     NEXT I
880   !
890   ! CALC COEFFICIENTS OF 6TH DEGREE POLYNOMIAL
900   !
910     Aaa(1)=Beta(1,1)*Beta(5,5)-Beta(1,5)*Beta(1,5)
920     Aaa(2)=2*Beta(1,5)*(Beta(1,4)+Beta(5,6))
930     Aaa(2)=Aaa(2)-2*(Beta(1,6)*Beta(5,5)+Beta(1,1)*Beta(4,5))
940     Aaa(3)=Beta(5,5)*(2*Beta(1,2)+Beta(6,6))+4*Beta(1,6)*Beta(4,5)+Beta(1,1)
*Beta(4,4)
950     Aaa(3)=Aaa(3)-(Beta(1,4)+Beta(5,6))^2-2*Beta(1,5)*(Beta(2,5)+Beta(4,6))
960     Aaa(4)=-2*Beta(2,6)*Beta(5,5)-2*Beta(4,5)*(2*Beta(1,2)+Beta(6,6))-2*Beta
(1,6)*Beta(4,4)
970     Aaa(4)=Aaa(4)+2*Beta(1,5)*Beta(2,4)+2*(Beta(1,4)+Beta(5,6))*(Beta(2,5)+B
eta(4,6))
980     Aaa(5)=Beta(2,2)*Beta(5,5)+4*Beta(2,6)*Beta(4,5)+Beta(4,4)*(2*Beta(1,2)+
Beta(6,6))
990     Aaa(5)=Aaa(5)-2*Beta(2,4)*(Beta(1,4)+Beta(5,6))-(Beta(2,5)+Beta(4,6))^2
1000    Aaa(6)=-2*Beta(2,2)*Beta(4,5)-2*Beta(2,6)*Beta(4,4)+2*Beta(2,4)*(Beta(2,
5)+Beta(4,6))
```

```
1010    Aaa(7)=Beta(2,2)*Beta(4,4)-Beta(2,4)*Beta(2,4)
1020  !
1030  ! FIND ROOTS OF POLYNOMIAL
1040  '
1050    FOR I=1 TO 7
1060      Dum(I-1)=Aaa(8-I)
1070      Idum(I-1)=0
1080    NEXT I
1090    Tola=1.E-18
1100    Tolf=1.E-18
1110    Itmax=50
1120    CALL Siljak(6,Dum(*),Idum(*),Tola,Tolf,Itmax,Dumr(*),Idumr(*))
1130    FOR I=1 TO 6
1140      Root(I)=Dumr(7-I)
1150      Iroot(I)=Idumr(7-I)
1160    NEXT I
1170    Mu(1)=Root(3)
1180    Mu(2)=Root(2)
1190    Mu(3)=Root(1)
1200    Imu(1)=Iroot(3)
1210    Imu(2)=Iroot(2)
1220    Imu(3)=Iroot(1)
1230  '
1240    FOR I=1 TO 6
1250      R1=Root(I)
1260      I1=Iroot(I)
1270      CALL Cmult(R1,I1,R1,I1,R2,I2)
1280      CALL Cmult(R1,I1,R2,I2,R3,I3)
1290      CALL Cmult(R1,I1,R3,I3,R4,I4)
1300      CALL Cmult(R1,I1,R4,I4,R5,I5)
1310      CALL Cmult(R1,I1,R5,I5,R6,I6)
1320      Rsol(I)=Aaa(1)*R6+Aaa(2)*R5+Aaa(3)*R4+Aaa(4)*R3+Aaa(5)*R2+Aaa(6)*R1+Aa
a(7)
1330      Isol(I)=Aaa(1)*I6+Aaa(2)*I5+Aaa(3)*I4+Aaa(4)*I3+Aaa(5)*I2+Aaa(6)*I1
1340      Sol(I)=Rsol(I)+Isol(I)
1350    NEXT I
1360  !
1370  ! CALC COEFFICIENTS LANDA AND DELTA
1380  !
1390    FOR J=1 TO 3
1400      CALL Cmult(Mu(J),Imu(J),Mu(J),Imu(J),R2,I2)
1410      CALL Cmult(Mu(J),Imu(J),R2,I2,R3,I3)
1420      CALL Cmult(Mu(J),Imu(J),R3,I3,R4,I4)
1430  !
1440      CALL Cmult(Beta(1,5),0,R3,I3,Rd1,Id1)
1450      CALL Cmult(Beta(1,4)+Beta(5,6),0,R2,I2,Rd2,Id2)
1460      CALL Cmult(Beta(2,5)+Beta(4,6),0,Mu(J),Imu(J),Rd3,Id3)
1470      L3(J)=Rd1-Rd2+Rd3-Beta(2,4)
1480      I13(J)=Id1-Id2+Id3
1490  !
1500      CALL Cmult(Beta(5,5),0,R2,I2,Rd1,Id1)
```

```
1510      CALL Cmult(2*Beta(4,5),0,Mu(J),Imu(J),Rd2,Id2)
1520      L2(J)=Rd1-Rd2+Beta(4,4)
1530      I12(J)=Id1-Id2
1540  !
1550      CALL Cmult(Beta(1,1),0,R4,I4,Rd1,Id1)
1560      CALL Cmult(2*Beta(1,6),0,R3,I3,Rd2,Id2)
1570      CALL Cmult(2*Beta(1,2)+Beta(6,6),0,R2,I2,Rd3,Id3)
1580      CALL Cmult(2*Beta(2,6),0,Mu(J),Imu(J),Rd4,Id4)
1590      L4(J)=Rd1-Rd2+Rd3-Rd4+Beta(2,2)
1600      I14(J)=Id1-Id2+Id3-Id4
1610  !
1620      CALL Cdivid(L3(J),I13(J),L2(J),I12(J),Landa(J),Ilanda(J))
1630      IF J=3 THEN CALL Cdivid(L3(J),I13(J),L4(J),I14(J),Landa(J),Ilanda(J))
1640      Landa(J)=-Landa(J)
1650      Ilanda(J)=-Ilanda(J)
1660    NEXT J
1670    R1=Mu(1)-Mu(3)
1680    I1=Imu(1)-Imu(3)
1690    CALL Cmult(Landa(3),Ilanda(3),R1,I1,R2,I2)
1700    CALL Cmult(Landa(2),Ilanda(2),R2,I2,R1,I1)
1710    R3=Mu(3)-Mu(2)
1720    I3=Imu(3)-Imu(2)
1730    CALL Cmult(Landa(3),Ilanda(3),R3,I3,R4,I4)
1740    CALL Cmult(Landa(1),Ilanda(1),R4,I4,R3,I3)
1750    Delta=Mu(2)-Mu(1)+R1+R3
1760    Idelta=Imu(2)-Imu(1)+I1+I3
1770  !
1780  ! CALCULATE THE NON-THERMAL STRESSES AT A POINT RA,TET
1790  !
1800    CALL Fxmat(Mu(*),Imu(*),Landa(*),Ilanda(*),Delta,Idelta,Tet,Ra,Aa(*),Fx(
*),Fqx(*))
1810  !
1820  !
1830    MAT T4= Fx*Sfo ! ROTATE THE NON-THERMAL STRESSES AT THE POINT
1840    FOR I=1 TO 6
1850      T5(I)=T4(I)+Pressure*Fqx(I)
1860    NEXT I
1870  !
1880  ! CALCULATE THE THERMAL STRESSES AT RA,TET
1890  !
1900    IF Tdelt=0 THEN 2100
1910  !
1920    Lna=LOG(10)
1930    C1=-E1*Talph*Tdelt/(2*(1-Mu1)*Lna)
1940    C2=1/99
1950    C3=10/Ra
1960    Lnr=LOG(C3)
1970  !
1980    Sigr=C1*(-Lnr-C2*(1-C3*C3)*Lna)   ! RADIAL STRESS
1990    Sigt=C1*(1-Lnr-C2*(1+C3*C3)*Lna)  ! TANGENTIAL STRESS
2000    Sigz=C1*(1-2*Lnr-2*C2*Lna)        ! AXIAL STRESS
```

```
2010  !
2020    T6(1)=Sigr
2030    T6(2)=Sigt
2040    T6(3)=Sigz
2050  !
2060    CALL Tetss(Tet,T2(*)) ' ROTATE STRESSES INTO XYZ SYSTEM
2070    MAT T3= INV(T2)
2080    MAT Heat= T3*T6
2090  !
2100    Stpt(1)=T5(1)+Heat(1) ' SUM THERMAL AND NON-THERMAL COMPONENTS
2110    Stpt(3)=T5(2)+Heat(2)
2120    Stpt(2)=T5(3)+Heat(3)
2130    Stpt(4)=T5(4)+Heat(4)
2140    Stpt(6)=T5(5)+Heat(5)
2150    Stpt(5)=T5(6)+Heat(6)
2160  !
2170    Froot=1
2180  SUBEND !*************************************************************
2190  SUB Orienh(D,B,Ah(*))
2200    OPTION BASE 1
2210  '
2220    IF ABS(D)=90 THEN 2420
2230  !
2240    Bx=B+270
2250    By=B+180
2260    Bz=B
2270  '
2280    Dx=0
2290    Dy=90-D
2300    Dz=D
2310  !
2320    Ah(1,1)=COS(Dx)*COS(Bx)
2330    Ah(1,2)=SIN(Dx)
2340    Ah(1,3)=COS(Dx)*SIN(Bx)
2350    Ah(2,1)=COS(Dy)*COS(By)
2360    Ah(2,2)=SIN(Dy)
2370    Ah(2,3)=COS(Dy)*SIN(By)
2380    Ah(3,1)=COS(Dz)*COS(Bz)
2390    Ah(3,2)=SIN(Dz)
2400    Ah(3,3)=COS(Dz)*SIN(Bz)
2410    SUBEXIT
2420    Ah(1,3)=-1
2430    Ah(2,1)=-1
2440    Ah(3,2)=1
2450  SUBEND !*************************************************************
2460  SUB Orien2(D,B,A(*))
2470    OPTION BASE 1
2480    Tet=90-D
2490    St=B+90
2500    IF St>360 THEN St=St-360
```

```
2510    IF St>180 THEN St=St-180
2520    IF B<90 AND B>=0 THEN 2550
2530    IF B<180 AND B>=90 THEN 2590
2540    IF B<270 AND B>=180 THEN 2590
2550    Betax=St+180
2560    Betay=St
2570    Betaz=St+270
2580    GOTO 2620
2590    Betax=St
2600    Betay=St+180
2610    Betaz=St+90
2620    Deltax=90-Tet
2630    Deltay=Tet
2640    Deltaz=0
2650  !
2660    A(1,1)=COS(Deltax)*COS(Betax)
2670    A(1,2)=SIN(Deltax)
2680    A(1,3)=COS(Deltax)*SIN(Betax)
2690    A(2,1)=COS(Deltay)*COS(Betay)
2700    A(2,2)=SIN(Deltay)
2710    A(2,3)=COS(Deltay)*SIN(Betay)
2720    A(3,1)=COS(Deltaz)*COS(Betaz)
2730    A(3,2)=SIN(Deltaz)
2740    A(3,3)=COS(Deltaz)*SIN(Betaz)
2750  SUBEND !*************************************************************
2760  SUB Tetss(Tet,Tss(*))
2770    OPTION BASE 1
2780    MAT Tss= (0)
2790    Tet2=2*Tet
2800    Tss(1,1)=COS(Tet)*COS(Tet)
2810    Tss(2,2)=Tss(1,1)
2820    Tss(1,2)=SIN(Tet)*SIN(Tet)
2830    Tss(2,1)=Tss(1,2)
2840    Tss(3,3)=1
2850    Tss(1,6)=SIN(Tet2)
2860    Tss(2,6)=-Tss(1,6)
2870    Tss(6,1)=-.5*Tss(1,6)
2880    Tss(6,2)=-Tss(6,1)
2890    Tss(6,6)=COS(Tet2)
2900    Tss(4,4)=COS(Tet)
2910    Tss(5,5)=Tss(4,4)
2920    Tss(4,5)=-SIN(Tet)
2930    Tss(5,4)=-Tss(4,5)
2940  SUBEND !*************************************************************
2950  SUB Fxmat(Mu(*),Imu(*),Landa(*),Ilanda(*),Delta,Idelta,Tet,Ra,Aa(*),Fx(*),
Fqx(*))
2960    OPTION BASE 1
2970    INTEGER I
2980  !
2990    DIM Ksi(3),Iksi(3),Sq(3),Isq(3),Gama(3),Igama(3)
3000  !
```

```
3010    IF Tet=0 THEN Tet=.001
3020    IF Tet=90 THEN Tet=89.999
3030    IF Tet=180 THEN Tet=179.999
3040    IF Tet=270 THEN Tet=270.001
3050  !
3060    MAT Fx= (0)
3070    MAT Fqx= (0)
3080  !
3090    FOR I=1 TO 3
3100      CALL Cmult(SIN(Tet),0,Mu(I),Imu(I),Z4,Iz4)
3110      Z4=Z4+COS(Tet)
3120  !
3130      CALL Cmult(Z4,Iz4,Ra,0,R1,I1)
3140      CALL Cmult(R1,I1,R1,I1,R2,I2)
3150      CALL Cmult(Mu(I),Imu(I),Mu(I),Imu(I),R3,I3)
3160      R2=R2-1-R3
3170      I2=I2-I3
3180      CALL Csqrt(R2,I2,Sq(I),Isq(I))
3190  '
3200      IF Tet>90 AND Tet<270 THEN Sq(I)=-Sq(I)
3210      IF Tet>90 AND Tet<270 THEN Isq(I)=-Isq(I)
3220  '
3230      R1=Sq(I)+R1
3240      I1=Isq(I)+I1
3250      CALL Cmult(0,1,Mu(I),Imu(I),R2,I2)
3260      R2=1-R2
3270      I2=-I2
3280      CALL Cdivid(R1,I1,R2,I2,Ksi(I),Iksi(I))
3290  '
3300      CALL Cmult(Delta,Idelta,Ksi(I),Iksi(I),R1,I1)
3310      CALL Cmult(R1,I1,Sq(I),Isq(I),R2,I2)
3320      CALL Cinv(R2,I2,Gama(I),Igama(I))
3330      Gama(I)=-Gama(I)
3340      Igama(I)=-Igama(I)
3350    NEXT I
3360  !
3370    CALL Cmult(0,1,Gama(1),Igama(1),R1,I1)
3380    CALL Cmult(R1,I1,Mu(1),Imu(1),R2,I2)
3390    CALL Cmult(R2,I2,Mu(1),Imu(1),R1,I1)
3400    CALL Cmult(Landa(2),Ilanda(2),Landa(3),Ilanda(3),R2,I2)
3410    R2=R2-1
3420    CALL Cmult(R1,I1,R2,I2,R4,I4)
3430    CALL Cmult(0,1,Gama(2),Igama(2),R1,I1)
3440    CALL Cmult(R1,I1,Mu(2),Imu(2),R2,I2)
3450    CALL Cmult(R2,I2,Mu(2),Imu(2),R1,I1)
3460    CALL Cmult(Landa(1),Ilanda(1),Landa(3),Ilanda(3),R2,I2)
3470    R2=1-R2
3480    I2=-I2
3490    CALL Cmult(R1,I1,R2,I2,R3,I3)
3500    R4=R4+R3
```

```
3510    I4=I4+I3
3520    CALL Cmult(0,1,Gama(3),Igama(3),R2,I2)
3530    CALL Cmult(R2,I2,Mu(3),Imu(3),R1,I1)
3540    CALL Cmult(R1,I1,Mu(3),Imu(3),R2,I2)
3550    CALL Cmult(R2,I2,Landa(3),Ilanda(3),R1,I1)
3560    R2=Landa(1)-Landa(2)
3570    I2=Ilanda(1)-Ilanda(2)
3580    CALL Cmult(R1,I1,R2,I2,R3,I3)
3590    R4=R4+R3
3600    I4=I4+I3
3610    Fx(1,1)=-R4
3620  !
3630    CALL Cmult(Gama(1),Igama(1),Mu(1),Imu(1),R2,I2)
3640    CALL Cmult(R2,I2,Mu(1),Imu(1),R1,I1)
3650    CALL Cmult(Mu(3),Imu(3),Landa(3),Ilanda(3),R3,I3)
3660    CALL Cmult(R3,I3,Landa(2),Ilanda(2),R2,I2)
3670    R3=Mu(2)-R2
3680    I3=Imu(2)-I2
3690    CALL Cmult(R1,I1,R3,I3,R4,I4)
3700    CALL Cmult(Gama(2),Igama(2),Mu(2),Imu(2),R2,I2)
3710    CALL Cmult(R2,I2,Mu(2),Imu(2),R1,I1)
3720    CALL Cmult(Landa(1),Ilanda(1),Landa(3),Ilanda(3),R3,I3)
3730    CALL Cmult(R3,I3,Mu(3),Imu(3),R2,I2)
3740    R2=R2-Mu(1)
3750    I2=I2-Imu(1)
3760    CALL Cmult(R1,I1,R2,I2,R3,I3)
3770    R4=R4+R3
3780    I4=I4+I3
3790    CALL Cmult(Gama(3),Igama(3),Mu(3),Imu(3),R1,I1)
3800    CALL Cmult(R1,I1,Mu(3),Imu(3),R2,I2)
3810    CALL Cmult(R2,I2,Landa(3),Ilanda(3),R1,I1)
3820    CALL Cmult(Mu(1),Imu(1),Landa(2),Ilanda(2),R2,I2)
3830    CALL Cmult(Mu(2),Imu(2),Landa(1),Ilanda(1),R3,I3)
3840    R2=R2-R3
3850    I2=I2-I3
3860    CALL Cmult(R1,I1,R2,I2,R3,I3)
3870    R4=R4+R3
3880    I4=I4+I3
3890    Fx(1,2)=-R4
3900  !
3910    CALL Cmult(Gama(1),Igama(1),Mu(1),Imu(1),R2,I2)
3920    CALL Cmult(R2,I2,Mu(1),Imu(1),R1,I1)
3930    CALL Cmult(Landa(2),Ilanda(2),Landa(3),Ilanda(3),R2,I2)
3940    R2=R2-1
3950    CALL Cmult(0,1,Mu(2),Imu(2),R3,I3)
3960    R2=R2+R3
3970    I2=I2+I3
3980    CALL Cmult(0,1,Mu(3),Imu(3),R3,I3)
3990    CALL Cmult(R3,I3,Landa(2),Ilanda(2),R5,I5)
4000    CALL Cmult(R5,I5,Landa(3),Ilanda(3),R3,I3)
```

```
4010    R2=R2-R3
4020    I2=I2-I3
4030    CALL Cmult(R1,I1,R2,I2,R4,I4)
4040    CALL Cmult(Gama(2),Igama(2),Mu(2),Imu(2),R2,I2)
4050    CALL Cmult(R2,I2,Mu(2),Imu(2),R1,I1)
4060    CALL Cmult(Landa(1),Ilanda(1),Landa(3),Ilanda(3),R2,I2)
4070    R2=1-R2
4080    I2=-I2
4090    CALL Cmult(0,1,Mu(3),Imu(3),R3,I3)
4100    CALL Cmult(R3,I3,Landa(1),Ilanda(1),R5,I5)
4110    CALL Cmult(R5,I5,Landa(3),Ilanda(3),R3,I3)
4120    R2=R2+R3
4130    I2=I2+I3
4140    CALL Cmult(0,1,Mu(1),Imu(1),R3,I3)
4150    R2=R2-R3
4160    I2=I2-I3
4170    CALL Cmult(R1,I1,R2,I2,R3,I3)
4180    R4=R4+R3
4190    I4=I4+I3
4200    CALL Cmult(Gama(3),Igama(3),Mu(3),Imu(3),R1,I1)
4210    CALL Cmult(R1,I1,Mu(3),Imu(3),R2,I2)
4220    CALL Cmult(R2,I2,Landa(3),Ilanda(3),R1,I1)
4230    R2=Landa(1)-Landa(2)
4240    I2=Ilanda(1)-Ilanda(2)
4250    CALL Cmult(0,1,Mu(1),Imu(1),R5,I5)
4260    CALL Cmult(R5,I5,Landa(2),Ilanda(2),R3,I3)
4270    R2=R2+R3
4280    I2=I2+I3
4290    CALL Cmult(0,1,Mu(2),Imu(2),R5,I5)
4300    CALL Cmult(R5,I5,Landa(1),Ilanda(1),R3,I3)
4310    R2=R2-R3
4320    I2=I2-I3
4330    CALL Cmult(R1,I1,R2,I2,R3,I3)
4340    R4=R4+R3
4350    I4=I4+I3
4360    Fx(1,6)=R4
4370    !
4380    CALL Cmult(Mu(1),Imu(1),Mu(1),Imu(1),R1,I1)
4390    CALL Cmult(R1,I1,Gama(1),Igama(1),R2,I2)
4400    CALL Cmult(R2,I2,Landa(3),Ilanda(3),R1,I1)
4410    R2=Mu(3)-Mu(2)
4420    I2=Imu(3)-Imu(2)
4430    CALL Cmult(R1,I1,R2,I2,R4,I4)
4440    CALL Cmult(Mu(2),Imu(2),Mu(2),Imu(2),R1,I1)
4450    CALL Cmult(R1,I1,Gama(2),Igama(2),R2,I2)
4460    CALL Cmult(R2,I2,Landa(3),Ilanda(3),R1,I1)
4470    R2=Mu(1)-Mu(3)
4480    I2=Imu(1)-Imu(3)
4490    CALL Cmult(R1,I1,R2,I2,R3,I3)
4500    R4=R4+R3
```

```
4510    I4=I4+R3
4520    CALL Cmult(Mu(3),Imu(3),Mu(3),Imu(3),R1,I1)
4530    CALL Cmult(R1,I1,Gama(3),Igama(3),R2,I2)
4540    CALL Cmult(R2,I2,Landa(3),Ilanda(3),R1,I1)
4550    R2=Mu(2)-Mu(1)
4560    I2=Imu(2)-Imu(1)
4570    CALL Cmult(R1,I1,R2,I2,R3,I3)
4580    R4=R4+R3
4590    I4=I4+I3
4600    Fx(1,4)=R4
4610  !
4620    CALL Cmult(0,1,Gama(1),Igama(1),R2,I2)
4630    CALL Cmult(R2,I2,Mu(1),Imu(1),R1,I1)
4640    CALL Cmult(R1,I1,Mu(1),Imu(1),R2,I2)
4650    CALL Cmult(R2,I2,Landa(3),Ilanda(3),R1,I1)
4660    R2=Mu(3)-Mu(2)
4670    I2=Imu(3)-Imu(2)
4680    CALL Cmult(R1,I1,R2,I2,R4,I4)
4690    CALL Cmult(0,1,Gama(2),Igama(2),R2,I2)
4700    CALL Cmult(R2,I2,Mu(2),Imu(2),R1,I1)
4710    CALL Cmult(R1,I1,Mu(2),Imu(2),R2,I2)
4720    CALL Cmult(R2,I2,Landa(3),Ilanda(3),R1,I1)
4730    R2=Mu(1)-Mu(3)
4740    I2=Imu(1)-Imu(3)
4750    CALL Cmult(R1,I1,R2,I2,R3,I3)
4760    R4=R4+R3
4770    I4=I4+I3
4780    CALL Cmult(0,1,Gama(3),Igama(3),R2,I2)
4790    CALL Cmult(R2,I2,Mu(3),Imu(3),R1,I1)
4800    CALL Cmult(R1,I1,Mu(3),Imu(3),R2,I2)
4810    CALL Cmult(R2,I2,Landa(3),Ilanda(3),R1,I1)
4820    R2=Mu(2)-Mu(1)
4830    I2=Imu(2)-Imu(1)
4840    CALL Cmult(R1,I1,R2,I2,R3,I3)
4850    R4=R4+R3
4860    I4=I4+I3
4870    Fx(1,5)=-R4
4880  !
4890    CALL Cmult(0,1,Gama(1),Igama(1),R1,I1)
4900    CALL Cmult(Landa(2),Ilanda(2),Landa(3),Ilanda(3),R2,I2)
4910    R2=R2-1
4920    CALL Cmult(R1,I1,R2,I2,R4,I4)
4930    CALL Cmult(0,1,Gama(2),Igama(2),R1,I1)
4940    CALL Cmult(Landa(1),Ilanda(1),Landa(3),Ilanda(3),R2,I2)
4950    R2=1-R2
4960    I2=-I2
4970    CALL Cmult(R1,I1,R2,I2,R3,I3)
4980    R4=R4+R3
4990    I4=I4+I3
5000    CALL Cmult(0,1,Gama(3),Igama(3),R2,I2)
```

```
5010    CALL Cmult(R2,I2,Landa(3),Ilanda(3),R1,I1)
5020    R2=Landa(1)-Landa(2)
5030    I2=Ilanda(1)-Ilanda(2)
5040    CALL Cmult(R1,I1,R2,I2,R3,I3)
5050    R4=R4+R3
5060    I4=I4+I3
5070    Fx(2,1)=-R4
5080  '
5090    CALL Cmult(Mu(3),Imu(3),Landa(3),Ilanda(3),R2,I2)
5100    CALL Cmult(R2,I2,Landa(2),Ilanda(2),R1,I1)
5110    R1=Mu(2)-R1
5120    I1=Imu(2)-I1
5130    CALL Cmult(Gama(1),Igama(1),R1,I1,R4,I4)
5140    CALL Cmult(Landa(1),Ilanda(1),Landa(3),Ilanda(3),R2,I2)
5150    CALL Cmult(R2,I2,Mu(3),Imu(3),R1,I1)
5160    R1=R1-Mu(1)
5170    I1=I1-Imu(1)
5180    CALL Cmult(Gama(2),Igama(2),R1,I1,R3,I3)
5190    R4=R4+R3
5200    I4=I4+I3
5210    CALL Cmult(Mu(1),Imu(1),Landa(2),Ilanda(2),R1,I1)
5220    CALL Cmult(Mu(2),Imu(2),Landa(1),Ilanda(1),R2,I2)
5230    R1=R1-R2
5240    I1=I1-I2
5250    CALL Cmult(Gama(3),Igama(3),Landa(3),Ilanda(3),R2,I2)
5260    CALL Cmult(R2,I2,R1,I1,R3,I3)
5270    R4=R4+R3
5280    I4=I4+I3
5290    Fx(2,2)=-R4
5300  '
5310    CALL Cmult(0,1,Mu(3),Imu(3),R1,I1)
5320    CALL Cmult(R1,I1,Landa(3),Ilanda(3),R2,I2)
5330    CALL Cmult(R2,I2,Landa(2),Ilanda(2),R1,I1)
5340    CALL Cmult(0,1,Mu(2),Imu(2),R2,I2)
5350    CALL Cmult(Landa(2),Ilanda(2),Landa(3),Ilanda(3),R3,I3)
5360    R3=R3-1+R2-R1
5370    I3=I3+I2-I1
5380    CALL Cmult(Gama(1),Igama(1),R3,I3,R4,I4)
5390    CALL Cmult(Landa(1),Ilanda(1),Landa(3),Ilanda(3),R1,I1)
5400    CALL Cmult(0,1,Mu(3),Imu(3),R2,I2)
5410    CALL Cmult(R2,I2,Landa(1),Ilanda(1),R3,I3)
5420    CALL Cmult(R3,I3,Landa(3),Ilanda(3),R2,I2)
5430    CALL Cmult(0,1,Mu(1),Imu(1),R3,I3)
5440    R1=1-R1+R2-R3
5450    I1=-I1+I2-I3
5460    CALL Cmult(Gama(2),Igama(2),R1,I1,R3,I3)
5470    R4=R4+R3
5480    I4=I4+I3
5490    CALL Cmult(0,1,Mu(1),Imu(1),R2,I2)
5500    CALL Cmult(R2,I2,Landa(2),Ilanda(2),R1,I1)
```

```
5510    CALL Cmult(0,1,Mu(2),Imu(2),R3,I3)
5520    CALL Cmult(R3,I3,Landa(1),Ilanda(1),R2,I2)
5530    R1=Landa(1)-Landa(2)+R1-R2
5540    I1=Ilanda(1)-Ilanda(2)+I1-I2
5550    CALL Cmult(Gama(3),Igama(3),Landa(3),Ilanda(3),R2,I2)
5560    CALL Cmult(R2,I2,R1,I1,R3,I3)
5570    R4=R4+R3
5580    I4=I4+I3
5590    Fx(2,6)=R4
5600  !
5610    CALL Cmult(Gama(1),Igama(1),Landa(3),Ilanda(3),R1,I1)
5620    R2=Mu(3)-Mu(2)
5630    I2=Imu(3)-Imu(2)
5640    CALL Cmult(R1,I1,R2,I2,R4,I4)
5650    CALL Cmult(Gama(2),Igama(2),Landa(3),Ilanda(3),R1,I1)
5660    R2=Mu(1)-Mu(3)
5670    I2=Imu(1)-Imu(3)
5680    CALL Cmult(R1,I1,R2,I2,R3,I3)
5690    R4=R4+R3
5700    I4=I4+I3
5710    CALL Cmult(Gama(3),Igama(3),Landa(3),Ilanda(3),R1,I1)
5720    R2=Mu(2)-Mu(1)
5730    I2=Imu(2)-Imu(1)
5740    CALL Cmult(R1,I1,R2,I2,R3,I3)
5750    R4=R4+R3
5760    I4=I4+I3
5770    Fx(2,4)=R4
5780  !
5790    CALL Cmult(0,1,Gama(1),Igama(1),R2,I2)
5800    CALL Cmult(R2,I2,Landa(3),Ilanda(3),R1,I1)
5810    R2=Mu(3)-Mu(2)
5820    I2=Imu(3)-Imu(2)
5830    CALL Cmult(R1,I1,R2,I2,R4,I4)
5840    CALL Cmult(0,1,Gama(2),Igama(2),R2,I2)
5850    CALL Cmult(R2,I2,Landa(3),Ilanda(3),R1,I1)
5860    R2=Mu(1)-Mu(3)
5870    I2=Imu(1)-Imu(3)
5880    CALL Cmult(R1,I1,R2,I2,R3,I3)
5890    R4=R4+R3
5900    I4=I4+I3
5910    CALL Cmult(0,1,Gama(3),Igama(3),R2,I2)
5920    CALL Cmult(R2,I2,Landa(3),Ilanda(3),R1,I1)
5930    R2=Mu(2)-Mu(1)
5940    I2=Imu(2)-Imu(1)
5950    CALL Cmult(R1,I1,R2,I2,R3,I3)
5960    R4=R4+R3
5970    I4=I4+I3
5980    Fx(2,5)=-R4
5990  !
6000    CALL Cmult(0,1,Gama(1),Igama(1),R2,I2)
```

```
6010    CALL Cmult(R2,I2,Mu(1),Imu(1),R1,I1)
6020    CALL Cmult(Landa(2),Ilanda(2),Landa(3),Ilanda(3),R2,I2)
6030    R2=R2-1
6040    CALL Cmult(R1,I1,R2,I2,R4,I4)
6050    CALL Cmult(0,1,Gama(2),Igama(2),R2,I2)
6060    CALL Cmult(R2,I2,Mu(2),Imu(2),R1,I1)
6070    CALL Cmult(Landa(1),Ilanda(1),Landa(3),Ilanda(3),R2,I2)
6080    R2=1-R2
6090    I2=-I2
6100    CALL Cmult(R1,I1,R2,I2,R3,I3)
6110    R4=R4+R3
6120    I4=I4+I3
6130    CALL Cmult(0,1,Gama(3),Igama(3),R1,I1)
6140    CALL Cmult(R1,I1,Mu(3),Imu(3),R2,I2)
6150    CALL Cmult(R2,I2,Landa(3),Ilanda(3),R1,I1)
6160    R2=Landa(1)-Landa(2)
6170    I2=Ilanda(1)-Ilanda(2)
6180    CALL Cmult(R1,I1,R2,I2,R3,I3)
6190    R4=R4+R3
6200    I4=I4+I3
6210    Fx(6,1)=R4
6220  !
6230    CALL Cmult(Gama(1),Igama(1),Mu(1),Imu(1),R1,I1)
6240    CALL Cmult(Mu(3),Imu(3),Landa(2),Ilanda(2),R3,I3)
6250    CALL Cmult(R3,I3,Landa(3),Ilanda(3),R2,I2)
6260    R2=Mu(2)-R2
6270    I2=Imu(2)-I2
6280    CALL Cmult(R1,I1,R2,I2,R4,I4)
6290    CALL Cmult(Gama(2),Igama(2),Mu(2),Imu(2),R1,I1)
6300    CALL Cmult(Landa(1),Ilanda(1),Landa(3),Ilanda(3),R3,I3)
6310    CALL Cmult(R3,I3,Mu(3),Imu(3),R2,I2)
6320    R2=R2-Mu(1)
6330    I2=I2-Imu(1)
6340    CALL Cmult(R1,I1,R2,I2,R3,I3)
6350    R4=R4+R3
6360    I4=I4+I3
6370    CALL Cmult(Gama(3),Igama(3),Mu(3),Imu(3),R2,I2)
6380    CALL Cmult(R2,I2,Landa(3),Ilanda(3),R1,I1)
6390    CALL Cmult(Mu(1),Imu(1),Landa(2),Ilanda(2),R2,I2)
6400    CALL Cmult(Mu(2),Imu(2),Landa(1),Ilanda(1),R3,I3)
6410    R2=R2-R3
6420    I2=I2-I3
6430    CALL Cmult(R1,I1,R2,I2,R3,I3)
6440    R4=R4+R3
6450    I4=I4+I3
6460    Fx(6,2)=R4
6470  !
6480    CALL Cmult(Landa(2),Ilanda(2),Landa(3),Ilanda(3),R1,I1)
6490    CALL Cmult(0,1,Mu(2),Imu(2),R2,I2)
6500    CALL Cmult(0,1,Mu(3),Imu(3),R3,I3)
```

```
6510    CALL Cmult(R3,I3,Landa(2),Ilanda(2),R5,I5)
6520    CALL Cmult(R5,I5,Landa(3),Ilanda(3),R3,I3)
6530    R1=R1-1+R2-R3
6540    I1=I1+I2-I3
6550    CALL Cmult(Gama(1),Igama(1),Mu(1),Imu(1),R2,I2)
6560    CALL Cmult(R2,I2,R1,I1,R4,I4)
6570    CALL Cmult(Landa(1),Ilanda(1),Landa(3),Ilanda(3),R1,I1)
6580    CALL Cmult(0,1,Landa(1),Ilanda(1),R2,I2)
6590    CALL Cmult(R2,I2,Landa(3),Ilanda(3),R3,I3)
6600    CALL Cmult(R3,I3,Mu(3),Imu(3),R2,I2)
6610    CALL Cmult(0,1,Mu(1),Imu(1),R3,I3)
6620    R1=1-R1+R2-R3
6630    I1=-I1+I2-I3
6640    CALL Cmult(Gama(2),Igama(2),Mu(2),Imu(2),R2,I2)
6650    CALL Cmult(R2,I2,R1,I1,R3,I3)
6660    R4=R4+R3
6670    I4=I4+I3
6680    CALL Cmult(0,1,Mu(1),Imu(1),R2,I2)
6690    CALL Cmult(R2,I2,Landa(2),Ilanda(2),R1,I1)
6700    CALL Cmult(0,1,Mu(2),Imu(2),R3,I3)
6710    CALL Cmult(R3,I3,Landa(1),Ilanda(1),R2,I2)
6720    R2=Landa(1)-Landa(2)+R1-R2
6730    I2=Ilanda(1)-Ilanda(2)+I1-I2
6740    CALL Cmult(Gama(3),Igama(3),Mu(3),Imu(3),R3,I3)
6750    CALL Cmult(R3,I3,Landa(3),Ilanda(3),R1,I1)
6760    CALL Cmult(R1,I1,R2,I2,R3,I3)
6770    R4=R4+R3
6780    I4=I4+I3
6790    Fx(6,6)=-R4
6800    !
6810    CALL Cmult(Mu(1),Imu(1),Gama(1),Igama(1),R2,I2)
6820    CALL Cmult(R2,I2,Landa(3),Ilanda(3),R1,I1)
6830    R2=Mu(3)-Mu(2)
6840    I2=Imu(3)-Imu(2)
6850    CALL Cmult(R1,I1,R2,I2,R4,I4)
6860    CALL Cmult(Mu(2),Imu(2),Gama(2),Igama(2),R2,I2)
6870    CALL Cmult(R2,I2,Landa(3),Ilanda(3),R1,I1)
6880    R2=Mu(1)-Mu(3)
6890    I2=Imu(1)-Imu(3)
6900    CALL Cmult(R1,I1,R2,I2,R3,I3)
6910    R4=R4+R3
6920    I4=I4+I3
6930    CALL Cmult(Mu(3),Imu(3),Gama(3),Igama(3),R2,I2)
6940    CALL Cmult(R2,I2,Landa(3),Ilanda(3),R1,I1)
6950    R2=Mu(2)-Mu(1)
6960    I2=Imu(2)-Imu(1)
6970    CALL Cmult(R1,I1,R2,I2,R3,I3)
6980    R4=R4+R3
6990    I4=I4+I3
7000    Fx(6,4)=-R4
```

```
7010  !
7020    CALL Cmult(0,1,Mu(1),Imu(1),R1,I1)
7030    CALL Cmult(R1,I1,Gama(1),Igama(1),R2,I2)
7040    CALL Cmult(R2,I2,Landa(3),Ilanda(3),R1,I1)
7050    R2=Mu(3)-Mu(2)
7060    I2=Imu(3)-Imu(2)
7070    CALL Cmult(R1,I1,R2,I2,R4,I4)
7080    CALL Cmult(0,1,Mu(2),Imu(2),R1,I1)
7090    CALL Cmult(R1,I1,Gama(2),Igama(2),R2,I2)
7100    CALL Cmult(R2,I2,Landa(3),Ilanda(3),R1,I1)
7110    R2=Mu(1)-Mu(3)
7120    I2=Imu(1)-Imu(3)
7130    CALL Cmult(R1,I1,R2,I2,R3,I3)
7140    R4=R4+R3
7150    I4=I4+I3
7160    CALL Cmult(0,1,Mu(3),Imu(3),R1,I1)
7170    CALL Cmult(R1,I1,Gama(3),Igama(3),R2,I2)
7180    CALL Cmult(R2,I2,Landa(3),Ilanda(3),R1,I1)
7190    R2=Mu(2)-Mu(1)
7200    I2=Imu(2)-Imu(1)
7210    CALL Cmult(R1,I1,R2,I2,R3,I3)
7220    R4=R4+R3
7230    I4=I4+I3
7240    Fx(6,5)=R4
7250  !
7260    CALL Cmult(0,1,Gama(1),Igama(1),R1,I1)
7270    CALL Cmult(R1,I1,Landa(1),Ilanda(1),R2,I2)
7280    CALL Cmult(R2,I2,Mu(1),Imu(1),R1,I1)
7290    CALL Cmult(Landa(2),Ilanda(2),Landa(3),Ilanda(3),R2,I2)
7300    R2=R2-1
7310    CALL Cmult(R1,I1,R2,I2,R4,I4)
7320    CALL Cmult(0,1,Gama(2),Igama(2),R1,I1)
7330    CALL Cmult(R1,I1,Landa(2),Ilanda(2),R2,I2)
7340    CALL Cmult(R2,I2,Mu(2),Imu(2),R1,I1)
7350    CALL Cmult(Landa(1),Ilanda(1),Landa(3),Ilanda(3),R2,I2)
7360    R2=1-R2
7370    I2=-I2
7380    CALL Cmult(R1,I1,R2,I2,R3,I3)
7390    R4=R4+R3
7400    I4=I4+I3
7410    CALL Cmult(0,1,Gama(3),Igama(3),R2,I2)
7420    CALL Cmult(R2,I2,Mu(3),Imu(3),R1,I1)
7430    R2=Landa(1)-Landa(2)
7440    I2=Ilanda(1)-Ilanda(2)
7450    CALL Cmult(R1,I1,R2,I2,R3,I3)
7460    R4=R4+R3
7470    I4=I4+I3
7480    Fx(5,1)=-R4
7490  !
7500    CALL Cmult(Gama(1),Igama(1),Landa(1),Ilanda(1),R2,I2)
```

```
7510    CALL Cmult(R2,I2,Mu(1),Imu(1),R1,I1)
7520    CALL Cmult(Mu(3),Imu(3),Landa(3),Ilanda(3),R3,I3)
7530    CALL Cmult(R3,I3,Landa(2),Ilanda(2),R2,I2)
7540    R2=Mu(2)-R2
7550    I2=Imu(2)-I2
7560    CALL Cmult(R1,I1,R2,I2,R4,I4)
7570    CALL Cmult(Gama(2),Igama(2),Landa(2),Ilanda(2),R2,I2)
7580    CALL Cmult(R2,I2,Mu(2),Imu(2),R1,I1)
7590    CALL Cmult(Landa(1),Ilanda(1),Landa(3),Ilanda(3),R3,I3)
7600    CALL Cmult(R3,I3,Mu(3),Imu(3),R2,I2)
7610    R2=R2-Mu(1)
7620    I2=I2-Imu(1)
7630    CALL Cmult(R1,I1,R2,I2,R3,I3)
7640    R4=R4+R3
7650    I4=I4+I3
7660    CALL Cmult(Gama(3),Igama(3),Mu(3),Imu(3),R1,I1)
7670    CALL Cmult(Mu(1),Imu(1),Landa(2),Ilanda(2),R2,I2)
7680    CALL Cmult(Mu(2),Imu(2),Landa(1),Ilanda(1),R3,I3)
7690    R2=R2-R3
7700    I2=I2-I3
7710    CALL Cmult(R1,I1,R2,I2,R3,I3)
7720    R4=R4+R3
7730    I4=I4+I3
7740    Fx(5,2)=-R4
7750    !
7760    CALL Cmult(Landa(2),Ilanda(2),Landa(3),Ilanda(3),R1,I1)
7770    CALL Cmult(0,1,Mu(2),Imu(2),R2,I2)
7780    CALL Cmult(0,1,Mu(3),Imu(3),R3,I3)
7790    CALL Cmult(R2,I2,Landa(2),Ilanda(2),R5,I5)
7800    CALL Cmult(R5,I5,Landa(3),Ilanda(3),R3,I3)
7810    R1=R1-1+R2-R3
7820    I1=I1+I2-I3
7830    CALL Cmult(Gama(1),Igama(1),Mu(1),Imu(1),R2,I2)
7840    CALL Cmult(R2,I2,Landa(1),Ilanda(1),R3,I3)
7850    CALL Cmult(R3,I3,R1,I1,R4,I4)
7860    CALL Cmult(Landa(1),Ilanda(1),Landa(3),Ilanda(3),R1,I1)
7870    CALL Cmult(0,1,Landa(1),Ilanda(1),R2,I2)
7880    CALL Cmult(R2,I2,Landa(3),Ilanda(3),R3,I3)
7890    CALL Cmult(R3,I3,Mu(3),Imu(3),R2,I2)
7900    CALL Cmult(0,1,Mu(1),Imu(1),R3,I3)
7910    R1=1-R1+R2-R3
7920    I1=-I1+I2-I3
7930    CALL Cmult(Gama(2),Igama(2),Mu(2),Imu(2),R3,I3)
7940    CALL Cmult(R3,I3,Landa(2),Ilanda(2),R2,I2)
7950    CALL Cmult(R2,I2,R1,I1,R3,I3)
7960    R4=R4+R3
7970    I4=I4+I3
7980    CALL Cmult(0,1,Mu(1),Imu(1),R2,I2)
7990    CALL Cmult(R2,I2,Landa(2),Ilanda(2),R1,I1)
8000    CALL Cmult(0,1,Mu(2),Imu(2),R3,I3)
```

```
8010    CALL Cmult(R3,I3,Landa(1),Ilanda(1),R2,I2)
8020    R2=Landa(1)-Landa(2)+R1-R2
8030    I2=Ilanda(1)-Ilanda(2)+I1-I2
8040    CALL Cmult(Gama(3),Igama(3),Mu(3),Imu(3),R1,I1)
8050    CALL Cmult(R1,I1,R2,I2,R3,I3)
8060    R4=R4+R3
8070    I4=I4+I3
8080    F*(5,6)=R4
8090    !
8100    CALL Cmult(Mu(1),Imu(1),Gama(1),Igama(1),R1,I1)
8110    CALL Cmult(R1,I1,Landa(1),Ilanda(1),R2,I2)
8120    CALL Cmult(R2,I2,Landa(3),Ilanda(3),R1,I1)
8130    R2=Mu(3)-Mu(2)
8140    I2=Imu(3)-Imu(2)
8150    CALL Cmult(R1,I1,R2,I2,R4,I4)
8160    CALL Cmult(Mu(2),Imu(2),Gama(2),Igama(2),R1,I1)
8170    CALL Cmult(R1,I1,Landa(2),Ilanda(2),R2,I2)
8180    CALL Cmult(R2,I2,Landa(3),Ilanda(3),R1,I1)
8190    R2=Mu(1)-Mu(3)
8200    I2=Imu(1)-Imu(3)
8210    CALL Cmult(R1,I1,R2,I2,R3,I3)
8220    R4=R4+R3
8230    I4=I4+I3
8240    CALL Cmult(Mu(3),Imu(3),Gama(3),Igama(3),R1,I1)
8250    R2=Mu(2)-Mu(1)
8260    I2=Imu(2)-Imu(1)
8270    CALL Cmult(R1,I1,R2,I2,R3,I3)
8280    R4=R4+R3
8290    I4=I4+I3
8300    F*(5,4)=R4
8310    !
8320    CALL Cmult(0,1,Gama(1),Igama(1),R2,I2)
8330    CALL Cmult(R2,I2,Mu(1),Imu(1),R1,I1)
8340    CALL Cmult(R1,I1,Landa(1),Ilanda(1),R2,I2)
8350    CALL Cmult(R2,I2,Landa(3),Ilanda(3),R1,I1)
8360    R2=Mu(3)-Mu(2)
8370    I2=Imu(3)-Imu(2)
8380    CALL Cmult(R1,I1,R2,I2,R4,I4)
8390    CALL Cmult(0,1,Gama(2),Igama(2),R2,I2)
8400    CALL Cmult(R2,I2,Mu(2),Imu(2),R1,I1)
8410    CALL Cmult(R1,I1,Landa(2),Ilanda(2),R2,I2)
8420    CALL Cmult(R2,I2,Landa(3),Ilanda(3),R1,I1)
8430    R2=Mu(1)-Mu(3)
8440    I2=Imu(1)-Imu(3)
8450    CALL Cmult(R1,I1,R2,I2,R3,I3)
8460    R4=R4+R3
8470    I4=I4+I3
8480    CALL Cmult(0,1,Gama(3),Igama(3),R2,I2)
8490    CALL Cmult(R2,I2,Mu(3),Imu(3),R1,I1)
8500    R2=Mu(2)-Mu(1)
```

```
8510    I2=Imu(2)-Imu(1)
8520    CALL Cmult(R1,I1,R2,I2,R3,I3)
8530    R4=R4+R3
8540    I4=I4+I3
8550    Fx(5,5)=-R4
8560  !
8570    CALL Cmult(0,1,Gama(1),Igama(1),R2,I2)
8580    CALL Cmult(R2,I2,Landa(1),Ilanda(1),R1,I1)
8590    CALL Cmult(Landa(2),Ilanda(2),Landa(3),Ilanda(3),R2,I2)
8600    R2=R2-1
8610    CALL Cmult(R1,I1,R2,I2,R4,I4)
8620    CALL Cmult(0,1,Gama(2),Igama(2),R2,I2)
8630    CALL Cmult(R2,I2,Landa(2),Ilanda(2),R1,I1)
8640    CALL Cmult(Landa(1),Ilanda(1),Landa(3),Ilanda(3),R2,I2)
8650    R2=1-R2
8660    I2=-I2
8670    CALL Cmult(R1,I1,R2,I2,R3,I3)
8680    R4=R4+R3
8690    I4=I4+I3
8700    CALL Cmult(0,1,Gama(3),Igama(3),R1,I1)
8710    R2=Landa(1)-Landa(2)
8720    I2=Ilanda(1)-Ilanda(2)
8730    CALL Cmult(R1,I1,R2,I2,R3,I3)
8740    R4=R4+R3
8750    I4=I4+I3
8760    Fx(4,1)=R4
8770  !
8780    CALL Cmult(Gama(1),Igama(1),Landa(1),Ilanda(1),R1,I1)
8790    CALL Cmult(Mu(3),Imu(3),Landa(3),Ilanda(3),R3,I3)
8800    CALL Cmult(R3,I3,Landa(2),Ilanda(2),R2,I2)
8810    R2=Mu(2)-R2
8820    I2=Imu(2)-I2
8830    CALL Cmult(R1,I1,R2,I2,R4,I4)
8840    CALL Cmult(Gama(2),Igama(2),Landa(2),Ilanda(2),R1,I1)
8850    CALL Cmult(Landa(1),Ilanda(1),Landa(3),Ilanda(3),R3,I3)
8860    CALL Cmult(R3,I3,Mu(3),Imu(3),R2,I2)
8870    R2=R2-Mu(1)
8880    I2=I2-Imu(1)
8890    CALL Cmult(R1,I1,R2,I2,R3,I3)
8900    R4=R4+R3
8910    I4=I4+I3
8920    CALL Cmult(Mu(1),Imu(1),Landa(2),Ilanda(2),R2,I2)
8930    CALL Cmult(Mu(2),Imu(2),Landa(1),Ilanda(1),R3,I3)
8940    R2=R2-R3
8950    I2=I2-I3
8960    CALL Cmult(Gama(3),Igama(3),R2,I2,R3,I3)
8970    R4=R4+R3
8980    I4=I4+I3
8990    Fx(4,2)=R4
9000  !
```

```
9010    CALL Cmult(Landa(2),Ilanda(2),Landa(3),Ilanda(3),R1,I1)
9020    CALL Cmult(0,1,Mu(2),Imu(2),R2,I2)
9030    CALL Cmult(0,1,Mu(3),Imu(3),R3,I3)
9040    CALL Cmult(R3,I3,Landa(2),Ilanda(2),R5,I5)
9050    CALL Cmult(R5,I5,Landa(3),Ilanda(3),R3,I3)
9060    R1=R1-1+R2-R3
9070    I1=I1+I2-I3
9080    CALL Cmult(Gama(1),Igama(1),Landa(1),Ilanda(1),R2,I2)
9090    CALL Cmult(R2,I2,R1,I1,R4,I4)
9100    CALL Cmult(Landa(1),Ilanda(1),Landa(3),Ilanda(3),R1,I1)
9110    CALL Cmult(0,1,Landa(1),Ilanda(1),R2,I2)
9120    CALL Cmult(R2,I2,Landa(3),Ilanda(3),R3,I3)
9130    CALL Cmult(R3,I3,Mu(3),Imu(3),R2,I2)
9140    CALL Cmult(0,1,Mu(1),Imu(1),R3,I3)
9150    R1=1-R1+R2-R3
9160    I1=-I1+I2-I3
9170    CALL Cmult(Gama(2),Igama(2),Landa(2),Ilanda(2),R2,I2)
9180    CALL Cmult(R2,I2,R1,I1,R3,I3)
9190    R4=R4+R3
9200    I4=I4+I3
9210    CALL Cmult(0,1,Mu(1),Imu(1),R2,I2)
9220    CALL Cmult(R2,I2,Landa(2),Ilanda(2),R1,I1)
9230    CALL Cmult(0,1,Mu(2),Imu(2),R3,I3)
9240    CALL Cmult(R3,I3,Landa(1),Ilanda(1),R2,I2)
9250    R2=Landa(1)-Landa(2)+R1-R2
9260    I2=Ilanda(1)-Ilanda(2)+I1-I2
9270    CALL Cmult(Gama(3),Igama(3),R2,I2,R3,I3)
9280    R4=R4+R3
9290    I4=I4+I3
9300    Fx(4,6)=-R4
9310  !
9320    CALL Cmult(Gama(1),Igama(1),Landa(1),Ilanda(1),R2,I2)
9330    CALL Cmult(R2,I2,Landa(3),Ilanda(3),R1,I1)
9340    R2=Mu(3)-Mu(2)
9350    I2=Imu(3)-Imu(2)
9360    CALL Cmult(R1,I1,R2,I2,R4,I4)
9370    CALL Cmult(Gama(2),Igama(2),Landa(2),Ilanda(2),R2,I2)
9380    CALL Cmult(R2,I2,Landa(3),Ilanda(3),R1,I1)
9390    R2=Mu(1)-Mu(3)
9400    I2=Imu(1)-Imu(3)
9410    CALL Cmult(R1,I1,R2,I2,R3,I3)
9420    R4=R4+R3
9430    I4=I4+I3
9440    R2=Mu(2)-Mu(1)
9450    I2=Imu(2)-Imu(1)
9460    CALL Cmult(Gama(3),Igama(3),R2,I2,R3,I3)
9470    R4=R4+R3
9480    I4=I4+I3
9490    Fx(4,4)=-R4
9500  !
```

```
9510    CALL Cmult(0,1,Gama(1),Igama(1),R1,I1)
9520    CALL Cmult(R1,I1,Landa(1),Ilanda(1),R2,I2)
9530    CALL Cmult(R2,I2,Landa(3),Ilanda(3),R1,I1)
9540    R2=Mu(3)-Mu(2)
9550    I2=Imu(3)-Imu(2)
9560    CALL Cmult(R1,I1,R2,I2,R4,I4)
9570    CALL Cmult(0,1,Gama(2),Igama(2),R1,I1)
9580    CALL Cmult(R1,I1,Landa(2),Ilanda(2),R2,I2)
9590    CALL Cmult(R2,I2,Landa(3),Ilanda(3),R1,I1)
9600    R2=Mu(1)-Mu(3)
9610    I2=Imu(1)-Imu(3)
9620    CALL Cmult(R1,I1,R2,I2,R3,I3)
9630    R4=R4+R3
9640    I4=I4+I3
9650    CALL Cmult(0,1,Gama(3),Igama(3),R1,I1)
9660    R2=Mu(2)-Mu(1)
9670    I2=Imu(2)-Imu(1)
9680    CALL Cmult(R1,I1,R2,I2,R3,I3)
9690    R4=R4+R3
9700    I4=I4+I3
9710    Fx(4,5)=R4
9720  !
9730    FOR I=1 TO 6
9740      IF I=3 THEN 9760
9750      Fx(3,I)=-(Aa(3,1)*Fx(1,I)+Aa(3,2)*Fx(2,I)+Aa(3,4)*Fx(4,I)+Aa(3,5)*Fx(5
,I)+Aa(3,6)*Fx(6,I))/Aa(3,3)
9760    NEXT I
9770  !
9780    FOR I=1 TO 6
9790      Fx(I,I)=1+Fx(I,I)
9800    NEXT I
9810  !
9820    CALL Cmult(Mu(3),Imu(3),Landa(2),Ilanda(2),R2,I2)
9830    CALL Cmult(R2,I2,Landa(3),Ilanda(3),R1,I1)
9840    CALL Cmult(Landa(2),Ilanda(2),Landa(3),Ilanda(3),R3,I3)
9850    R3=R3-1
9860    CALL Cmult(0,1,R3,I3,R2,I2)
9870    R1=Mu(2)-R1+R2
9880    I1=Imu(2)-I1+I2
9890    CALL Cmult(Gama(1),Igama(1),R1,I1,Z1,Iz1)
9900  !
9910    CALL Cmult(Landa(1),Ilanda(1),Landa(3),Ilanda(3),R2,I2)
9920    CALL Cmult(R2,I2,Mu(3),Imu(3),R1,I1)
9930    R2=1-R2
9940    I2=-I2
9950    CALL Cmult(0,1,R2,I2,R3,I3)
9960    R1=R1-Mu(1)+R3
9970    I1=I1-Imu(1)+I3
9980    CALL Cmult(Gama(2),Igama(2),R1,I1,Z2,Iz2)
9990  !
10000   CALL Cmult(Mu(1),Imu(1),Landa(2),Ilanda(2),R1,I1)
```

```
10010   CALL Cmult(Mu(2),Imu(2),Landa(1),Ilanda(1),R2,I2)
10020   R3=Landa(1)-Landa(2)
10030   I3=Ilanda(1)-Ilanda(2)
10040   CALL Cmult(0,1,R3,I3,R4,I4)
10050   R1=R1-R2+R4
10060   I1=I1-I2+I4
10070   CALL Cmult(Gama(3),Igama(3),R1,I1,Z3,Iz3)
10080 !
10090   CALL Cmult(Mu(1),Imu(1),Mu(1),Imu(1),R4,I4)
10100   CALL Cmult(R4,I4,Z1,Iz1,R1,I1)
10110   CALL Cmult(Mu(2),Imu(2),Mu(2),Imu(2),R4,I4)
10120   CALL Cmult(R4,I4,Z2,Iz2,R2,I2)
10130   CALL Cmult(Mu(3),Imu(3),Mu(3),Imu(3),R4,I4)
10140   CALL Cmult(R4,I4,Landa(3),Ilanda(3),R5,I5)
10150   CALL Cmult(R5,I5,Z3,Iz3,R3,I3)
10160   Fqx(1)=R1+R2+R3
10170 !
10180   CALL Cmult(Landa(3),Ilanda(3),Z3,Iz3,R1,I1)
10190   Fqx(2)=Z1+Z2+R1
10200 !
10210   CALL Cmult(Mu(1),Imu(1),Z1,Iz1,R1,I1)
10220   CALL Cmult(Mu(2),Imu(2),Z2,Iz2,R2,I2)
10230   CALL Cmult(Landa(3),Ilanda(3),Mu(3),Imu(3),R4,I4)
10240   CALL Cmult(R4,I4,Z3,Iz3,R3,I3)
10250   Fqx(6)=-(R1+R2+R3)
10260 !
10270   CALL Cmult(Landa(1),Ilanda(1),Mu(1),Imu(1),R4,I4)
10280   CALL Cmult(R4,I4,Z1,Iz1,R1,I1)
10290   CALL Cmult(Landa(2),Ilanda(2),Mu(2),Imu(2),R4,I4)
10300   CALL Cmult(R4,I4,Z2,Iz2,R2,I2)
10310   CALL Cmult(Mu(3),Imu(3),Z3,Iz3,R3,I3)
10320   Fqx(5)=R1+R2+R3
10330 !
10340   CALL Cmult(Landa(1),Ilanda(1),Z1,Iz1,R1,I1)
10350   CALL Cmult(Landa(2),Ilanda(2),Z2,Iz2,R2,I2)
10360   Fqx(4)=-(R1+R2+Z3)
10370 !
10380   Fqx(3)=-(Fqx(1)*Aa(3,1)+Fqx(2)*Aa(3,2)+Fqx(4)*Aa(3,4)+Fqx(5)*Aa(3,5)+Fqx
(6)*Aa(3,6))/Aa(3,3)
10390 !
10400 SUBEND !*************************************************************
```

U. S. Government Printing Office: 1985/5-587-002/24077

Technical Information Department · Lawrence Livermore National Laboratory
University of California · Livermore, California 94550